AN ARCHAEOLOGICAL AND ENGINEERING EXAMINATION OF NAVAL GUN FAILURE PATTERNS UTILIZING FINITE ELEMENT ANALYSIS

By

James R. Fowler

May 2026

Director of Thesis: Dr. Nathan Richards

Department of History

Abstract

Because of their material composition and massive bulk, cannons are ubiquitous in the archaeological record and commonplace throughout the world. Historical developments in metallurgy and material science paralleled progress in artillery design. However, seemingly random catastrophic gun failures continued to plague militaries well into the nineteenth and twentieth centuries with sometimes significant repercussions. The purpose of this research is to generate a multidisciplinary study that combines archaeological, historical, and engineering methodologies to answer complex questions concerning cannon failure patterns. Specifically, this research analyzes an attempt to utilize engineering Computer Aided Design (CAD) software to conduct Finite Element Analysis (FEA) on models of 17th century, 18th century, and 19th century naval guns to simulate how they fail.

The results of the simulations are then compared to the archaeological data, and the trends are discussed at length. The impact of variables such as age, surface finish/corrosion, material composition, casting techniques, cannon design, and history are quantified to help understand the historical and archaeological record and explain why some guns failed in the way that they did. The objective of this research is to identify a categorization of cannon failure modes to help archaeologists and historians record damaged cannons and extrapolate a gun's service history and cause of failure with confidence.

AN ARCHAEOLOGICAL AND ENGINEERING EXAMINATION OF NAVAL GUN FAILURE PATTERNS UTILIZING FINITE ELEMENT ANALYSIS

A Thesis

Presented to the Faculty of the Department of History

East Carolina University

In Partial Fulfillment of the Requirements for the Degree

Master of Arts in Maritime Studies

By

James R. Fowler

May, 2026

Director of Dissertation: Nathan Richards, Ph.D.
Dissertation Committee Members:
Jason T. Raupp, Ph.D.
Eric O. Oakley, Ph.D.

Dedication

To my wonderful wife Abigail Fowler, the Zephyrus to my doldrums.

Acknowledgements

Like so many undertakings in life, this thesis is a culmination of work and support from many people in my life. I would foremost like to thank my wife Abigail Fowler, who has furnished me with ample love and patience throughout the entire thesis writing process, even the stressful parts. I would also like to extend my sincere gratitude to my advisor Dr. Nathan Richards, who with magnanimous patience helped me to narrow down my thesis topic and was ever present with words of encouragement and stalwart guidance. Many thanks also to Dr. Eric Oakley, whose hospitality in office hours I have taken advantage of on more than one occasion. Thanks also to Dr. Jason Raupp, who made me aware of the gun failure phenomenon and enthusiastically supported my interest in pursuing this topic.

A special thanks goes to the Maritime Archaeological Society of Finland and the Finnish Heritage Agency, which made fieldwork in the Finland and the Baltic possible for me under research permit MV/00971/2025, especially Markku Luoto, Dr. Minna Koivikko, and all my Finnish friends who welcomed me to Finland with open arms. Additionally, thank you to Jim McKee and Edwin Scollon who provided me with data and information in this search. A huge thank you must go out to Addison Costa who helped conduct research for my thesis and aided in testing out new measurement methodology. Your endless enthusiasm made every day brighter. And I cannot forget Don Swanbeck, who helped measure my first round of cannons in the pouring rain. Your dedication to precision paid off greatly. To the rest of my cohort, a hearty thank you. I could not imagine undergoing this degree and fieldwork with any other group–from the mud of Mallows Bay to the alligators in the Cape Fear River.

Lastly, to my family and my parents Michael Fowler and Dr. Julie Bunck, for always offering to help review and revise, and for unending love and support throughout this process.

Table of Contents

Table of Figures

Table of Equations

List of Abbreviations

ASME	American Society of Mechanical Engineers
BTU	British Thermal Unit
BTU/lb F	British Thermal Units per Pound Fahrenheit
BTU/ft h F	British Thermal Units per Foot–Hour Fahrenheit
°C	Degrees Celsius
CAD	Computer Aided Design
cm	Centimeter
ECU	East Carolina University
°F	Degrees Fahrenheit
FEA	Finite Element Analysis
FHA	Finnish Heritage Agency
FMA	Failure Modes Analysis
FoS	Factor of Safety
Ft	Feet
GPa	Gigapascal
HCF	High Cycle Fatigue
In.	Inch
KSI	Kilo-pound per Square Inch
LCF	Low Cycle Fatigue
m	Meter
mm	Millimeter

MPa	Megapascal
MAS	Finnish Maritime Archaeological Society
PFD	Process Flow Diagram
PSI	Pound per Square Inch
Ra	Surface Roughness
TMF	Thermo–Mechanical Fatigue
UTS	Ultimate Tensile Strength

Preface

My search for failed guns in the archaeological record led me on a path to broaden our understanding of naval ordinance and its effect on course of history. While thus engaged, I became aware of the vast lexicon utilized to describe weapons of war, and I believe it is only appropriate to describe some of this terminology that I later utilize throughout this work. The words *naval gun*, *gun*, *cannon*, and *artillery* are all used to describe what is relatively the same piece of technology, although each of these words contains a slightly different connotation. The word *cannon* is utilized in common parlance to describe any large smooth–bore artillery device firing solid shot or explosive shells. However, I acknowledge that in some technical phraseology, *cannon* refers to a very particular size and shot–weight artillery system, as described by Iver Cooper in *Arming the Warship: Naval Weapons Technology and Gunnery from the Spanish Armada to the Cold War* (Cooper 2024:5). Thus, throughout this study the term *cannon* is used as a generalist term to describe any artillery piece which is not specifically known to be for naval usage. Similarly, the term *gun* is commonly understood to be a portable, shoulder–able small–arm, however it is important to note that the term *gun* serves a different meaning altogether in naval parlance. In this case, I use the term *gun* to indicate a crew–served cannon permanently mounted on a ship firing broadly flat–trajectory projectiles. For example, and to help indicate the degree of similarity between such weapons, a naval *gun* could be requisitioned by a terrestrial military and utilized as a *cannon* or as *artillery*. For this thesis, the term *gun* or *naval gun* is utilized to describe weapons explicitly found on board warships or designed for naval usage. *Artillery* is utilized as a synonym for *cannon,* and both will be utilized as a generalist catch–all term.

Technically speaking, this study explores cannon failure characteristics with a focus on naval gun failures, not the failing of terrestrial artillery or cannons. The fieldwork focused on naval guns located on coastal fortifications or naval guns located on shipwrecks. Often the historical context of any cannon located in the archaeological context is unknown, and therefore it is not apparent if it was a *gun* or a *cannon.* It is worth mentioning that in software simulations, the processes that work for analyzing naval guns would also work for any terrestrial cannon or artillery, that is to say, the terms are utilized for theoretical distinction amongst military branches more than any functional distinction, and do not affect the outcome of the research.

Chapter 1: A Multidisciplinary Analysis of Failed Naval Guns

Introduction

Warfare on the high seas is a concept as old as ships themselves. Warring factions consistently utilized sea power to dominate and subjugate neighboring groups, a tradition that stretches well into antiquity (Mahan 1890; Lambert 2018). A key aspect to naval warfare has always been the weapons of war that enable it, and none is more recognizable than the naval gun. Perhaps the single most recognizable symbol of sea power in the world, the naval gun represents many things. To some, it represents order, control, and prosperity. To others, it is a manifestation of European domination. To those unlucky enough to be on the receiving end of one, it can represent death itself. To others using one to ensure victory, it can be a savior. Regardless, the naval gun has been an essential aspect of naval warfare since its conception in the early 14th century (Padfield 1974:19). The naval gun has changed drastically in its design, engineering, and usage over the intervening half millennium, but the basic form has remained the same, and the dangers associated with operating one remained mostly unchanged. Historical developments in metallurgy and material science reflected progress in artillery design. However, seemingly random catastrophic gun failures plagued militaries well into the nineteenth and twentieth centuries with sometimes significant repercussions (Taylor 1984:148–149).

The objective of this thesis is multifaceted, including aspects of archaeological theory and engineering theory informed upon a broad foundation of historical research. Initially, a collection of guns present in the archaeological record was located and recorded in detail, including notation of all dimensions and identifying marks. Additionally, photogrammetry was utilized where possible to obtain further detailed data. Failed guns from several different centuries and caused by several different failure modes were located and recorded. The archaeological data was then matched to historic engineering drawings, and all deviations noted. Archives around the world were combed for historic engineering data on cannon manufacturing and construction, and historic treatises and gunnery manuals searched thoroughly for all mention of naval gun failures. From this foundation, engineering technology was utilized to reconstruct the cannon failure dynamics in a software simulation, to glean answers as to how, why, and when naval guns fail.

The history of naval gun design and usage is inextricable from the driving metallurgical developments pioneered throughout the era. To understand naval gun history, and failed naval guns in the archaeological record, is to understand the engineering developments that drove advances in cannon manufacturing. Only from a historical and technical understanding can gun failure patterns become apparent. In this thesis, the history of naval gunnery and cannon metallurgy is cataloged and followed by a primer on the basic engineering considerations that may affect the naval gun failures found in the archaeological record. Engineering fundamentals and first principles such as material science, metallurgy, and fatigue are discussed at length, and hopefully the complicated world of cannon manufacturing processes and considerations will become palatable to a broader audience.

Once all variables are accounted for, engineering simulation testing and comparison commenced. Utilizing Computer Aided Design (CAD) software, computer models of each gun type were built using the primary source engineering documents in their intended role. The CAD models were then imported into a Finite Element Analysis (FEA) suite, and a regime of simulations conducted on the models. The purpose of the simulations was to locate and identify weak points in the designs and provide quantitative data on the expected performance of the selected naval guns in the field throughout their designed lifetime. From this analysis a compilation of failure modes was generated. A cannon's failure mode can be defined as a general pattern in which the cannon repeatedly fails given the correct combination of variables. The results of the FEA simulations were then compared to their archaeological counterparts and assessed.

The research was used to explain and confirm known gun failure modes, while also providing a reference for future archaeological analysis of failed guns. A categorization was created, driven by data derived from the simulations and archaeological analysis, to aid in the interpretation of other failed guns found in the archaeological record. No such categorization currently exists, and no work had been done to explain failed guns. On the contrary, failed guns are often overlooked in their potential value to explain the historical and archaeological record. This thesis seeks to remedy that gap in knowledge and provide a foundation for future research.

Research Questions

The objective of this research is to expand the understanding of naval gun failures. Through an archaeological analysis of the material culture coupled with an examination of many different factors in the historic manufacture of naval guns was used to inform an engineering analysis of the material culture. The objectives were categorized into several secondary questions to facilitate an understanding of the primary objective.

Primary Question

- Can engineering technology be utilized to broaden knowledge of naval gun failures found in the archaeological record while also aiding in the interpretation of historical instances of cannon failures?

Secondary Questions

- Can a categorization of naval gun failure modes be generated?
- What are the non–engineering related factors influencing instances of historic gun failures?
- Can engineering software successfully replicate a gun failure to corroborate evidence found in archaeological record?
- How do archaeological considerations such as transformation processes and site formation influence the identification of failed guns?
- How many engineering factors can be identified that influence the failure of guns?

Previous Research

Almost no previous research exists on this specific topic, a fact which resulted in several unforeseen challenges. Failed guns are often ignored in most archaeological publications, because failed guns are not seen as a means to understand history but instead as a broken version of ubiquitous artifacts (Cook et al. 2016:375; Eriksson and Rönnbyn 2017:103; Martin 2020:429). However, as is argued in this study, failed guns can help historians and archaeologists peer deeper into the ambiguities of history and learn more about the cultures, tendencies, and societal minutia of historic militaries. In archaeological publications, often failed guns are simply referred to once in a catalog of artifacts or in a map but otherwise receive little attention (Cook et al. 2016:375; Eriksson and Rönnbyn 2017:103; Harris and Richards 2018:411–412). However, this isn't always the case. Lake Champlain Maritime Museum (LCMM) recovered an exploded gun from the gunboat *New York* in the early 2000s, and much research was conducted on contextualizing the find (Cohn et al. 2003:86–92). Avocational archaeologist Edwin Scollon has spent considerable time tracking down the historical context of that gun failure, even locating the gravesites of some of the killed crew members, however few publications have developed from this (Scollon 2025, pers comm.). Additionally, an exploded cannon was located near Brunswick Town/Fort Anderson State Historic Site (BTFA) in Winnabow, North Carolina (NC), and site manager Jim McKee has invested significant resources into documenting and conserving the failed cannon. Believed by McKee to possibly be from the wreck of the 18th century Spanish privateer *La Fortuna*, significant effort has been made to contextualize the cannon (McKee 2025, pers. comm.). However, no official publications have been written to catalog that research.

Cannons, damaged or otherwise, are ubiquitous in the archaeological record and appear in many relevant publications, too numerous to catalog here (McBride 1976:189,193,196; Brown 1990:18–21; Overmeer 2012:1–93; Cook et al. 2016:375). It is worth noting that failed cannons are much more common in the underwater archaeological record than the terrestrial archaeological record, however no rigorous testing has been undertaken to understand why that may be the case. Perhaps failed guns on land were recycled and remelted, while those situated below the surface were lost or deemed too expensive to recover simply to recycle. Regardless, failed guns appear underwater in greater numbers (McBride 1976:189, 193, 196; Brown 1990:18–21; Overmeer 2012:1–93; Cook et al. 2016:375; Eriksson and Rönnbyn 2017:103; Martin 2020:429; Harris and Richards 2018:411–412; Delgado and Goold 2022:357). Many failed guns located underwater are included in this study (Cohn et al. 2003:86–92; Wessex Archaeology 2013:10, 22; Shipwreck Preservation Society of Newfoundland and Labrador 2020; Maritime Archaeological Society of Finland 2025). Despite the numerous archaeological publications that mention failed cannons, few suppose a causation, or draw any meaningful analysis from the failed guns. Thus, this thesis aims to provide a foundation for reevaluation of these findings, and provide a framework for future analysis of exploded, burst, or otherwise failed guns in both the terrestrial and underwater archaeological context.

Furthermore, the engineering community has forwarded no rigorous attempts to evaluate historical gun explosions, nor has engineering methodology been utilized systematically within the archaeological community to answer material culture questions. Some studies exist, such as Kristina Fricker's work on utilizing FEA software to model collision dynamics in Greco–Roman naval conflicts (Fricker 2019). Additionally, FEA was utilized in prehistoric archaeology to model and simulate ancient tool systems, including the usage patterns of recurve bows (Almeida 2013:209–270). Others used FEA and CAD systems to model static systems such as ancient architecture, as was demonstrated by Richard Levy and Peter Dawson (Levy and Dawson 2009:2298–2307). More recently, FEA was utilized to simulate amphora dispersion patterns on ancient European shipwrecks (Sviličić et al. 2025:373). Broadly speaking, however, the use of engineering techniques is heavily underutilized and poses a new avenue for solving advanced questions concerning the archaeological record.

It is hoped that other scholars in these fields will utilize multidisciplinary engineering and archaeological methodologies to answer material culture questions. Engineering methodologies, while advanced, are accessible and easy to learn, and could revolutionize the field of archaeology if widely accepted and utilized. Great care was taken to make this thesis as accessible as possible to archaeologists and historians of all backgrounds, to hopefully allow the easy utilization of this technology to future archaeological projects. Photogrammetry technology is widely accepted and has seen widespread adoption; FEA analysis is the next logical step for photogrammetric data or CAD models to test digital artifacts in simulation software. This thesis represents a type of experimental archaeology, one where no physical artifacts are risked, but instead a digital representation can be thoroughly tested and broken in many different ways to further understand the material culture.

Structure of Thesis

To fully appreciate the outcomes of this thesis, an overview of the thesis structure is necessary. Chapter One initiates the thesis and orients the reader with the project's objectives. Chapter Two provides a detailed overview of the history of naval gun usage on board warships and gives an overview of gun manufacturing techniques and material sourcing. It concludes with a detailed recollection of many historical instances of cannon failure, focusing on naval usage. Chapter Three familiarizes the reader with the primary theoretical frameworks utilized in examining failed guns. The chapter begins with an overview of archaeological theory, including the site formation theory utilized to contextualize the archaeological record. Then, engineering theory is examined in detail. To fully understand the many factors at play in instances of gun failure, a primer on engineering first principles is included. This information is important for fully understanding the results of the FEA simulations on exploded guns. Chapter Four outlines the Process Flow Diagram (PFD) utilized in this study, which provides the methodological process by which the archaeological data was acquired, the historical information obtained, CAD models constructed, and the FEA simulations undertaken. This chapter is of importance to any future researcher hoping to build upon this study. In Chapter Five, the archaeological fieldwork which included the documentation of failed guns, conducted by the author and by many other researchers, is compiled and examined. Technical, historical, and archaeological details for every failed gun is listed. Chapter Six outlines the utilization of engineering FEA software on failed guns and analyzes the trends. The guns are categorized according to failure pattern, and each failure mode is analyzed via one or more archetypal guns representing each individual failure pattern. FEA was conducted on the CAD models of the guns, and all other similarly failed guns are compared and contrasted to the archetype. Finally, Chapter Seven reviews the objectives of the thesis and concludes the study, providing clear avenues for further research and outlines the next steps which should be undertaken to increase the understanding of failed guns.

Chapter 2: The History of Naval Ordnance

Introduction

Exploded guns are found throughout the archaeological record, but instances of gun explosions also appear in the historical record with significant frequency. In this chapter, the usage of guns onboard ships is reviewed, complete with an overview of weapon manufacturing during the age of sail. Material sourcing played a substantial role in the final quality of the cast iron product, and thus a short exploration of the iron trade as it applies to iron guns is introduced. Additionally, treatises on gun design were thoroughly searched, and a complete picture of the historic knowledge of gun failures compiled. These ingredients are essential to understand when analyzing damaged or failed guns in the archaeological record.

Naval Warfare Before the Gun

To understand the influence of guns on naval warfare, an analysis of warfare just prior to the advent of the gun is necessary. In the Middle Ages, the primary method of conducting warfare on land was to replicate the great battles of the classic period, exemplified by building castles to survive massive sieges. The Siege of Tyre by Alexander the Great in 332 B.C.E., the bloody Siege of Carthage during the Third Punic War in 149 B.C.E., and Julius Caesar's decisive victory against Vercingetorix at the Siege of Alesia in 52 B.C.E. all provided inspiration to the medieval world for conducting effective campaigns (Hammond 1996:xl; Mueller 2012:290-304). Early European warfare at sea was a development upon this paradigm. Ships were designed with high structures on the quarterdeck and forecastle to replicate this method; ostensibly ships were viewed as large floating castles and siege engines, designed to battle with each other in close proximity (Tucker 1989:1). Early naval battle tactics often revolved around ships laying "siege" to other ships, or even to coastal fortifications (Martin 2001:58). The terminology, tactics, and strategy were direct developments upon the tested understanding of terrestrial warfare. King Edward III once stated, “Lay me against the Spainard who is coming, for I wish to joust with him” (Tucker 1989:1). Figure 1 depicts the chaotic Battle of Sluys in 1340 and demonstrates the close quarter combat style utilizing an infantry assault over the bulwarks of a ship, before the gun changed the tactics naval warfare (Niderost 2021:71).

Figure 1: The Battle of Sluys, 1340. Painting from Jean Froissart’s *Chronicles* (Niderost 2021:71).

Not only did the height advantage afforded by high castles aid in providing a location to attack over an enemy's bulwarks, it also provided a location to retreat to if the spar deck amidships were to be taken by the enemy. A defense in depth strategy was highly desirable in the chaos of such rapid and close quarter sea battles; it was not unheard-of for a ship's crew to retake the ship using its castles as a launching point for a counterattack.

Origins of Gun Manufacturing

This paradigm shifted with the adoption of shipboard ordnance. Although metallurgy was harnessed by humanity for thousands of years, only in the last several hundred years has this technology been utilized in the production of guns. Early projectile warfare on ships was conducted with the use of burning arrows and spears, as well as *triboli* –a three-pronged piece of iron– that when hurled onto the deck of a ship would spell devastation for the crew (Tucker 1989:2). The first projectile weapons utilizing gunpowder to generate pressure (as opposed to pressure generated by the human lungs in the form of blowguns and darts) were created by the Chinese in the 11th or 12th century (Andrade 2016:66). The spread of this technology was gradual, seeing use in southeast Asia, India, and the Middle East before reaching Europe. In 1313, in the city of Ghent, several municipal officers refer to the invention of "guns" –from the Middle English word "gunne" or "gonne"– and their manufacture in that town and their exportation to England, though earlier references to gunpowder can be found even earlier (Oxford English Dictionary 2026). Friar Robert Bacon wrote the recipe for a crude gunpowder in 1249, and Fredrick Robertson supposedly replicated in his book titled *Histoire d'Artillerie* (Robertson 1921:62). Because *Histoire d'Artillerie* isn't easily located in 2025, however, it is hard to corroborate. Much academic controversy surrounds the use of cannon in 1346 in the battle between King Edward III and the forces under Philip VI at the Battle of Crécy. It is believed that this is one of the earliest accounts of cannon being utilized for a siege (Robertson 1921:64).

Initial European guns were more akin to pots, vases, or barrels than to the modern image of a cannon. Two distinct types of early artillery were developed at this time, both utilizing technologies already commonplace on the battlefield. The first utilized a pot or a vase complete with a long narrow neck. Inside the neck, a crossbow bolt was placed, and the pot was filled with gunpowder. When ignited, the bolt was discharged from the pot at high velocity. The other primary method was designed to fire stones and consisted of a long barrel–like structure of relatively crude construction and filled with gunpowder (Robertson 1921:63). A stone was inserted into the muzzle and the contraption lit. These early guns were noticeably ineffective, and throughout the 1300s various versions of this technology were tested to little effect. A more repeatable and relatively safer version of the technology became commonplace in Europe around the year 1400, and terrestrial artillery was utilized on the battlefield primarily as a method to conduct a siege, though this rapidly changed (Andrade 2016:75–103).

Early guns were limited in usefulness by the manufacturing techniques used to construct them. The first European and Asian cannon were in some cases not made from metal, but instead constructed of timbers arranged with metal bands, in a similar fashion to the construction of wooden barrels. These weapons were inexpensive to construct but lacked durability and power. Wood does not have a high ultimate tensile strength, and thus it is not suitable for repeated high-pressure loading. Ultimate tensile strength (UTS) will be explained in depth in Chapter Three, which is an engineering term used to describe the maximum force a certain unit of material can withstand before the stress-strain relationship moves from elastic deformation region through the plastic deformation region and into the region of force that requires the material to fail (Groover

2012:50–55). In the case of wood, often the region where plastic deformation occurs is very small, and wood reaches its UTS quickly and fractures.

The wooden weapons were replaced by metal versions, which did not perform much better, although some new design developments were implemented. The difficulty inherent in heating enough iron to the temperature required to flow into a large cannon mold meant that many early guns were not cast (Tucket 1989:2; Cooper 2024:38). Instead, longitudinal strips of iron were arranged on a mandrel and welded together to form a tube, in a similar manner to the wooden guns (Mehl 2002:13). The voids in between each strip of metal were then filled with molten lead (Tucket 1989:2). For additional strength, hoops or bands of iron were strapped around the tube to provide additional radial stress mitigation, often added while red–hot, and when they cooled, they constricted around the barrel, providing additional strength (Cooper 2024:38).

Breechloading capability was another development which influenced the trajectory of early gun design. Instead of consisting of a single hollow tube with one end closed, a breechloading gun was comprised of two parts. The barrel was a tube with an opening on both ends, and a breech block was designed to fit up against the tube and be held in place by a large wedge (Mehl 2002:13). Gunpowder was loaded into the breech block, which ostensibly was a large chamber with a hole in one end which allowed the loading of the gun away from the barrel itself. These early metal guns often constituted long, narrow, and heavy weapons that possessed an alarmingly high rate of self-destruction. Metal guns could be made of iron or bronze, but neither was a perfect material, for a variety of reasons. No robust empirical process was commonplace to guide cannon manufacturing, and the physics and chemistry of metallurgy was not well understood. Unsurprisingly, such weapons were often more of a danger to their crews than to the enemy (Tucket 1989:2). Additionally, no design standardization had been devised. Each individual gun was different from most others, which led to many quality control issues to be addressed in time. The categories of individual types of guns are staggering in their variety. There existed twelve types of culverin, five types of demi–cannon, five types of saker, and many other categorizations such as demi–culverin, curtowes, moyens, sparrows, pellicans, aspics, shrimps, and lizards, just to name a few (Carpenter 1993:9).

Adoption of Naval Guns Onboard Warships

The first naval guns were adopted onboard warships sometime in the 14th century, although to what extent is poorly understood (Robertson 1921:3–4). Scholars have argued for decades over the consequences of the naval gun on the development of western civilization. Peter Padfield argues that God, the gun, and the sailing ship were the three pillars on which the foundation of western civilization were built (Padfield 1974:9). Padfield surely agreed with Carlo Cipolla, who earlier advanced the argument that the development of better sailing ships, stronger guns, and the merging of the two into a collaborative, drilled fighting force was the catalyst for European domination (Cipolla 1967:137–138; Padfield 1974:9). John Law argues for a similar paradigm: documents, devices, and drilled people resulted in Portuguese expansion in the Atlantic (Law 1984:234, 253–258). As Padfield argues, Cipolla's argument implies that it was the failure of the Muslims, Chinese, Japanese, Koreans, and others to develop an answer to the sailing ship which ensured western domination. Padfield, though, believes differently, arguing that the Chinese mastered the implementation of naval guns on ships well before the western powers, but the reason for losing dominance in sea power was the result of several other overlapping factors. The social, cultural, and political situation in Asia during the two hundred years during which Europe rapidly developed the naval gun was tumultuous, full of internal political strife and a refocus away from foreign policy to towards domestic policy (Padfield 1974:9, Hobson 2004:50–74). The many naval wars which took place in the English Channel, of which there were no equal counterparts in the East, allowed Europeans to solidify naval tactics regarding guns and ships, to produce a devastating fighting force (Lavery 1992:7–10). The effects the naval gun had on the propagation of sea power is inexorably connected to the rise of Europe as the world dominant cultural force, as discussed by Alfred T. Mahan and later Julian Corbett (Mahan 1890:11–28, Crobett 1911:10–12), and revisited in the modern era by scholars of sea power such as Andrew Lambert and Benjamin F. Armstrong (Lambert 2018:1–17). These later authors argued, as have others, for a more complete understanding of sea power, and include often soft skills as well as hard assets like offensive weapons in their analysis (Armstrong 2023:119–156). Regardless, all above agree that the combination of great sailing machines, standardized tactics and approaches, and drilled men ensured a European world.

The adoption of cannon for use on ships was understandably slow. The concept of bringing a large, heavy object that uses explosions and fire to operate and is prone to random catastrophic self–destruction onto a ship made from wood, canvas, tar, and other flammable materials was not incredibly attractive to most navies of the time. However, the promise of unfathomable destruction to an enemy's ship drove some forward-thinking navies to adopt the technology in limited quantities to gain an upper hand in combat (Tucket 1989:1–4). In addition, the construction style of vessels required significant development before guns could be utilized in any great numbers. The clinker vessels of northern Europe were built in the shell-first method, with frames inserted in critical locations after the planks defined the shape of the hull (Steffy 1994:100). This method was effective at creating ships well-suited for the environment, but such vessels were prone to hogging and sagging under too much unsupported weight. Cutting gun ports through any strake weakened every strake placed above it, because the clinker design philosophy dictated that the structural strength of the vessel was reliant on the unison of the strakes, not the frames. This meant that guns were less likely to incur damage to clinker-built ships if they were mounted on the spar-deck, without cutting structurally compromising gunports. Unfortunately, this moved the center of gravity of the ship well above a stable location. Additionally, because of the clinker design philosophy, the deck structure on these vessels were not designed to support significant point loading (Robertson 1921:3), and heavy guns created a very heavy point load wherever placed onboard (Tucket 1989:3–6). This introduced the additional factor of horizontal distribution, which affected the usage of warships from a tactical and operational standpoint (Cooper 2024:30–31). From henceforth, the weight of guns was a critical factor of warship design up to and through the dreadnought era (Brown 1997:201,208–213). Only with the development of carvel constructed ships did naval gunnery truly come into its own.

A carvel constructed ship was more conducive to the application of terrestrial cannons at sea and was an additional technology necessary to the full implementation of naval guns. Carvel construction, also known as "skeleton–first" or "frame–first", was based on a different design philosophy, that of a ship's frames being the primary load–bearing structure, not the exterior planking (Hocker 2004:5–6; Pomey et al. 2012:235–236). This change happened at different times, at different rates, and at different places throughout the first millennium, but in Europe it only became prevalent and widespread when more weight was required by the new generation of ships (Pomey et al. 2012:235). By the 7th century, frame–first construction was widespread, and the earlier forms of clinker–construction were well out of fashion (Batchvarov 2002:13–14). Regardless, carvel construction allowed for the load–bearing aspects of the hull to be much strengthened, and the exterior planking to be relegated to a supporting role in the strength of a ship. Thus, gun ports could be situated between upright frames, and not at all interfere with the rigidity and sea worthiness of the hull. The exterior planking which would have gun ports cut into it would not be load bearing and would not weaken the strength of the hull above it. With this development, more and heavier guns could be placed into ships, which opened the door for tactical and strategical evolution to blossom (Cooper 2024:32–33).

Even with the development of better suited vessels, it wasn't until the 16th century that the cannon construction process itself become well enough understood for an empirical approach to be implemented (Guilmartin 2003:305). The development of gun technology was bottlenecked by the dominant naval architecture of the time, and once carvel and gunport technology were mature, a rapid advancement of guns followed. The invention of the reliable blast furnace in the mid-16th century made casting guns a viable and quasi-repeatable method and harkened in the development of muzzle-loading guns to replace the older, and significantly more dangerous, breechloading guns (Tucker 1989:6–7). Breechloading technology wasn't revisited again in earnest until the 18th century. The blast furnace not only allowed for much hotter conditions for the thorough melting and processing of raw ore, it also allowed for a more repeatable application of carbon into the molten iron, producing a metal more conducive to the creation of guns.

Gun Casting Techniques

The process of early gun design and testing was not defined by a greater knowledge of the first principles of physics but instead established by the catastrophic explosion of any method that radically departed from the norm, often resulting in the sudden death of its architect. For example, King James II of Scotland was an early proponent of cannons being utilized on the battlefield and established a large personal collection of different guns (Mallet 1856:323). He was killed in action in 1460 when a cannon he was personally overseeing exploded, sending a red–hot shard through his leg thus “snapping” his thigh, leading to bloody and quick death that was mourned throughout Scotland (Lesley 1830:31).

This process defined early naval gun design, ensuring slow but steady innovation where the more efficient methods gradually became apparent and antiquated methods slipped into obscurity (Guilmartin 2003:305–306). Simply because no development of theory was driving development of technology does not indicate that technological development was not happening, nor that new technology could not emerge in other forms. The design of naval guns in the 1600s is a good example of the development of technology not supported by engineering theory but instead supported by traditional methodology. Even today with modern casting technology, it is very hard to successfully cast such a large piece of metal as a naval gun; it remains as much of an art form today as ever (Carpender 1993:88–93). Many considerations were weighed to make the casting of a gun easier, with possibly the most important being the choice of material.

The general approach to casting a large cannon did not evolve much from the late 15th century until the early 19th century, however the techniques and conceptual understanding were influenced by advancements in engineering theory. Cannons were typically cast upright in a large pit, often within a facility specifically designed for their casting (Smith 2017:56; Cooper 2024:40). Specialized foundries for cannon manufacturing were often constructed centered around a blast furnace. Due to the large quantities of molten iron required to cast such a large object, the molds were usually placed as close to the casting arch as possible to ensure very little heat was lost during the transfer of the liquid iron from the furnace to the mold. A casting arch is often the largest arch of a blast furnace and it is through this structure that workers gain access to the hearth area and from where the iron flows into the molds.

To construct a mold for the cannon entailed first constructing a model of the cannon to–scale. This was built utilizing a large tapered wooded post to serve as the primary volume of the gun, often mounted horizontally for construction of the model on a mandrel (Cooper 2024:40). A rope would then be wound around the wooded post, while liberal amounts of grease were lathered onto it. Upon this foundation, a replica of the gun was constructed using layers of animal dung and brick dust to slowly build up the shapes of the outside profile. Each layer was dried, often by lighting a fire underneath the mandrel and rotating the post about its axis on the mandrel to expose all quadrants of the post to the heat of the fire. To create the trunnions, wooden patterns were fashioned and attached to the model at the appropriate locations, secured by nails. Any ornamental decorations were created in wax and secured to the model where necessary (Smith 2017:56).

The mold was overlayed onto this model, after the finished model was heavily greased. The mold was usually about 10 centimeters (cm) thick and made of a similar material to the model –primarily of clay, dung, loam, and other binder materials (Cooper 2024:40). When the mold was completed, it was cinched together with iron hoops, not unlike the construction of a wooden barrel. To remove the model from the mold, first the trunnions were removed through holes cut in the mold, thus slid out of the mold along the axis of the trunnions. The resulting hollow hole were capped off with a plug of mold material, often with any trunnion identification marks embossed onto the interior face of the plug, which thus appeared on the end of the trunnions on the casted product. The heavily greased wooden post inside the model was accessed through the muzzle end of the mold and removed completely. This void was then packed with flammable material and burned, which consumed the rope and caused the model to shrink in on itself and collapse, and thus it could then be smashed up with hammers and removed from the mold (Smith 2017:56).

The hollow barrel would be assembled into the mold by inserting a large post or iron bar, sometimes wrapped with rope or wire, into the mold and held in place with a crown–iron (Smith 2017:56). The fully assembled mold was placed into the pit and oriented with the breech down, and the muzzle facing upwards (Guilmartin 1982:140). The molten iron was then poured directly into the mold, and the cannon was left to cool over the course of multiple days. Once cool, it was then removed from the pit and the mold broken up. The feeder head was detached from the cannon mold, and the barrel core was pulled out of the cannon. For early cannon, the process at this point was largely finished. For later cannon, at this point the barrel was reamed out using a large watermill driven lathe to ensure a smooth interior bore (Smith 2017:56). Towards the end of cast–iron gun manufacturing, and when steam powered boring equipment became more prevalent in machine shops around the world, often the barrel core was skipped entirely and instead the barrel bored out of the solid cannon. This was a very time intensive and power–hungry job which only became viable with advancements in technology around the late 19th century.

Other methods were also experimented with to help create a barrel that exhibited strength radially out from the centerline of the barrel. The Rodman process, commonly implemented after the United States (US) Civil War in American gun manufacturing, called for the barrel to cast hollow and not bored out, but to achieve radial robustness the bore was cooled first by passing water through the hollow bore (Cooke 1875:121). This also had the effect of reducing internal strain within the metal, allowing the cast to exist closer to equilibrium, thus reducing the tendency for newly cast barrels to burst under their own internal strain. These methods represent some of the last major developments in bulk cast iron gun manufacturing before the widespread adoption of steel barrels.

Gun Material Sourcing and Manufacturing Facilities

Many factors influence the choice of a material when designing a cannon, and a poor choice of material will result in many different types of failures. As discussed later in Chapter Three, the two primary metals as far as gun manufacturing is concerned are cast iron and cast bronze. Cast iron is an iron alloy containing about 2.1% to 4% carbon depending on the refinement technique, and somewhere between 1% and 3% silicon (Groover 2012:22). Bronze is a copper alloy, usually consisting of around 90% copper and 10% tin for the standard modern material (Groover 2012:26). In antiquity, these ratios were harder to control, and often both types of metal were alloyed in various ratios depending on a variety of factors, including the ore's location of origin. Though bronze and iron were used in every manner of gun, high quality guns were often made from bronze. Despite being an easier and more favorable material to work with, these were very expensive and prone to work-hardening which significantly reduced their safe lifespan. The alternative was iron, which has a much lower elasticity and is much more brittle, while also being heavier for a similar strength, and more prone to corrosion. In almost all regards, bronze is a superior material, but it is an alloy of two relatively uncommon materials which are often not found at the same location and expensive to acquire.

Perhaps of the few variables which could be controlled by early gun manufacturers, the most important was the location at which the raw metal ore was mined. Regional metal quality played a large role in the durability of the gun. In some regions, iron and bronze quality was noticeably poor, while metal mined from other locations was noted to produce much higher quality products. Nordic iron, from countries such as present Norway, Sweden, and Finland, were considered the best building material due to the quality of the iron ore mined from those areas (Boëthius 1958:149). Iron export has been a primary driver of the Swedish economy since the 15th century, with similar trade taking place throughout the Baltic (Ducoing and Olsson-Spjut 2021:1–12; Weihed 2022:412). The primary reason Baltic iron was so highly prized for its use in guns has much to do with the purity of the raw ore. The industry experienced a metamorphosis when English blast furnace technology was used in Sweden, and Swedish iron bar exports surged from 11,000 tons a year to well over 40,000 tons a year during the height of the industrial age (Boëthius 1958:150–153; Axelsson 2021). Indeed, the quality of Swedish iron for the use in cannon was so great that the export of Swedish ordinance single handedly supported military expansion in the new country of Holland for two centuries (Cipolla 1967:52–60). After Spain recognized Holland as an independent nation in 1609, the Dutch government designed their national defenses around the steady supply of high-quality Swedish cannon which did not indebt them to a central European superpower. With Holland's success at that endeavor, England began importing Baltic iron, primarily from Sweden, partially for use in arming it's battlefleet, with the first shipment arriving in 1632 (Cipolla 1967:64). The Swedes also mastered the use of carbon in their iron, balancing the ratios to ensure a stable and long–lasting iron. This technological advantage differentiated Nordic guns from those built in competing regions and demonstrated a hierarchy in manufacturing capability and quality assurance.

In addition to exporting iron, the Baltic region also exported large amounts of copper, for use in the alloying of bronze. Sweden exported so much copper that a copper standard was introduced to back Swedish currency (Edvinsson 2012:303–315). Though the material could be found in a variety of places, the purity of the ore from locations in the north significantly out preformed ore mined in central or southern Europe. Although copper was available in mines located in northern Britian and in select regions throughout Europe, the expense and time required to extract it allowed a competing Baltic copper economy to flourish. Some of these regions witnessed mining operations for many centuries –the Swedish copper mining industry began in earnest during the 13th century. The copper mines in the Swedish town of Falun, located only 100 miles north–west of the country's capital, was operational for many hundreds of years (Weihed 2022:409,412). During the Tudor dynasty, English copper mining operations increased dramatically in the regions of Cumberland and Cornwall, and eventually royal mines broke ground in Swansea to further ensure a strong supply of copper for Royal government use. This operation did not shutter its doors until well into the Victorian period. Although not as important to the greater European economy as compared to the Baltic iron trade, the copper trade from the Nordic countries provided another high-quality material source for the smelting of bronze and the creation of bronze guns even as other countries allocated significant resources into acquiring copper (Weihed 2022:412).

While many guns were cast in the Baltic and shipped south for use in other militaries, England required a source of guns to furnish the Royal Navy that did not rely on maintaining delicate treaties in the Baltic. However, it was well understood that iron mined in the British Isles was significantly inferior to that gathered in the Baltic and in parts of western Russia (Greener 1858:90). The first blast furnace, known as the Weald, was built in southern England in 1490 and remained operation for some 323 years. One hundred and nineteen blast furnaces are recorded to have been in operation in England during the height of English cannon manufacturing, and of those thirty-eight were specifically designed for use in the construction of guns. Thus, cannon foundries operated all throughout the British Isles, including in the Midlands, South Wales, Shropshire, and the Forest of Dean (Smith 2017:56).

The specific casting technique utilized to produce either a bronze or cast-iron gun also played an important role in determining the quality and lifespan of the weapon. One benefit of using bronze was the ability to easily remelt and recast it into a new weapon (Tucker 1989:10; Ciarlo et al., 2023:1–28). Casting bronze was complicated by the fact that it had a higher toughness and higher ductility, and lower bulk modulus. This meant that bronze guns could not withstand the shock and internal pressures as well as iron, and higher-strength alloys of bronze were often too brittle. This concept will be explained in Chapter Three. However, both were prone to bursting (Dawson and Dawson 2007:17).

Additionally, bronze is prone to the development of a casting defect known as microporosity, also discussed in detail in Chapter Three. In short, microporosity occurs when a network of small voids becomes trapped in the pour, resulting in a sponginess of the metal. This can occur due to the alloy nature of bronze, which suffers from different solidification rates for different component metals in the alloy (Groover 2012:134). In both historic iron and bronze gun manufacturing, microporosity occasionally occurred due to moisture or gas emanating from the organic wooden bore core (Hodson 2003:76). However, microporosity most often occurred due to non–uniform solidification. Tin has one of the lowest melting points of all metals, and thus it often solidifies long before copper. This results in a non–homogeneous casting profile. If this defect was present in large areas or critical areas, a cannon explosion could be catastrophic with no forewarning.

Hence, most features of cannon design were direct responses to difficulties experienced during the casting process. For example, when a bronze cannon is cast in an upright orientation (as was normal), the composition of the alloy was non-homogeneous throughout the process. Tin and copper tend to segregate themselves within the melt, and the tin could congregate at whichever location was last to solidify. This tended to be the breech area of the cannon, thus leaving the muzzle with a really low density of tin per unit copper. Cannons thus displayed highly ductile muzzles and highly brittle breeches, which were not conducive to safe firing or long service lives. The internal stress on the cannon caused by firing resulted in strain being the highest around the breech area, adding to the problem. To combat this, cannon manufacturers often designed a cannon to have a thicker breech area to combat brittleness, and flared muzzle end to combat warping due to ductility (Guilmartin 2003:310–312).

Iron guns had similar problems, but mostly because iron is simply more brittle than bronze. Additionally, although iron is not considered an alloy in the truest sense of the word, the iron utilized in the early creation of guns was indeed often contaminated with other elements (usually carbon) and could thus suffer from defects more commonly associated with more conventional alloys. Cast iron is more susceptible to stress fractures and microscopic surface imperfections that can multiply during repetitive cycles. These fatigue-related issues resulted in iron guns failing after long lifespans, and often for no apparent reason. To combat this, iron cannon were often cast far larger than necessary, with much thicker walls to mitigate such issues. For this reason, iron guns were considerably heavier and larger than bronze guns of the same shot weight. This significantly affected their implementation on the battlefield, as a ship could carry many more bronze guns than iron ones (Cooper 2024:38–40).

Both in cast iron and cast bronze cannon, the uniformity of the metal's crystalline structure is of utmost importance (Guilmartin 2003:307). Both varieties of cannon were cast with the muzzle facing up, which had the effect of compressing the molten metal at the breech of the weapon and allowing for more uniform cooling and a denser and stronger alloy. As machining capability increased in the 1750s, advances in boring machines made it possible to cast solid barrels and bore the entire core of the cannon out to produce the hollow bore. This machining process produced more accurate weapons and improved weapon quality because imperfections in the molten metal tend to concentrate at the center of mass, which tended to be along the axis of the cannon. Thus, many imperfections were removed during the boring process (Guilmartin 1999; Cooper 2024:40–42).

Iron cannon had less alloy-related issues but were instead challenging to cast because of the heat required to render liquid iron. Large blast furnaces were utilized, but the quality of the hot iron was highly suspect. Although not represented in the archaeological record in the same way bronze defects are (Guilmartin 2003:307–313), iron has a slew of common defects itself which can be present. A casting defect common to metal not poured at high enough temperature is the 'cold shot.' A cold shot is a defect that results from splattering or a low temperature pour, causing large areas of pre-frozen metal 'inclusions' to enter the casting and situate before the remaining melt solidifies, thus becoming entrapped in the casting (Groover 2012:133). This can cause many discontinuity problems in the crystalline structure or result in air pockets trapped within the casting. These can in turn cause internal fatigue or stress fractures to develop, resulting in seemingly random catastrophic failure to occur while firing. Like microscopic voids, these were impossible to detect at the time.

After these major improvements, cannon technology remained somewhat stagnant between 1600 and 1850. A well-made bronze cannon from 1600 was very similar in essence and ballistic performance when compared with a cannon from 1850. A gun from the 19th century were slightly shorter and a bit lighter, and a bit safer to use, but internal and external ballistic performance were largely the same (Guilmartin 1999; Guilmartin 2003:49). Between 1600 and 1850, cannons changed primarily in material composition and subtly in design. Naval guns switched primarily to being made from iron, due to the decreasing cost of using the material. Founding processes changed dramatically to produce more reliable and safe weapons, but the profile and design intent did not. It is important to note that this chapter offers only a brief overview of the different considerations influencing the design and manufacture of cannons over a very large period, from 1350 through 1850.

History of Gun Proofing

To mitigate gun explosions, many militaries implemented a system of proofing requirements to more strictly regulate what weapons entered service, as well as to document and track gun quality (Greener 1858:244). Before a military or a private buyer would accept an order of guns from a manufacturer, it had to be examined to ensure safety (Cooper 2024:49). In England, this process took place initially at the Tower of London, but later at various gun proofing facilities at Woolwich, many of which are still active today (Smith 2017:56). The gun, after all manufacturing processes were completed, was measured throughout its bore to determine whether it fell within manufacturing tolerances. This process was often completed with a pair of calipers. Additionally, a tool called a "searcher" was implemented to check the interior of the bore for surface imperfections. The searcher comprised of a long pole with a constellation of metal "L" shaped prongs sticking out the end, which was pulled through the bore. If the searcher encountered a pit or flaw, the prongs sprung outwards into the deviation, and the location was noted. After this was completed, the cannon was subjected to a test utilizing a proof load (Cooper 2024:49).

The proof load was a quantity of the propellant, usually gunpowder, which was significantly above the quantity of propellant the gun was designed to be subjected to –often a double load, or twice the amount of black powder (Cooper 2024:49). If the gun survived this over–pressure test, it would be stamped with a proof mark and released for use. If it did not survive, it would not be released for use. Other post–proofing processes included a “waterproof”, which recently proofed guns pumped with water after the touchholes and muzzles were tightly plugged. The water would work its way into any spongey area, and once the cannon was drained, if water continued to weep from the interior barrel after the rest of the gun had dried, the gun was considered too spongey and condemned (Verbruggen 2013:99–100). Early proofing processes for use on light weight guns consisted of firing them at a higher rate than usual instead of using a larger gunpowder charge. If the piece survived firing two or three hundred rounds in rapid succession without bursting, it was considered good enough for service (Muller 1768:111). Obviously, this placed gun crews at significantly higher risk, among other issues, and was dropped as a viable method. There is evidence that gun manufacturers released un–proofed weapons into service, but those did not have a proof mark and thus were considered less reliable (Greener 1858:244). A proof mark was applied to the barrel utilizing a die–stamp, but if the gun was modified or damaged throughout its career, this was sometimes revoked, and the gun was considered “out of proof.” In some instances, guns which were out of proof or rejected during the proofing process were stamped with a mark signifying them as condemned. For example, Dutch cannon marked with an XD, XS, or XW failed tests associated with dimensions, by the searcher, or by the water–proofing process, respectively (Verbruggen 2013:100).

The more standard process of proofing cannons remained unchanged for a vast span of history, however in 1858 the general process was well outlined in William Greener’s treatise on gun manufacturing. Before guns were proofed, often the manufacturer, who was sometimes accompanied by a military representative, visually inspected all the as of yet un–proofed guns and compared them to a standard gun (Cooke 1875:123). This process weeded out any obvious rejections (Verbruggen 2013:99). Many barrels were often proofed together, first taken into a separate building designed for the proofing process. The building was usually strongly built, made from brick or of an equally strong material. In later proofing buildings, sheet iron was used to line the walls throughout the building to ensure safety. Even the windows had sheet iron over them, utilizing a contraption reminiscent of a venetian blind (Greener 1858:254). This is visualized in Figure 2.

Figure 2: A typical mid–19th century proofing house during a test (Greener 1858:254).

The new, un–proofed barrels were then placed on large iron frames which run the length of the room. Against the opposite wall of the room, sand piled up in a large mound to provide a backstop to catch the cannon balls after they were fired from the guns. Behind the barrels, against the wall behind the guns, exists enough large berm of sand, this was used to catch the dislodged cannons if they are propelled backwards off the frame by the force of the proofing explosion. To secure the cannons to the frame, a large iron bar was placed behind them with holes cut out large enough to fit the cascabel or rear portion of the cannon without room for the entire cannon to fit through. The barrels were oriented belly–up, to allow the touch holes to face down. Underneath the proofing rack, each cannon had a groove which terminated underneath the touchhole, both of which were filled with gunpowder, ostensibly creating a fuse to be lit from a safe distance (Greener 1858:255). In larger proofing houses common in the 19th century, guns were ignited simultaneously, however it is unlikely that early proofing houses were this efficient. The room was first locked down, with every window blind closed and the door bolted shut, and a red–hot iron was passed through a hole to light off the trail of gunpowder. A tremendous explosion took place, and once the room aired out, the guns were inspected for failures (Greener 1858:254-256).

It was not uncommon to find many different types of failures during proofing. In one test, it was typical to have some cannons found to be in perfect condition, while others were destroyed. Some barrels were found twisted out of shape, but a more common failure was a bulge or swelled region on the cannon, where softer iron deformed permanently. At this point, the barrels received their proof marks. In later tests, an additional proof mark would be added for barrels which had been significantly bored out, documenting which size bore was finally utilized to achieve a nominal interior surface finish. Cannons that failed the proof but only bulged or swelled were often be sent back to the manufacturer, who hammered the swellings back into tolerance and resubmitted the barrel. Often at that point, the barrel passed the proofing test. In 1857 alone, over 416,000 barrels were "proofed" in this manner (Greener 1858:254-256).

Some non–compliance regulations existed to control the sale of un–proofed or out of proof guns, but the practice was considered common enough. In 1815, Parliament enacted regulation to make the sale of guns without proof in any circumstance illegal, and liable to a penalty of twenty pounds for each un–proofed barrel sold to any buyer. Further regulation was enacted through the passing of the Gun Barrel Proof Act of 1855, which delegated further powers to the Birmingham and London proofing companies. However, before 1815, much of the gun trade was unregulated, and un–proofed guns likely made it into circulation (Greener 1858:244–245).

History of Gun Failures

Gun failures and explosions have been a constant threat to militaries from the present day back into antiquity. This subsection recounts many of the most famous gun and cannon explosions, from the 15th century through the late 20th century. As mentioned previously, the earliest recorded instance of a cannon explosion (certainly others happened earlier but were never recorded) occurred when the King of Scotland, James II, was killed by a bursting cannon (Lesley 1830:31). Another instance happened four years later during the Siege of Bamburgh Castle, when several large cannons were utilized, and one catastrophically burst, likely killing its crew (Greener 1910:28). The first example of naval gun failure (which blew the bow off an ottoman galley) is recorded by sources in 1517 (Guilmartin 2003:27, 30). Failed guns were found aboard *Mars* (1563), which sank in the mid-1500s (Eriksson and Rönnby 2017:103). In the archaeological evidence of the Spanish Armada ship *El Gran Grifon,* failed or damaged guns were found in situ, dating to 1588 (Martin 1972:63; Muckelroy 1978:104).

Examples of naval gun failures become more common in primary sources dating to the seventeenth and eighteenth centuries. In 1647, the Dutch ship *Groeningen* sank off the coast of Elmina, Ghana, after a gun exploded while saluting Elmina castle (Cook et. al 2016:375). During the 1702 Siege of the Castillo de San Marcos, during the War of Spanish Succession, more instances of gun explosions are recorded. An iron 16–pounder exploded, killing four men and seriously wounding another six (Manucy 1949:48). Two 18–pounders exploded on USS *Bonhomme Richard* during its engagement with HMS *Serapis* in 1779, killing several sailors and maiming others (McGrath 2014:295; Naval History and Heritage Command 2025). Amasa Delano mentions in his journal that a gun exploded onboard the EIC ship *Panther* due to overheating in 1791. During an attack on the ship by New Guinean natives, a forecastle gun exploded at the breech, spraying molten shrapnel into a pig pen on deck and snapping the legs of multiple pigs (Delano 1817:94–95).

Throughout the 19th century, in a multitude of different primary and secondary sources, gun explosions appear often. During the 1813 Pacific cruise of HMS *Racoon*, a gunnery accident killed two men (and maybe an additional six), and wounded at least 21, a large portion of the sloop's complement (Rees 2012:8). During the Second Barbary War in 1815, exploding guns killed more US sailors than enemy action against the Algiers pirates. Commodore Stephen Decatur lamented the constant failure of his guns onboard USS *Guerriere*, and worried that the almost endemic rate at which exploding guns in the US Navy "would be injurious to the service beyond the loss of the men occasioned thereby" (Leiner 2006:99). William Lewis, commander of *Guerriere*, wrote later "So much for our contract artillery! The effect produced…is beyond the loss of a few lives. It will by & by destroy the confidence which men should have in the sufficiency of the weapons with which they fight, and the bravest man will go into action trembling with the apprehension that the first discharge of his gun will blow him to pieces" (Leiner 2006:99–100). In 1817 in the port of Callao, a sailor of *Le Bordelais* had his hands mangled in an incident involving a misfiring cannon (Roquefeuil 1823:20).

According to the 19th century artillery engineer William Greener, during the period between 1840 and 1860, which spanned the First and Second Anglo–Sikh Wars, the New Zealand Wars, and the Crimean War, it was noted that the British Army and Royal Navy lost almost as many gun crews to bursting mortars and exploding naval guns as they did to enemy action (Greener 1858:84–85). And though William Greener was in a position to exaggerate such claims to push for the adoption of his own gun manufacturing processes, this does not lessen the severity of the issue which plagued the British Military. In some instances, guns burst after having fired only fifteen, ten, or even five rounds, "killing the gunners in great numbers" (Greener 1858:85).

US Secretary of State Abel Upshur and Secretary of the Navy Thomas Walker Gilmer shared a similar fate when the massive twelve–inch muzzleloader named "Peacemaker" exploded onboard USS *Princeton* in 1844 during a celebratory salute. Not only were the Secretary of State and the Secretary of the Navy instantly killed, but also Captain Beverly Kennon, Chief of the Bureau of Construction, Equipment and Repairs, as well as David Gardiner, Virgil Maxcy, and President John Tyler's enslaved valet named Armistead (United States Congress House Committee on Naval Affairs 1844; Pearson 1966:163–183). President Tyler himself was spared from the accident by luck alone –he had retreated below decks for a break in the festivities. The Peacemaker gun explosion resulted in the death of more top–ranking US government officials than any other tragedy in American history. The event shocked the American public and brought the danger of large caliber naval gun explosions into public recognition. An illustration of this event can be seen in Figure 3.

Figure 3: The USS *Princeton* gun explosion. Lithograph published by N. Currier (Miles 1926:2225).

During the Siege of Fort Sumter in 1863, heavy caliber Parrott guns were trained on the fort and neighboring Charleston, SC, lobbing shells in some instances over 4,290 yards. However, the endurance of those guns was always in question. One particular weapon, known as the “Swamp Angel” burst at the breech after firing only 36 rounds (Manucy 1949:54). A similar weapon, also utilized during the siege, is depicted burst in Figure 4. In 1895, Coxswain John N. Johnson, the captain of the number three gun onboard USS *Olympia*, took his place besides the 5–inch breechloader under his command. Upon firing, the gun failed and dislodged itself from its carriage, flying across the deck and crushing the young man’s skull, killing him instantly (*San Francisco Call* 1895:1). Perhaps the most recent example of a gun explosion occurred on 19 April 1989, when the center gun in the number two turret of USS *Iowa* (BB–61) exploded, killing forty-seven of the ship’s crew and sparking a national outrage (Conahan 1990:1). Indeed, this modern instance is only the most recent event in a long history of naval gun explosions which plagued militaries for as long as naval guns have been utilized in combat. In so many instances throughout history, cannon were more likely to kill their crews than damage the enemy.

Figure 4: A 300–pounder Parrott Rifle, located on Morris Island, near Charleston, South Carolina. The Photo was taken in 1863 by Haas and Peale (Cooper 2024:45).

Even the quality of the gunpowder utilized significantly affected the likelihood of a gun explosion (Muller 1768:xxvi). Not only was larger grain gunpowder known at the time to be a more effectual propellant, it was also deemed less likely to cause a gun burst event (Greener 1858:35). This is primarily due to the speed at which different size gunpowder grains combust when exposed to an ignition source. A fine–grain gunpowder will ignite completely while the cannon ball has not yet left the barrel, or perhaps not even travelled more than a third the way down the barrel. Thus, all the force of that weight of gunpowder is exerted on the area between the breech and ball (Holley 1865:301). A slower–burning gunpowder, even at the exact same weight and capable of generating a similar amount of pressure, reached its peak pressure at a point when the cannon ball has traveled completely down the barrel or left the barrel entirely, thus distributing its pressure load over a much larger area while generating the same explosive force. Additionally, Newton's first law of motion also holds sway over the interaction between the cannon ball and the various types of gunpowder explosions. A fine powder does not have time to move the cannonball from a state of rest before it reaches its peak pressure, whereas a slower burning powder can "lift" the charge during the low–pressure stage of the explosion and start the ball on its journey down the barrel, thus placing the object in motion, before reaching its maximum pressure (Greener 1858:35). If time is not allowed for the cannonball to react to the expansive force of the explosion, the force will be exerted primarily on the barrel of the cannon and not the cannonball. A further complication to this is found when comparing the size of gunpowder to the size of the cannonball. A tight–fitting cannon ball rapidly accelerates with fine powder and not allow any pressure to escape around the cannonball and relieve the pressure on the inside of the cannon, thus causing the cannon to burst. William Greener supposed that the quality of the gunpowder used to proof the gun may allow a poorly–made gun to pass proof when using very large–grain powder, but when that same gun was subjected to fine powder it may immediately explode, seemingly for no apparent reason (Greener 1858:51).

Gun metal also plays a significant role in the likelihood of a gun bursting. By the mid–19th century, it was common knowledge that brass and bronze guns were significantly less likely to burst when compared to iron guns yet they had much lower service lives. At both the Siege of Badajos and Siege of San Sebastian, iron guns continually fired at a rate of 12 rounds a minute and 22.5 rounds a minute respectively, for 104 hours and 15.5 hours respectively (Greener 1858:60-63). This was possible with a bronze or brass gun, which required a fire rate of one third that displayed on the aforementioned sieges to remain fully operation for the indicated time periods.

It has been known for some time that what is understood today as metal fatigue played a large role in seemingly random catastrophic gun explosions. An early example of a confirmed fatigue failure is readily apparent when analyzing French gun explosions during the Siege of Antwerp in 1832. The French at the time constructed several enormous mortars for use in lobbing shells into Antwerp from well behind the front lines (Mallet 1856:342; Holley 1865:125). One particularly large mortar fired 10 or 12 shots with a full charge of gunpowder but exploded when firing a shell with a much lower quantity of gunpowder. At the time, it was determined that vibrations in the iron caused a breakdown in the cohesiveness of the metal, which resulted over time in a slow weakening of the structure (Greener 1858:66). Instances like that indicate that historic gun manufacturers were aware that the strength of guns eroded over time and exploded randomly even at much lower powder loads. It should be noted that vibration failure is indeed a phenomenon which theoretically could destroy a gun, such a failure was likely due to interrupting the resting frequency of the metal. Assuredly, in this case, the failure of the French mortar more resembles that of a classic fatigue failure. In some instances, as during the aforementioned Siege of Castillo de San Marcos in 1702, colonial isolation played a significant role. In far–flung regions of the world, ordnance was sometimes pressed into service even if it had served longer than the normal 1,200 round lifespan recommended for an iron gun (Manucy 1949:48).

Another way guns failed during use can be traced to the methods used to secure them, and the angle at which they are elevated to fire. During the Siege of San Sebastian, in 1813, cast iron guns fired shot at a range of 1,500 yards, with some guns firing as many as 3,000 rounds before being retired from the field (Greener 1858:88). However, during the Crimean War, guns built to the same design specifications exploded after only one fourth the number of rounds were fired through them. The difference between these scenarios can be traced to the angle at which the guns were elevated to place shots on targets at great distances. Of the known guns that exploded during the Siege of Sebastopol, all exploded after firing when aimed at high elevation to hit distant targets (Holley 1865:121). During the Siege of San Sebastian, the guns were onboard warships or mounted to carriages on the plains surrounding the city fired at an elevation of zero to six degrees, thus directing almost all force backwards, allowing the gun carriages and/or the rope tackle to dampen much of the rearward force exerted on the trunnions. However, when a gun was elevated even slightly, to an elevation of as little as 30 degrees, a substantial enough portion of the force was exerted downwards onto the relatively immobile deck of the ship or the floor of the battery and thus receives no dampening (Greener 1858:88). A gun elevated at six degrees could possibly fire 200 rounds before failure, while a gun elevated at thirty may only survive 50 rounds. This evidence is corroborated in other historical reports, where the high elevation of guns used during the Siege of Charleston placed undue stress on the cannon's structure (Holley 1865:56). The failure occurs at the trunnion area, which is the primary location which attaches the gun to the carriage. The trunnions are subjected to intense, undampened shearing forces when fired at a high elevation, and thus likely guns which display sheared–off trunnions are evidence of firing at extreme angles for range. During the Bombardment of Suomenlinna fortress in Finland during the Crimean War, the British thirteen-inch mortars fired an average of 120 rounds before failing at the trunnions, "the fracture in all was peculiarly alike; being at right angles to the supports [trunnions]" (Greener 1858:89; Holley 1865:582). The non–symmetrical nature of the trunnions, thus being located further below the centerline of the gun as opposed to in line with the centerline, added to this problem. Even though five minutes were given for these guns to cool between each firing to reduce fatigue, they still continually failed due to shearing trunnions, or splitting down the middle as if some large knife had cut them in half (Greener 1858:144; Holley 1865:125). Between both the Siege of Sebastopol and the Bombardment of Suomenlinna, at minimum 12 guns exploded, and the only data available as to the causes of these explosions indicate that they were highly elevated (Holley 1865:124). However, British commander Scott claimed "nearly the whole of mortars employed either burst, or were rendered unserviceable; the best, that of the *Growler,* cast in 1813, standing only 355 rounds only" at the Bombardment of Suomelinna (Holley 1865:125).

Excessive heating of the gun due to firing was known to cause a perceived weakness in the weapon, however some propose that this is due to excessively heated powder and not an inherent weakness in the metal at high heat. As discussed in Chapter Three, heat does play a part in the strength of materials, but some engineers argued that the heat of iron between zero and 600 degrees is less of a concern when compared to heated gunpowder, which will burn more quickly and thus reach peak pressure before the projectile has travelled the appropriate distance down the barrel, resulting in the pressure load being distributed over a much smaller area (Holley 1865:285). Although the heat generated by repetitive firing was known to weaken guns, often other points failed before a gun burst due to heat–related dilapidation (Muller 1768:xxii). Perhaps reports of metal failing around the cannon's vent is related to heat–induced failure (Holley 1865:64,117).

The symmetry of the gun also plays a significant part in its durability. Guns tend to fail where the thickness of the barrel wall decreases, and as such, some guns are designed with inherent weak points. For example, the British ten–inch, 86–pounders had a significant design flaw which was corroborated by the fact that such weapons saw more failures during the Siege of Sebastopol than any other British long–barrel artillery piece, with the exception of several mortar designs (Greener 1858:117–118). This design can be seen in Figure 5. This is because the British ten–inch, 86–pounder was non–symmetrical –the cannon had a uniform bore diameter, but as it approached the breech the bore tapered, and was not mirrored by the outside diameter. Such weapons would likely fail where the tapered section met the non–tapered section of the bore. It was also known that the quality or type of metal affected the amount of taper any gun could withstand. A gun made from bronze or soft iron required almost no taper, whereas a gun made from cast iron could have significant taper (Cooke 1875:61).

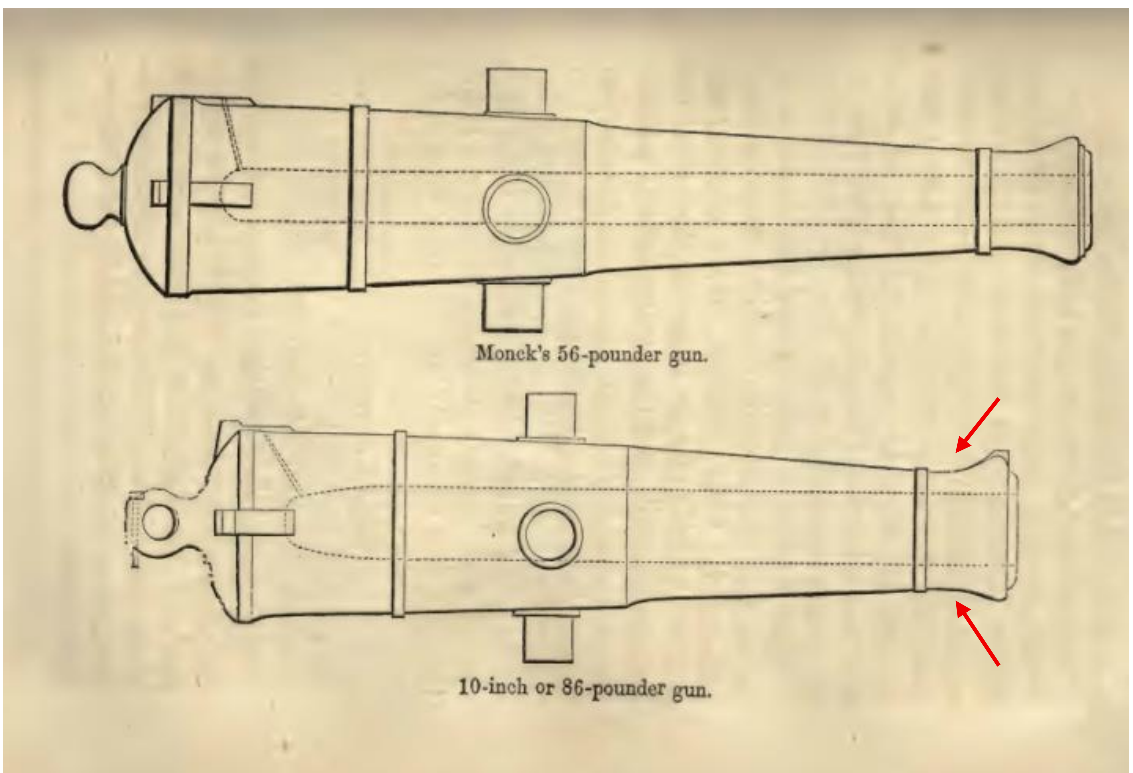

Figure 5: British ten–inch, 86–pounder (Right) vs a Monck 56–pounder (Left). Note the tapered muzzle with thin bore wall, indicated by the red arrows (Greener 1858:117).

Other factors are known historically to heighten the likelihood of a cannon exploding. The cannon ball will accelerate down the barrel reaching velocities of more than 1,300 feet per second, and the air is compressed in front of the cannon ball, causing the rapidly expanding pressure in front to place extreme stress on the tip of the muzzle, as this is the location at which the pressure to wall–thickness ration becomes the smallest, before the cannonball leaves the muzzle and the system returns to a state of equilibrium (Greener 1858:277). Greener (1858) indicates that this is the cause of cannons which burst at their muzzles. Another possible multiplying factor is the length of the projectile. A ball is the lightest object, for its maximum height is the same as its length. However, with longer projectiles, such as bar shot, double shot, chain shot, or any cylindrical, oval, bullet–, or pill–shaped object, the stress is increased significantly, as the inertia to overcome such a heavy object coupled with the additional friction places significant stress on the weapon (Greener 1858:280). This effect was well understood and of concern during the testing of early rifling in large caliber weapons.

Human error is also known to cause the burst of a gun; this is especially prevalent onboard ships. Sometimes during the misfire of a naval gun, due to wet powder or powder which does not burn fully due to the short barrel length common to naval guns, sailors assumed the powder was fully burnt and rammed another load of powder into the gun and tried to refire it. In some instances, this process was repeated as many as three times, when finally, all the powder lit properly, and caused the gun to burst (Muller 1768:xv). This often killed entire gun crews and sometimes also adjacent crews. Crew training was important to mitigate such events, as the wellbeing of the entire vessel depended on proper operation of the guns. John Muller summarized this neatly: "[if neither guns nor crews can] bear a brisk firing, the bursting of a piece in action might create such a confusion as to cause the loss of the ship" (Muller 1768:57).

Conclusion

Any single topic touched on above could be explored in more depth as it applies to the history of naval warfare, the implementation of guns on warships, cannon design and manufacturing, cannon proofing, and cannon failures. Included above is simply an abbreviated overview of an expansive field of knowledge which does not need to be restated at length here. The historiographic corpus of naval operations and tactics, sea power strategy, and naval warfare is robust, and contains much information on the utilization of cannon throughout this time. However, modern literature created to review historic cannon engineering is sparse, and thus historic sources on cannon engineering were consulted at length and pieced together. Thus, this chapter on the history of cannon utilization, and specifically manufacturing and engineering, fits in a niche that is underappreciated in the greater study of the history of firearms. With additional research, more information might be gleaned to fill out this less–well understood aspect of military history. In the next chapter, the engineering theory and archaeological approaches alluded to in this chapter are explored and explained. This in turn prepares the reader to fully appreciate a modern approach to test historic cannon engineering. Utilizing the historic sources expounded upon in this chapter, Chapter Four explains how this historic information can inform modern engineering analysis.

Chapter 3: The Theoretical Foundations of Gun Failure

Introduction

The primary objective of this research is archaeological in concept, but to answer complex archaeological questions associated with gun explosions, a complete understanding of more than archaeological theory is required. Archaeological theory in its own right is of central importance to the interpretation of the archaeological evidence in so far as what factors impacted the state of the evidence post–deposition, as well as contextualizing the pre–deposition environment. As Keith Muckelroy pointed out, archaeological theory of transformation processes and site formation comes into play during and after the process of deposition, the time before the deposition event is of little interest (Muckelroy 1978:157–159). However, other theoretical frameworks, such as engineering theory, must also be implemented to fully understand the dynamics of gun failures.

It is for this reason that a complete understanding of engineering theory in what ways it applies to the archaeological interpretation of exploded guns is vital. This is to say, a two-hundred-year-old exploded gun has had a multitude of physical forces acting upon it from the moment it was conceived in the mind of its creator up until the present moment. Some of these factors can be well understood through the lens of archaeological theory, however, discernment must be maintained: damage that may appear due to archaeological processes may instead be due to pre–archaeological processes in the historical record, more readily defined through engineering theory. However, as described by Michael Schiffer, archaeological site formation considers pre–deposition status (Schiffer 1983:675-706, 1987:1-10, 1995:171-176), and thus in the instance of this thesis, the engineering theory operates within the purview of archaeological site formation theory. Schiffer's understanding of site formation theory implies that other theoretical frameworks can be utilized under the umbrella of archaeological theory to further understand the archaeological record –therefore, engineering theory is utilized within the framework of archaeological theory to support the tenets of site formation theory. For example, identifying a gun which was damaged due to a gun explosion and a gun damaged by a dredging operation while deposited on a shipwreck are handled by engineering theory oriented within an archaeological site formation theory framework. With this in mind, the following work leans heavily on engineering theory, but as a form of archaeological site formation theory.

To accurately deduce the service history of a damaged gun, researchers must first determine if the damage is due to archaeological processes or engineering processes. This chapter serves two purposes to this extent: firstly, to explain applicable archaeological theory and relate the theory as it applies to damaged cannons; and secondly, to familiarize the reader with the applicable engineering theory and demonstrate in what circumstances engineering theory is in play. However, although the evidence under examination in this thesis is archaeological, the purpose of this study is to use archaeology to answer historical questions concerning patterns in gun explosions. This supposes that most research here is focused on damage found on exploded guns that resulted from engineering shortcomings and inform on historical realities in such broad categories as 18th century manufacturing techniques, historic quality control standards, military culture surrounding gun upkeep and repair habits, and not focused on necessarily examining how guns are affected by archaeological processes. In this way, the engineering theory, which is used to directly answer these questions, is of the utmost importance. The archaeological theory is consulted only to confirm that the damage on the gun is indeed due to engineering shortcomings and not archaeological in nature. As is demonstrated in Chapters Five and Six, some exploded guns show damage from both archaeological and engineering processes, and such situations must be explained.

Archaeological theory, because it serves as the umbrella theory under which engineering theory operates, is discussed first. Focus is directed to transformation processes, site formation processes, and behavioral archaeology generally, as these are the primary lenses through which the archaeological evidence is analyzed. The archaeological theory section is followed up with a second section covering engineering theory in depth as it applies to many different aspects of cannon engineering, including material science, work hardening, material fatigue, and surface finish, among others. This section will necessarily be explanation heavy. The goal is to succinctly explain, in simplified and straightforward terms, why engineering theory is useful to the archaeologist interested in damaged guns, and in what ways it affects the artifacts found in the archaeological record. Later, in Chapter Four, the engineering theory is revisited to explain how the archaeological artifacts were tested for engineering theory-related defects, to help explain the patterns in the archaeological record. Through the combination of multiple approaches an answer to the question at hand may be generated.

Archaeological Theory

Several key archaeological theory regimes were utilized to interpret damaged cannons within the archaeological record. A multifaceted approach will require the overlapping of fundamental archaeological theory with recent developments in archaeological site formation. Such an approach is recommended to fully appreciate the complex pressures at play which have influenced the development of cannons from historical objects to archaeological artifacts (Trigger 1989:359–361). The primary lens utilized will be processual in nature, incorporating developments upon what Lewis Binford coined “Middle Range Theory” to link past human agency with the remains on the sea floor while simultaneously limiting assumptions and guaranteeing the utmost explicitness (Binford 1962:218-220; Renfrew and Bahn 2012:40-41,176). The thesis's archaeological objectives are not simply to describe the damaged cannons but to understand what human factors motivated and drove the actions which resulted in the deposition of artifacts and the formation of sites, in a way to differentiate between solely archaeological processes and engineering processes which affected the archaeological record. To complete such a task, archaeological site formation theory must be well understood.

Site Formation and Transformation Processes

The theoretical framework of archaeological site formation processes as proposed by Michael Schiffer, Keith Muckelroy, and others (Muckelroy 1978:157-160; Schiffer 1983:675-706, 1987:1-10, 1995:171-176, 2002, 2010:31-53; Schiffer and Skibo 1987; Keith 2016:2-3) are used in this study to understand archeological examples. Like the ships to which they are so fundamentally linked, cannon also undergo site formation processes after deposition in their archaeological context which may introduce complications to an analysis that would not be present on a newly cast or even newly retired naval gun. Considering that examples of failed naval guns exist (and perhaps are more commonly found) in the underwater context, site formation theory is applied. Additionally, the physical aspects of the archaeological material whether influenced by cultural or non–cultural (environmental) transformation processes is considered (Schiffer 1987:7). By examining the guns through the archaeological theoretical framework subtle variables may be identified and considered. The utilization of site formation theory within the context of behavioral archaeology has been applied many times before to contextualize the archaeological record, this project follows such precedent (see for example Fox 2015; O'Brien 2022; Pawelski 2023; Phipps 2024**).**

Underwater archaeological site formation theory was pioneered by Keith Muckelroy, who developed a system to frame the wrecking process and evolution of a shipwreck over time. According to Muckelroy, a submerged site or artifact experiences a life cycle of use before the wrecking or deposition event, which leaves telltale signs on the archaeological evidence. During deposition, the object is subjected to more change, and some material is lost to the environment (Muckelroy 1978:158–159). Factors such as salvage, disintegration, and seabed movement impact the site. When the area is excavated by archaeologists, even more of the site is disturbed and destroyed. The influential work provided by Muckelroy on wreck site formation laid the groundwork for its application to watercraft and other submerged archaeological artifacts.

Michael Schiffer's work complements Muckelroy's research with a focus on what Schiffer labeled transformation processes, divided further into cultural and noncultural processes (Schiffer 1983:675-706, 1987:1-10, 1995:171-176, 2010:31-53; Schiffer and Skibo 1987). Cultural transforms, or c–transforms, are processes enacted on the site or object to transform the object from the systemic context into the archaeological context via cultural drivers. Examples of c–transforms include any human–driven causation of deposition, such as purposeful burial, disposal, or abandonment. Noncultural transforms, or n–transforms, operate in a similar manner but produce the result through noncultural drivers, such as environmental forces, deposition due to flora or fauna, or other phenomena such as natural disasters. Both transforms can continue to affect the archaeological site, influencing the quality of preservation, damage to the site, as well as the formation of the site. Deposition of cannon into the archaeological record can happen due to both types of transformation processes and identifying how transformation processes can damage guns is of the outmost importance to this study. Some guns were deposited by c–transforms, such as by being purposefully abandoned, thrown overboard, or sunk onboard a ship in battle. Other guns were lost due to n–transforms, such as during a severe storm. Transformation processes continue to affect naval guns once in the archaeological record. Some of the case study guns covered in Chapter Five and Six have been damaged by dredging operations or other similar c–transforms, while other guns have been significantly impacted by n–transforms such as natural site disturbance, shifting bathometry, water salinity, and a myriad of other influences. Locating and accounting for transformation processes will be a central part of determining each gun's history.

Engineering Theory

When compared to archaeological theory, the engineering theoretical framework is complementary while simultaneously different. Based on the understanding and utilization of engineering first principles and the underpinning laws for Newtonian mechanics, engineering theory must be broken down into a digestible and approachable synopsis. Once the archaeological record is understood, and site formation theory and transformation processes accounted for, an engineering analysis will need to be conducted to understand what c–transforms caused damage. This would include any which occurred to the gun before it was deposited into the archaeological record. Any utilization of engineering software to replicate the archaeological material will need to be conducted after accounting for any archaeological damage (i.e., damage which occurred after deposition into the archaeological record) to produce a quantitative analysis of failure modes. These theoretical considerations are denoted and explained at length in the following sections.

The subsequent subsections will provide a very brief overview of several aspects of engineering theory and how they relate to gun manufacturing and failure. The Material Composition subsection introduces the reader to the two primary materials used in early gun manufacturing: iron and bronze. It will also focus on orienting the reader to several fundamental engineering theoretical laws. The Work Hardening subsection will relate the concept of repetitive straining to create a boundary of hardened material which is tougher but more susceptible to brittle cracking, a phenomenon routinely observed within the barrels of bronze weapons. The Fatigue subsection will explain how cyclic loading scenarios can lead to microcracks developing within the structure of a cannon, which can lead to devastating and random gun explosions. The Surface Finish subsection will outline the drastic effects a bad surface finish can have on the durability of a gun, resulting in sometimes as much as a 50% decrease in overall strength. The Casting Techniques and Defects subsection will allow an appreciation for the many different possible faults which may occur during the manufacturing process of guns and explain in engineering terms the theory and stumbling blocks of casting processes as it applies to gun founding. The Cannon Design subsection acts as a catch all section for several miscellaneous aspects of cannon engineering which play a role in the longevity and likelihood of failure, primarily from a design perspective.

Material Composition

Material composition is the primary factor in determining whether a cannon fulfills its design intent –that is, whether the cannon fails on its first shot, or its thousandth shot. The importance of material composition cannot be understated in its relation to cannon manufacturing and utilization. So deeply is material science connected to cannon founding, that entire navies were designed around the material of the guns to be utilized (Rodger 1996:302–303). The primary tangible (and arguably oversimplified) means in which material composition affected the construction and utilization of guns is in weight and reliability. It may seem straight forward that different materials have different densities and mass, but the relationship between material composition and cannon design is deeper than this surface level observation, a fact which will be methodically unpacked in this subsection.

The two primary choices of metals, in so far as gun manufacturing in the years before steel technology became mature in the mid–19th century, are cast iron and cast bronze. Cast iron is not pure iron, instead it is technically an iron alloy containing about 2.1% to 4% carbon depending on the refinement technique, and somewhere between 1% and 3% silicon. The carbon is introduced into the elemental iron during the smelting process, as soot and other carbon combustion byproducts are incorporated into the molten mixture. Additionally, other trace elements are often present, but those are of negligible quantities in most cases and do not measurably affect the material science of cast iron at the resolution in which the topic is analyzed here. Bronze is a copper alloy, usually consisting of around 90% copper and 10% tin for the standard modern material (Groover 2012:22,26). In antiquity, the ratios were harder to control, and often both types of metal were alloyed in various ratios depending on a variety of factors. The quality of bronze often depends on the quality of its composite materials, most importantly copper. High quality copper free of inclusions and other contamination was sometimes hard to source, which in some cases limited the use of bronze. Whether bronze or cast iron, for all subsequent engineering modeling and analysis of gun failures in future chapters, the American Society for Mechanical Engineers (ASME) standards for each material will be used, as it is sufficiently close to the historic material composition to lend useful results (American Society for Mechanical Engineers 2025).

The topic of material science is so intrinsic to cannon design, that in some form it influences almost every type of gun failure. Modern engineering theory outlines several primary variables which affect the selection of a material: the material’s strength in relation to any given temperature, the material's thermal conductivity, the material's yield strength, and the material's bulk modulus of elasticity are very important properties that influence a material's suitability for use in guns. Also important are the toughness of the material and the material's ductility under different conditions. A short synopsis of these properties, clearly explained, will shed light on failure patterns common in naval artillery. Some of these variables were understood in antiquity, and others were deduced mathematically or otherwise very recently, when the ability to test and quantify data became more precise.

An important aspect of material choice as it affects the design of guns is the relationship between strength and temperature for different materials. A general trend repeated in most metals is that the strength of the metal is influenced by the heat the metal is subjected to (The Engineering Toolbox 2008a). As the metal heats up, the strength (and thus resistance to failure) decreases, as depicted in Figure 6.

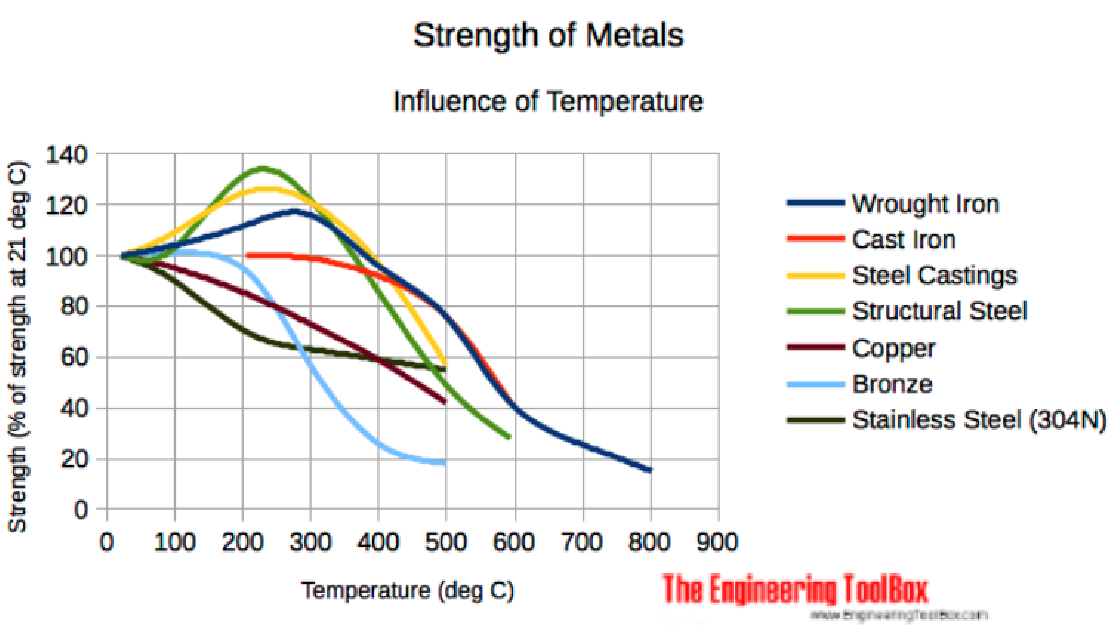

Figure 6: Strength of Metals and the Influence of Temperature (The Engineering Toolbox 2008a).

This profoundly affects cannon design, because continued firing of a gun exposes the material to an increase of energy in the form of heat. As discussed previously in Chapter Two, it was not uncommon for guns to be fired multiple times in short succession, and if the rate of fire surpasses the material's rate of heat transfer, i.e., the rate at which the gun can cool off, it will continue to heat up until a failure occurs. Even in the 16th century, military officers were aware that heat causes a gun to fail and recommended less than eight shots per hour to ensure the gun remained cool (Tucker 1989:10). As depicted in Figure 6, cast iron resists a loss of strength much longer than bronze does under the same thermal loading. At 200°C (392°F), both cast iron and bronze remain at around 100% strength, but as the metal heats up to 300°C (572°F), cast iron remains at around 100% strength, but the strength of bronze has reduced dramatically to less than 60% of its original strength. This means that all else being equal, a cast iron gun can fire more shots in an hour than a bronze gun can before the gun fails due to heat-induced weakness. Guns that have failed due to thermal loading may show the associated signs, but to separate thermal failure from deformation due to archaeological site formation processes can be challenging– an example of such a gun is discussed in Chapter Five. A gun at BTFA shows significant deformation due to heat, but it uncertain if this was incurred during the firing process as an c–transform, or later as a n–transform (see Figure 48 and Figure 49 for a visual depiction of this). For example, a high–temperature environment such as a ship–board fire could deform a gun after or before a failure has occurred (regardless of its failure mode) and thus consideration of archaeological site formation theory and transformation processes must be observed to correctly identify heat–related damaged, regardless of material.

Closely related to the strength-temperature relationship are material properties known as thermal conductivity and specific heat. These material properties vary for different metals, and thus material choice (even specific alloy choice) can greatly influence gun failure patterns. A material's thermal conductivity represents the quantity of heat gained or lost due to a temperature gradient over time. More specifically, this is a denotation of the ability of heat to transfer from molecule to molecule only utilizing thermal motion, with no transfer of mass taking place (Groover 2012:75). This phenomenon is commonly encountered when utilizing metal cookware on a stovetop: it takes a longer time for a cast–iron skillet to heat up compared to one made of copper, that is in part because both metals display different thermal conductivity properties. Bronze has a thermal conductivity of 15 British thermal units per foot–hour Fahrenheit (BTU/ft h F), where cast iron has a much higher thermal conductivity of 30.1 BTU/ft h F (The Engineering Toolbox 2005). This means that a bronze gun cools more quickly than an iron gun, when subjected to the same period to cool to ambient temperature, but also heats up equally as quickly, resulting in more frequent rest times. So, iron's strength is less influenced by heat, and it heats up more slowly, but additionally, it takes longer to cool. This is reflected in the other variable mentioned earlier, Specific Heat. Closely related, this is a measure of the quantity of heat required to increase or decrease the temperature of a unit mass of material by a single degree (Groover 2012:74). The specific heat of cast iron is around .107 British thermal units per pound Fahrenheit (BTU/lb F), where bronze is around .088 BTU/lb F (The Engineering Toolbox 2003). This indicates that it requires less energy in the form of heat to raise the temperature of bronze one degree when compared to cast iron. These factors are taken into consideration when conducting an engineering simulation of metals.

Another important factor in gun manufacturing is a material's yield strength. An aspect of the material's stress–strain relationship, a material's yield strength describes the maximum force a certain unit of material can withstand before the stress-strain relationship moves from elastic deformation region to plastic deformation region, often denoted on a graph as the yield point (Groover 2012:50–55). Figure 7 displays a typical stress–strain graph for metals, which succinctly summarizes the metal's tensile material properties. Simply, stress is the force exerted on the material, and strain is the resulting deformation of the material in reaction to the stress. The curve for every metal is very complex and often the curves are not as simple as the one shown below, and much work has been done to quantify the complexity of cast iron and bronze curves (Morrev 2019). However, for these purposes, a simplified understanding will suffice.

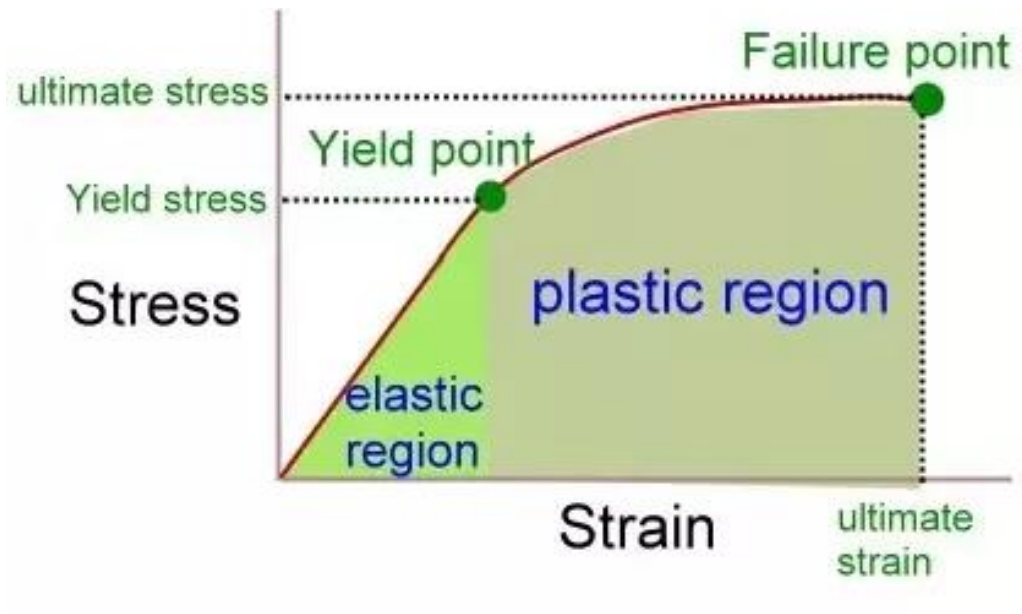

Figure 7: A typical Stress-Strain curve (Universal Engineering Services 2021).

In the region low in stress and low in strain, elastic deformation occurs when a metal is deformed by force but is capable of returning to its original shape, like a spring. This region is denoted as light green in Figure 7. When higher levels of stress and strain are encountered, plastic deformation occurs, specifically when a material is subjected to so much force that it deforms in a way that will not allow it to return to its original shape, referred to as a material's yield strength, or yield point. Beyond the yield strength is a material's ultimate tensile strength (UTS), sometimes referred to simply as tensile strength or failure point, which equals the maximum stress and strain the material can withstand before failing outright. Such relationships are utilized at length throughout Chapter Four and Chapter Six, because if an iron gun reaches its yield strength, it becomes damaged, and at the tensile strength, localized or catastrophic failure can occur. A good example of this is repeatedly bending a paperclip until fatigue failure, when the paperclip reaches its ultimate strain and ultimate stress. This phenomenon is further explored in the fatigue subsection but suffice to say plastic deformation will eventually lead to fatigue failure. Obviously, this is bad if a cannon is inflated by pressure to such an extent that the interior of the bore remains in a different shape and stays that way without returning to its pre-pressure form. As alluded to above, many of the guns tested in Chapter Six are subjected to pressures which overcome the yield strength, and sometimes the ultimate tensile strength, and result in iterative failure. Too much repetition of this, and the cannon will catastrophically fail, similar to bending a paperclip repeatedly bent back and forth until it breaks. Cast iron has a yield strength of 275 MPa (39,885.4 psi), and bronze has a yield strength of anywhere between 125 MPa and 800 MPa (18,129.7 psi – 116,030 psi), meaning that some modern bronze alloys are much more resistant to yielding than cast iron (Groover 2012:53). As indicated in Chapter Six, the detonation of gunpowder within the bore of a cannon can result in pressures of 100,000 psi or higher, and the resultant force can be substantially larger than the yield strength or tensile strength of the material, sometimes several times higher. Notably, this large variability in the yield and tensile strength of different metals, including cast iron but especially bronze alloys, are deceptive. Low strength bronzes used today in additive manufacturing are in the 125-150 MPa range (18,129.7 psi – 21,755.7 psi) and less resistant to stress than iron (He et al. 2019:653). However, engineering analysis on bronze archaeological artifacts has helped narrow down the types and alloys of bronze used in historic metallurgy (Sik 2009:1269–1272). Cannons and other bronze objects were made out of a high-tin bronze alloy, which would often display yield strengths around 150–200 MPa (21,755.7 psi – 29,007.5 psi), comparable but noticeably worse than cast iron. However, because bronze can sustain significant high strain deformation and return to its pre-stress state (i.e. these bronzes have a relatively high yield strength) they were competitive with iron. However, cast iron has less resistance to strain, but can sustain much more stress. This means that it behaves in a more brittle fashion and is not as effective at returning to its original form if pushed beyond the elastic region.

A material's bulk modulus of elasticity is very closely related to yield strength and strain, but notably different. This is the measure of a material's elastic or volumetric response to a hydrostatic pressure with equilateral tension (U.S. Department of Energy 1993). More simply put, this is a material's resistance to uniform compression by a pressure or force, maybe better described as a measure of the inherent stiffness of a material to resist changes in volume (The Engineering Toolbox 2008b; Groover 2012:52). In cannon design this is crucial because a cannon experiences a large, uniform pressure every time it is ignited. In this department, cast iron has a bulk modulus of between 62.1 Gigapascals (GPa) to 250 GPa (9,006.8 ksi – 36,259.4 ksi), and bronze has a generally lower bulk modulus of between 70 and 138 GPa (10,152.6 ksi – 20,015.2 ksi). Hence, cast iron is more resilient to pressure forces and less likely to change volumetrically, but also capable of sustaining less strain.

A material's toughness describes the way a material reacts to sudden impacts (U.S. Department of Energy 1993). Toughness is thus defined as the amount of work required to deform a unit of metal until it fractures. Copper alloys such as bronze are significantly tougher than cast iron, and thus less likely to shatter under impact. Toughness is closely related to ductility, and materials that are more ductile tend to display higher toughness as well. Bronze is significantly more ductile than iron, and thus when bronze naval guns fail, they tend to tear and shear in comparison to cast iron cannons, which blow to pieces like a bomb (Tucker 1989:10; Guilmartin 1999).

More standard material properties relationships exist within material science to help explain the different behaviors between cast iron and bronze, but the primary ones that hold specific bearing on the topic of gun explosions have been covered. With a basic understanding of these concepts, a more focused inspection of gun failures can be attempted. In the next subsection, the concept of work hardening is introduced and explained.

Work Hardening

Work hardening, also referred to as strain hardening, is an important factor to consider when designing metal components, such as cannons. Work hardening happens when a material is deformed repeatedly at the beginning of the plastic deformation region on the stress–strain diagram. This results in the material being deformed plastically, but not to the point of failure. Instead, as stress and strain on the material decrease, the material then returns to the elastic region with slight plastic deformation. This deformation region is denser and stronger than the unaffected region and thus is hardened and made more resistant to further deformation. The process can be repeated to achieve a very durable layer of strain hardened material and is depicted in Figure 8.

To relate this to more common knowledge, it is this process which is utilized to create very hard swords and blades. Historic blacksmiths understood the process in a traditional sense: if one smashes a hot blade with a hammer enough times (plastically deforming the metal) and

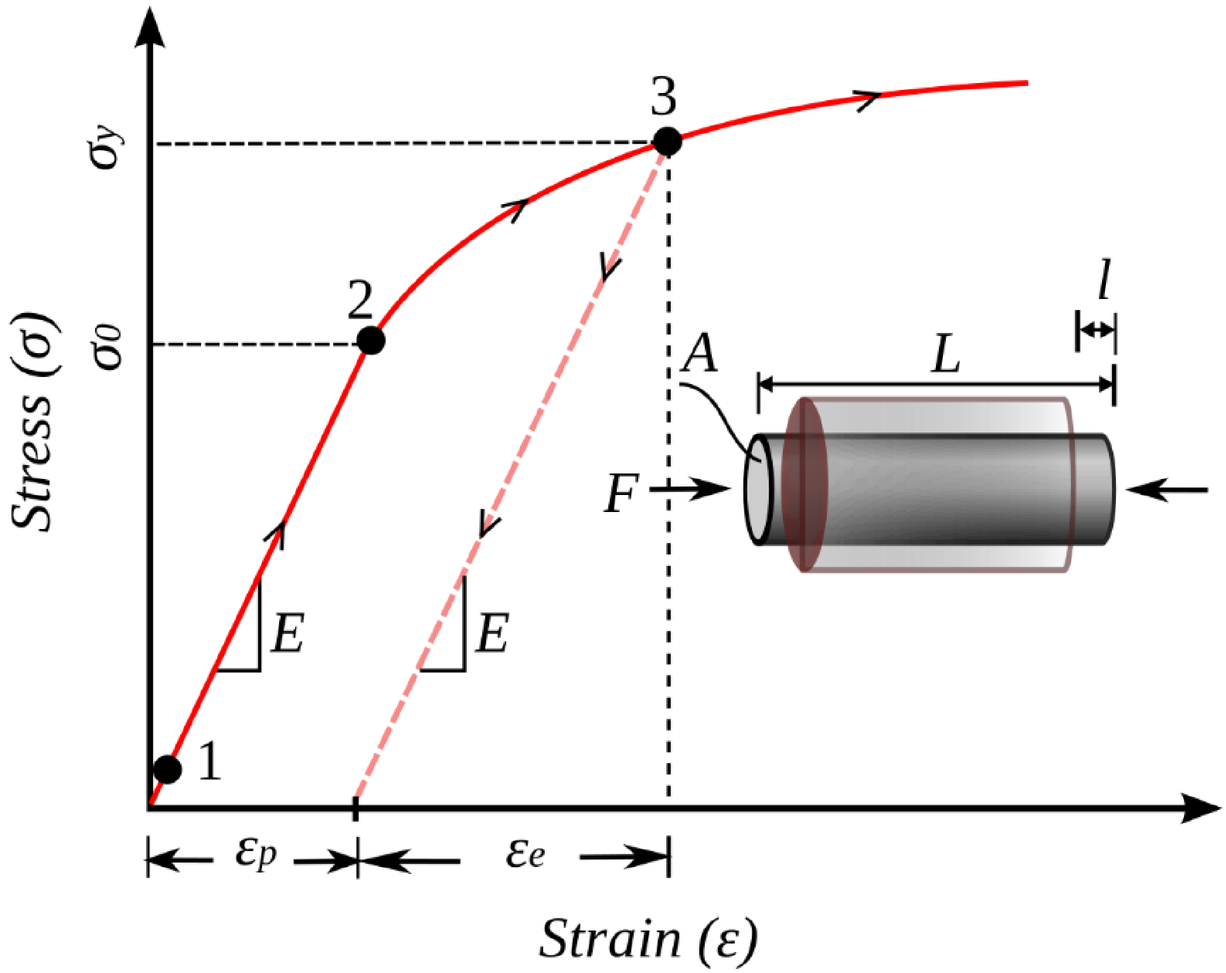

Figure 8: An example of the work hardening process (Quizlet 2024).

lets it cool quickly (letting it return into the elastic region), then the blade will be tougher and stronger than if it hadn't been hammered. A thin layer of super-hardened metal will exist in every place where the metal has been struck with a hammer. The same process is in play when a cannon is fired repeatedly. Instead of being smashed with a hammer to produce heat and force, the explosion of gunpowder creates a concentration of heat and force, leaving a work hardened inner shell throughout the interior of the bore, as if the entire inner bore has been smashed with a hammer. The process of work hardening is especially prevalent in ductile materials such as bronze, and thus this affects bronze cannons more than iron cannons.

Work hardening can be useful or detrimental, depending on the use case. While work hardening does create a harder surface that resists penetration (a very useful aspect if designing the armor scheme to a dreadnought battleship), it is not useful for cannon manufacture, as it results in brittleness (Brown 1997:77,202; Guilmartin 2003:312). Work hardening slowly builds up in bronze guns over time, and results in a brittle inner layer that causes a greater chance of explosion (Tucket 1989:6–8). To combat this, the life span of a bronze cannon had to be adjusted, and once a cannon had become hardened enough to chance explosion, it was taken out of service and melted down to be recast.

Fatigue

The concept of fatigue is probably the single most important causation of failure on seemingly well–built guns, which served a long lifetime and exploded "randomly." Fatigue is referenced many times in Chapter Six, because almost every exploded or otherwise failed gun exhibits some form of fatigue failure. Metal fatigue is a concept in material science which outlines the generation and propagation of microscopic cracks in a metal due to cyclical loading, causing the part or object to fail even when subjected to loads well below its yield strength (Budynas and Nisbett 2015:275; DeLuca 2025). A more precise definition is "the process of progressive localized permanent structural change occurring in a material subjected to conditions that produce fluctuating stresses and strains at some point or points and that may culminate in cracks or complete fracture after a sufficient number of fluctuations" (Pedersen 2024:1). Fatigue failure is especially dangerous in all aspects of the engineering discipline because it happens very suddenly. When a part fails statically, usually it develops a large deflection and then fails, providing a visible warning in advance (Budynas and Nisbett 2015:275). However, fatigue failure is sudden and total, with no warning and without any visible indication of imminent failure.

The fatigue life of an object is the theoretical duration of the object from creation to fatigue failure, and is comprised of two distinct phases, the crack initiation phase and the crack propagation phase. In all objects subjected to such stress, including cannons, the crack initiation phase occurs when the object reaches stress amplitudes below its yield strength but is violent enough to cause cyclic slip to initiate, thus slowly eroding material a few molecules at a time. In time, a micro crack will occur and drive the process onward to the crack propagation phase. In this stage, the crack will grow in a stable and predictable manner according to fracture mechanics, and result in a sudden failure of the part once the remaining cross section is unable to sustain the applied loading (Pedersen 2024:2).

There are four primary forms of fatigue which could affect almost all metal components: high cycle fatigue (HCF), low cycle fatigue (LCF), thermal fatigue, corrosion fatigue, and thermo–mechanical fatigue (TMF) (DeLuca 2025). HCF becomes present during cyclic loading comprised of low amplitude, high frequency elastic strain. An example of this might be the tip of a turbine blade on a jet engine, as it encounters faster moving air and slower moving air in different regions of its 360-degree rotation around the engine's axis. Over time, this vibration will erode and cause the fan blade to fail—hence why airlines sometimes replace turbine blades which show signs of wear. LCF is characterized by cyclic exposure to high amplitude, low frequency plastic strain. An example of LCF would be bending a paperclip, to repeat an example from earlier. If a paperclip is bent apart, and then bent back to its original orientation, a single cycle of LCF has been imparted on the object. Repeated cycles will cause the paperclip to fail due to LCF. It may be obvious that cannon discharges are primarily examples of LCF, with "low" cycles of a few hundred discharges, one thousand being almost unheard of in some designs. “High” cycles of fatigue present in HCF situations being instead many hundreds of thousands of cycles, as demonstrated by the rounds per minute of a jet engine. A cannon would rarely be exposed to HCF, but it is not impossible. Thermal fatigue failure results when an object is subjected to drastic heating and cooling cycles, which causes thermal expansion and contraction within the object to initiate and propagate cracks. A good example of thermal fatigue are cracks in a highway after years of harsh winters and scorching summers –the expansion and contraction of the asphalt cause it to crack. The same effect can happen within other materials, especially metals, and more specifically poorly–mixed metal alloys with differing thermal expansion coefficients (Suresh 1998:115–117). Metals like non–homogenous bronze that are allowed to cool slowly are more prone to this type of fatigue. Needless to say, cannons undergo extreme cyclic heating and cooling cycles and thus expand and contract due to heat constantly, making this fatigue common in exploded guns. Corrosion fatigue occurs due to cyclic exposure to a corrosive environment. The combination of stress and corrosion can accelerate the creation of microcracks and the propagation of them once initiated, leading to failure. The salt environment onboard ships and on coastal fortifications make this type of fatigue prevalent on poorly maintained naval guns.

Compared to the above types of fatigue, TMF is a more multidimensional concept, which considers the relationship between heat and strength. As mentioned above, the rate of heat gain, and the relationship between heat and strength, greatly impacted the lifespan of a cannon. Bronze was more susceptible to heat-related failure, but both iron and bronze guns could be affected. TMF is induced when the effects of cyclical *mechanical* loading are coupled with those of cyclical *thermal* loading. A gun, when fired repeatedly, is subjected to all the ingredients that may result in high amplitude, low frequency thermo-mechanical fatigue failure: the mechanical loading is the force and pressure associated with the discharge of gunpowder, and the thermal loading is the heat energy generated by such an explosion. Three primary mechanisms are present to propagate TMF: material creep (seen sometimes in cannon as 'droop' in the muzzle, where material has sagged down as if the cannon had melted), fatigue cracks, and higher levels of oxidation. These three work in tandem to weaken a cannon, both in–phase and out–of–phase: creep happens in–phase (when the cannon is subjected to high mechanical and thermal loads simultaneously) and thus causes fatigue and oxidation, which occur between firing, hence out–of–phase. Oxidation weakens the surface of the material, creating flaws and allowing for the propagation of fatigue cracks. The system is then put through another cycle of firing, and the creep continues to act, creating a negative feedback loop. TMF is still poorly understood, and several models have been developed to help engineers identify TMF. TMF is specifically present in systems subjected to high temperature gradients and adverse conditions under intense mechanical loads, specifically turbine systems such as jet engines and turbofans (Nagesha et al. 2010). However, cannons at sea may also represent an example of such a failure pattern, abet at a slower rate.

It is important to note that although material fatigue is almost unavoidable, there are certain characteristics that hasten the process. Cyclic loading is the primary fundamental cause, although obviously this is unavoidable when engineering a naval gun. Additionally, material defects significantly hasten fatigue failure because preexisting cracks, inclusions, impurities, voids, and grain boundaries serve and stress concentration areas, focusing local stress and initiating fatigue cracks. Finally, design flaws are particularly insidious. Sharp corners which have no internal chamfer, poor stress relief from associated regions of the object, and other poor design methodologies can significantly weaken a part and make it susceptible to fatigue. In the case of guns, fatigue may propagate where reinforcement bands junction with the barrel of the gun, or where trunnions terminate in the body of the gun. Other factors of engineering theory are applicable to fatigue failure, namely casting defects and surface finish play a substantial role in the initiation and propagation of fatigue cracks. These are both covered in the next two subsections.

Surface Finish

Another aspect that causes gun failure is imperfections in surface finish. Surface finish, or surface roughness, is essentially the level of imperfections the surface of a material has on it. A smooth surface finish will be mirror–like, and a poor surface finish will be sandpaper–like, or worse. Casting processes are notorious for producing very, very poor surface finishes, and this can significantly reduce the lifespan of the part (Groover 2012:137). Surface finish is measured in Roughness, or Ra, and is displayed in Figure 9.

Figure 9: An example of different Surface Roughness textures in Ra (Unity Manufacture 2023).

A high Ra value means a poor surface finish, where a small value indicates a smooth finish. When calculating tensile and yield strength for different materials, like bronze and iron, a perfect surface finish is usually assumed for simplicity. But surface finishes are almost never perfect and can drastically affect the realistic performance of a material. Figure 10 represents a graph produced to show the relationship between surface factor and tensile strength for an additive manufacturing project at NASA's Marshall Space Flight Center, and the results are telling. High surface finish parts have a surface factor of close to 1 (100%), but as surface finish gets worse, the surface factor sinks father below 1. The surface factor is a ratio applied to the fatigue limit of a part to indicate how much the part could be affected by surface roughness, as a percentage.

As described by Figure 10, a very, very poor surface finish of any given tensile strength could induce reductions up to 50% (.5), which is massive. As anyone who has felt the surface of a cannon knows, cannons have very poor surface finishes. The casting techniques, combined with saltwater corrosion, and the effect of thermo-mechanical and low cycle fatigue heavily affect the lifespan of naval guns. However, site formation theory dictates that n–transforms such as water immersion will also heavily impact this variable on archaeological artifacts, as what surface finish was present on the gun when it failed may not be the surface finish present on the gun after it entered the archaeological record and was subjected to site formation processes.

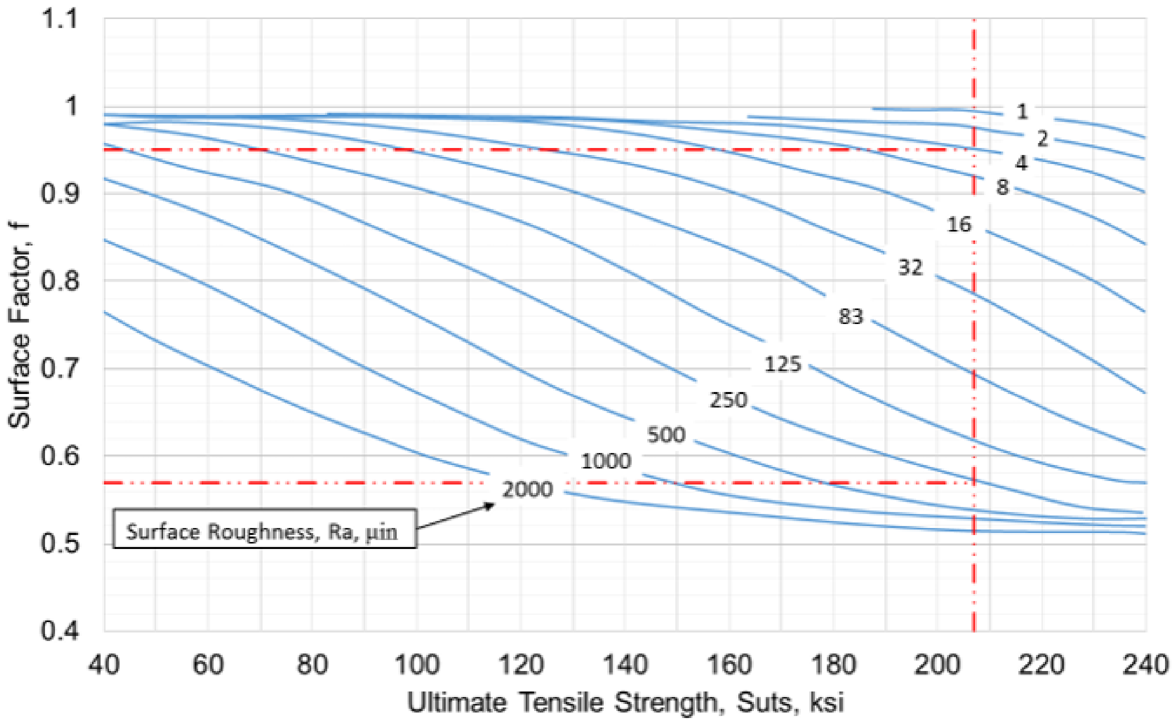

Figure 10: Surface Factor plotted against Tensile Strength (Lambert 2016).

Unfortunately, the effect that the Ra variable has on the propagation of fatigue cracks and failure patterns in naval guns has never been fully explored. When conducting engineering computer analysis on cannon solid models, the Ra variable will be based not on what is displayed in the archaeological record, but instead on an estimated Ra value based on modern attempts to cast cannon.

Casting Techniques and Defects

The specific casting technique utilized to produce either a bronze or cast-iron gun plays an important role in determining the quality and lifespan of the weapon, and their susceptibility to many different types of failure, including fatigue failure. One benefit of using bronze was the capability to easily remelt and recast the bronze into a new weapon, thus allowing weapons to be quickly recycled and rebuilt before issues such as fatigue became a problem (Tucker 1989:10).

However, using bronze guns was complicated by the fact that bronze had a higher toughness and higher ductility, and lower bulk modulus. This meant that bronze guns could not withstand the shock and internal pressures as well as iron, and higher-strength alloys of bronze were often too brittle. Modification of bronze alloy for gun manufacturing was akin to walking a tightrope between making bronze enough like iron to resist the stress of firing, but not less ductile enough to explode like a bomb when it failed (Guilmartin 1999; 2003:307–310). Additionally, bronze is prone to the development of a casting defect known as microporosity. Microporosity occurs when a network of small, microscopic voids is caused by non-uniform freezing of the liquid metal. What results are a dendritic void network distributed throughout the casting. This sponginess of the metal is resultant of the alloy nature of bronze, where the different composite metals solidify at different rates. Tin has one of the lowest melting points of all metals, and thus tin often solidifies long before copper, and this results in a non–homogeneous casting profile. The resultant casting exhibits weakness wherever microporosity occurs, and although this can be inspected for today using standard quality control procedures such as radiographic methods, magnetic particle tests, and supersonic testing (Groover 2012:134-135), these defects were historically impossible to detect. If this defect was present in large areas or critical areas, a cannon explosion could be catastrophic with no forewarning. Additionally, large grain boundaries and drastic contrasts between different metal material within the casting of the gun were ripe for fatigue crack initiation and propagation to occur, as mentioned in the previous subsection. To limit microporosity was to simultaneously limit the chances for fatigue failure to occur earlier than it might otherwise, as well as to limit immediate failure during proofing due to weak points and voids within the cannon.

Both in cast iron and cast bronze cannons, the uniformity of the metal's crystalline structure is of the utmost importance (Guilmartin 2003:307). Both varieties of cannon were cast with the muzzle facing up. This had the effect of compressing the molten metal at the breech of the weapon, allowing for more uniform cooling and a denser and stronger alloy. As mentioned in Chapter Two, machining capability increased in the 1750s, and advances in boring machines made it possible to cast solid barrels and then bore the entire core of the cannon out to produce the hollow bore. This machining process produced more accurate weapons and improved weapon quality because imperfections in the molten metal tend to concentrate at the center of mass, which tends to be along the axis of the cannon. Thus, many imperfections were removed during the boring process (Guilmartin 1999). However, non–homogenous metal was still a major problem in any cast metal gun. The problem of non–homogenous metal only went away when non–casting dependent gun making processes were introduced during the latter half of the 19th century.

Cast-iron cannons had less alloy-related issues when compared to bronze guns but were instead challenging to cast because of the heat required to render liquid iron. Large blast furnaces were utilized, but the quality of the hot iron was highly suspect. Although not represented in the archaeological record in the same way as bronze defects (Guilmartin 2003:307–313), iron has a slew of common defects which most likely are present in the archaeological record. A casting defect common to metal not poured at high enough temperature is the 'cold shot.' A cold shot is a defect that results from splattering or a low temperature pour, causing large areas of pre-frozen metal 'inclusions' to enter the casting and situate before the remaining melt solidifies, thus becoming entrapped in the casting (Groover 2012:133). This can cause many discontinuity problems in the crystalline structure or result in air pockets trapped within the casting. Those in turn can cause internal fatigue or stress fractures to develop, resulting in a random catastrophic failure while firing. This can happen during the proofing process, or later due to fatigue failure. Like microscopic voids, these were impossible to detect at the time, but modern techniques have allowed for testing.

Cannon Design

Cannon design for naval guns at the time was directly related to the knowledge of casting science. Most features of cannon design were direct responses to difficulties experienced during the casting process. For example, when a bronze cannon is cast in an upright orientation (as was normal), the composition of the alloy was non-homogeneous throughout the casting. As mentioned before, tin and copper tend to segregate themselves within the melt, and the tin would congregate at whichever location was last to solidify. This tended to be the breech area of the cannon, thus leaving the muzzle of the cannon with a low density of tin per unit of copper. Cannons thus displayed highly brittle muzzles and highly ductile breeches, which resulted in burst muzzles. The internal stress on the cannon caused by firing resulted in strain being the highest around the breech area, but the brittle muzzle area was often the first to fail. To combat this, manufacturers often designed cannon with a thicker breech area and a flared muzzle end to mitigate these effects (Guilmartin 2003:310–312). Identifying these factors in the archaeological record can be difficult, as site formation processes can drastically change the physical profile of the gun, obscuring legitimate damage incurred during the failure process from n–transforms and c–transforms. Identifying design intent from modification due to site formation processes may also pose a challenge, as some damaged cannons were used as bollards for many years, and damage incurred during this period of their use may not be consistent with damage incurred during firing. Examples of cannons which were used as bollards are discussed in Chapter Five.

Iron guns had additional problems, but mostly because, as demonstrated earlier, iron is simply more brittle than bronze. Cast iron is not an alloy, but it is more susceptible to stress fractures and microscopic surface imperfections that can multiply during repetitive cycles. To combat this, iron cannons were often cast way larger than necessary, with much thicker walls to mitigate such issues. For this reason, iron guns were considerably heavier and larger than bronze guns of the same shot weight. This had the adverse effect of limiting the amount of iron guns which could be mounted onboard a ship in comparison to bronze guns. It also demarcated where in the ship guns cast from different material were placed; iron guns were often located on the lower decks if placed onboard the same ship as bronze guns.

Conclusion

With the information imparted in this chapter, the archaeological and engineering theory utilized to analyze failed cannons can be fully appreciated. As described by Schiffer (1983), different approaches can be nestled within archeological theory to fully explain the archaeological record. In this work, a complex engineering theory corpus was utilized to further complement the archaeological approach, and provide further insight into the lifespan of guns, and their deposition into the archaeological record. The archeological theoretical framework is based heavily off the work of Schiffer: the purpose is to not only record and measure the cannons but also understand the human factors which played a role in the history of the gun. Differentiating between n–transforms and c–transforms was aided by understanding concepts from engineering theory.

Specifically, the engineering theory is utilized to determine the cause of failure noted in the archaeological record. To this end, several engineering fundamentals were described in detail which may play a role in the history of a failed gun. The material composition of cast iron and bronze were both explained, because cannon design (and poor design decisions) was universally linked to material composition. Iron guns react differently than bronze guns, and thus iron guns must be approached through a different design framework. Despite excluding bronze guns from this study, the design of iron guns was directly related to that of bronze guns, and thus an understanding of both was required. As later described in Chapter Six, material yield and tensile strength characteristics play a huge role in determining the likelihood of failure. Cast iron's toughness, bulk modulus, and temperature characteristics are all physical properties that engineering modeling software considers to accurately model the reaction of a cast iron gun to the effects of repeated firing, and thus to understand what the program is simulating one must first understand these fundamentals. Work hardening, although hard to model in engineering software, no doubt plays a huge role in the likelihood of failure and should be acknowledged and explained. Additionally, the presence of fatigue imparts a higher likelihood for failure: a gun which has been misused, under–maintained, or used for long periods of time can be more susceptible to fatigue, and thus more readily fail at the exact wrong time. Although this study does not attempt to quantify the effects of fatigue, its presence is often noted and statements are made to indicate the likelihood of its presence on a failed gun. Other aspects, such as surface finish, also compound or otherwise modify factors such as fatigue, and thus the effects of surface finish must be mentioned. In the employed software, a high surface finish is automatically assumed, however this introduces a degree of uncertainty into the simulations that should be acknowledged.

Additionally, the theory behind engineering processes also falls within the greater category of engineering theory. Casting techniques and defects, well understood today, were less well accounted for in historic casting processes. Issues such as microporosity, cold shots, and non–homogenous solidification are all examples of quality issues which plagued early cast iron products. Furthermore, cannon design itself evolved throughout the period covered by this study. Some guns noted in Chapter Five were cast in the early 18th century, others in the mid–19th century, and as stated in Chapter Two, the intervening 150 years between 1700 and 1850, there was much engineering development that effected the likelihood for failure. In short, cannon design in the 19th century improved, and with it, design processes, such as casting techniques. In the subsequent chapter, the precise methodology utilized to model all these factors is described in depth, and all processes to replicate the work are expounded upon.

Chapter 4: Gun Failure Quantification Methodology

Introduction

Without the proper and conscious utilization of a preconceived methodology, no quantitative or qualitative analysis can be conducted with any amount of intellectual robustness. The purpose of methodology is to determine the process and outline the steps necessary to collect and organize data, as well as to acknowledge the methods of analysis, limitations of the analysis, and explain the analysis process. However, as is displayed in this chapter and in Chapter Six, this is an iterative process. The mode of analysis is an integral part of the methodology and hence modifications to one affect the other. The methodology utilized for this study incorporates a sequence of four primary phases outlined in the Process Flow Diagram (PFD), depicted in Figure 11.

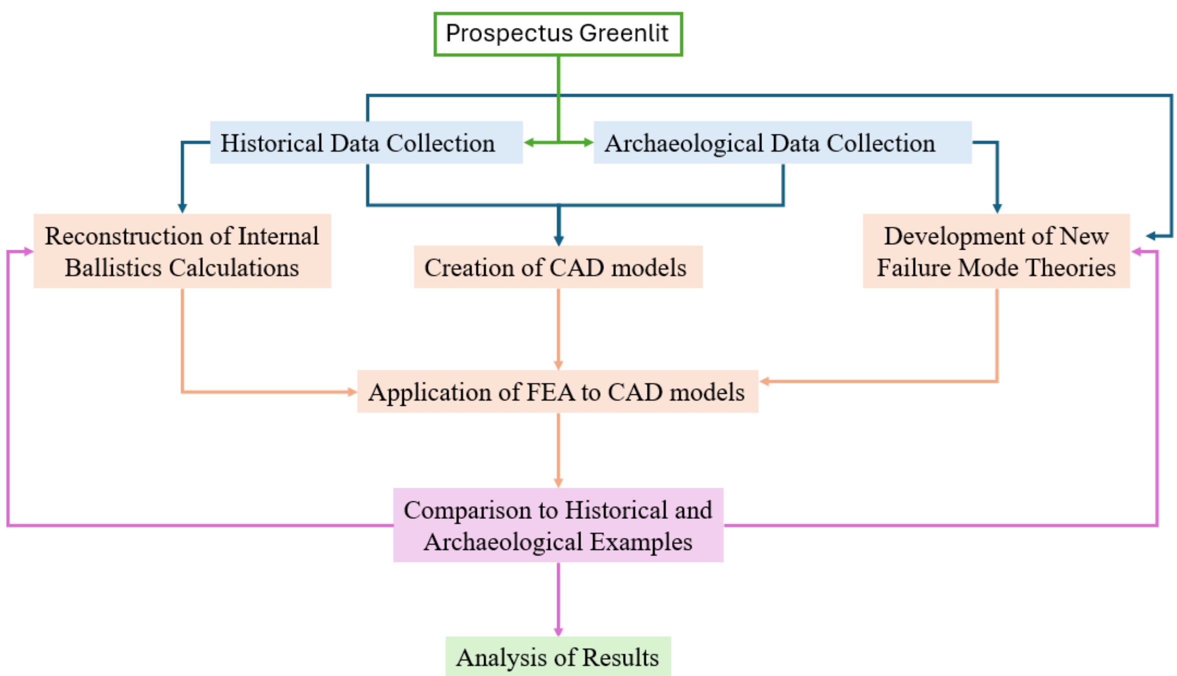

Figure 11: Process Flow Diagram (PFD). (Image by James Fowler.)

The initial step consisted of the project prospectus receiving permissive authority to commence. After the acceptance of the prospectus, the other four primary phases in the PFD were completed, indicated in Figure 11 by color. It is important to note that the PFD does not map onto, nor represent a breakdown of content within individual thesis chapters, but instead provides a workflow from which the thesis chapters were generated.

The first step was the Acquisition of Data phase (indicated in blue), where archaeological and historical data was collected in the field. This phase included traveling to, and the measuring of, guns in the field, as well as contacting archives and acquiring historical documents such as blueprints and technical reports on gun testing and conducting any necessary research on historical background. The historiography of gun manufacturing, raw material acquisition, and gun design were also compiled in this step. Historical data collection informed the creation of CAD models through the utilization of historic blueprints. Additionally, historical sources were consulted in recreating internal ballistics calculations to identify variables necessary to the implementation of FEA, discussed later in this chapter. Consultation of any historic gun testing reports also informed the development of new failure mode theories. A culmination of guns measured during this phase can be found in Chapter Five, and a synopsis of the historiographic information collected during this phase can be reviewed in Chapter Two.

The second step in the PFD was the Generation of Models phase (indicated in orange), where the archaeological and historic data was consulted and distilled to create a selection of cannon models in CAD, used to then generate FEA analysis reports. The creation of CAD models was sourced from a variety of data, including but not limited to historic blueprints, archaeological drawings, photogrammetry, and cannon measurements. Once a CAD model was built, FEA was applied to the model to understand how the real object might have reacted in the physical world. Several different FEA tests, one for each identified failure mode (such as fatigue, thermal, and overpressure) were run to produce generated reports on the behavior under each loading circumstance. The archaeological data provided a source for a new failure mode analysis, and new test regimes were designed from the results. Additionally, if historical data existed (such as documents concerning testing and cannon proofing), that was also utilized to inform the development of new failure mode analyses.

The third step in the PFD was the Comparison to Historical and Archaeological Examples phase (indicated in purple). In this phase, the results of the FEA simulations were critically analyzed and compared to the historical and archaeological data. If lacking in congruency, a new failure mode analysis (FMA) was initiated to develop new concepts on why the cannon failed, and a new bank of tests was designed to try and simulate the failure conditions. Additionally, if the FEA analysis indicated anomalies or otherwise failed, a reexamination of the engineering variables was necessary, which would require a second attempt at reconstructing the internal ballistics calculations to hone critical values such as bore pressure. This step of the PFD was utilized to create Chapter Six.

The final step in the PFD was the Analysis of Results phase (indicated in green). This phase required the results to be cross-compared, and conclusions to be drawn between different failure mode analyses and how they impacted the FEA simulation. From this analysis, a categorization of cannon failure modes could be generated, along with a telltale list of common features of each failure, to help researchers correctly identify the origins of an exploded cannon. This was achieved by comparing similar cannon explosions, and testing each cannon for every kind of failure mode identified, to see how the cannon might react. This step was also utilized in the creation of Chapter Six and Chapter Seven.

Due to the iterative nature of this study, the PFD overlaps between chapters; it is intentionally organized in this way to provide a framework within which to conceptualize the analysis process in relation to the greater methodology. Direct analysis of the cannon data are not discussed in this chapter, only the framework through which analysis is conducted. A careful review of the PFD indicated the iterative nature of this study. Adherence to the methodology resulted in comparative analysis, but the results in the analysis will be fed back into the methodology for reiteration, resulting in new and more accurate results ready for comparison. As the process matures, a more accurate understanding can be gained from the results. This becomes clearer throughout the subsequent explanation of the process. The PFD with the chapter focus underlay is depicted in Figure 12. The Comparison of Historical and Archaeological Examples step and the Analysis of Results step belong squarely in Chapter Six, and thus that aspect of the methodology will be saved for Chapter Six.

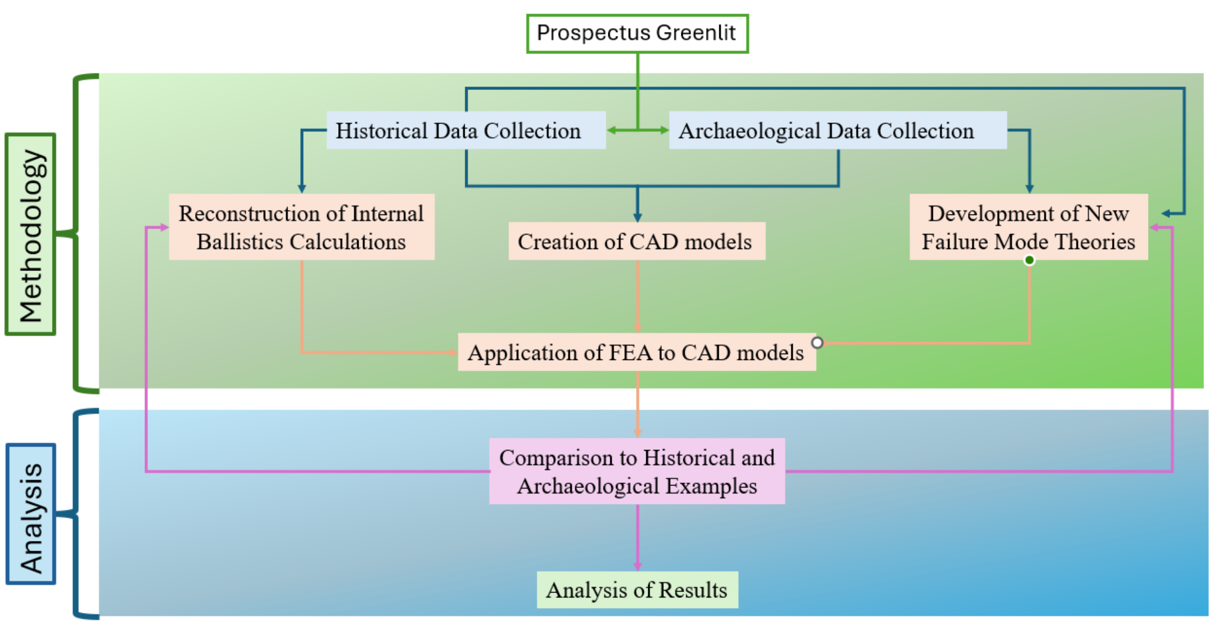

Figure 12: Process Flow Diagram (PFD) with chapter focus underlay– methodology chapter and analysis chapter. (Image by James Fowler.)

Historical Data Collection

The Data Collection phase consists of two parts, historical and archaeological data collection. The historical data collection methodology is relatively standard; however, some notation is necessary to outline all assumptions and review the techniques utilized. In this case, the historical material was selected to understand the historical perspective on the explosion and damage of guns, which may differ from the current understanding. As John Arnold argues throughout his book *History: A Very Short Introduction*, history is more than simply a re-telling of a set timeline interspersed with new data accumulation, instead it is in essence an ever–evolving argument, prone to re–interpretation, and constantly dynamic in its influence on current affairs (Arnold 2000). It is through this lens which the historical perspective was filtered and re-interpreted to drive at further understanding of the complex history of cannon failure patterns. In the spirit of what John Sumida and David Rosenburg propose in their essay within *Doing Naval History: Essays Toward Improvement*, this research is designed to be contextually–driven; a response to a call within the naval history community to refocus on the influence of greater systems to explain individual instances (Sumida and Rosenburg 1995:25–35). For this reason, the historical sources utilized range in a broad variety to add context to this historical instance: archival material, technical treatises, and engineering blueprints (Robins 1805:7,74; Griffith 1856:56–57; Mallet 1856:323–350; Greener 1858:254,277; Holley 1865:120–121,582; Cooke 1875:61,120–121; Greener 1910:28), all focused on gun manufacturing, are supplemented with material in a larger context, such as sources which focus on economic, strategic, diplomatic, and cultural influences. As indicated in Chapter Two, this research considers many different aspects that impacted gun design and manufacture, and also impacted the likelihood of guns exploding. Iron ore quality, design constraints, location of origin, military culture, strategic objectives, economic forces, and many other factors all play a role in determining the reason why a gun failed.

The historical data collection methodology utilized is primarily focused on the interpretation of primary-source documents. Historic cannon blueprints were located in archives and supplemented with many primary–source treatises and accounts, which are discussed later in this chapter. The objective of this study is to combine primary source documents, secondary source documents, and material culture evidence to support a hypothesis, while simultaneously filtering poor sources. In the case of cannon explosions, often not much choice is available in the quality of the sources. Part of the objective of this research is to provide future researchers with a blueprint to help understand gun explosions, thus allowing for a better filter on historical data relative to gun explosions.

Locating instances of gun explosions in history poses a difficult problem: famous gun explosions are often recorded and easy to corroborate with other sources, but as is often a problem in the study of the history of technology, in many instances the "failures" are forgotten to history. Only the ideas that survive are remembered. So, it often is with gun explosions. As indicated in Chapter Two, and corroborated by archaeological examples in Chapter Five, exploded guns were thrown overboard, remelted, or perhaps used as fill material. No one at that time wanted to remember guns which were rejected, they were not only useless as objects of war, but they had no place as memorials or the like. Many cannons which exploded were bitterly disposed of as garbage. However, from historical accounts, it is clear that many guns exploded, in some instances regularly. To account for this, a historical methodology focused on reading "in between the lines" of history to grasp allusive concepts was necessary.

After initial internet searches for exploded cannon were exhausted, the ability to reliably locate data for the study dropped substantially. The collection of gun explosions documented here, both archaeological and historical, were often located through the reading of sources completely off the topic, and no other more suitable methodology has arisen. For example, Stephen Decatur's mention of cannons exploding on the frigate *Guerriere* could only be located by reading about the battle in a book on the Barbary Wars –the book itself does not have "cannon" in the index (Leiner 2006:99). The author, Frederick C. Leiner, only mentioned the gun explosions offhand in the text. Decatur himself only mentions it briefly in his letters. Such is the experience of searching for historical instances of gun explosions –no one today, or then, has given it much attention or found it worthy of denoting. The historical methodology for locating sources is rudimentary and sporadic. No database of exploded guns exists, only dozens of footnotes in a random assortment of history books. Hopefully this research provides a staging ground that did not previously exist for future forays into this obscure but important aspect of naval history.

Archaeological Data Collection

The archaeological data collection methodology is much more straight forward. In this subsection, the different measurement techniques are explained, the documentation process outlined, and different approaches outlined for different scenarios. As shown on the PFD, this step in the process goes hand in hand with the historical data collection process -both are intertwined. Historical instances of gun explosions are used to track down archaeological instances, and archaeological instances are used to locate historical documents thus related. However, unlike historical data collection, the archaeological aspect is more quantitative in nature, in part to make up for the data often missing in the historical sources.

The cannons considered by this study were measured in a variety of locations, some underwater, and some above. Some cannons were measured with no time restraint; others were measured quickly due to deteriorating weather conditions or other uncontrollable variables which limited accuracy. The condition of the gun is also of the utmost importance and impacts on the quality of the data. The archaeological significance of the gun is only as good as the context recorded during its recovery, and in many instances, guns have been removed indiscriminately and are thus devoid of context. As with any archaeological artifact, the ability to record the gun in situ is considered optimal for understanding the context in which it was deposited (Bowens et. al 2009:201-202). Often, this context is underwater. However, guns already salvaged, archaeologically or otherwise, are still extremely useful and have a place in this study. The goal of this research is not to understand the context of the gun, but the failure of the gun itself, so while context is key, it is not required to gain much understanding, as detailed in Chapter Five and Chapter Six.

Standard Cannon Recording Techniques

The simplest cannon to measure, exploded or otherwise, is the one preserved and on land. The process of measuring, recording, documenting, and preserving cannons in the archaeological context, and more specifically *nautical* archaeological context, is well understood (Wilkes 1971:238–242; Muckelroy 1976:126,190; Bowens et. al 2009:201–212; Ciarlo et al 2023:3–12; Koivikko et al. 2025:2–27). The proper preservation of the gun can reveal high levels of detail which in some instances are distinct enough to evaluate at a micro level and deduce failure origin, as represented by several guns in this study. All possible methods can be used to measure such a well-preserved gun, and a much higher resolution of archaeological data can be gathered. The methods used depend on whether the gun is above water or under it, however the objective remains the same: to retrieve proper dimensions and measure and record any notable features. A description of a gun's orientation, the construction material, the overall dimensions such as length and width, maximum diameter, minimum diameter, bore diameter, the presence (or otherwise) of external features such as trunnions, lifting dolphins, cascabels, and reinforcement bands, distance between trunnion faces and diameter of the trunnions, inscriptions or cast stampings, and evidence of the carriage and/or breeching ropes are the minimum necessary data generally understood to be needed to identify the gun (Bowens et al. 2009:202). However, for the purposes of this study, much more data was required to perfectly replicate a gun in a CAD platform. A complete version of cannon recording proforma utilized is available in Appendix A. Additionally, copies of all recorded cannon data for the guns analyzed using FEA are located in Appendix B.

For all dimensioning operations intended for engineering application, it is advisable to follow the fundamentals of geometric dimensioning and tolerancing as outlined by ASME to ensure maximally accurate measurements are obtained (Krulikowski 2013:10–18). This calls for the determination of a set datum on the cannon from which to measure every dimension, to ensure uniformity across all measurements. In most cases, the datum designated is in a planar form, represented by the plane created by the flat face of the muzzle of the gun. A straight edge is placed (when necessary) on the flat face of the muzzle to serve as a datum to measure offsets from to each feature. This method is the standard approach utilized in measuring guns. In some instances, a second datum will need to be determined, in some instances the cascabel, in order to achieve accurate measurements. It is good practice to measure each feature from both datums, and possibly a third, to achieve maximum accuracy, however often time restraints limit redundancy. This process will avoid tolerance stack up and allow for cross references.

Additionally, standard operating procedure calls for the use of the exact same measuring device, to remove any error which may accumulate between differing devices. For the purposes of this study, a measurement accuracy of one centimeter was considered nominal. This was not always possible, in some instances an accuracy to the nearest half meter or so was all that could be ensured, dependent on the environment. In this way, the location and dimension of every single feature on the gun must be measured in exact detail when possible. The exact location of each reinforcement band, the band's width and length, and location relative to the datum must be measured. The goal of the measurements is to produce a reverse–engineered blueprint of the cannon to then feed into a CAD suite.

Archaeological Photography and Video Inspection

Archaeological photographs were taken of many of the guns. The methodology of archaeological photography utilized was to get several photos of each gun. One photo of the full gun, taken from a distance which allowed a full image, was taken. Additional photographs were taken of any distinguishing markings, and of any areas which display damage. Where possible, these images included a scale item of some kind. However, some photographs were taken in a candid fashion, especially when failed guns were encountered unexpectedly in the field. In some of these photos, no formal scale item was on–hand, and thus makeshift scale items, such as a one–euro coin, were utilized. An example of this technique was utilized during the recording of exploded guns in Malta. These guns were unexpectedly found and no formal scale item was present. Several camera types were utilized. Thus, some guns were recorded utilizing a DSLR–style Canon EOS, others were captured utilizing the phone camera on an iPhone 8s, and others using an iPhone 16. Regardless, the image quality achieved from all these devices was more than adequate.

Often, as explained in Chapter Two, the origination point of a cannon failure is inside the bore. It is very difficult to collect photographic evidence on the interior of a gun barrel, or to inspect the interior bore, utilizing standard cameras. To solve this problem, a new method was devised to inspect the interior of a gun's bore by taking inspiration from the ramrods used in the past to load naval guns. A long collapsable inspection pole was requisitioned, with a camera and light attached to the end (Figure 13). Additionally, a ninety–degree viewing attachment was requisitioned, consisting of a small mirror, oriented at forty–five degrees to the barrel of the bore cam. This allowed the camera to focus on the sides of the interior of the cannon bore, and not the back breech. A close–up of the ninety–degree attachment is depicted in Figure 14.

Figure 13. The bore cam, a Teslong Telescopic Pole Inspection Camera, was utilized by James Fowler to inspect the interior of the cannon barrels. (Photo by James Fowler.)

Figure 14. The mirror attachment that allowed the Bore Cam to view ninety–degrees to the axis. (Photo by James Fowler.)

The original design intent of such a system was to inspect drainpipes and other similar plumbing scenarios; however, it was re conceptualized for this purpose. The pole was run down the barrel of the gun to inspect the interior walls of the cannon in search of signs of failure. The video and images taken from this system can be recorded, and are standard formats and thus may be meshed with the standard photogrammetry to create full interior and exterior photogrammetry models of non–submerged cannon. This step was not conducted during this study, because no video was recorded. Incidentally, no interior bore damage was found utilizing this tool on the cannons inspected with the device.

Possible modification or replication of the system could be conducted to allow for use underwater, however, given the build–up of concretion and debris in most archaeological sites, the system is much better suited for terrestrial use. The bore cam was utilized to inspect the bore interior of guns in Suomenlinna, Finland, and in Edenton, NC. Although the camera can record video, technical issues ensued which limited the full implementation of the bore cam during this study. The bore cam connects to a smartphone utilizing a long USB–C cable, and the phone must have updated software to utilize the bore cam's recording feature. During the trip to Finland, the proper software was not downloaded correctly onto the smartphone and thus no video was recorded, although the camera was still utilized to inspect the interior of the bores, in the function of a non–recording bore scope. The bore cam was operated by one individual who controlled it, while another inspected the video feed for any anomalies, as seen in Figure 15.

Figure 15: James Fowler utilizes the bore cam on a cannon in Edenton, NC. Addison Costa (foreground) views the live feed through a phone app. (Photo by Abigail Fowler.)

Photogrammetry

Photogrammetry has proven very effective in producing highly accurate renderings which can be measured to the millimeter (mm) scale, if not even higher resolution. For the purposes of this study, photogrammetry was utilized extensively to capture cannons in situ, as well as to document preserved guns. Photogrammetry is most useful when cross referenced with traditional measurements when possible, and in this study was used to check measurements made by hand. Photogrammetry has been utilized substantially in many archaeological projects, so a complete documentation of its use would be superfluous (Eriksson and Rönnby 2017: 92–107; Wessex Archaeology 2017a; Phipps 2023:9–12; BU Archaeology 2025; Koivikko et al. 2025; Maritime Archaeological Society of Finland 2025a, 2025b). However, an abbreviated description of the lessons learned applicable to conducting photogrammetry on cannons specifically is included.

The basic process of photogrammetry is to circle an object with a camera, taking a photograph of the object after every few degrees of change, thus creating a sphere of photographs from every angle, all focused on the object. Then a photogrammetry software determines minute differences in the 2D photographs, orienting the perspectives to create a 3D image. When conducting photogrammetry on cannons, several things must be noted. Cannons, especially conserved cannons, are often almost black in color. This means that very little texture is apparent, and to achieve the appropriate detail, the exposure on the camera needs to be adjusted up to allow the texture to be recorded by the camera. The addition of bright lights, shining at an angle relative to the lens, aided in mitigating exposure issues. This is of particular importance when trying to document the underside of the cannon, which suffers from a shadow.

Basic Workflow for Photogrammetric Model Creation

In this section, a basic workflow for the creation of photogrammetric models is described. For this study, Agisoft Metashape was utilized for the creation of all photogrammetric models. Some photogrammetric models were created utilizing video data shot on an iPhone 16, and others were created from photos captured on a Canon DSLR camera. After opening the program the creation of a photogrammetric model began by selecting Add Photos under the Workflow tab. If video data was utilized, Import Video was selected, and a frame step of “2” was selected to ensure two stills were pulled from every second of video. Once the photos were added to the chunk, the Align Photos function was selected to allow the program to orient the photos in three–space. Generic Preselection was ensured to be checked, and OK was selected. Utilizing Gradual Selection under the Model tab, all inaccurate Tie Points were at this time deleted from the mesh. Then, after clicking Workflow, a mesh was built by selecting Build Mesh. After the mesh was generated, all unnecessary background data was cropped out. From this point, a texture was generated by selecting Build Texture. At this point, all photogrammetric models were scaled by adding markers on the scale items in the photos and describing the distance between those markers in the software. When the photogrammetric model was scaled, the process is finished, and the photogrammetric model can be analyzed and viewed from any angle. For detailed information on utilizing Agisoft Metashape, the Agisoft Metashape User Manual was consulted (Agisoft Metashape 2026:20–90).

A Note on Photogrammetry for CAD Models

The ability to utilize a photogrammetric model to create a CAD model for FEA analysis does appear to exist, however this was not tested during this study. Theoretically, a CAD model would be created by uploading the photogrammetric model into RhinoCAD or a similar product, and “shrink–wrapping” the mesh to create a solid model part file. However, such a path was not utilized for this study. That is because the guns recorded utilizing photogrammetry in this study were already failed, and thus a CAD model of an already failed gun removes the ability to test how a complete version of the gun would fail. To make a simple comparison: one cannot conduct a crash test on a car that has already crashed. However, potential exists to further pursue this option. For example, if two identical guns were found: one that failed and one that is pristine, then photogrammetry could be utilized to create a CAD model of the pristine one and test it utilizing FEA, and then the results could be compared to the photogrammetric model of the failed gun. However, this proved difficult to complete for this study, because identical and pristine versions of the failed guns were not located. Thus, simply recreating the guns utilizing manual measurements, archaeological drawings, and engineering blueprints proved more viable, and thus CAD models were created in this fashion. Photogrammetry for this study was still critical, however, it was utilized instead to obtain models which could be accurately measured and provide a means to inspect failed guns digitally from any angle and at any scale, to help inform the manual creation of CAD models.

Creation of CAD Models

Once a cannon has been fully measured and documented, and photogrammetry conducted on it if necessary and practical, the next step is to use the measured dimensions to recreate the cannon as a CAD solid model. CAD programs, simply put, are computer design software systems which allow the user to create objects in a virtual space, and have been used in maritime archaeological contexts before (Green 2004:202–203). However, each program has its own workflow. The workflow for creating a CAD model from an engineering blueprint is relatively straight forward and is comprised of three primary operations. First, the historic engineering drawing or archaeological measurements must be transformed into a CAD solid model. Second, the CAD model must be fully defined and meshed, ready to be analyzed in an FEA simulation. Third, an FEA simulation must be run on the CAD model and the results observed and any tweaks made. This process is illustrated in Figure 16.

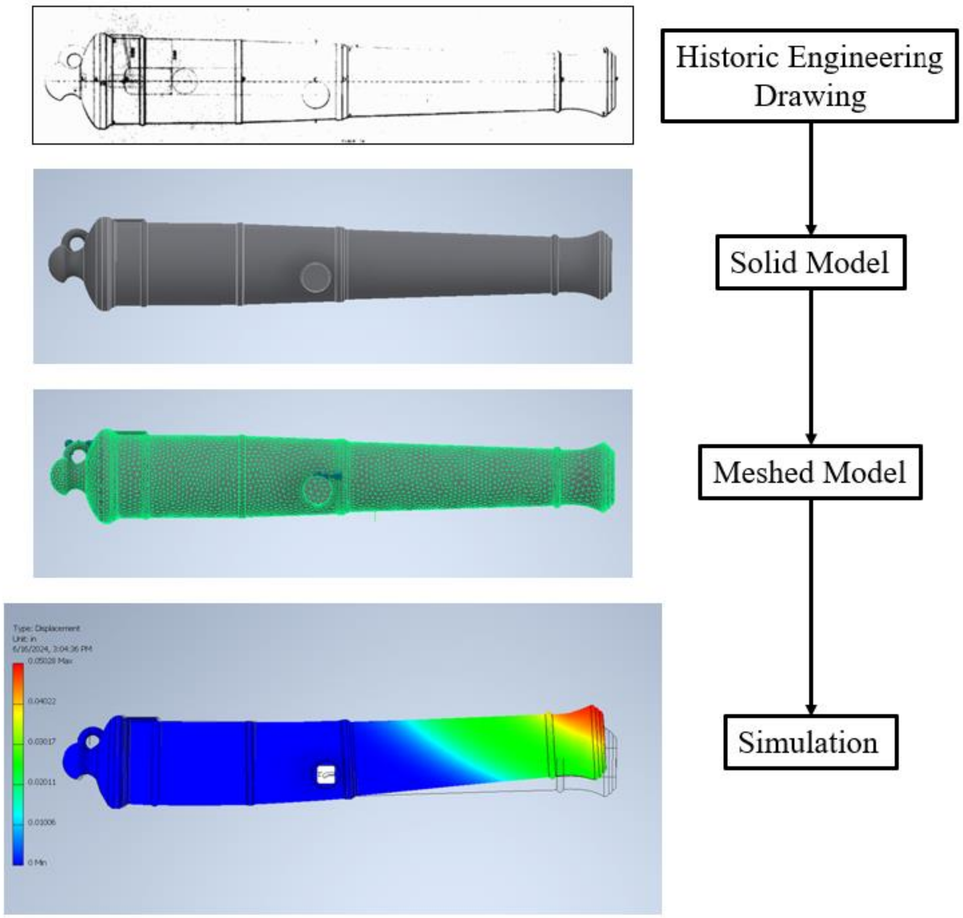

Figure 16: The basic CAD modeling process used for any FEA analysis. (Images by James Fowler from Autodesk Inventor.)

Basic Workflow for CAD Model Creation

As described in more detail later, even the most advanced CAD projects begin with a single point, referred to as the origin. From this point, lines can be drawn to create a 2D shape, and then that shape can be embossed to create a 3D shape of a certain depth, and so on and so forth, adding and subtracting space to create very complex shapes. CAD is utilized throughout the engineering field to design, develop, and reiterate parts in real time, significantly decreasing the amount of time necessary to get a product from the design phase into production. CAD programs are an extremely powerful tool which not only can be utilized for engineering tasks but can also be repurposed to help answer archaeological and historical questions by using engineering techniques. The CAD program utilized for this study is Autodesk Inventor Professional.

To create a cannon in a CAD program, the first step is to create a half profile of the cannon along the cannon's x–axis, that is, the axis of the bore. The creation of CAD models is where the extremely detailed measurements of the cannons, taken in the field, come into play. Utilizing the dimensions, a very accurate half profile can be created. Alternatively, a historic cannon blueprint can be utilized and simply traced onto the YZ Plane, as is visualized in Figure 17. To do this, under the Sketch tab, Start 2D Sketch is selected, and then the YZ Plane is selected as the base for the 2D sketch. From this, the blueprint is traced, or the cannon recording proforma consulted, to generate a 2D outline of the cannon.

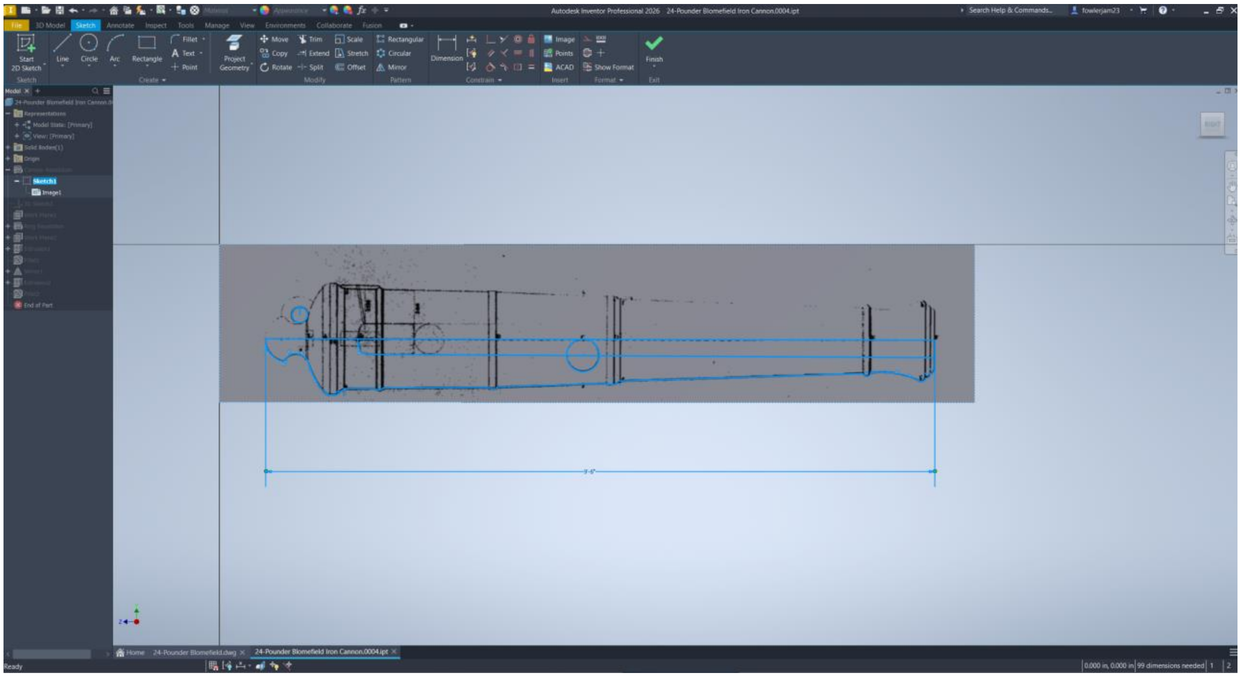

Figure 17: A cannon blueprint is traced in the YZ Plane. (Image by James Fowler from Autodesk Inventor.)

Cannons are considered roughly “axially symmetric,” which means any portion of the surface is equally distant from the centerline of the gun to any other portion of the surface, in a 360-degree arc perpendicular to the axis of symmetry, as depicted in Figure 18. This is very conducive to quick modeling. The first task is to consult the measurements and determine the diameter of the bore and halve that value to determine the radius of the bore. This value determines how far from the x–axis the profile of the bore will be drawn. Utilizing the archaeological measurements, the profile of the cannon is recreated, using the datum determined on the gun as described in the early subsection on Archaeological Data Collection– this is usually the front face of the gun, or some other conducive location. Each reinforcement ring is drawn in, every axially symmetric feature included. It is important to note that the end goal is to complete a “revolve” command, and revolve the profile around the x–axis, which means that only one half of the profile is necessary, as depicted in Figure 18.

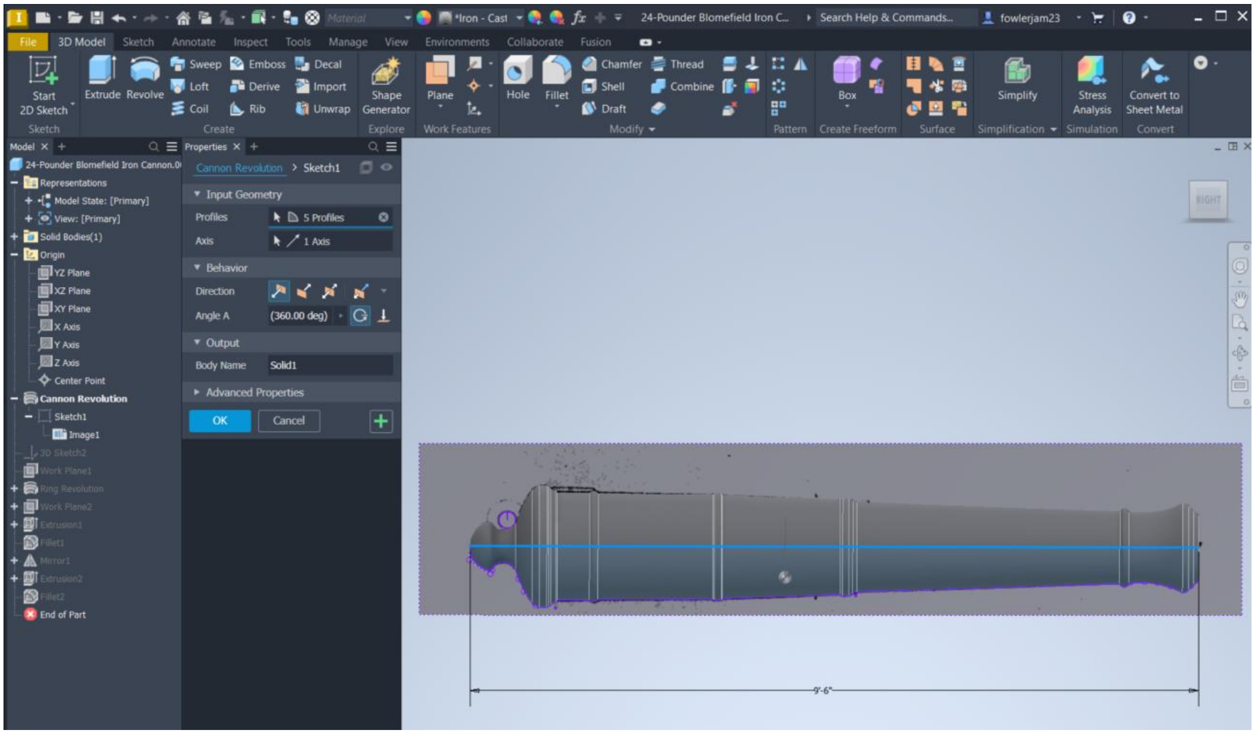

Figure 18: The Revolution window open, with the half cannon outline selected as Profile. (Image by James Fowler from Autodesk Inventor.)

This completes two tasks simultaneously: it halves the work necessary to complete the profile, but it also limits any misalignment and ensures a perfect “revolve.” Once the profile is complete, the “revolve” command can be processed and a solid model will be generated. To complete a revolve, under the 3D Model tab, select Revolve. When the Revolution Properties window is opened, the traced outline of half the cannon is selected as Profile. The centerline of the cannon is selected as Axis. This can also be seen in Figure 18.

From this point, all non–symmetrical features are added onto the cannon, including any cascabel rings, trunnions, or lifting rings. Once the cannon profile is revolved around the x–axis, further extrusions can be made to create the trunnions. Often, trunnions have a slight taper to them, and this must be accounted for. The circumference of the trunnion must be measured both at its end as well as where it terminates into the body of the cannon. It is to be noted that the length circumference of the trunnion is not the same as the length of the seam the trunnion makes as it intersects the cylindrical form of the cannon at different lengths along the trunnion's axis. That is to say, the length of the seam between trunnion and cannon is not equal to the circumference of the trunnion, that would only be true if the trunnion terminated into a flat plane that bisected it perpendicular to its axis. Instead, it is important to achieve a measurement of the trunnion's circumference exactly perpendicular to the trunnion's axis, as close to the cannon's body as possible. To add a feature like a trunnion, the profile of the cascabel is traced onto the YZ Plane from the blueprints, or oriented by utilizing the archaeological measurements. This method was similarly used for all non–symmetrical additions. Once a circle representing the trunnion on YZ Plane is present in the correct spot, it is extruded outwards perpendicular to the YZ Plane to create the trunnion. This is visualized in Figure 19.

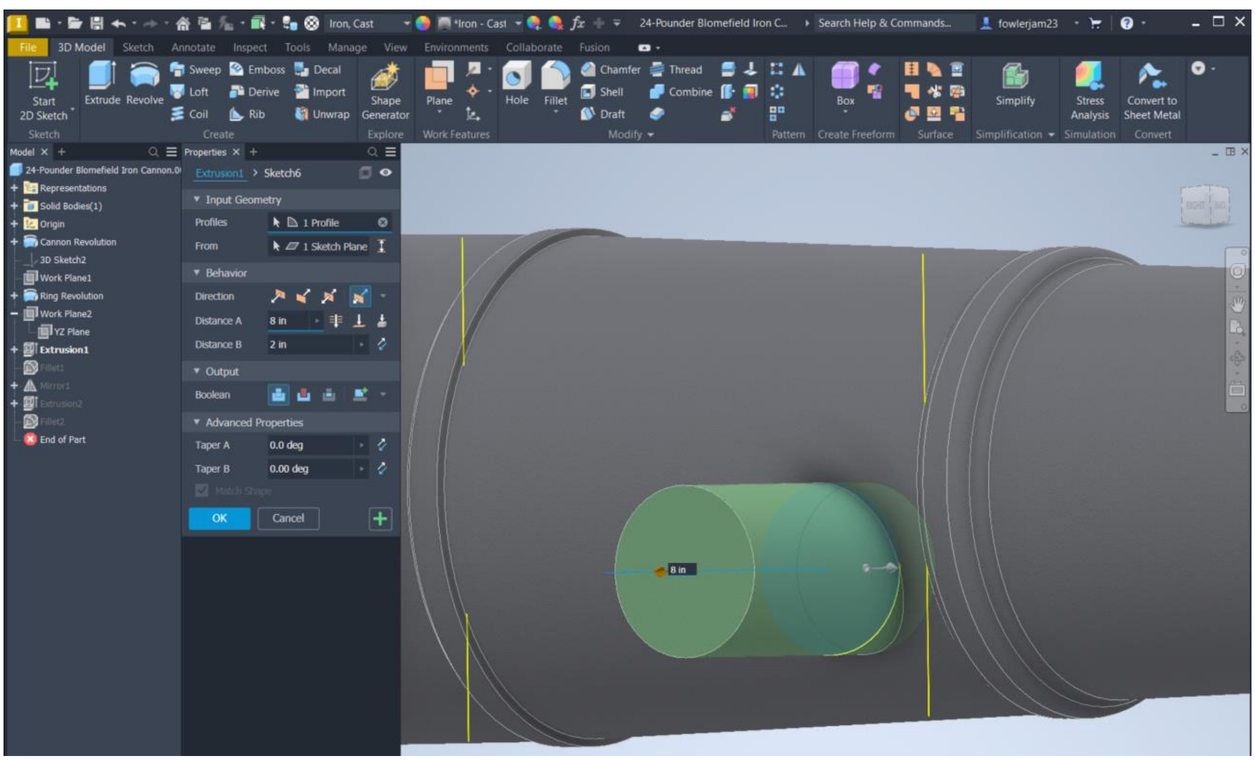

Figure 19: The Properties dropdown tab for a trunnion extrusion. (Image by James Fowler from Autodesk Inventor.)

Under the 3D Model tab, Extrude was selected, and the trunnion profile utilized for Profiles. The From box was filled by selecting the YZ Plane. Symmetric was chosen for the Direction box, indicating that the trunnions on both sides of the cannon are symmetrical to each other. Utilizing blueprints or archaeological measurements, the length of the trunnions originating at the centerline are input into the Distance A box. If the trunnions are non-symmetrical, a Distance B box will be present to input the other distance into. Boolean is selected for Output, to indicate that the extrusion is a net positive of material to the model. If any taper is indicated on the blueprint, or recorded in the archaeological measurements, it can be input in the Advanced Properties tab. Other details can be added in this stage, such as fillets, chamfers, or holes, if the model requires it. A very simplistic cannon may not have any of these features, but a more complex gun, such as the Blomefield 24–pounder utilized in the example, may require many additional features if called for in the blueprints. Sometimes the addition of other planes, such as offset planes, may be necessary to orient a feature correctly. For example, sometimes an additional plane is necessary to orient the bore of a weapon. To do this, under the 3D Model tab, Plane is selected, then Offset Plane. The new plane must be offset from an existent plane, and in the case of a bore, this plane would be the XY Plane. At this point, the plane is manually dragged out in front of the cannon model, however it is possible to input specific values to dictate the exact position of the plane. This is illustrated in Figure 20.

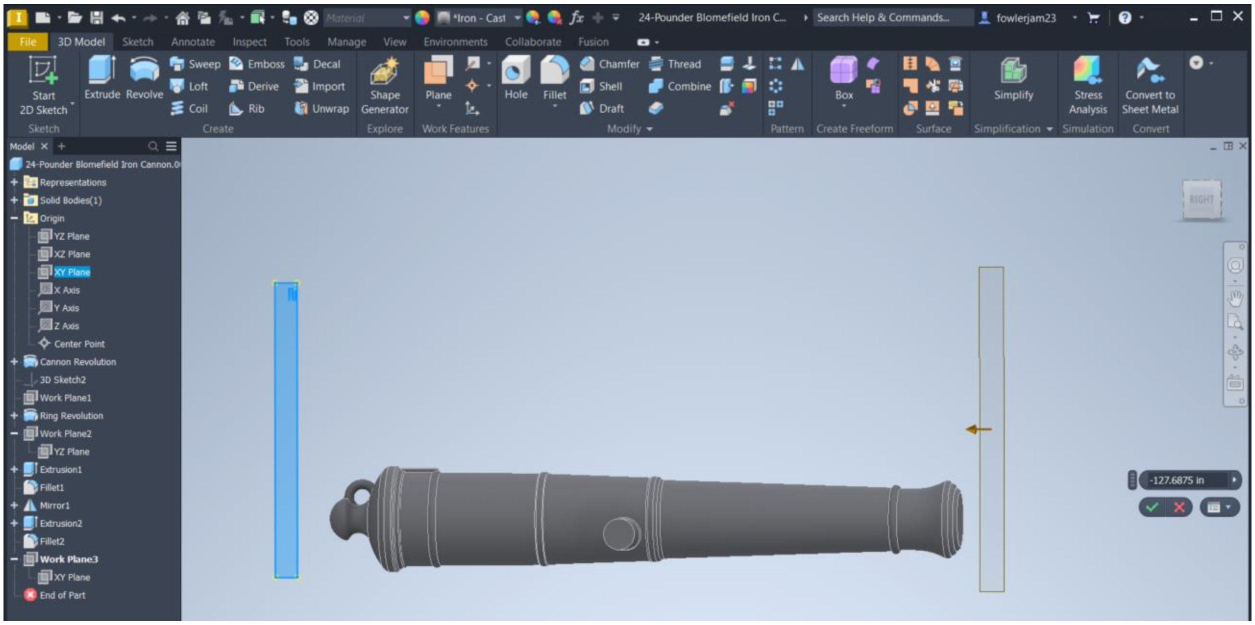

Figure 20: A new plane being created infront of the muzzle to facilitate adding a bore. (Photo by James Fowler from Autodesk Inventor.)

The final step is to assign all physical properties to the cannon, to help the program determine any applicable calculations. As it stands, a newly created model's material is "undefined," and to conduct FEA, the program needs that physical property defined. The material, as explained in Chapter Three, is related to everything– it defines yield strength, behavior at different temperatures, toughness, ductility, bulk modulus of elasticity, and all the other different aspects touched on. Many different types of cast iron material profiles exist, each which have their own specifications. For the purposes of this study, the most basic form of cast iron was utilized. To select this material, first the Tools tab was selected, then Material was clicked. In the Material Browser tab, "Iron, Cast" was chosen from the Inventor Material Library, and added to the model. It is at this point that a complete solid model for a cannon was made, and the model is fully prepared for analysis in the FEA suite. It is important to double check the dimensions of the cannon model, which can be done by opening the Tools tab, and selecting

Measure, and then utilizing the Measure tool to confirm the model dimensions match the archaeological data or the blueprint.

Educated Estimation during the Modeling Process

It is important to note that some dimensions cannot be easily measured during the archaeological evaluation, or are not included in the blueprints, and thus during the modeling stage, some estimation will always be required. A good example of a dimension that is very hard to measure is the profile of the interior breech end of the bore. Sometimes during the manufacturing process this is bored out as a cone, other times the bore terminates in a semicircle, yet other times it is simply a flat face. This depends on the design of the cannon, but regardless it is very difficult to measure precisely without cutting the cannon in half. If blueprints exist, utilize them here to gain this profile. If no such data exists, the methodology used here is observational in essence. With a flashlight, the cannon bore should be inspected and some determination made as to the profile of the breech end. Then, measurements of the depth of the barrel should be recorded. The rest is estimated, and this will be reflected in the cannon solid model. An easy stand in, if the breech profile is not known, is to assume it is a flat end, and simply draw the bore as a cylinder consisting of the depth of the cannon bore and the width of the bore radius.

Reconstruction of Internal Ballistics Calculations

The CAD model is of no use if the contextual data which drives the FEA is not fully understood. To achieve this, the appropriate forces that the cannon is subjected to need to be quantified. This includes the internal pressure of the powder explosion, among other things. Internal ballistics calculations are often developed to calculate a theoretical muzzle velocity, and several iterations of these calculations have been utilized over the centuries. The iteration selected to determine bore pressure for this study is derived from calculations of Benjamin Robins, who authored *New*

Principles of Gunnery, originally published in 1742 and republished as a second edition in 1805 (Robins 1805:7). This work includes Robert's theories of determining the internal ballistics of a black powder cannon, including a version of the bore force equation, which will be necessary to understand the force exerted upon the interior of a cannon to cause it to fail. If this number is known, it can be utilized in FEA to define the force expended on the interior of the gun. The next several paragraphs outline the methodology utilized to obtain a realistic estimation for pounds per square inch of pressure exerted on interior bore. This allows for the FEA software to accurately simulate cannon bursting dynamics. The Robins model is discussed, and then a contemporary alternative considered.

The Robins Equation

Robins made several assumptions to develop his equation, which is not expounded upon here for the sake of brevity. However, although more complex modern equations exist today which consider more variables, the Robins equation is accurate enough in limited instances. Additionally, it is one of the only equations designed specifically to measure bore pressure in early muzzle loading guns. The Robins equation was used extensively to design cannons during the late 18th century and was chosen as a starting point for this work due to its simplicity and relative accuracy (Robins 1805:74; Cooper 2024:163–174). The Robins equation has been iterated upon over the intervening centuries and was the basis for much of the work conducted by John Dahlgren in the 1850s, to design the last iteration of black powder muzzle loading guns (Cooper 2024:173).

The Robins equation considers several assumptions which are worth noting. Robins assumes that the force of the powder on the cannonball ceases as soon as the ball leaves the barrel. Robins also assumes that all powder of the charge is burned completely and converted into gas before the ball begins to move. Although these are both known to be inaccurate assumptions, and upon which a more contemporary mathematical solution exists, the difference if assumed otherwise in *some* cases is statistically insignificant and have been considered reliable (Ingalls 1912:2–3). Importantly, Robins acknowledges that as the cannon ball moves further down the barrel, the spike in pressure will decrease, followed by a rapid de–pressurization of the area behind the ball when it leaves the chamber completely (Robins 1805:74-75). Robins depicted this in a diagram, reprinted in Figure 21. Other authors have iterated upon this equation, including Charles Hutton in the 1770s and 1790s. Benjamin Thomnpson also built upon the Robins equations in the late 1790s, and designed experiments to measure pressure generated within a gun (Ingalls 1912:3–5). J. G. Benton in 1862 corroborated these results to some extent, and in the 1840s T. J. Rodman built further upon J. G. Bentons work by creating a similar graph utilizing a 42–pounder cut down at caliber intervals to obtain pressure readings at each interval (Guilmartin 2003:299; Benton 1862:29, Ingalls 1912:8–9). Robin's version of the pressure equation produced the diagram is depicted in Figure 21, and Guilmartin's version of the pressure diagram generated from T. J. Rodman's data is depicted in Figure 22.

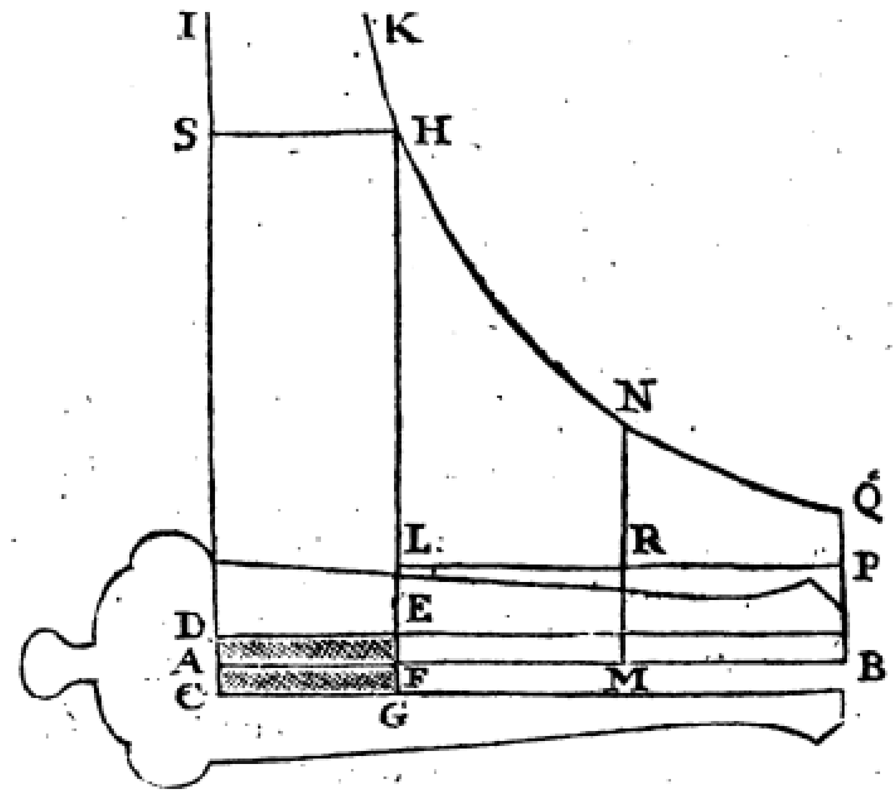

Figure 21: The pressure gradient as at different points within the cannon's barrel (Robins 1805:75).

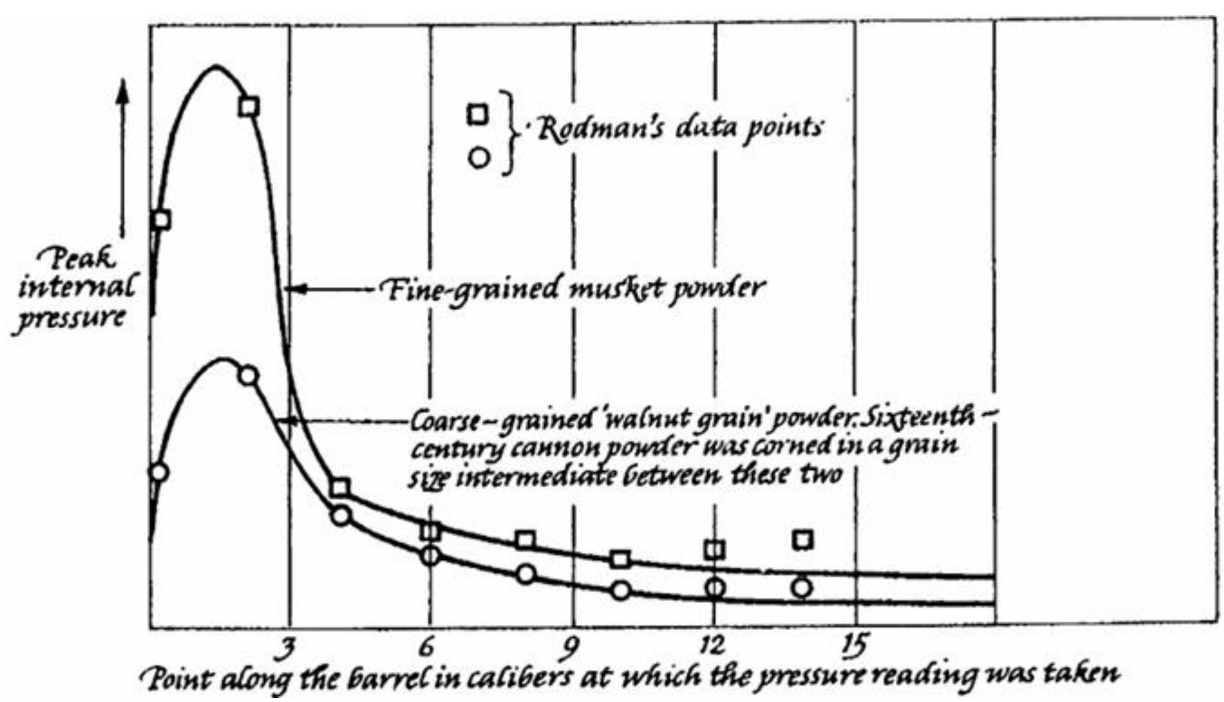

Figure 22: Bore pressure along the length of a cannon barrel, created by John F. Guilmartin based on data from T. J. Rodman's work (Guilmartin 2003:299).

In chapter one of his *New Principles of Gunnery*, Robins outlined the basic equation in Proposition VII, which defineds the pressure on the cannonball given any distance between the internal breech and the ball (Robins 1805:74–75, Collins 2025). The resulting Robins equation is depicted below in Equation 1:

Equation 1. $$F(x) = \frac{RP_{atm}Ac}{x}$$

Where:

$F(x)$ is the force exerted on the cannon ball.

R is the initial ration of gun powder gas to atmospheric pressure.

P_{atm} is the atmospheric pressure.

A is the cross-sectional area of the bore (or projectile).

c is the length of the barrel which contains powder before firing.

x is the distance from the internal breech face to the cannon ball.

Robins explained his equation in imperial units, and estimated R to equal roughly 1000/1, which is the value utilized for all the calculations (Robins 1805:76; Cooper 2024:163). P_{atm} is simply 1 atmosphere of pressure, equal to 14.7 pounds per square inch. A depends on which cannon is being measured. This equation was built upon, and more modern alternatives exist. As the propellant burns, it generates a predictable chemical energy, which is converted into pressure within the bore. This can be easily quantified in ideal gas law (Moran et al. 2018:90), stated below in Equation 2:

Equation 2. $$P_0V_0 = nR_uT$$

Where P_0 is pressure.

V_0 is volume.

n are moles of gas.

R_u is the gas constant.

T is temperature.

Modified Equation for Internal Bore Pressure

For this application, it is not known the exact moles of gas generated by the combustion of the propellent, nor is an exact temperature known. Both of these would be very hard to estimate with any degree of accuracy. Therefore, a new version of this equation must be derived that takes into account these unknown variables. However, as a means to combat Robin's assumption that all propellants are instantaneously converted to gas, the equation is multiplied by f, representing the fraction of chemical energy converted to gas pressure. f is often assumed to be around 0.5, considering only half the powder is utilized in generating pressure. This is because a good portion of the energy is expended in the form of heat, light, radiation, noise and kinetic energy of the gas. Some sources claim an f value a bit lower around 0.43, others higher; for this study the value of 0.43 was used (Guilmartin 2003:300; Sasser and Ford 2020:31). Additionally, the adiabatic exponent, also known as specific heat ratio, for gunpowder gas propellant was determined to be around 1.2 to 1.3, with some sources claiming as high as 1.4 (Sarrau 1883:6–8; Prentiss 1923a:117–122, 1923b:184–188). For the purposes of this study, 1.3 were used. Equation 3, the rearranged equation for internal energy of an ideal gas during an adiabatic process is as follows:

Equation 3. $$U = \frac{P_0 V_0}{\gamma - 1}$$

Where U is equal to internal energy.

γ is the adiabatic exponent for the propellant gas.

Rearranging again for pressure results in Equation 4:

Equation 4. $$P_0 \cong \frac{U(\gamma - 1)}{V_0}$$

Additionally, it is known that U, internal energy, can be described as the relationship of mass times specific energy, because specific energy is simply energy per unit of mass (Moren et. al 2018:230). This relationship is described in Equation 5.

Equation 5. $$U = E_g = fE = fm_p q$$

Where E_g is the energy of the gas.

E is the total energy.

m_p is the mass of the propellant.

q is the specific energy.

The specific energy of black powder was quantified to be around 3.5 megajoules per kilogram, and thus this value was utilized for q (Salzano and Basco 2012:727). However, m_p is not known, so to find m_p, Equation 6 was used:

Equation 6. $$m_p = \rho V_i$$

Where ρ represents the specific density of black powder.

V_i represents the initial volume taken up by the gunpowder charge.

The specific density of black powder was found to be roughly 1.7 to 1.8 grams per cubic cm (Benton 1862:44; Sasse 1985:9,18; PyroGuide 2025). Additionally, if initial volume of gunpowder is not known, a rule of thumb indicates that m_p is often equal to roughly 0.33–0.50 times the poundage of the gun. Thus, a complete equation for determining an approximate internal bore pressure, referred to now as Equation 7, is shown below:

Equation 7.
$$P_0 \cong \frac{(f m_p q)(\gamma - 1)}{V_0}$$

This equation was utilized to provide the FEA software with an accurate pressure load value to apply when constraining the simulation. It should be noted that this is a relatively simplistic equation that isn't designed for pinpoint accuracy, but instead provides a rough estimation of bore pressure given projectile location. A more accurate equation could have been constructed utilizing differential equations; however, this was avoided for simplicity's sake. It is of the utmost importance to ensure that all units are compatible so that the equation is calculated correctly. It is also important to note that as Robins pointed out in 1743, the pressure behind the projectile decreases as the projectile moves down the bore of the gun. The above equation accounts for this: as the volume of the space behind the bore increases, the pressure inversely decreases. Therefore, when modeling the cannons, the projectile was manually moved, and each associated volume value was input into the equation to generate accurate pressure values for that stage of the explosion and subsequent location of the projectile. For each gun, these values are cataloged in Appendix C.

Each cannon chosen for further analysis was subjected to a bank of pressure tests. This includes a pressure simulation at 20 cm (7.87 in) intervals, beginning at the initial location of the projectile when seated properly, with enough space between the projectile and the breech for propellant, wading, etc. From this point, 20 cm (7.87 in) intervals down the barrel of the gun were tested, utilizing a new volume measurement to inform an accurate pressure value. As the cannon ball proceeds down the barrel, the internal bore pressure drops off as the internal void behind the accelerating cannon ball increases, as depicted in Figure 21. This methodology allows each cannon to be tested at multiple stages of pressurization, to see if the changing pressure vessel profile can account for why some cannons failed the way they did. To initially set up Equation 7 properly, that means the value of x is set first to 20 cm (7.87 in), or the length of space which was taken up by the propellant, wading, etc., if known, and then increased from there in 20 cm (7.87 in) intervals. There are some limitations in this method, which are discussed in Chapter Six.

Application of FEA to CAD Models

Once a CAD model has been created, and the appropriate force determined from the modified equation, then all the ingredients necessary to conduct FEA are present. In this subsection, the appropriate method to subject a model to FEA are unpacked. However, it is important to note that there are several limitations and assumptions that must be acknowledged beforehand.

Explanation of Limitations and Justification of Assumptions

The nature of the CAD software implies several limitations and requires several assumptions on the part of the analyst. As described above, Robins determined in 1743 that the pressure within the gun decreases rapidly as the projectile moves down the barrel. However, in Autodesk Inventor Professional 2026, a functionality to analyze the dynamics of an explosion in an FEA suite is not included. Other software platforms are capable of such dynamic analysis but were not utilized in this study. Thus, several assumptions were made. To represent the ball in the chamber, a "plug" measuring 10 cm (3.93 in) long was placed within the barrel, creating in essence a sealed chamber. This plug was moved in intervals, and differing pressures were simulated at intervals or 20 cm (7.87 in). The initial interval was decided to be 10 cm or 20 cm (3.93 in or 7.87 in), depending on the size of the cannons bore, to replicate the space taken up by the powder charge. The plug was modeled to have a flat face oriented towards the explosion, as opposed to a hemispherical face, for two reasons. Firstly, the CAD software continuously failed to reliably mesh on high resolution in the region where the hemisphere interfaced with the bore wall. Additionally in examples when the mesh did not fail, more issues arose: because the hemisphere was fully stationary and not dynamic (like a ball would be in real life), the FEA software indicated incredibly unrealistic stress concentrations in the acute angle region between the hemisphere and the bore wall. These results were well beyond reasonable internal ballistics portfolios, and if used, would have heavily skewed the data. When a flat face on the plug was utilized, the stress characteristics fell within an expected and realistic range. Thus, given the limitations of the software, a less–realistic but acceptably–accurate representation of the ball was created utilizing instead a flat–faced cylindrical plug.

Process Workflow for FEA Modeling

Once a model of a cannon is completed, the next step is to apply Finite Element Analysis to the model. Simply put, Finite Element Analysis deconstructs larger objects into a matrix of polygonal surfaces, the utilizes partial differential equations to simulate the dynamics of each polygon relative to each other, and relative to a defined three–dimensional axis. This functionality allows the software to estimate how the object will behave by analyzing the matrix of individual polygons (Autodesk 2026). The software does this by solving complex mathematical equations which approximate the real–world laws of physics. According to Autodesk, "FEA software can handle far more complex geometries, multiple physics effects simultaneously, and large-scale problems quickly and accurately [when compared to manual calculations]" (Autodesk 2026). The purpose of the software is to accurately model real–word forces such as stress, vibration, heat, fluid dynamics, and fatigue to help engineers understand how an object will react under a variety of conditions.

This requires beginning a simulation. Two programs were utilized to conduct FEA analysis: the onboard stress analysis simulation software within Autodesk Inventor Professional 2026, as well as Autodesk Nastran FEA software, which is a more advanced software plugin to Autodesk Inventor Professional 2026. Both have very similar workflows. The simulation process was initiated in Autodesk Inventor. In the 'Environments' tab, the 'Stress Analysis' tool was selected. Conversely, if Autodesk Nastran was utilized, the 'Autodesk Inventor Nastran' tool was selected. This opened a new tab at the far right of the tab ribbon called 'Analysis'. The material assigned to the model must be confirmed, thus allowing the FEA software to select those material properties for the simulation. To do this, the 'Material Assign' tab was selected, and the material was confirmed. If for some reason the default material was incorrect from the one selected during the CAD modeling process, simply search for and select the correct material in the 'Material Browser'. For more information on the material properties critical to accurate FEA simulation, refer to Chapter Three. The layout of the ‘Analysis’ tab is visualized in Figure 23.

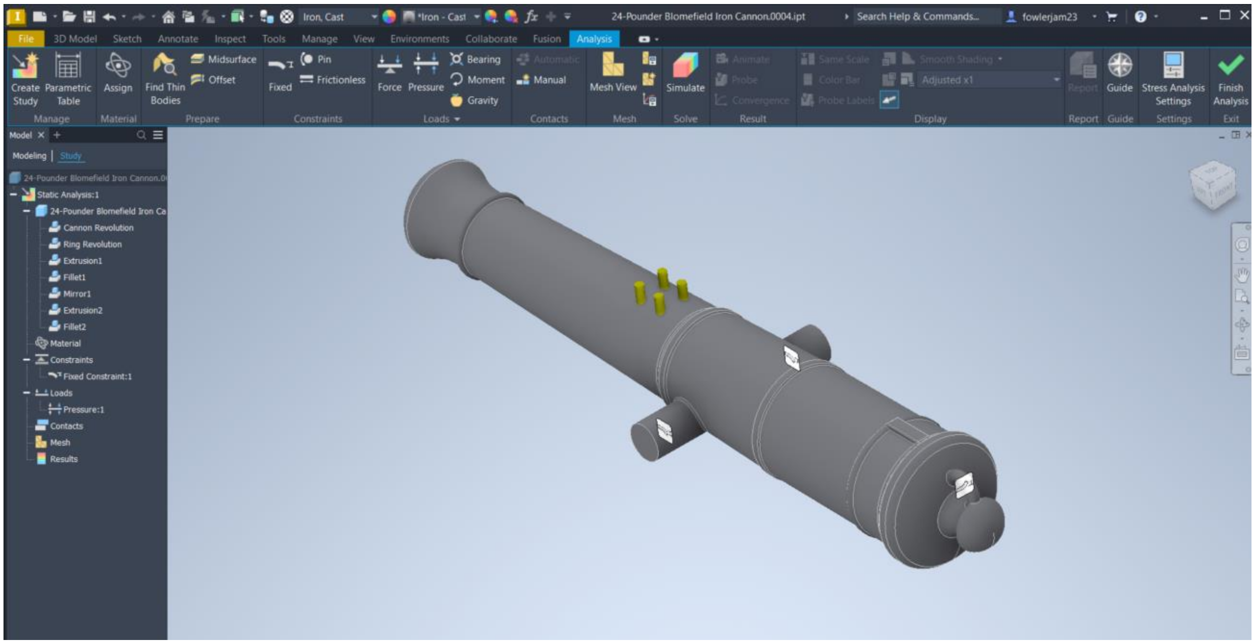

Figure 23: The Analysis tab in Autodesk Inventor, utilized for conducting FEA simulations. (Image by James Fowler from Autodesk Inventor.)

Additionally, the model must be constrained in a realistic way. This was achieved by using a fixed constraint option on the trunnions and cascabel of the guns, simulating the weapon being mounted to a carriage, and secured with breeching lines around the cascabel. To complete this, the ‘Fixed Constraints’ tool was selected after first selecting the faces of the constrained features. At this stage, forces of gravity were selected for the FEA simulation, to ensure the model was subjected to the forces of its own weight in the vertical axis. This was done by selecting ‘Gravity’ in the ‘Loads’ tool in the ‘Analysis’ tab. Additionally, a force was subjected to the weapon. This was done by selecting the interior bore walls, interior breech face, and interior surface of the projectile, forming an enclosed three-dimensional volume. Sometimes it was easiest to select these faces if a cross section of the cannon model was created during the CAD process. To set up the pressure force, the ‘Pressure’ tool was selected in the ‘Loads’ tab under the ‘Analysis’ tab. The ‘Pressure’ window will open, and this was where the very important pressure value, determined by the modified equation derived in the above Modified Equation for the Internal Ballistics Calculations subsection, was input. Once all the above-mentioned settings are in order, the model was meshed. A meshed model is illustrated in Figure 24.

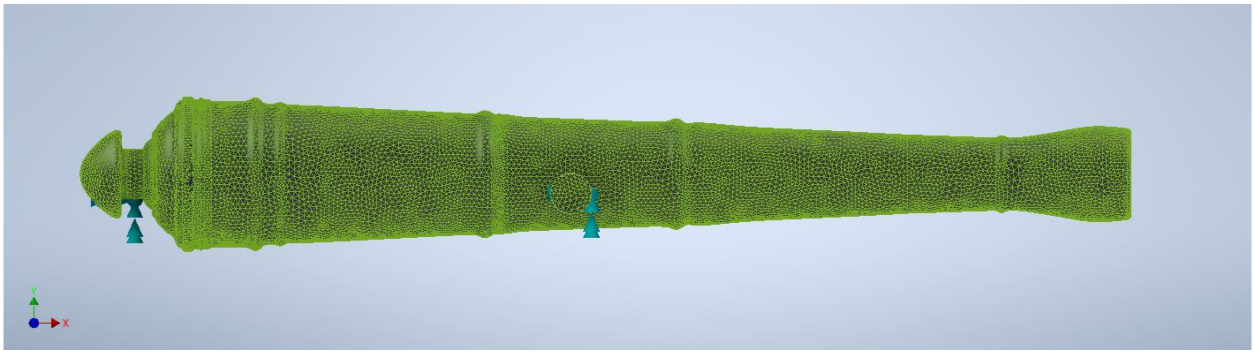

Figure 24: A meshed model of a cannon. Note the arrows on the trunnion and the cascabel indicating those regions have been constrained. (Image by James Fowler from Autodesk Inventor Nastran.)

To mesh a model, the ‘Mesh View’ tool was selected and a mesh was run. If the mesh fails to generate, it is good practice to access the ‘Mesh Settings’ tool and decrease the maximum size of the polygons, which will take longer to mesh, but will result in a higher–definition model which is less likely to crash. At this point the model was prepared for a simulation.

To run a simulation, the ‘Simulate’ tool was selected in the ‘Solve’ tab within the ‘Analysis’ tab, and the simulation was run, and the results were displayed. For each distance of the projectile within the bore evaluated, the model was edited, the cylindrical plug was relocated the correct distance from the interior breech face, and the simulation was re–run. Extensive examples of completed simulations are displayed in Chapter Six.

When analyzing the FEA results, the quantity of different force graphs which become generated can be overwhelming. Displacement, 1st Principle Stress, 3rd Principle Stress, Von Mises Stress, and Factor of Safety graphs are the primary five that most FEA software platforms generate by default. Only a few of these are important for this analysis. When determining a material's yield strength, often this is done by utilizing a simple tensile test to reach the material's yield point. However, in application, systems of stress are often much more dynamic and harder to model. The material often has both shear and stress components acting in all three axes: the x–, y–, and z–axis. The Von Mises Stress graph is a derivation to convert this very complicated stress profile into an equivalent tensile strength, to aid in direct comparisons (Autodesk 2014). Thus, this study focused on the Von Mises Stress results, as well as the Displacement graph results, and the Factor of Safety results.

Value Parameters for FEA Analysis

An integral aspect of the methodological process is the accurate interpretation of results. To aid in this, some information is divulged to clarify the methodology for interpretation of various engineering parameters, such as Von Mises Stress, Displacement, and Factor of Safety. An explanation of what is considered a high, nominal, or low value is required to fully appreciate the analysis technique. While initially complex, such parameters are easily explained to allow for complete understanding.

Von Mises Stress Parameters

As discussed at length in Chapter Three, what determines the parameters for the observed stress within a cannon is directly related to the physical properties of cast iron. As stated earlier, the materials' Von Mises Stress is a method to convert a matrix of stress vectors into an equivalent tensile strength. Cast iron has a yield strength of around 39,885.4 psi (275 MPa) and an ultimate tensile strength of around 58,015–116030 psi (400–800 MPa) depending on metal grade (Groover 2012:53). For the purposes of this study, any Von Mises Stress seen below 39,885.4 psi (275 MPa) will be considered nominal, any above that will be considered high. Because the exact grade of cast iron utilized on the guns in this study is currently unknown, an estimation will need to be made, and therefore any Von Mises Stress seen above 72,519 psi (500 MPa) will be considered at or exceeding the material's ultimate tensile strength, and the metal will be considered to have failed within whatever isolated region such parameters are met.

Displacement Parameters

Displacement is more relativistic to properly gauge, and thus no fixed numerical value is associated with "high" versus "low" displacement. However, cast iron, as described in Chapter Three, is very brittle relative to other materials, and cannot undergo significant deformation before failure. Therefore, any deformation of below 1% of the material's overall dimension will be considered nominal, anything above this value will be considered substantial. For example, if a cannon barrel 20 cm (7.87 in) in diameter bulges 0.5% in displacement, the displacement value would be 2 mm (0.07 in). For example, if 1 mm (0.04 in) of displacement is measured, then it would be considered nominal. If, however, the observed displacement was 3 mm (0.12 inn), this would be considered a high displacement and not nominal.

Factor of Safety Parameters

Factor of Safety (FoS) parameters are simple to define. As stated earlier, FoS is a unitless, always–positive ratio describing the ability for a system to withstand its required load. Mathematically, FoS is described as the material's strength divided by the applied stress (Budynas and Nisbett 2015:18). Thus, if the material's strength equals the applied stress, the FoS equals 1.0. However, in "real life," a FoS should never be as little as one. Instead, systems are always over engineered to withstand loads larger than the bare minimum to account for misuse, wear and tear, and fatigue. For this study, a FoS of 1.0 will be considered nominal. A FoS between 3.0 and 1.0 will be considered optimal. Any FoS lower than 1.0 but larger than 0.0 will be considered too low and will be interpreted to indicate imminent failure within whatever isolated region such parameters are met.

The Correct Interpretation of FEA Results

Additionally, the FEA graphs are generated in a color spectrum, however it is important to note that the colors themselves do not mean anything when disconnected from the scale. An example of an FEA graph is that generated for BR–01, the 24–pounder Blomefield, which is depicted in Figure 25. The color red indicates high values, blue indicates low, green is in the middle. However, what is depicted red, indicating a high value for one graph might be considered a low value for another graph, and shown in blue. For example, large 36–pounder gun might show Von Mises Stress on the inside surface of the barrel at 39,885.4 psi (275 MPa) and be depicted in its FEA Von Mises Stress graph in the color red, indicating a high stress parameter. However, in a different graph, for perhaps a smaller 6–pounder cannon, under the same gunpowder load, very high Von Mises Stress values may be encountered, and the peak stress observed is 72,519 psi (500 MPa). In this case, the 39,885.4 psi (275 MPa) stress may be depicted as blue, because it is not nearly the highest stress seen in that FEA simulation.

Furthermore, when an FEA result graph of a cannon is generated, the researcher has the option to view the cannon in “realistic displacement” or “exaggerated displacement.” Exaggerated displacement is useful for instances when the displacement values are relatively low, such as less than an inch, and differentiating between a graph with displacement and without displacement may prove difficult to the naked eye. Cast iron, which has a very low displacement tolerance, is a good candidate for utilizing the exaggerated displacement feature, to allow researchers to more readily identify the areas where displacement is occurring. This feature will often result in graphs which appear unrealistically “ballooned” or deformed, however this is not a realistic representation but instead an exaggerated representation to more readily visualize trends. All exaggerated displacement graphs will be labeled as such in this study. An example of an exaggerated displacement graph can be seen in Figure 25.

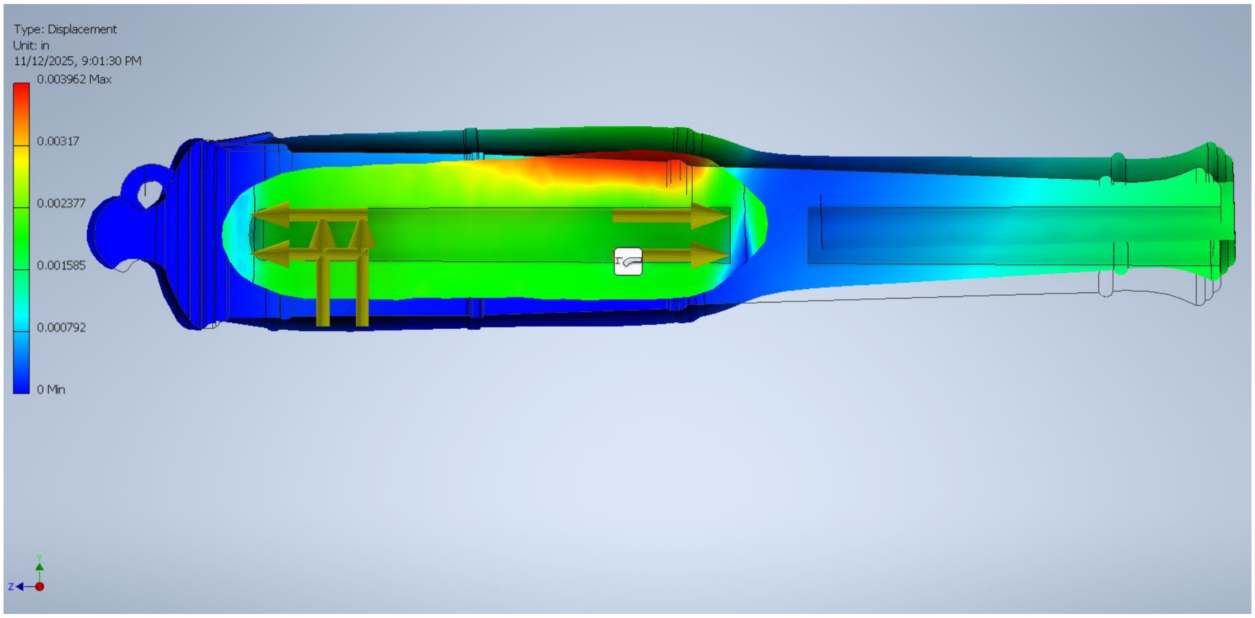

Figure 25: FEA graph for BR–01. Exaggerated displacement is shown. Note the scale on the left, indication of the type of graph displayed, the values associated with the colors, and the axis in the lower left corner. Also present are yellow arrows indicating the pressure values assigned to the barrel, the back breech face, and the front projectile face. (Created in Autodesk Inventor by James Fowler.)

Additionally, it is worth noting other features within a cannon FEA graph. Yellow arrows within the graph are indicators of the presence of pressure values assigned to various surfaces of the CAD model. These are not important to the study themselves; they only indicate to the operator that various forces are present but otherwise should be ignored for the interpretation of results. It can also be noted that in the bottom left corner, a small axis exists which may help inform the reader as to the orientation of the gun in three-dimensional space. Graph type, units, and a timestamp of the simulation are also included. An outline is also present, indicating the original location of the cannon before the discharge took place.

Methodological Limitations

The unfortunate reality is that no large collection of exploded guns exists in one easy location. Exploded guns are sprinkled throughout the world, in accessible and inaccessible places, both on land and underwater. Perhaps the most challenging limitation encountered was the required travel to access and measure guns around the world. This resulted in several statistical skews that should be acknowledged. The best data on cannons is pulled from locations in which the research was the easiest to carry out. For example, cannons on the east coast of the United States were easily accessible to the author and comprise the foundational corpus of high–resolution data. These cannons were accessible, and time was often not a consideration when measuring and recording them. As much time as was necessary to achieve very detailed accounts of the cannon could be spent, and thus very detailed measurements could be achieved.

This contrasts with data collected on cannon located in far-off places, especially where research was not the primary objective of the trip. In these instances, only a small amount of time could be dedicated to quickly record what was possible. An example of this situation would be data collected on cannons recorded on the island of Malta. Due to time constraints, data from cannons recorded in Malta are limited to scaled archaeological photos and some photogrammetric data. No detailed site recordings, measurements, or detailed descriptions exist for these guns.

A third category of data resolution is comprised of cannons recorded not by the author but by another source. Sometimes these are recorded by trained archaeologists or historians, other times by citizen scientists. Considering the wide range of training, any data pulled from this pool must be examined with a critical eye. However, a global study such as this would not be possible on one graduate student's budget, and thus this data is exceptionally useful despite its low resolution and must be considered. For example, guns recorded through past East Carolina University field schools, or by archaeological organizations around the world, represent a high–resolution example of this kind of data. Even though these organizations were not recording guns with the knowledge of what the data would be later used, they did so with such precision that further analysis is feasible. An example of a low–resolution dataset would be an individual taking a few photos of a gun and posting them to a website. Often, no scale items exist in such reports and no archaeological measurements are recorded, but from the photos alone, a reasonable evaluation of the gun's condition and failure mode can be made.

Determining Cannon Failure Classifications

A final word must be said to acknowledge the methodology of cannon failure classifications, outlined in the next chapter and in Chapter Six. A useful classification for cannon failures can be developed in several ways, however simply describing the physical, visual characteristics of cannon failures does not imply causation, and isn't useful in interpretation of cannon failure modes. An arbitrary classification based on visual cues of any kind will not only be unhelpful but in some cases down–right misleading. A cannon which fails 10 cm (3.93 in) aft of the muzzle may be visually similar to a cannon which fails 40 cm (15.75 in) aft of the muzzle, and it might be tempting to include both these as similar failures in an arbitrary visual classification– an argument can be made for both.

A classification could also be built without reference to the visual characteristics at all and only based on interpretation of engineering simulation data. However, because of the vast and minute differences in cannon material makeup, as well as various design characteristics which cannot be quantified in the accessible engineering analysis software, this method would result in a different set of limitations. A cannon failure classification cannot be generated with any degree of accuracy based solely on data from simulations, because such methods are only a tool through which information can be processed. Without a dialogue between the archaeological evidence and the simulation evidence, no truly precise and useful picture of failure profiles can be generated.

Additionally, a classification could be determined only through consulting historic primary sources on cannon failure. These sources are often very detailed and contain precise interpretations from engineers at the time, interpreting how and why cannons failed the way they observed. However, this method has some rather obvious flaws as well: it would not consider the limitations in precise analysis technology available when those sources were first generated. In Chapter Six an attempt is made to reconcile all three possible rationales for failure classification to generate a useful method for interpreting physical examples of failed cannons in the archaeological record, as well as a method to interpret descriptions of exploded cannons in the historical record. Only at the intersection between archaeological data generated in the field, data gathered from analyzing historic sources, and trends indicated from the implementation of engineering software can a useful classification be generated.

Chapter 5: Failed Guns in the Archaeological Record

Introduction

To feasibly compare cannon failure patterns, a robust collection of various exploded cannons extant in the archaeological record must be recorded. In this chapter, a comprehensive list of the recorded guns is presented. Some of these guns are later be subjected to FEA simulations in Chapter Six as archetypes of various failure patterns, however this chapter aims to catalog and discuss the larger database in detail, with information given on the location, condition, archaeological status, and fieldwork conducted on the guns. Throughout the data collection process, many cannons were recorded or otherwise documented. Guns were recorded in multiple locations around the world. Most of the exploded guns documented are located in either the United States, Malta, and Finland, and thus results are skewed for those regions. This is due to multiple reasons, including funding constraints, opportunities to conduct research in these regions, and a high density of preserved guns located in these places. The global scale of this project is displayed in Figure 26.

Figure 26: Global locations of various exploded guns recorded for this study. British guns are demarcated in red, Swedish in blue, and unknown in yellow. (Image created by James Fowler using Google Earth.)

Exploded guns located in Europe are displayed in Figure 27, and those recorded in North America are displayed in Figure 28. British guns are indicated in red, Swedish guns are indicated in blue, and unknown guns are indicated in yellow.

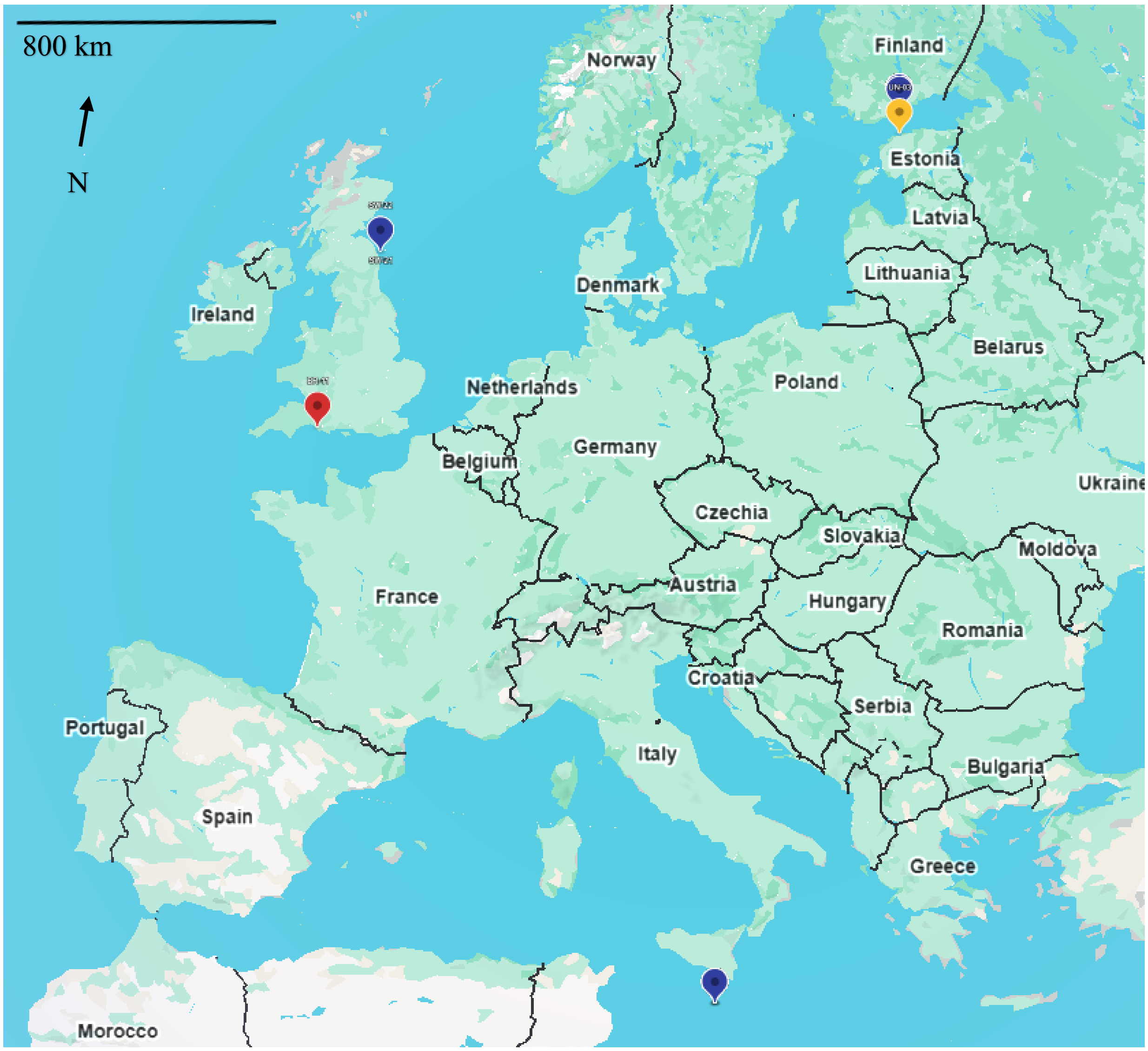

Figure 27: The locations of exploded guns in Europe. British guns are demarcated in red, Swedish in blue, and unknown in yellow. (Image created by James Fowler using Google Earth.)

Figure 28: The locations of exploded guns in North America. British guns are demarcated in red, Swedish in blue, and unknown in yellow. (Image created by James Fowler using Google Earth.)

Close up maps of the location of some guns documented for this study are included. Figure 29 depicts the locations of failed guns located at Fort St. Elmo, in Valetta, Malta. Figure 30 indicates the location of failed guns at Suomenlinna Fortress in Helsinki Harbor, in Finland.

Figure 29: The locations of exploded guns in Fort St Elmo, Malta. British guns are demarcated in red, Swedish in blue. (Image created by James Fowler using Google Earth.)

To categorize this study, each cannon was assigned a unique identifier to aid in differentiating every gun. The cannons are organized in alphabetical order according to their nation of manufacture (if known) and the nomenclature of the unique identifiers is as follows: AA– ##. The first two letters indicate the national origin of the gun. British guns were designated "BR," Swedish guns "SW," and Unknown guns "UN." The second two numbers were assigned in numerical order to identify the gun relative to others in the category of national origin. Of course, many other national origins exist, but no guns manufactured in other nations besides those listed above were recorded for this study. Additionally, a condition has been assigned to each cannon, to indicate "at a glance" the level of preservation observed; these are "excellent," "good," "poor," and "very poor."

Figure 30: The location of a large cluster of failed Swedish guns at Suomenlinna Fortress, Finland. (Image created by James Fowler using Google Earth.)

Excellent indicates a level of preservation such that all markings were clearly legible. Good indicates that some of the markings were legible, or that fine details on the gun were mostly preserved. Poor indicates that few markings and fine details were visible. Very poor indicates that the gun was heavily corroded or poorly preserved, and no fine details were observable at all. A complete list of all known failed guns, both those used for this study and those not included, can be seen in Appendix D.

British Cannons

British guns often prove easy to identify and also common in the archaeological record. British guns are characterized by muted and utilitarian designs, which in the later 18th century become highly standardized, driven by the need to simplify logistics aboard ships (McConnell 1988:17,69,144). Perhaps most ubiquitous are the Armstrong and Bloomfield pattern cannons, however later developments produced the Millar pattern guns used during the Crimean War and other mid–19th century conflicts (McConnell 1988:27–28, 150; Tucker 1989:96–99,118). Armstrong guns are identifiable by their round cascabels, simplistic and robust barrel design, and less ornate embellishments. Bloomfield pattern guns are very recognizable due to the presence of a large breech ring on top of the cascabel (Tucker 1989:118). Most British guns have easily–identified and standardized markings on them, which have been thoroughly cataloged to aid in identification (Brown 1989:321–329). Guns cast before the widespread implementation of gun standards within the British royal armed forces still tend to follow some trends, although these are often harder to positively identify. What follows is a list compiled of every British gun recorded for this study which showed signs of damage.

Cannon BR–01: British Blomefield 24–Pounder

This cannon was recorded by East Carolina University graduate student Raymond Phipps during the 2022 ECU Field School to the island of Antigua, and is depicted in Figure 31 (Phipps 2023:9–12). The gun is in excellent condition, is currently located on the Blockhouse Ruins at the Nelson's Dockyard National Park, and is roughly 1.27 m (3.28 ft) in length, and 48 cm (18.89 in) in diameter.

Figure 31: A photogrammetric model of Cannon BR–01, 2022. (Image courtesy of East Carolina University Maritime Studies Department.)

Thomas Blomefield (1787–1815) designed the British Blomefield line of naval guns specifically to answer the artillery needs of the Royal Navy (McConnell 1988:27–28; Tucker 1989:118). The weapon was intentionally designed in a more robust fashion to lessen the likelihood of bursting or other failures (Henry 2004:45). The weapons were produced in various weights, but the 18– and 24–pounder variants saw the most widespread adoption (Tucker 1989:149–150; Mehl 2002:30).

The breech of the weapon is characterized by a more rounded, convex profile, and the inclusion of a large loop cast into the top of the cascabel, as seen in Figure 32 (Tucker 1989:118). This loop was included in the design to facilitate better control of recoil. Traditionally, "breeching lines" were employed to control recoil by fastening both ends to iron loops attached to the inner hull of the ship, on either side of the gunport (Cooper 2024:114–115, 117). The midsection of the rope was then wound around the cascabel, and then the whole rig was tightened to prevent uncontrolled recoil. In previous iterations of naval guns, the breeching line was simply wrapped around the cascabel, but on the Blomefield design, a loop was included on the top of the cascabel to eliminate any possibility of the breeching line slipping from the cascabel during firing (Mehl 2002:29).

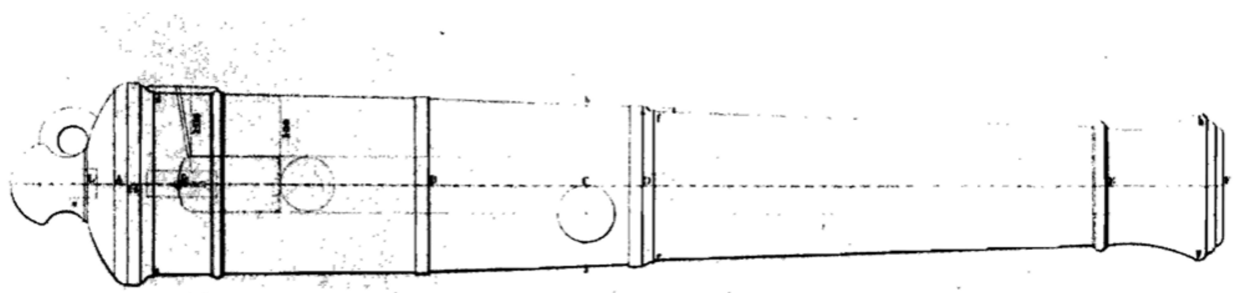

Figure 32: British Blomefield 24–pounder engineering drawing (McConnell 1988:74).

Cannon BR-01 has the coat of arms of George III cast into the top of the barrel between the second and third reinforcement bands, directly over the trunnions (Mehl 2002:28). An English “broad arrow” symbol, utilized to demarcate weapons owned by the British royal military, is also located in this region, between the first and second reinforcement bands (ECU Maritime Studies 2022). Both trunnions include identification marks. The left trunnion is stamped with “WCo,” indicating that this particular weapon was cast by the Samuel Walker and Company Foundry in Rotherham, United Kingdom (UK) (Mendel 1965:178; Brown 1988:105). The right trunnion is stamped with the numbers “505,” indicating the weapon’s serial number. The top of the piece has a vent platform drilled to accept a flintlock ignitor, indicating previous deployment onboard a Royal Navy vessel (Tucker 1989:32). The cannon was retired from front line service in the Royal Navy and relinquished to Antigua to be used as a coastal defense gun

(ECU Maritime Studies 2022). Once retired, the gun likely saw less routine maintenance and a lower standard of upkeep, resulting in a degradation of the gun's condition. This example is missing the entire barrel about one meter forward of the trunnions. No diagnostic information is available concerning the gun's failure, only that it exploded during firing.

Cannon BR–02: British 8–inch 65–Pounder Smoothbore Shell Gun

This cannon is likely an early 1840s shell gun recorded by James Fowler at Fort St Elmo in Valletta, Malta, on 6 December 2024, and is in good condition, as depicted in Figure 33. Not much is known about this gun aside from its general level of preservation and the large portion of the weapon that is missing. It is surmised that this is an 8–inch 68– or 65–cwt (hundredweight) Shell Gun with a Millar pattern breeching ring, as depicted in Figure 34 (McConnell 1988:96–99; Tucker 1989:150; Mehl 2002:38). This class of weapon was developed as an iteration on the Blomefield Pattern guns, replacing them in the battle line in the mid-1800s (Tucker 1989:148). The Millar pattern breeching ring was the first widely utilized feature to fully replace the cascabel, in essence combining the cascabel with the breech ring.

These weapons saw extended service in the British empire throughout the mid–1800s, participating the Crimean War and other colonial conflicts (Mehl 2002:38). Considering the timeframe for these guns, it is not surprising that the coat of arms of Queen Victoria is cast into the top of the barrel directly above the trunnions, forward of the first reinforcement band (McConnell 1988:96–99). Additionally, the number "13" is cast directly forward of the crest, possibly a serial number. On the right trunnion, the letters "B.P. & Co" are cast into the face, indicating manufacture by the Bailey, Pegg and Company, as seen in Figure 35 (Royal Archives 2025). Additionally, the serial number ("728 ov") is barely legible above the manufacturer's stamp.

Figure 33: Cannon BR–02, 6 December 2024. (Photogrammetric model created using Agisoft Metashape by James Fowler.)

The face of the trunnion is heavily corroded, further conservation may indicate that the markings were misidentified by the recorder. Two large lines run across the face of the trunnion, one from top to bottom and one from left to right. On the top of the barrel a large English broad arrow stamp is present, indicating service in the British military. Additionally, the number “4” is located aft of the broad arrow. This marking is heavily corroded. The left trunnion has no discernable markings whatsoever. These can be seen in Figure 36.

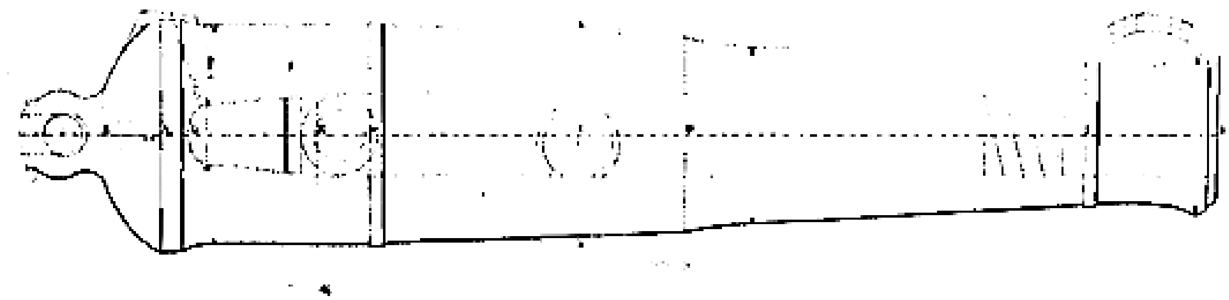

Figure 34: 8–inch Millar Pattern Breechloading Gun Engineering Drawing (McConnell 1988:99)

Figure 35: Cannon BR–02, left trunnion, recorded 6 December 2024. (Image courtesy of James Fowler.)

Figure 36: Cannon BR–02, top view, note the crest and the broad arrow stamp, recorded 6 December 2024. (Model created in Agisoft Metashape by James Fowler.)

Cannon BR-02 shows significant damage consisting of a variety of sources. The most obvious failure is the barrel, sheared off directly forward of the trunnions. The failure point on the barrel is somewhat anomalous, and it cannot be determined if the cannon failed due to a burst barrel, or instead if the barrel was cut off using an acetylene torch. Either way, this weapon was subjected to significant n–transforms and c–transforms. Possible damage due to an acetylene torch is depicted in Figure 37 and Figure 38.

Figure 37: Cannon BR–02, damaged Millar–pattern breech ring, recorded 6 December 2024. (Image courtesy of James Fowler.)

The cut region shows signs of bubbling due to molten iron, and a curious ring is visible, possibly indicating a first pass, followed by a second pass with a cutting torch. Possibly, the cannon was used as a bollard and was later cut up and removed as a bollard, resulting in the barrel being removed, as was exceedingly common in Malta, depicted in Figure 39. Additionally, the entire breech area of the gun shows distinct signs of n–transforms such as corrosion not present on the forward area of the gun, further indicating possible burial of that portion of the weapon, shown in Figure 40. The weapon is roughly 1.52 m (4.99 ft) in length and 53 cm (20.87 in) in diameter.

Figure 38: Cannon BR–02, damaged area, possibly cut with an acetylene torch, 6 December 2024. (Image courtesy of James Fowler.)

Figure 39: Cannons used as bollards are common in Malta. Several holes in the sandstone, where bollards used to exist but were removed, were also noted. This example was located in Valletta Harbor, near Fort St. Elmo (author for scale). Recorded 7 December 2024. (Image courtesy of James Fowler.)

Figure 40: Cannon BR–02, red arrow indicates breech area heavily corroded, consistent with damage from burial, recorded 6 December 2024. (Image courtesy of James Fowler.)

Cannon BR–03: British 6– or 8–Pounder (uncertain)

This cannon is likely a mid-1700s 6– or 8–pounder recorded by James Fowler at Fort St Elmo in Valletta, Malta, on 6 December 2024, and is in poor condition. The weapon is heavily damaged and missing the last 30 cm (11.81 in) of the muzzle, as indicated in Figure 41. Additionally, it is missing the left trunnion.

Figure 41: Cannon BR–03, damaged muzzle. (Model created in Agisoft Metashape by James Fowler.)

This is likely a British gun, considering the context of its location and general profile and shape of the breech area and cascabel. No identifying marks, such as crest, numbers or letters, or engravings in the right trunnion, were readily apparent on any part of the weapon (Manucy 1949:42). The cascabel is notably oval in shape, not round, and the gun is characterized by a curved breech area with five concentric rings, both consistent with early 18th century British manufacture, as seen in Figure 42 (Manucy 1949:42).

Figure 42: Cannon BR–03, breech area, recorded 6 December 2024. (Image courtesy of James Fowler.)

The barrel has three reinforcement bands, one located near the touch hole, one located just aft of the trunnions, and one located just forward of the trunnions. Corrosion patterns indicate that the muzzle of the weapon may have been buried prior to conservation and display. A large compression or groove was noted to wrap around the muzzle of the gun about 20 cm (7.87 in) aft of the breakage location. Ostensibly this was not on the cannon when it was cast and is likely an area of localized n–transform corrosion which has since been stabilized and painted over. A closeup of this region can be seen in Figure 43. Although no precise measurements were taken, photogrammetric data was recorded for the breakage location, as were overall photographs of the weapon.

Figure 43: Cannon BR–03, damaged muzzle (model created in Agisoft Metashape by James Fowler).

Cannon BR–04: British 6– or 8–Pounder (uncertain)

This cannon is also likely a mid-1700s 6– or 8–pounder recorded by James Fowler at Fort St Elmo in Valletta, Malta, on 6 December 2024, and is in very poor condition. It is assumed that this is a British gun, considering the context of its location and general profile and shape, however no identifying marks were readily apparent (Manucy 1949:42). The weapon is heavily damaged and missing approximately 25 cm (9.84 in) of the muzzle, as seen in Figure 44. Unfortunately, the tip of the left trunnion is also missing, the location where identifying marks would have been cast. No discernable markings or identification marks were present on any part of the weapon, including no crest, no numbers or letters, and no engravings in the right trunnion. The gun is approximately 1.20 m (3.94 in) long and 20 cm (7.87 in) in diameter at the breech.

The barrel has three reinforcement bands, one located near the touch hole, one located just aft of the trunnions, and one located just forward of the trunnions. The breech portion of the weapon is significantly more corroded than the muzzle, and the heavily ribbed section near the breech indicates that this weapon was exposed to significant n–transforms such as saltwater and humidity corrosion in that region for extended periods of time.

Figure 44: Cannon BR–04, note the one–euro coin at muzzle end used as ad–hoc scale item, equal to 23.25 mm, recorded 6 December 2024. (Image courtesy of James Fowler.)

It is almost certain that this gun was buried past the trunnions and exposed to constant encroachments of salt water. The forward portions of the gun are also heavily corroded and show pitting similar to that observed on rear portion cannon BR–02, as seen in Figure 40. Additionally, significant deep pitting, likely an n–transform, was observed on the left side of the barrel just aft of the breakage location, inconsistent with corrosive patterns observed in similar guns, and is observable in Figure 45. It is surmised that this gun was partially buried, with the breech above ground, exposed to salt water. In similar fashion to cannon BR–03, this gun also has a strange groove in the barrel located in this example directly forward of the trunnions.

Figure 45: Cannon BR–04, muzzle area, recorded 6 December 2024. 1 Euro coin = 23.25 mm. (Image courtesy of James Fowler.)

Cannon BR–05: British 6– or 8–Pounder (uncertain)

This cannon is also likely a mid-1700s 6– or 8–pounder. BR–05 was recorded by James Fowler at Fort St Elmo in Valletta, Malta, on 6 December 2024, and is in poor condition. It is assumed that this is a British gun, considering the context of its location and general profile and shape, however no identifying marks were readily apparent. Due to the flat breech area, however, it may be a Swedish gun (Mehl 2002:24, 42). The weapon is heavily damaged and missing the last 30 cm of the muzzle, as depicted in Figure 46. No discernable markings or identification marks were present on any part of the weapon, including no crest, no numbers or letters, and no engravings in the right trunnion. This weapon is approximately 1.45 m (4.76 ft) long and about 25 cm (9.84 in) in diameter.

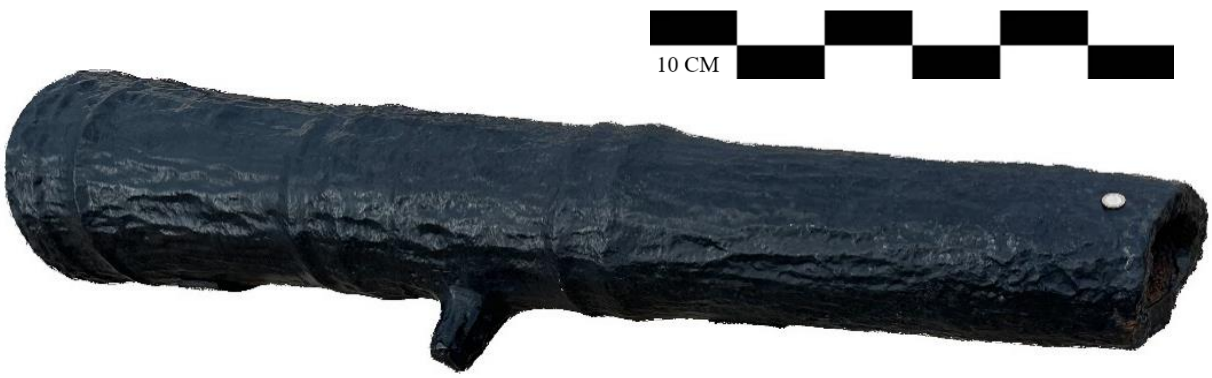

Figure 46: Cannon BR–05, recorded 6 December 2024. 1 Euro coin = 23.25 mm. (Image courtesy of James Fowler.)

The barrel has six reinforcement bands, two located near the touch hole, two located just aft of the trunnions, and two located just forward of the trunnions. On this piece, a vent platform is readily observable between the second and third reinforcement bands, just forward of the breech. The entire weapon is heavily ribbed and pitted, indicating possible n–transforms such as prolonged exposure to salt water and humidity. The trunnions are especially wanting; both are heavily corroded with all markings erased by time.

Cannon BR–06: British 6–Pounder (uncertain)

This cannon is also likely a mid-1700s 6–pounder. BR–06 was recorded by James Fowler at Fort St Elmo in Valletta, Malta, on 6 December 2024, and is in poor condition. It is assumed that this is a British gun, considering the context of its location and general profile and shape, however no identifying marks were readily apparent (Manucy 1949:42). The weapon is heavily damaged and missing the last 25 cm of the muzzle, as depicted in Figure 47. No discernable markings or identification marks were present on any part of the weapon, including no crest, no numbers or letters, and no engravings in the right trunnion. Three reinforcement bands are present, one near the breech, one aft of the trunnions, and one wide directly above trunnions. The forward portion of the gun indicates possible burial up to the trunnions, with pitting consistent with other examples, such as cannon BR–02 and cannon BR–04. This weapon is similar in size to the others in the collection, at approximately 1.5 m (4.92 ft) long and 30 cm (11.81 in) in diameter.

Cannon BR–07: British 6–Pounder (uncertain)

This cannon is also likely a mid-1700s 6–pounder recorded by James Fowler at Fort St Elmo in Valletta, Malta, on 6 December 2024, and is in very poor condition. It is assumed that this is a British gun, considering the context of its location and general profile and shape, however no identifying marks were readily apparent (Manucy 1949:42). The weapon is heavily damaged and missing a portion of the muzzle, observable in Figure 48 and Figure 49.

Figure 47: Cannon BR–06, recorded 6 December 2024. 1 Euro coin = 23.25 mm. (Image courtesy of James Fowler.)

Figure 48: Cannon BR–07, recorded 6 December 2024. 1 Euro coin = 23.25 mm. (Image courtesy of James Fowler.)

No discernable markings or identification marks were present on any part of the weapon, including no crest, no numbers or letters, and no engravings on either trunnion. Four reinforcement bands are present, one very near the breech, one aft of the trunnions, and two directly above trunnions. The forward portion of the gun indicates possible c–transforms such as burial up to the trunnions, with n–transforms visible such as pitting consistent with other examples, such as BR–02, BR–04, and BR–05.

Figure 49: Cannon BR–07, damaged muzzle, recorded 6 December 2024. 1 Euro coin = 23.25 mm. (Image courtesy of James Fowler.)

The breech portion of the weapon is also corroded, but in a different pattern than the muzzle. The heavily ribbed section near the breech indicates that this weapon was exposed to n–transforms such as saltwater and humidity corrosion in that region for extended periods of time, as is observable on cannon bollards, as seen in Figure 39. It is almost certain that this gun was buried past the trunnions and exposed to constant encroachments of salt water with the breech above ground. Heavy pitting was also observed in various places on the left side of the barrel, indicating heavy corrosion or perhaps a manufacturing defect, also seen in Figure 48. This weapon is similarly sized compared to others in the collection, at roughly 1.40 m (4.59 ft) in length and 30 cm (11.81 in) in diameter.

Cannon BR–08: British swivel gun

This weapon was recorded by James Fowler on 7 June 2024, during the 2024 ECU summer field school in BTFA (NC). BR–08 is in poor condition, as depicted in Figure 50. No identifying markings were located on the weapon to properly identify the country of origin, nor any information on its recovery. Despite this, the gun is likely a mid-18th century British swivel gun, common in the British colonies at the time (Mehl 1989:32). The weapon's shot weight was impossible to accurately measure due to the poor preservation of the gun; however, it is some variation of swivel gun and thus likely fired a sub-1-pound ball. This weapon shows extensive damage, including a heavily damaged muzzle and a missing cascabel, as depicted in Figure 51.

Figure 50: Cannon BR–08, photographed by James Fowler. (Image courtesy of East Carolina University Program in Maritime Studies.)

This weapon is about 62 cm (24.41 in) long and around 18 cm (7.09 in) wide. BTFA Manager Jim McKee indicated that earlier preservation attempts at the State Park had tried to use epoxy resin to stabilize the weapon, but that such conservation procedures had crudely encapsulated large portions of the muzzle and thus no detailed observations of fracture points are readily achievable (McKee 2024, pers. comm.). McKee also stated that before its epoxy treatment, the weapon showed signs of melting and deformation due to heat, as depicted in Figure 51.

Figure 51: Cannon BR–08, note the melted or otherwise damaged muzzle portion, photographed by James Fowler. (Image courtesy of East Carolina University Program in Maritime Studies.)

Cannon BR–09: British Armstrong 3–Pounder

This cannon was recorded by James Fowler and Don Swanbeck in June 2024, during the 2024 ECU summer field school in Edenton, NC. It was identified as a late 1700s Armstrong-Fredrick Pattern 3–pounder (Mehl 1989:32). The cannon is currently partially buried up to the trunnions, making proper identification currently impossible. The breech end of the weapon is completely inaccessible. The left trunnion is missing, but otherwise the piece is intact, and in good condition. It currently has a large bronze teapot affixed to the muzzle, making identification of the poundage uncertain, although measurements of the muzzle flare and muzzle circumference of the gun indicate that it is likely a 3–pounder. This can be seen in Figure 52.

Figure 52: Cannon BR–09, photographed by James Fowler. (Image courtesy of East Carolina University Program in Maritime Studies.)

Cannon BR–10: British 32–Pounder

This cannon was recorded by Wessex Archaeology on an underwater wreck site located at Chesil Beach in Dorset, UK, in 2017 and has been identified as a British 32–pounder. Due to its current deposition underwater, the gun is in poor visual condition, however under the concretion layers, it may be good condition. The gun is part of a larger site containing 8 cast iron guns manufactured between 1650 and 1725. The site appears to be a merchant shipwreck (Wessex

Archaeology 2017a). The gun rests upside down and shows signs of muzzle failure with a distinctive notch noted on the underside of muzzle, as can be seen in Figure 53.

Figure 53: A Photogrammetric model of Cannon BR–12. Red arrow indicates region of muzzle failure (Wessex Archaeology 2017b).

Swedish Cannons

Swedish Cannons are perhaps more widely distributed throughout the globe than any other national origin of gun, naval or otherwise. The Swedes steadily manufactured guns for several centuries, exporting most of them to locations all over Europe, North America, South America, Africa and beyond (Mehl 2002:24; Cohn et al. 2003:92; Herry 2004:99; Brown 2007:1–4; Chavonnes Battery Museum 2025; Koivikko et al. 2025:12–6). This is partially due to the high quality of Swedish iron and copper, and the relative ease with which it was mined (Bindler et al. 2017:1–4). The primary Swedish export gun was known universally as the *Finbanker* and is identified due to is angular geometry and often flat breech area (Mehl 2002:24). It is worth noting, many guns are identified as Finbankers without much quantitative evidence to support such an identification; researchers often cite "personal communications" or "consultation with an expert", while conveniently leaving out what source was actually consulted (see McBride

1975:248; Oldham et al. 1993:326 as examples of this). It is apparent that Swedish Finbankers were of two distinct categories: “flat breech” weapons and those which some indicate as “Dutch Finbankers” or “Dutch breech” Finbankers (i.e., Finbankers built to the specifications required by the Dutch when purchasing cannons for their military). Such weapons include a much more rounded breech (Mendel 1965:184; Martin 2005:192). Some scholars, notably historian Ruth Brown, have categorized them as Type A and Type B Finbankers, respectively (Parham et al. 2013:408–409). Additionally, Finbankers often have “double molded” reinforcement bands, a feature visible in Figure 29 and Figure 30 (Wilson 1988:87; Auer 2004:271). Other Finbankers have rectangular reinforcement bands, which are unlike other varieties of cannons. Regardless of overall design, the quality of Swedish iron was widely sought after, and nations without conducive supplies of iron would routinely purchase guns from Sweden to outfit their militaries (Franklin 1777:1; Cohn et al. 2003:92; Brown 2007:1–3).

Cannon SW–01: Swedish 32–Pounder

This cannon was recorded by James Fowler, Markku Luoto, and Mina Koivikko on 14 May 2025. James Fowler collaborated with the Maritime Archaeological Society of Finland (MAS) and the Finnish Heritage Agency to conduct thesis research in the Baltic Sea on the *Kronprins Gustav Adolf* wreck, permit ref MV/00971/2025 (Fowler 2025:10; Fowler 2026:1–12). *Kronprins Gustav Adolf* was a 62 gun third–rate ship of the line which sank as a result of action during the Russo–Swedish War of 1788 (Anderson 1910:246; John Tredrea and Eduard Sozaev 2010:470; Roio 2022:187–189). This cannon was identified as a Swedish Finbanker 36–pounder, and is currently underwater on the wreck site, as depicted in Figure 54. This weapon is about 2 m (6.56 ft) in length and around 50 cm (19.69 in) wide.

Figure 54: A photogrammetric model of Cannon SW–01 broken in half, denoted by the red boxes (Maritime Archaeological Society of Finland 2023).

The weapon was heavily encrusted and broken in half aft of the trunnions, but in good condition in the areas where the concretion was removed. Archaeological work was focused on the right trunnion, as seen in Figure 55. Detailed photogrammetric data was collected on the gun, and encrustation was removed from the right trunnion, which exposed the letter “E,” or possibly “M,” as depicted in Figure 56. No de–encrustation was conducted on the aft section of the cannon due to time constraints, so no markings were recovered on that section.

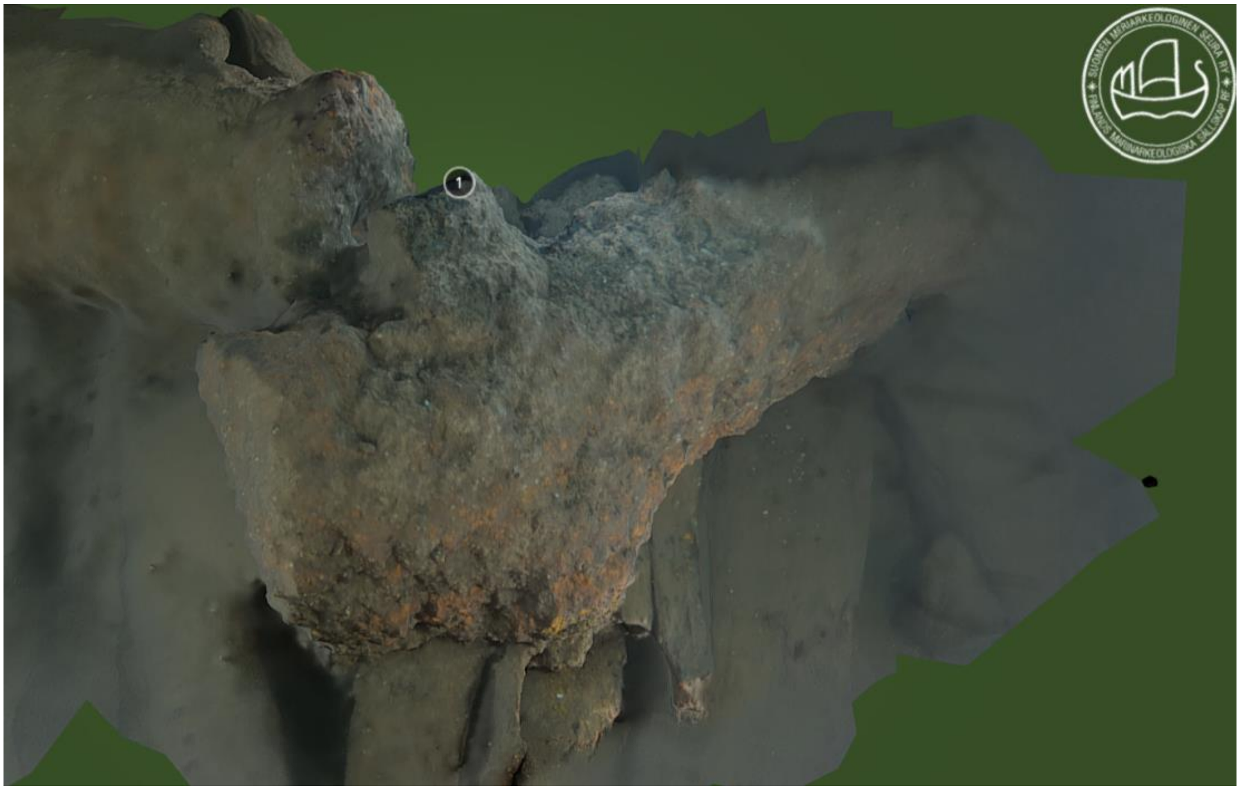

Figure 55: The forward half of SW–01, photogrammetric model by Markku Luoto. “1” indicates the location of the exposed trunnion (Maritime Archaeological Society of Finland 2025).

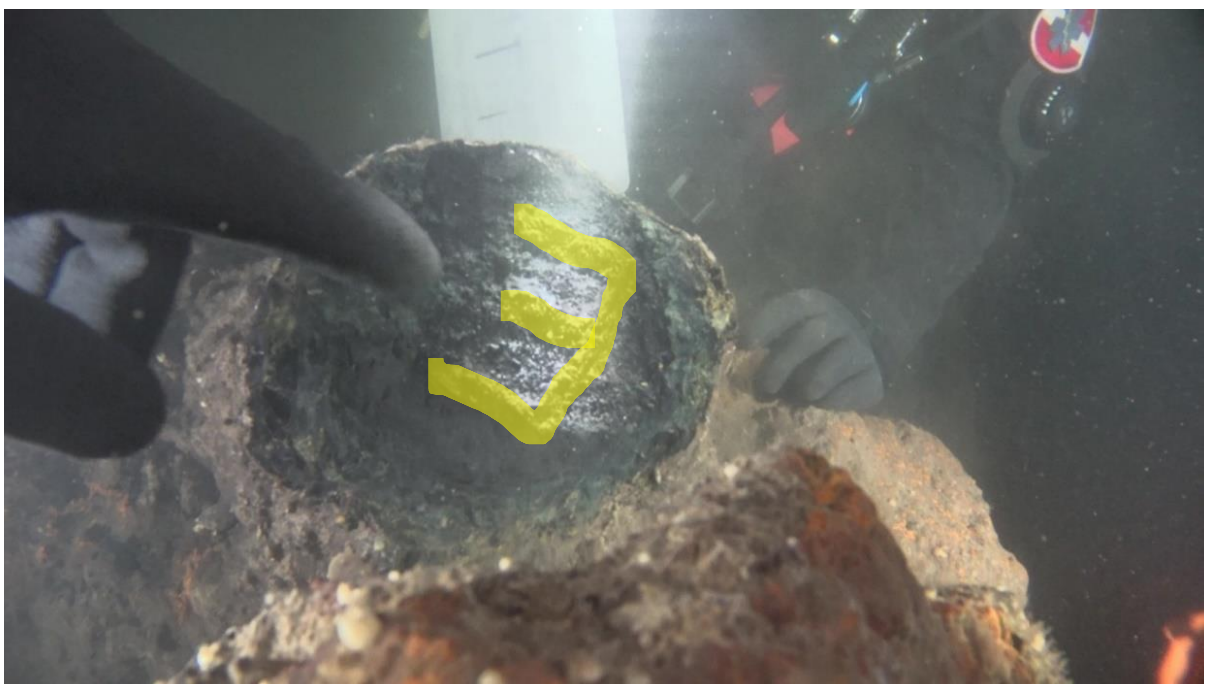

Figure 56: Cannon SW–01, the letter “E” on the trunnion, denoted in yellow, recorded 14 May 2025. Image by Markku Luoto, (Maritime Archaeological Society of Finland 2025).

Cannon SW–02: Swedish 24–Pounder

This cannon was recorded by James Fowler, Markku Luoto, and Mina Koivikko on 14 May 2025, underwater on the *Kronprins Gustav Adolf* wreck site. The weapon is heavily encrusted and broken in half at the trunnions, as depicted in Figure 57. Detailed photogrammetric data was collected on the gun, however no encrustation was removed, and no further analysis was conducted. Due to the encrustation buildup, high–resolution analysis for this study is not possible. However, this weapon provides an additional case study for guns broken aft of the trunnions. Additional archaeological work on this site may be directed towards further analysis of this gun.

Figure 57: A photogrammetric model of Cannon SW–02, broken in half. Photogrammetric model by Markku Luoto (Maritime Archaeological Society of Finland, 2023).

Cannon SW–03: Swedish 12–Pounder

This cannon was documented by James Fowler at Suomenlinna, Finland on 16 May 2025. It is a Swedish Finbanker, likely a 12–pounder (Paulaharju et al. 2025). The weapon is in excellent condition. The muzzle shows signs of spalling and damage, and the cascabel is missing. A cannonball is concreted into place at 20 cm (7.87 in) into the bore. Its naval heritage is assumed due to an anchor symbol engraved into the top of the barrel aft of the trunnions. The letters "6e" and "N40" are engraved in the side of the barrel aft of the right trunnion, as visible in Figure 58. The number "63" is engraved on the top of the barrel, towards to aft end. Additionally, the number "9" is engraved into the top of the barrel. It is uncertain what these engravings mean, however it is speculated that these are serial numbers or batch numbers. This weapon is approximately 2.5 m (8.20 ft) in length and roughly 35 cm (13.78 in) in diameter.

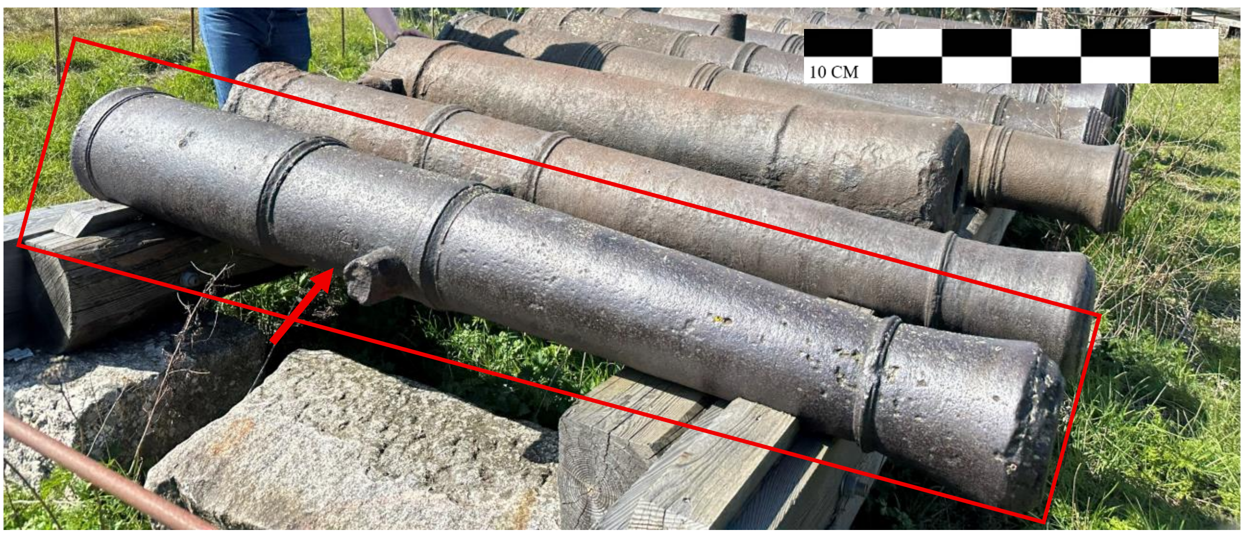

Figure 58: Cannon SW–03, note the spalling around the muzzle. Red arrow indicates location of engravings, recorded 16 May 2025. (Image courtesy of James Fowler.)

Cannon SW–04: Swedish 12–Pounder

This cannon was documented by James Fowler at Suomenlinna, Finland on 16 May 2025. It is a Swedish Finbanker, also likely a 12–pounder (Paulaharju et al. 2025). The weapon is in good condition, depicted in Figure 59. A cannon ball is lodged 20 cm (7.87 in) into the bore. A letter "W" is embossed on the right trunnion, likely indicating the cannon was manufactured in Wergeland Iron Works, in Copenhagen (Mendel 1965:178). Additionally, both the cascabel and the left trunnion are missing, the former indicated in Figure 60. The forward portions of the gun are significantly better preserved than the aft portions of the gun, which indicate heavy corrosion, also observable in Figure 60. Also noteworthy is the “Flat Breech” design on this gun, typical of Finbankers. This weapon is approximately 2.5 m (8.20 ft) in length and roughly 35 cm (13.78 in) in diameter.

Figure 59: Cannon SW–04, recorded 16 May 2025. (Image courtesy of James Fowler.)

Figure 60: Cannon SW–04, note the missing cascabel, recorded 16 May 2025. Cannon SW–03 is located partially out of frame on the right, also with missing cascabel. (Image courtesy of James Fowler.)

Cannon SW–05: Swedish 18–Pounder

This cannon was documented by James Fowler at Suomenlinna, Finland on 16 May 2025. It is a Swedish Finbanker in good condition, and this is the largest weapon in the collection of damaged guns at Suomenlinna, depicted in Figure 61. Sources claim this is a 12–pounder, however, it is more likely an 18– or 24–pounder that has been misidentified or otherwise overlooked (Paulaharju et al. 2025). The entire weapon aft of the trunnions is missing, as seen in Figure 62. Both trunnions have a “ribbon” symbol embossed, similar in shape to a sideways “alpha” letter, as depicted in Figure 63.

Figure 61: Cannon SW–05 denoted in red box, front half broken aft of the trunnions, recorded 16 May 2025. (Image courtesy of James Fowler.)

Figure 62: Top perspective of cannon SW–05 photogrammetric model, 1 Euro coin = 23.25 mm. (Created in Agisoft Metashape by James Fowler.)

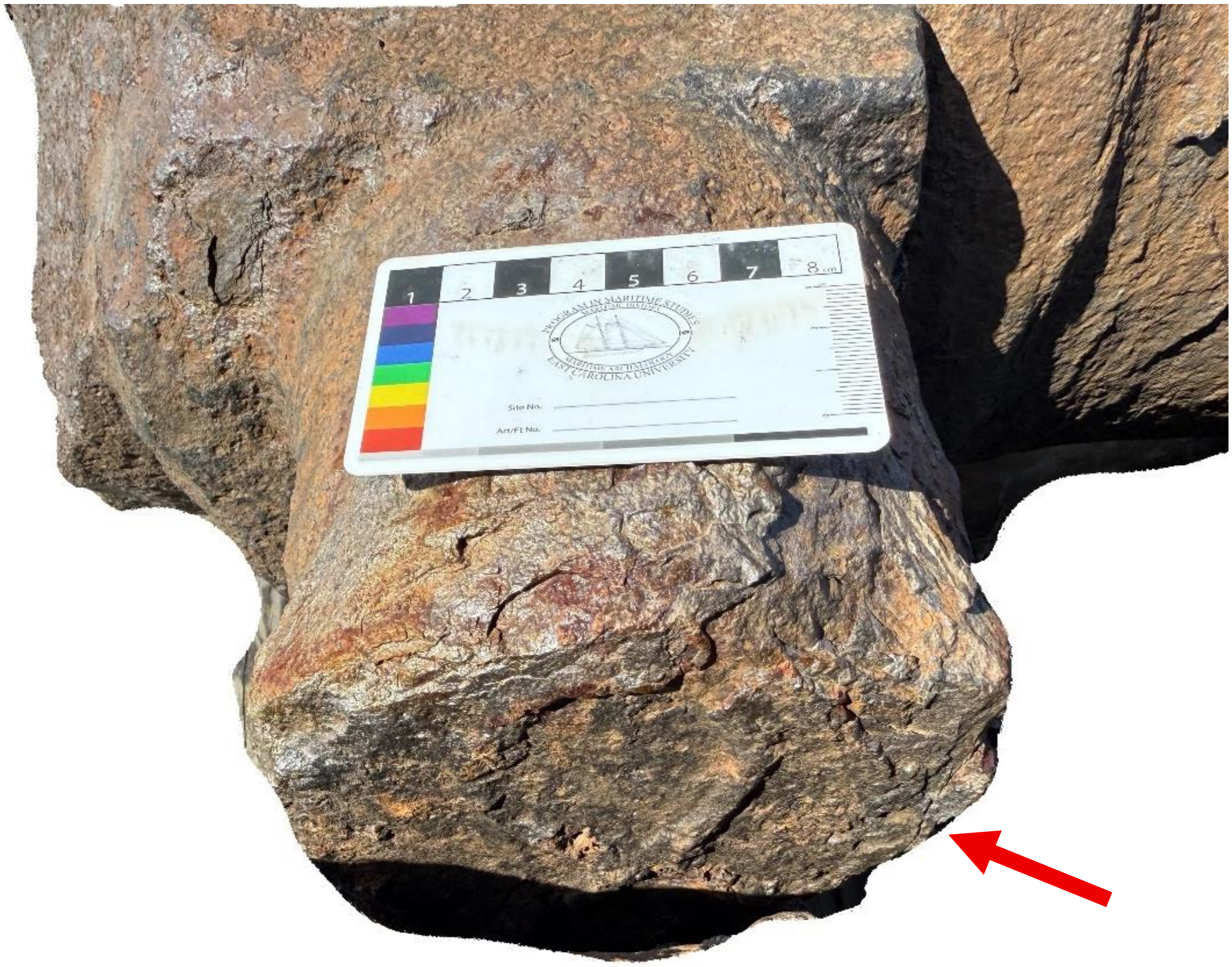

Figure 63: Right trunnion of SW–05, note the “ribbon” symbol, recorded 16 May 2025. (Image courtesy of James Fowler.)

Significant spalling and pitting were observed on and around the muzzle of Cannon SW-05, which appear to be n–transforms. The sheared region aft of the trunnions is clearly visible in Figure 64. This weapon is approximately 1.75 m (6.74 ft) in length, however, would have been closer to 3 m (9.84 ft) if both pieces were intact. SW–05 is roughly 50 cm (19.69 in) in diameter.

Figure 64: A photogrammetric model of Cannon SW–05, displaying the sheared portion aft of the trunnions looking forward. (Created in Agisoft Metashape by James Fowler.)

Cannon SW–06: Swedish 12–Pounder

This cannon was documented by James Fowler at Suomenlinna, Finland on 16 May 2025. It is a Swedish Finbanker in good condition, also likely a 12–pounder, depicted in Figure 65 (Paulaharju et al. 2025). The cascabel is missing and a cannon ball is lodged deep in the bore. A bore scope analysis indicated that significant "bubbling" of the metal within the bore may have jammed the ball into place, after long periods left loaded. No markings were observed on this weapon. This weapon was approximately 2.5 m (8.20 ft) in length and roughly 38 cm (14.96 in) in diameter.

Figure 65: Cannon SW–06, recorded 16 May 2025. (Image courtesy of James Fowler.)

Cannon SW–07: Swedish 6– or 8–Pounder (uncertain)

This cannon is also likely a mid-1700s 6– or 8–pounder recorded by James Fowler at Fort St Elmo in Valletta, Malta, on 6 December 2024, seen in Figure 66. It is assumed that this is gun of

Swedish origin in very poor condition, considering the shape of the breech and the general profile and shape, including the flat breech area (Brown 2007:1–2; BU Archaeology 2025). It does appear to be a “Flat breech” Finbanker (Mendel 1965:184). However, no identifying marks were readily apparent to confirm this identification. The weapon is roughly 1.5 m (4.92 ft) long and 25 cm (9.84 in) in diameter.

Figure 66: Cannon SW–07, viewed from the front, recorded 6 December 2024. (Image courtesy of James Fowler.)

Cannon SW-07 is heavily damaged and missing a large portion of its muzzle. The end of the muzzle shows signs of splaying and bursting, as depicted in Figure 67. No discernable markings or identification otherwise were present on any part of the weapon, including no crest, no numbers or letters, and no engravings on either trunnion. Three reinforcement bands are present, one very near the breech, one aft of the trunnions, and one directly forward of the trunnions. The forward portion of the gun indicates c–transforms such as possible burial up to the trunnions, with pitting consistent with other examples, such as cannon BR–02. The breech portion of the weapon is also corroded, but in a different pattern than the muzzle, possibly indicating n–transforms. The heavily ribbed section near the breech indicates that it may have been exposed to saltwater and humidity corrosion in that region for extended periods of time. It is almost certain that this gun was buried past the trunnions and exposed to constant encroachments of salt water. The forward portions of the gun are also heavily corroded and show pitting like that observed on rear portion cannon BR–02, BR–04, and BR–05. It also appears that areas of the muzzle have flaked off, as the muzzle cross section drastically decreases in diameter in the first meter of the weapon, by several centimeters.

Figure 67: Cannon SW–07, detailing the splayed and damaged muzzle area, recorded 6 December 2024. (Image courtesy of James Fowler.)

Cannon SW–08: Swedish 12–Pounder

This cannon was documented by James Fowler at Suomenlinna, Finland on 16 May 2025 (Figure 68). It is a Finbanker in excellent condition, also likely a 12–pounder (Paulaharju et al. 2025).

Figure 68: Cannon SW–08, 16 May 2025. (Image courtesy of James Fowler.)

The cascabel is missing and a cannon ball is lodged approximately 30 cm (11.81 in) into the bore. Letters “B” and “M” were observed cast into the gun near the muzzle, otherwise no markings were observed elsewhere. It is unknown what these markings mean. The letter “F” was observed on the left and right trunnion, indicating manufacture at the Finspong iron works in Sweden (Mendel 1965:174, Brown 1989:322; Auer 2004:272). The weapon is approximately 2.5 m (8.20 ft) in length and 40 cm (15.75 in) in diameter.

Cannon SW–09: Swedish 12–Pounder

This cannon was documented by James Fowler at Suomenlinna, Finland on 16 May 2025 (Figure 69). It is a Swedish Finbanker in excellent condition, also likely a 12–pounder (Paulaharju et al. 2025). The cascabel is missing. No accurate observation of the interior of the bore was possible due to the presence of a large wasp’s nest in same. The letters “IEC” were observed cast into the right trunnion, as depicted in Figure 70. This indicates that this gun was made by Jasper Ehrencreutz, founder of the Erencahl Works in Sweden (Mendel 1965:176). This mark was used up until 1750, suggesting this weapon was cast before that date. Further research did not turn up a meaning for these letters. On the left trunnion, the letters “E/M” were cast, also unknown in meaning. The weapon is about 2.5 m (8.20 ft) in length and around 35 cm (13.78 in) diameter.

Figure 69: Cannon SW–09, recorded 16 May 2025. (Image courtesy of James Fowler.)

Figure 70: Cannon SW–09, “IEC” cast into the right trunnion, recorded 16 May 2025. (Image courtesy of James Fowler.)

Cannon SW–10: Swedish 12–Pounder

This cannon was documented by James Fowler at Suomenlinna, Finland on 16 May 2025. It is a Swedish Finbanker in excellent condition, also likely a 12–pounder (Paulaharju et al. 2025). The cascabel and both trunnions are missing, the latter observable in Figure 71. On the second reinforcement band, the alphanumerical “Z3NO70” was inscribed. These markings are unknown in meaning. Adjacent to this is the marking “1778”, possibly indicating a year of manufacture. Additionally, for unknown reasons the numbers “6617” are cast into the barrel forward of the third reinforcement band. A cannon ball was observed 10 cm into the barrel. The weapon is like others in the collection, and measures approximately 2.5 m (8.20 ft) in length and around 30 cm (11.81 in) in diameter.

Figure 71: Cannon SW–10, recorded 16 May 2025. (Image courtesy of James Fowler.)

Cannon SW–11: Swedish 12–Pounder

This cannon was documented by James Fowler at Suomenlinna, Finland on 16 May 2025. This gun is depicted in Figure 72. It is a Swedish Finbanker in good condition, also likely a 12–

Figure 72: Cannon SW–11, recorded 16 May 2025. (Image courtesy of James Fowler.)

pounder (Paulaharju et al. 2025). The cascabel is missing, and a cannon ball was observed 20 cm (7.87 in) into the barrel. The left trunnion had the letter “C,” or possibly “G,” cast in, likely indicating a foundry (Brown 1989:322). The weapon is also about 2.5 m (8.20 ft) long and around 30 cm (11.81 in) in diameter.

Cannon SW–12: Swedish 12–Pounder

This cannon was documented by James Fowler at Suomenlinna, Finland on 16 May 2025. It is a Swedish Finbanker in good condition, also likely a 12–pounder (Paulaharju et al. 2025). The cascabel is missing, and a cannon ball was located 20 cm (7.87 in) into the barrel. The left trunnion had the cast numbers “1713”, indicating a possible manufacture date. The letters “VB” was also observed on the right trunnion (Figure 73), the mark of founder Ulla Berchner, successor to Gert Storning at Stafsio Iron Works in Sweden (Mendel 1965:178; Brown 1989:322). The gun (Figure 74) was about 2.5 m (8.20 ft) long by 30 cm (11.81 in) in diameter.

Figure 73: “VB” embossed onto the right trunnion of SW–12. Photograph taken at a very acute angle relative to the trunnion face, recorded 16 May 2025. (Image courtesy of James Fowler.)

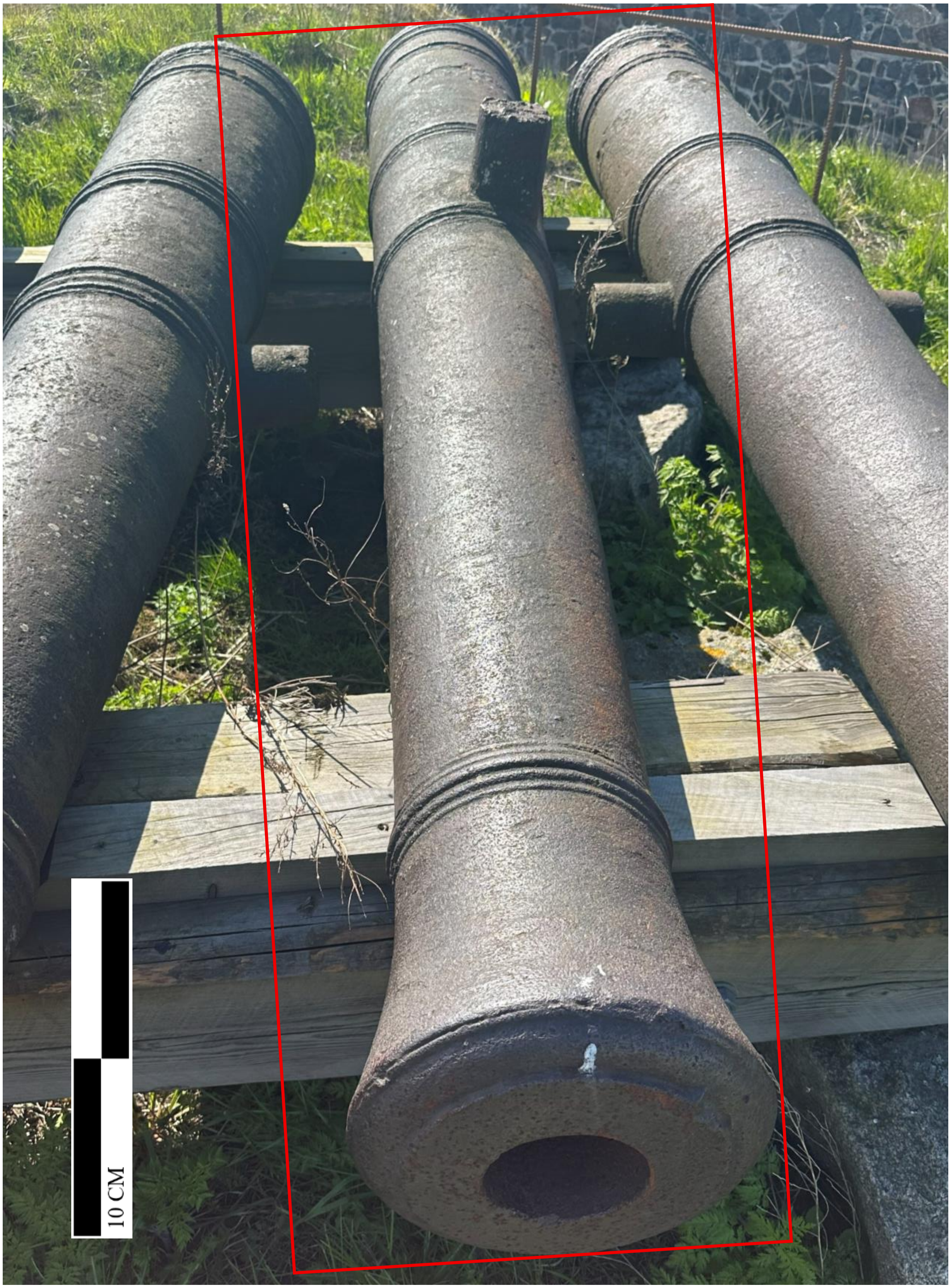

Figure 74: Cannon SW–12, recorded 16 May 2025. (Image courtesy of James Fowler.)

Cannon SW–13: Swedish 12–Pounder

This cannon was documented by James Fowler at Suomenlinna, Finland on 16 May 2025. This weapon is depicted in Figure 75. It is a Swedish Finbanker, also likely a 12–pounder

Figure 75: Cannon SW–13, 16 May 2025. (Image courtesy of James Fowler.)

(Paulaharju et al. 2025). The cascabel is missing, and a cannon ball was observed 20 cm into the barrel. The left trunnion also had the numbers “1713” cast into it, indicating a possible manufacture date, as depicted in Figure 76. The letters “NLH” were observed cast into the barrel forward of the fourth reinforcement band, close to the touch hole. The meaning of these letters is not understood. This weapon was almost identical to SW–12, of the same length and diameter.

Figure 76: “1713” embossed onto the left trunnion of SW–13. 16 May 2025. (Image courtesy of James Fowler.)

Cannon SW–14: Swedish 12–Pounder

This cannon was documented by James Fowler at Suomenlinna, Finland on 16 May 2025. It is a Swedish Finbanker in good condition, also likely a 12–pounder (Paulaharju et al. 2025). The cascabel and right trunnion were missing, and a cannon ball was observed 20 cm (7.87 in) into the barrel. No markings were observed anywhere on the weapon, and no photos of it were taken.

Cannon SW–15: Swedish 12–Pounder

This cannon was documented by James Fowler at Suomenlinna, Finland on 16 May 2025. It is a Swedish Finbanker in excellent condition, also likely a 12–pounder (Paulaharju et al. 2025). The cascabel and right trunnion were missing. Near the breech of the weapon, an anchor symbol was clearly visible, which may indicate naval service (Figure 77). The numbers “61874/1674” were inscribed into the barrel, meaning unknown. Additionally, upon inspection with the bore cam, a strange amber–colored sap–like substance was observed concreted throughout the entire length of the bore. Due to the bore cam malfunctioning during the fieldwork, no video or photographic evidence of this was recorded. The bore cam allowed for visual confirmation of the substance, however further research failed to uncover any clues about it or how it got into the bore.

Figure 77: Cannon SW–15, anchor symbol highlighted in yellow, recorded 16 May 2025. (Image courtesy of James Fowler.)

Cannon SW–16: Swedish 12–Pounder

This cannon was documented by James Fowler at Suomenlinna, Finland on 16 May 2025. It is a Swedish Finbanker, also likely a 12–pounder (Paulaharju et al. 2025). The cascabel is missing, and a cannon ball was observed 20 cm (7.87 in) into the barrel. Near the muzzle of the weapon on top, a small “Z” symbol was clearly visible. On the left trunnion, the numbers “173” were embossed (Figure 78).

Figure 78: Cannon SW–16, “173” embossed on the left trunnion, recorded 16 May 2025. (Image courtesy of James Fowler.)

The meanings of these are not known. On the right trunnion, the letters “IEC” were embossed, similar to cannon SW–09. The weapon is similar in size to others in the collection, around 2.5 m (8.20 ft) in length and 30 cm (11.81 in) in diameter.

Cannon SW–17: Swedish 12–Pounder

This cannon was documented by James Fowler at Suomenlinna, Finland on 16 May 2025. It is a Swedish Finbanker in excellent condition, also likely a 12–pounder (Paulaharju et al. 2025). The cascabel is missing, a cannon ball was observed 20 cm (7.87 in) into the barrel. For unknown reasons, “V:IX:XV:11” and “:X/1.XV” were inscribed on top of the barrel near the breach, partially depicted in Figure 79. The length and diameter of the cannon are 2.5 m (8.20 ft) and 30 cm (11.81 in), respectively.

Figure 79: Cannon SW–17, “V:IX:XV:11” and “:X/1.XV” inscribed on the barrel, recorded 16 May 2025. (Image courtesy of James Fowler.)

Cannon SW–18: Swedish 12–Pounder

This cannon was documented by James Fowler at Suomenlinna, Finland on 16 May 2025. It is a Swedish Finbanker in excellent condition, also likely a 12–pounder (Paulaharju et al. 2025). The cascabel is missing. On the top of the barrel behind the third reinforcement band the letter "P" is clearly inscribed, as depicted in Figure 80. The number "63" is also demarcated behind the 2nd reinforcement band. The meaning of these marks remains unknown. The left trunnion has the letters "1714" cast into it, possibly indicating a manufacturing date. A cannon ball was observed within the barrel. The gun is of similar dimensions to others in the collection, with a length of roughly 2.5 m (8.20 ft) and a diameter of around 30 cm (11.81 in).

Figure 80: Cannon SW–18, "P" inscribed on the barrel, recorded 16 May 2025. (Image courtesy of James Fowler.)

Cannon SW–19: Swedish 12–Pounder

This cannon was documented by James Fowler at Suomenlinna, Finland on 16 May 2025. It is a Swedish Finbanker in good condition, also likely a 12–pounder (Paulaharju et al. 2025). The cascabel is missing. On top the barrel is the marking "#047" near the breach end, as shown in Figure 81. None of these markings can be explained, perhaps more can be learned with additional research. Some undiscernible markings exist near the muzzle. A cannon ball was observed in the barrel. The weapon is approximately 2.5 m (8.20 ft) in length and 30 cm (11.81 in) in diameter.

Figure 81: Cannon SW–19, "#047" inscribed on the barrel, recorded 16 May 2025. (Image courtesy of James Fowler.)

Cannon SW–20: Swedish 18–Pounder

This cannon was recorded by James Fowler and Don Swanbeck in June of 2024 during the 2024 ECU summer field school in Edenton, NC (Figure 82). It is believed that this is gun of Swedish origin, considering the shape of the breech and the general profile and shape, however no identifying marks were readily apparent (Brown 2007:1–2).

Figure 82: Cannon SW–20. (Image courtesy of East Carolina University Program in Maritime Studies.)

This Finbanker demonstrates a classic “flat breech” design (Mendel 1965:184). The weapon is in good condition. The cascabel has been removed from this piece, possibly during an attempt to render it unusable or some other c–transform. Some unclarity exists concerning the shot weight of this weapon. It is presumed to have arrived in the United States as part of the “Borritz order” of guns during the American Revolutionary War, however the order indicates that only 18–and 24–pounders were shipped over from Europe (Franklin 1777:1). All other guns in the Borritz order still extant are 18–pounders, including those at the North Carolina State Capitol building, and others in Edenton. This gun shows a smaller diameter than nominal for an 18–pounder. The bore measurements for this gun are smaller, perhaps this is due to corrosion buildup not present on the other guns, or a different standard for 18–pounder shot.

Cannon SW–21: Swedish 6–Pounder

This cannon was recorded by Wessex Archaeology in 2013 on a wreck site located at Gun Rock, Outer Farne Islands, UK, and has been identified as a Swedish Finbanker 6–pounder (Wessex Archaeology 2013:10,22) Referred to as Cannon 6002 in Wessex Archaeology literature, this gun shows signs of failure forward of the trunnions on the top side of the barrel, with a large chunk of its barrel missing, as depicted in Figure 83 and Figure 84. Due to its location underwater and heavily concreted, the weapon is in unknown condition, and it is unknown if this damage is due to n–transforms or c–transforms. It was found amongst many guns showing damage, including three guns with muzzles “blown out” (known to Wessex Archaeology as ref 6006, 6009, and 6018) and two with muzzles missing large parts of the top of the gun (known to Wessex Archaeology ref 6010 and 6011). However, this example was the only one with available and clear photogrammetric data to indicate failure. Both the trunnions and the cascabel are intact, however no identifying marks were recorded due to the advanced concretion enveloping the gun. Previous surveys documented the letters “F” and “S” stamped into the trunnions, likely indicating a Finspong gun (Mendel 1965:174; Wessex Archaeology 2013:16). The exact identity of these guns remains elusive. It is not known if these were being carried as cargo or as ballast, a practice observed in other archaeological contexts (Auer 2004:269).

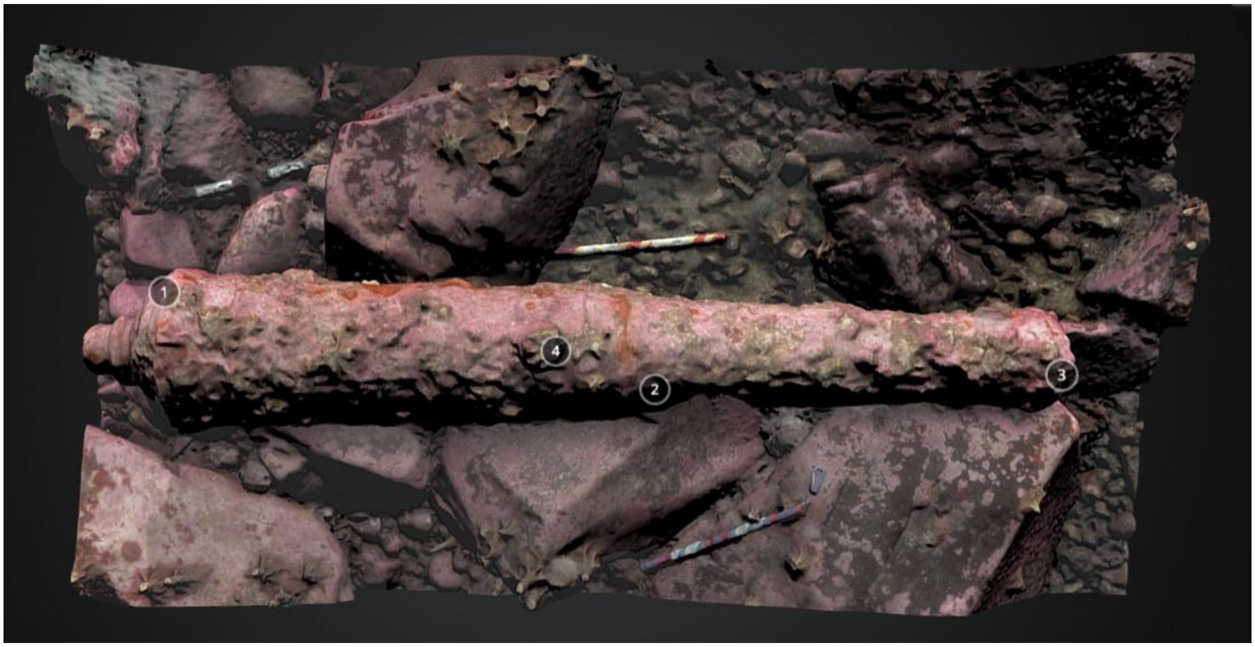

Figure 83: A photogrammetric image of Cannon SW–21 (Wessex Archaeology 2015a).

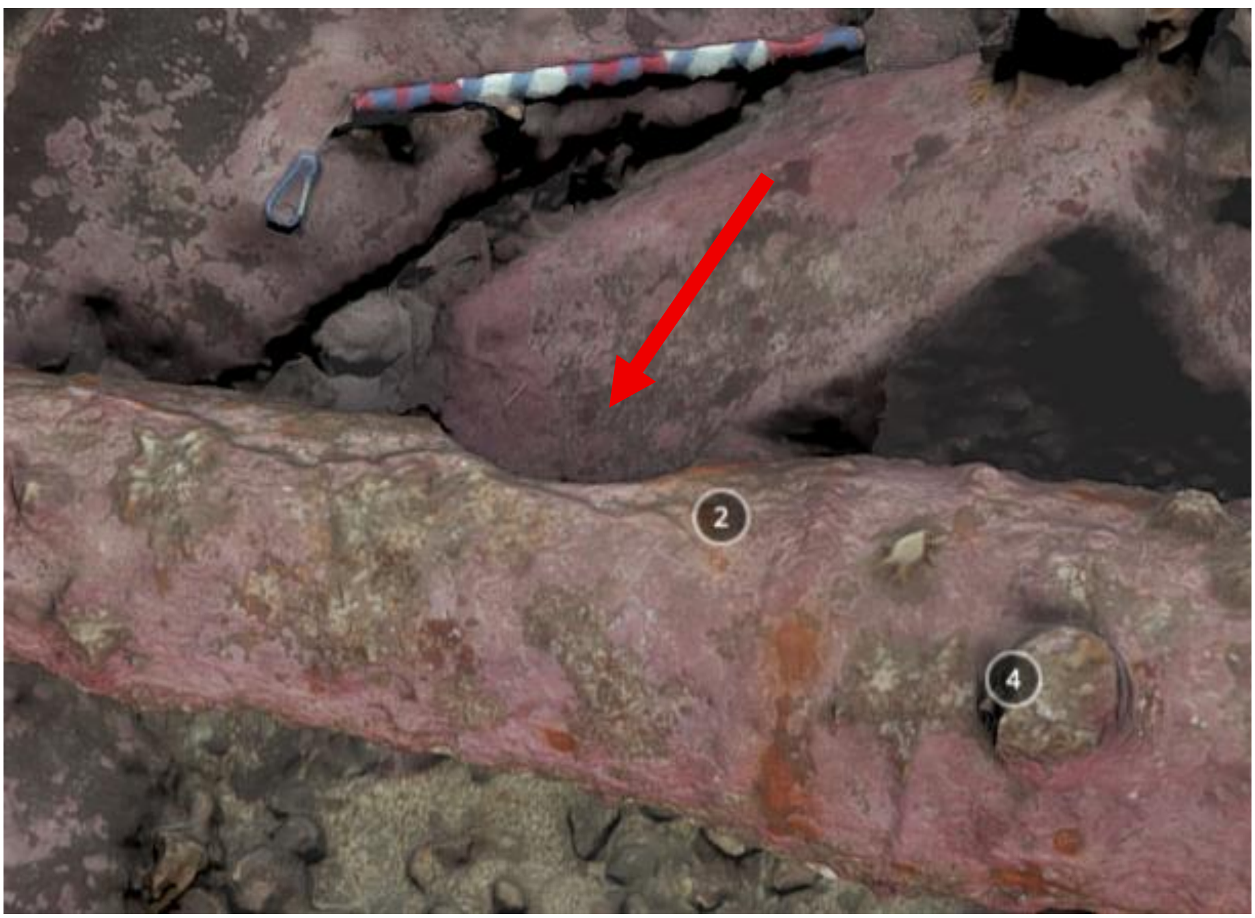

Figure 84: Detail from a photogrammetric image of Cannon SW–21, note the chunk missing from the top of the barrel indicated by red arrow (Wessex Archaeology 2015a).

Cannon SW–22: Swedish 6–Pounder (uncertain)

This cannon was recorded by Wessex Archaeology in 2013 on a wreck site located at Gun Rock, Outer Farne Islands, UK, and has been identified as a Swedish Finbanker 6–pounder seen in Figure 85. This weapon is in unknown condition due to advanced concretion and its location underwater. Referred to as Cannon 6011 in Wessex Archaeology literature, this gun shows signs of failure at the muzzle (Wessex Archaeology 2013:10,22). Both the cascabel and trunnions are intact. See Cannon SW–21 above for additional information on this site.

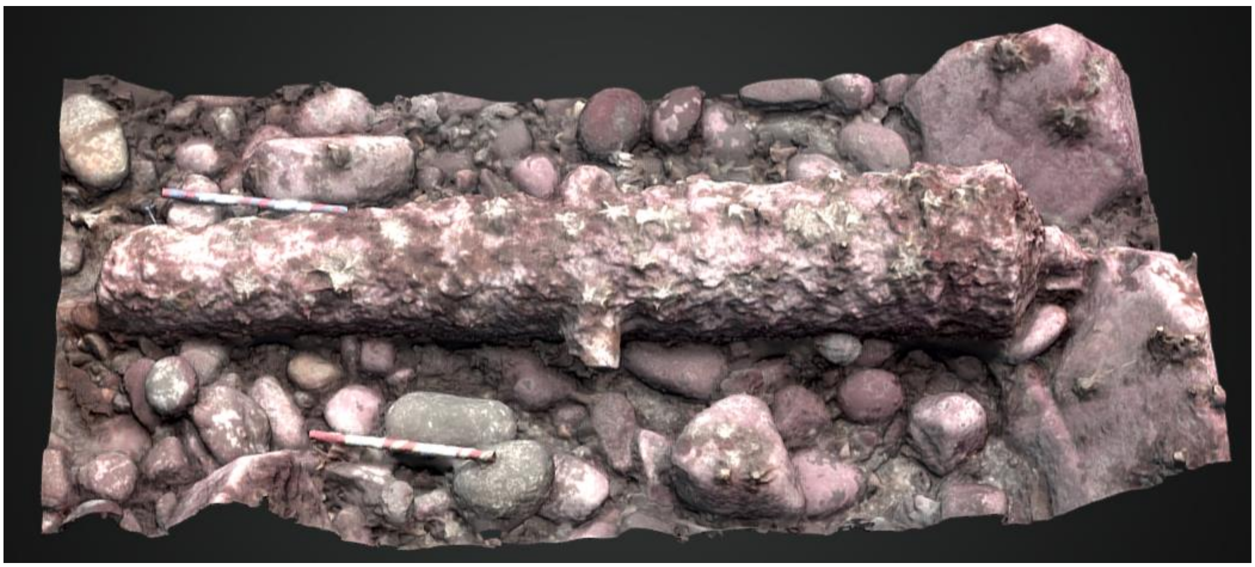

Figure 85: A photogrammetric image of Cannon SW–22. Note the heavy encrustation (Wessex Archaeology 2015b).

Cannon SW–23: Swedish 6–Pounder

This weapon was recovered in two pieces near the gunboat *New York* on Lake Champlain through a project sponsored by the LCMM. The first collection of pieces was located in the early 2000s by Edwin Scollon and the team of the Valcour Bay Research Project (Cohn et al. 2003:86–92), and the second set of pieces in 2025 during a follow up investigation. The cannon is in excellent condition. The breech area was found during a recent reanalysis of the site (Cohn et al. 2003:v,viii; Scollon 2025, pers. comm.). In the battle between British and Revolutionary forces on 11 October 1776, the gunboat *New York's* gun burst during firing, injuring a sergeant in the right arm, and killing Lieutenant Thomas Rogers (Cohn et al. 2003:v,52). Several fragments of the cannon were recorded, which were used to piece together the gun and its story, as depicted in Figure 86.

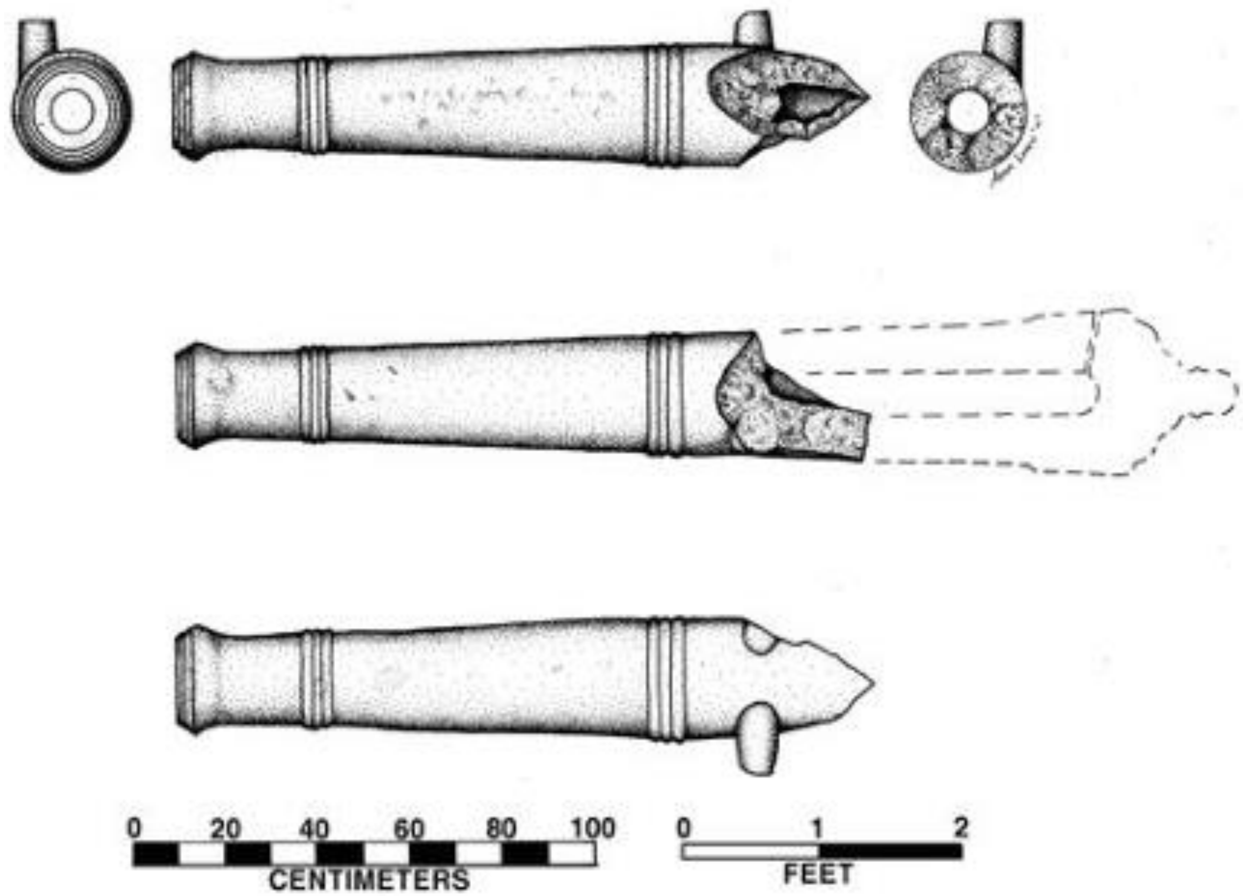

Figure 86: Scaled drawing of Cannon SW–23, referred to in LCMM literature as artifact 99–01. Image in the LCMM collection, drawn by Gordon Cawood, inked by Adam Loven (Cohn et al. 2003:86).

The weapon has been determined to be a 6–pounder of Swedish origin, due to its lack of British markings and similarity to other guns of the era confirmed to be a Swedish Finbanker (Cohn et al. 2003:92, 136). The gun appears to be of the "Dutch breech" variety, characterized by its rounded breech and stubby cascabel with little neck (Mendel 1965:184).

The failure occurred behind the trunnions, with large portions of the mid-section of the gun missing, as seen in Figure 86. The breech area is heavily damaged, with a large crack running through the left side of the breech. On the muzzle section, only the right trunnion remains intact, although the base of the left trunnion is present. On the right trunnion, an unidentified marking is present, resembling two numbers (“6”), with the second number mirrored about its vertical axis. On the muzzle, the letters “NoXII” are readily apparent, but the meaning is currently unknown. Other muzzle portions were discovered in the area, including a large portion of the breech (Cohn et al. 2003:87–92).

Unidentified Cannons

Many cannons located in the archaeological record are hard to identify, since many countries did not implement a standardization regiment and thus guns in their arsenals could be varied or collected from a wide range of sources. Additionally, in the case of some countries of origin, little academic research has been conducted to provide a foundational corpus of work to aid in identification. The origins of guns included in this category unknown, and no sources were located to further ascertain origin.

Cannon UN–01: Spanish/British 6–Pounder demiculverin

This weapon was recorded by James Fowler on 7 June 2024 during the 2024 ECU summer field school in BTFA (Figure 87). The 6–pounder is in excellent condition, due in part to Site Manager Jim McKee, who oversaw the conservation of this weapon (McKee 2024, pers. comm.).

Figure 87: A Photogrammetric image of the bottom view of UN–01, note the pock marks and damage. (Created by James Fowler in Agisoft Metashape.)

This gun was recovered from the Cape Fear River during a dredging operation in 2017. The gun shows definite signs of damage both during and before its exposure to site formation processes; notable on the muzzle–end of the weapon is significant marring due to propeller strikes. The weapon is 2.3 m (7.55 ft) long and 35.5 cm (13.98 in) in diameter, (Figure 88).

Figure 88: Cannon UN–01, photographed by James Fowler, (image courtesy of East Carolina University Program in Maritime Studies).

It is assumed that this is an early 18th century demiculverin of British origin considering the shape of the breech and the general profile and shape, however no identifying marks were readily apparent and thus it could be a Spanish or French weapon. The gun is heavily damaged and missing a large portion of the muzzle (Figure 89). An engine hoist was utilized to weigh

Figure 89: Cannon UN–01, broken portion of the muzzle, photographed by James Fowler, (image courtesy of East Carolina University Program in Maritime Studies).

the gun, which amounted to 1554 pounds (704.8 kg). Additionally, a long spiraling feature can be observed within the gun, embedded into the wall. It is likely that this shape is a piece of wire cast into the inner wall of the bore during the casting process. The casting process included wrapping a wooden post with a bundle of wires to form the bore, then the post and wires were removed. It seems in UN–01, a wire became detached from the bundle and was cast into the inner wall. Additionally, the weapon shows other signs of damage, including large chunks missing around the trunnion area and severe pitting towards the muzzle. The weapon was conserved by the site manager Jim McKee, but it is known that the gun was in very poor shape when recovered from the river. Pitting is present throughout the gun, which may be attributable to n–transform site formation processes, as described in Chapter Three. The manufacturing history before deposition into the archaeological record is not known, making identifying site formation processes difficult. Additionally, large streaks were observed in the muzzle, possibly representing prop strikes from passing boats.

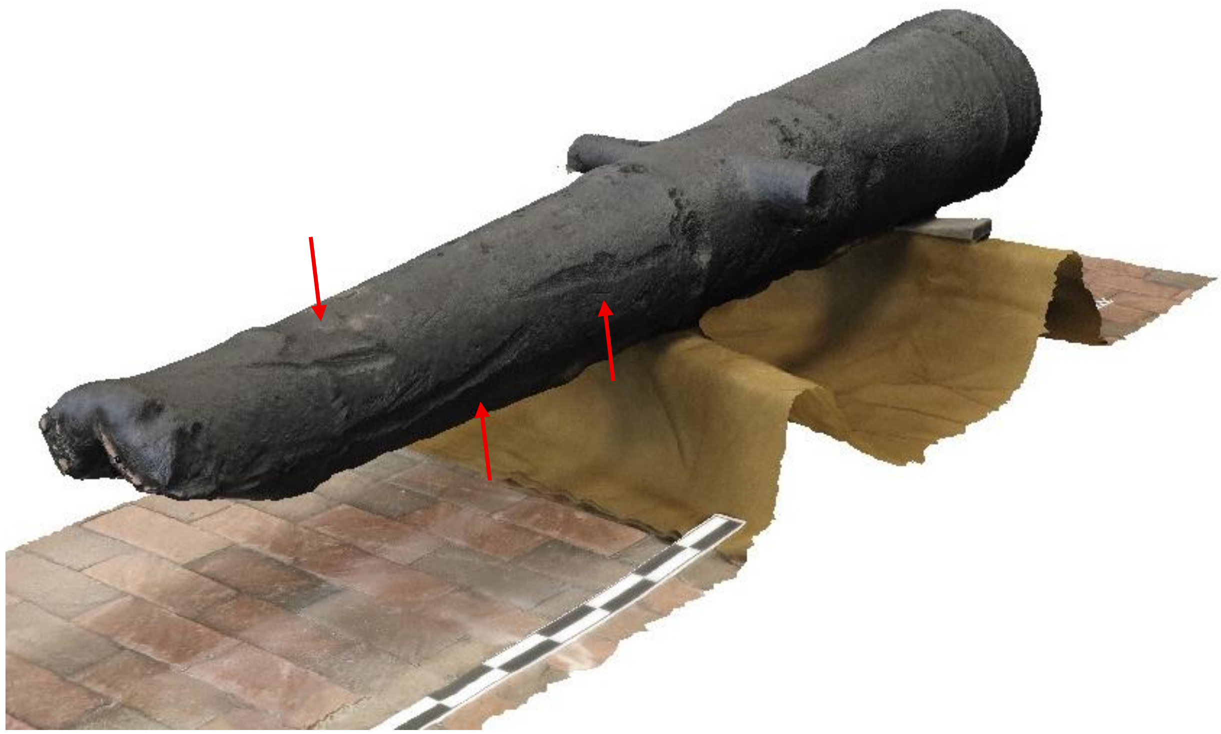

Figure 90: A photogrammetric Image of the ventral surface of UN–01, note the propeller strikes indicated in red. (Created by James Fowler in Agisoft Metashape.)

Cannon UN–02: Unknown 12–Pounder breechloader

This cannon was saved from the scrapyard due to the historical significance it played in the history of Cape Town, South Africa. The cannon was utilized as a part of a larger network of coastal defenses in guarding Table Bay, South Africa (Seemann 1992:1–4). This gun was part of the Amsterdam Battery, which was created in 1787, and is in excellent condition, seen in Figure 61.

Figure 91: Cannon UN–02 with catastrophically damaged barrel (Chavonnes Battery Museum 2025).

The cannon was utilized as a part of a larger network of coastal defenses in guarding Table Bay, South Africa (Seemann 1992:1–4). During the christening ceremony of the Amsterdam Battery, the gun was test fired for the first time by Governor Jacob Cornelius van de Graaff and exploded. Both gunners were killed and another five men were injured, including the Governor (Chavonnes Battery Museum 2025). It is likely that this cannon was of Dutch or Swedish manufacture, considering other weapons in context with this one were of similar origin. However, unlike the other guns in the collection, this weapon appears to be a breechloader, due to the large breech hole visible in the rear of the gun, although this is not confirmed. More research is needed to determine the exact origin of this weapon, and whether Dutch or Swedish breechloading weapons were in development in the 1780s. The gun exploded in the trunnion area, and thus no trunnions exist. No information was available as to any dimensions or markings present on the weapon; however, it was noted to have been buried for many years prior to its disposal (Chavonnes Battery Museum 2025). Of particular interest is the very clean breakage pattern on the rear of the weapon, like that observed on BR–02.

Cannon UN–03: Probably Swedish 18–Pounder (uncertain)

This cannon was documented by James Fowler in Tallinn, Estonia, on 17 May 2025. Little is currently known about this weapon, and few scaled images or archaeological photos exist of it due to the happenstantial documentation of it. It is currently located outside the Kiek in de Kök Museum & Bastion Tunnels, as depicted in Figure 92. The weapon is in good condition.

Figure 92: Cannon UN–03, recorded 17 May 2025. (Image courtesy of James Fowler.)

There is writing on the left trunnion, however it appears to be in a non–English language and proved elusive to translate for this thesis. The bottom alphanumerical engraving seems to be

“A Z A 2,” which meaning is unknown. This is depicted in Figure 93. The cannon displays catastrophic failure aft of the trunnions, shearing off in a clear wedge fracture pattern. The weapon seems to be of early 18th century vintage or even before, however no information could be gained to clarify.

Figure 93: Left trunnion of cannon UN–03, depicted the “A Z A 2” embossment. 17 May 2025. (Image courtesy of James Fowler.)

Cannon UN–04: Probably British or Spanish 16–Pounder

This weapon is located at the Castillo De San Marcos, St. Augustine. The gun is missing the entire breech portion, including the trunnions (Figure 94). Only the muzzle of the weapon is extant. It exploded during the English invasion of St Augustine on 10 November 1702 (Meide

2002:11). The weapon is in poor condition, and has no markings or dimensions associated with it.

Figure 94: Cannon UN–04, photograph by Chuck Meide (Meide 2002:11).

Cannon UN–05: Unknown Cannon

UN–05 is one of three cannons located off Bauline, Newfoundland, depicted in Figure 95 (Shipwreck Preservation Society of Newfoundland and Labrador 2020). Little is currently known about this gun, however, the area of damage is immediately noticeable. Due to concretion and its location underwater, the gun is in very poor visual condition. Additionally, it cannot be determined if the damage is due to n–transforms or c–transforms. A large chunk of the gun is missing from the top of the weapon, in a very similar fashion to the damage recorded on SW–19. It is presumed that this cannon was likely used as ballast (Shipwreck Preservation Society of Newfoundland and Labrador 2020).

Figure 95: Cannon UN–05, damage indicated by red arrow (Shipwreck Preservation Society of Newfoundland and Labrador 2020).

Conclusion

To fully appreciate the wide variety of cannon failure patterns, a collection of different failed guns was collected, documented, and selected for analysis. The guns described in this chapter were both accessible to the author and representative of different types of weapons. Many more examples of failed guns likely exist elsewhere in the world, and as more museums and archives digitize their collection of artifacts, hopefully more examples will become readily apparent. The niche aspect of exploded guns, as well as the vague terminology utilized to describe them, makes identifying and tracking them very difficult. Often, it is not recognized in archaeological literature that a gun is even broken, and thus they are not tagged or described as such. For example, in "A proposed standard in the reporting of historic artillery," Rudi Roth never mentions the measurements and details needed if a failed cannon is encountered (Roth 1989:191–202).

The collection of guns described above indicate several different breakage patterns. Some guns broke in half aft of the trunnions, others broke in half forward of the trunnions. Additionally, some guns are missing trunnions or cascabels altogether. Other weapons showed significant damage to the muzzle area, with severe cracking or splaying. A few guns seem otherwise undamaged, except for large chunks of metal missing from parts of the barrel. Perhaps these different failure patterns point towards larger trends in cannon failure. In the following chapter, an attempt is made to connect the examples of failure patterns shown above to different failure causes. The utilization of engineering theory and technology, in accordance with archaeological data and methodology, hopefully shed light on how and why the various guns shown above failed.

Chapter 6: Utilizing Engineering Software to Analyze Failed Gun

Introduction

Through analysis of all the data collected in Chapter Five, four types of primary failure profiles were generated. The methods for determining the following classifications were discussed at length in Chapter Four. These are based on creating an archaeological catalog and then subjecting the failed guns to engineering analysis while considering their historical and archaeological context. A Type I is classified as a "muzzle failure," defined as a fracture anywhere in the first 30 cm (11.81 in) of the cannon. Type II is labelled a "barrel failure forward of the trunnions" and is defined as any failure of the barrel between 30 cm (11.81 in) aft of the muzzle and forward of the trunnions. A Type III failure is classified as a "barrel failure aft of the trunnions" and describes any failure in the aft section of the barrel and the breach. A Type IV failure is classified as a "extremity failure" and describes any failure which effects one of the "extremities" of the gun: trunnions, cascabels, cascabel rings, hoisting dolphins or hoops, or other protrusions from the gun. In this chapter, each profile is reviewed in depth, and one or two examples of each are modeled and tested in engineering software and examined as a case study.

Each model is explained, and the combination of physical forces involved which resulted in the failure mode are examined and described. Any additional combinations of engineering simulations used are noted and explained, and the results discussed. The goal of this chapter is to determine if modern CAD and FEA engineering methodology can accurately replicate gun failures. To do so, guns were modeled and tested as outlined in Chapter Four, and then the results of the test compared with the archaeological data and contextualized within history. Additionally, this chapter helps determine *what* engineering factors can be measured accurately and helps determine whether cannon failures occurred before or after archaeological deposition.

It is also important to note that the textual order in which each failure type is analyzed in this chapter were arbitrarily assigned. For example, there is no reason that "muzzle failure" was chosen as Type I and "extremity failure" was not; no priority is implied. Additionally, Chapter Four, subsection Value Parameters for FEA Analysis should be consulted for any questions regarding Von Mises Stress, Displacement, or Factor of Safety.

Type I: Muzzle Failure

Cannons BR–07, BR–08, SW–07, and UN–01 represent suitable examples of a Type I failure. Of these weapons, UN–01 was selected as an archetype for several reasons. Substantial research was previously conducted on this gun by the management team at BTFA. Site Manager Jim McKee invested significant resources to conserve and document this weapon and generously provided his measurements and personal notes to aid in this research project. UN–01 was chosen because it is the most thoroughly recorded, complete with detailed photogrammetric data, known archaeological context, and multiple sets of highly accurate measurements corroborated by multiple individuals. The other examples of muzzle failures collected during this study were utilized to enhance this analysis and provide a dataset for comparison. Because many photos were taken of all the Type I examples, the breakage patterns of the entire dataset was compared and contrasted to UN–01 with ease.

Muzzle Failure FEA Simulations

As stated in Chapter Five, UN–01 is a demi-culverin 6–pounder likely of Spanish or British origin and recovered from the Cape Fear River during a dredging operation in 2017 (Jim McKee 2024, pers. comm.). A photo of this weapon can be seen in Figure 86. While it is in good condition overall, a large chunk of the muzzle located on the dorsal surface of the gun is missing. The weapon shows signs of damage both before and after being deposited into the archaeological record, including those resulting propeller strikes and severe pitting from deterioration, as depicted in Figure 95 and in the archaeological drawing depicted in Figure 96. Further analysis indicates that the missing forward section of the barrel was not due to damage during the dredging operation but is evidence of a cannon explosion. A spiraling crack–like feature was located within the barrel which terminated into the missing section. An archaeological drawing of this gun after conservation is depicted in Figure 96, and a photogrammetric model of this gun is presented in Figure 97. A scaled engineering drawing of the CAD model is depicted in Figure 98.

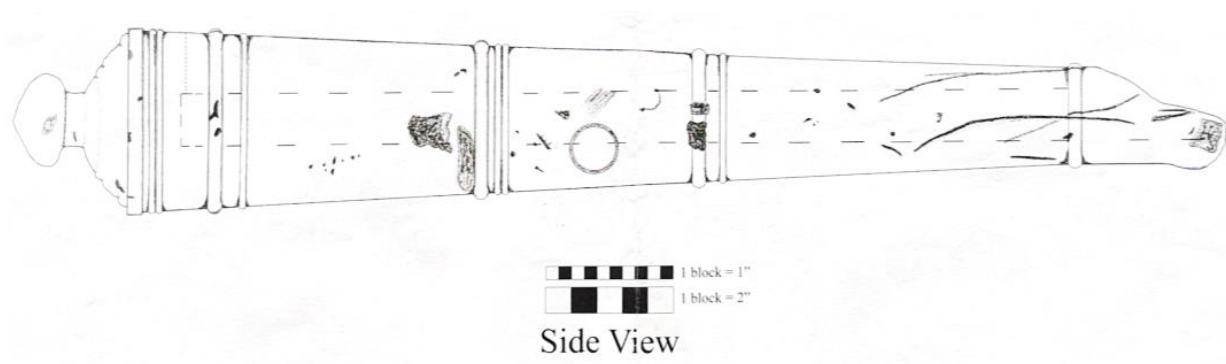

Figure 96: An archaeological drawing of UN–01, a demi-culverin 6–pounder, (courtesy of Jim McKee, Brunswick Town/Fort Anderson State Park).

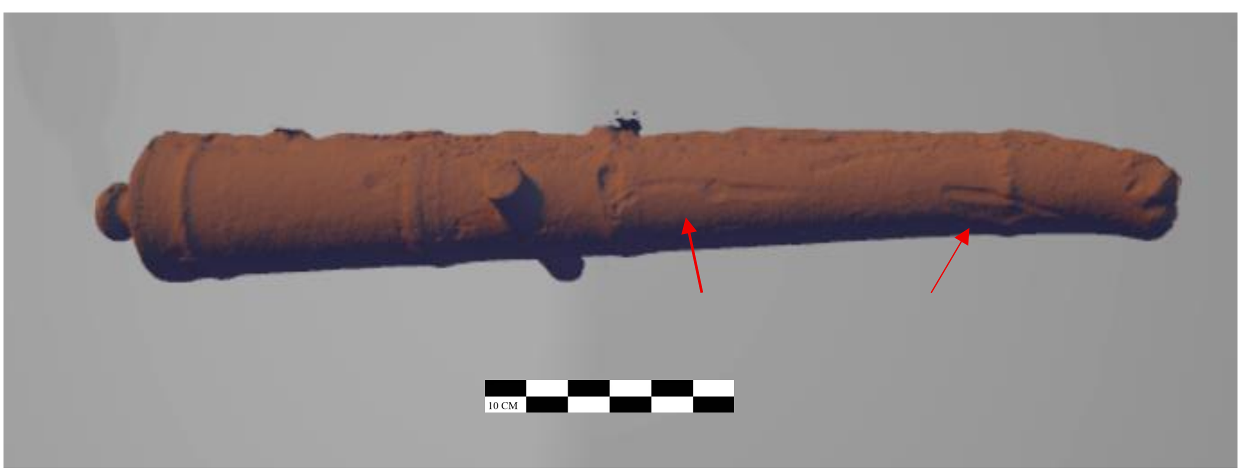

Figure 97: The Photogrammetric model of UN–01, ventral perspective. Note blade prop strikes, indicated by the red arrows. (Model created by James Fowler in Agisoft Metashape.)

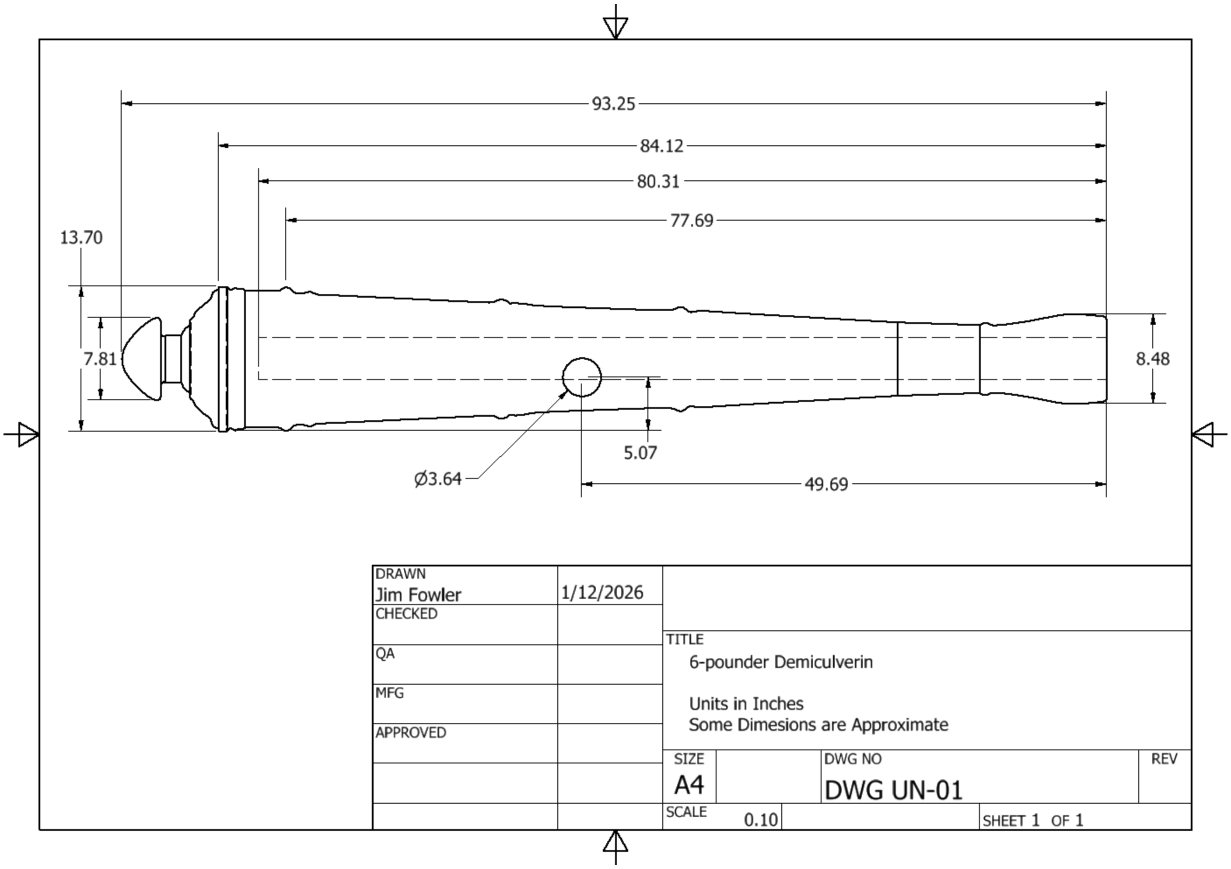

Figure 98: A dimensioned engineering drawing of the UN–01 CAD model. (Created by James Fowler in Autodesk Inventor.)

BTFA Site Manager Jim McKee believes the spiraling crack is a sprung core mold wire. According to McKee, the cannon was cast with a mold for the interior bore made from a fence post wrapped in metal wire (McKee 2024, pers. comm.). This method is a known manufacturing process utilized to cast guns of this type during the 18th century (Cooper 2024:40–41). Upon close examination, it appears one of the wires became trapped in the casting (Figure 98). The engineering solid model is depicted in Figure 99 and a close-up photo of the spiraling metal wire embedded in the interior of the bore can be seen in Figure 100.

Figure 99: UN–01 6–pounder Demiculverin CAD model, (Created by James Fowler in Autodesk Inventor.)

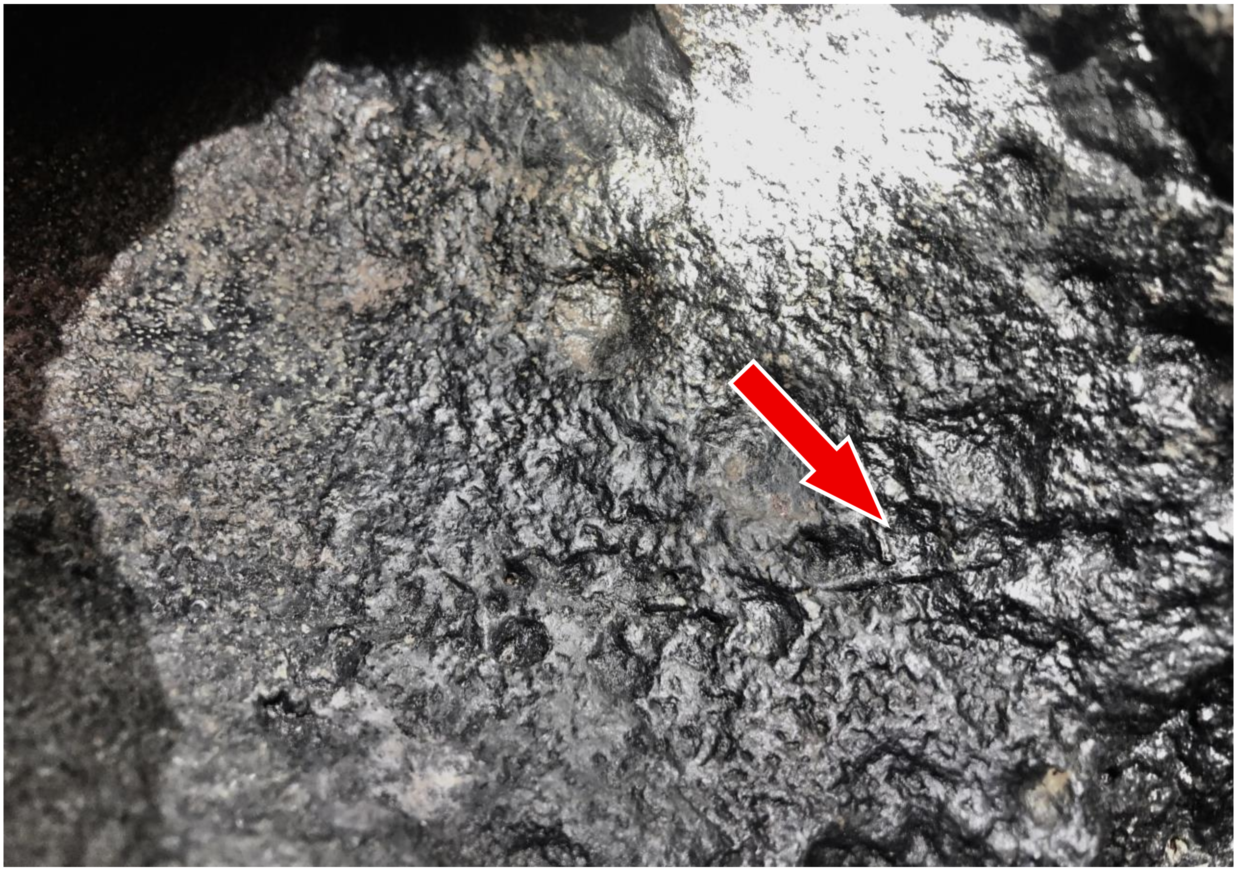

Figure 100: The wire embedded in the bore interior wall (visible in the lower half of the image). (Image by James Fowler.)

Example: UN–01

Initially, the model was created without the embedded wire to produce a baseline model for Type I failure analysis. Utilizing the pressure equation methodology described in Chapter Four, a momentary peak bore pressure of 100,100.04 psi (690.2 MPa) was calculated, with a mean bore pressure of 12,100.16 psi (83.4 MPa). The first number represents a momentary pressure spike, which rapidly decreases as the ball moves down the barrel. This was determined to be a realistic peak bore pressure for a cannon of this size, considering some 1850s tests of slightly larger guns returned peak bore pressures in the high 160,000s psi (1103.2 MPa) and resulted in bursting

(Cooper 2024:163–164). The bore pressure relative to the cannonball location graph for UN–01 is depicted in Figure 101.

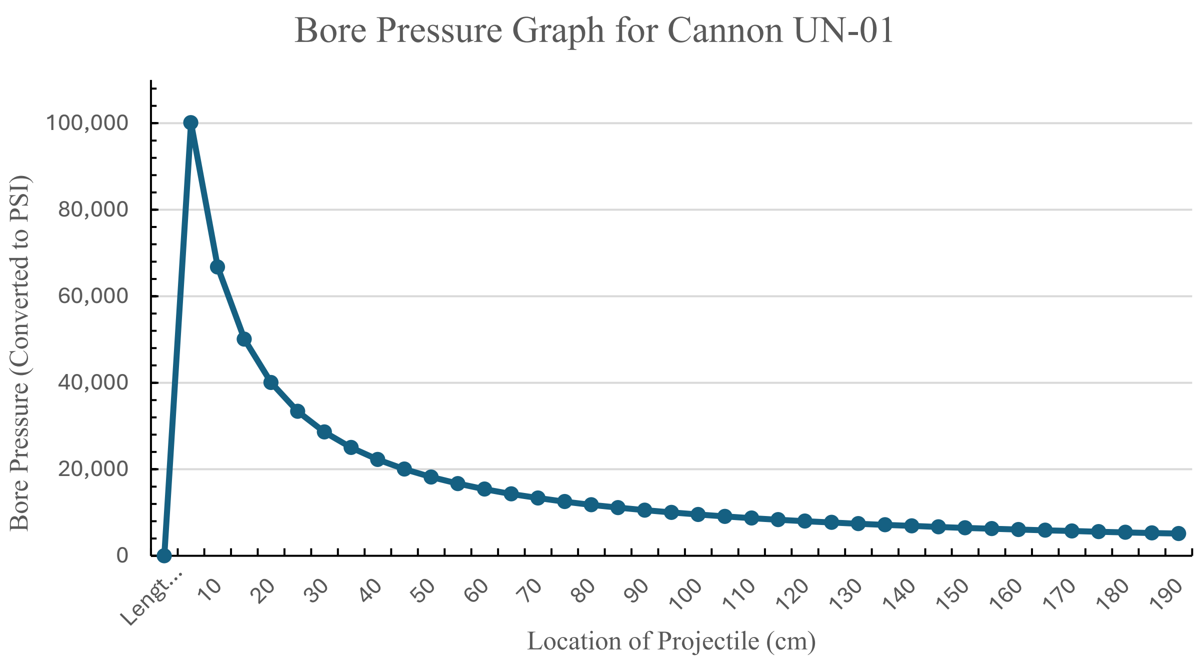

Figure 101: Bore Pressure Graph for UN–01 (Graph created in Microsoft Excel by James Fowler).

The cannon ball was initially located 10 cm offset from the interior breech face to allow room for the powder charge, as described in Chapter Four. The cannon was tested at bore pressures at each interval of 20 cm (7.87 in). The first interval (when the cannon fired initially, and the ball has yet to move) is depicted in Figure 102 and Figure 103 and shows that the cannon does deform by a maximum displacement of 0.04 cm (0.02 in). The FoS graph indicates that some regions of the cannon's interior encounter a minimum FoS of 0.57, indicating that the cannon could fail under the applied load of 100,100.04 psi (690.2 MPa) in this region. However, the external surfaces are well within a safe FoS range, varying between 6.0 and 9.0, which indicates that it may take some time for fatigue fractures to compromise this part.

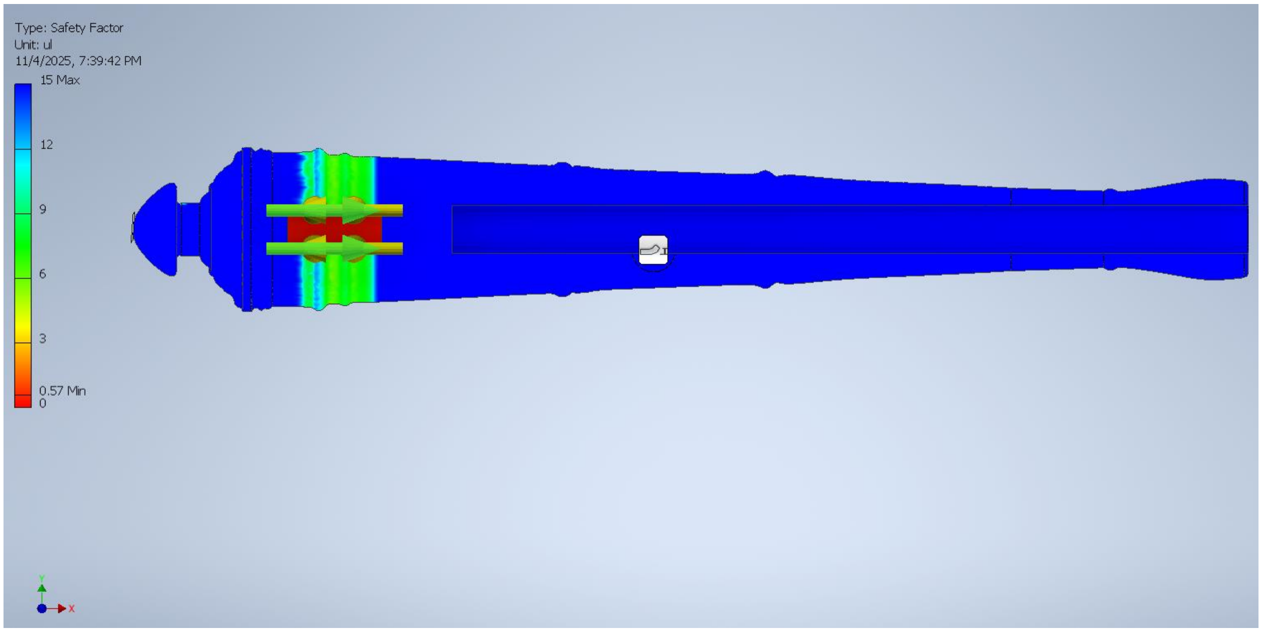

Figure 102: The Factor of Safety graph for UN–01 at the 10 cm interval; actual displacement shown. (Created by James Fowler in Autodesk Inventor.)

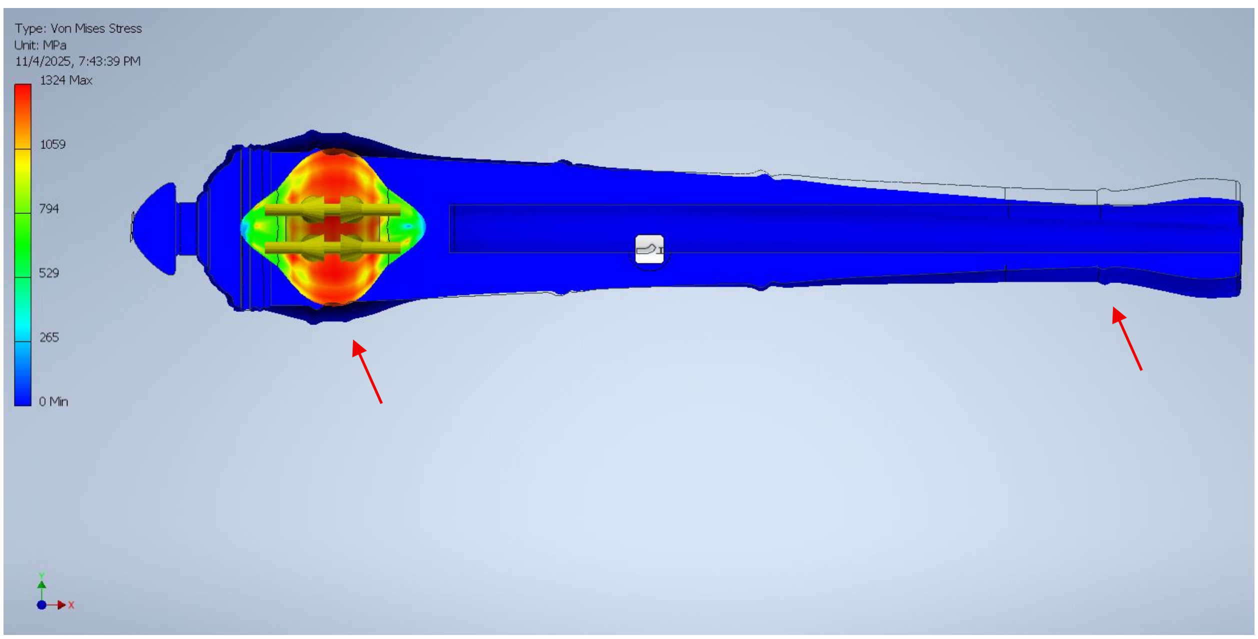

Figure 103: The Von Mises Stress graph for UN–01 at the 10 cm interval; exaggerated displacement indicated by red arrows. (Created by James Fowler in Autodesk Inventor.)

As seen in Figure 103, regions of the interior bore wall reach a maximum Von Mises stress of 1324 MPa (192 ksi), well over the material's yield strength. However, the Von Mises stress encountered on the outside surface is in the low 200s MPa (29 ksi), indicating that the thick-walled structure of the gun initially contains any material yield. Although fatigue will set in over cyclical use, the weapon is less likely to fail in this region. As the cannon ball travels down the barrel, however, some interesting results were observed. At 120 cm (47.24 in), the pressure equation indicated that the internal pressure would be around 57.5 MPa (8,341.7 psi). The FoS increases to a minimum of 4.6 as the pressure spike decreases as seen in Figure 104.

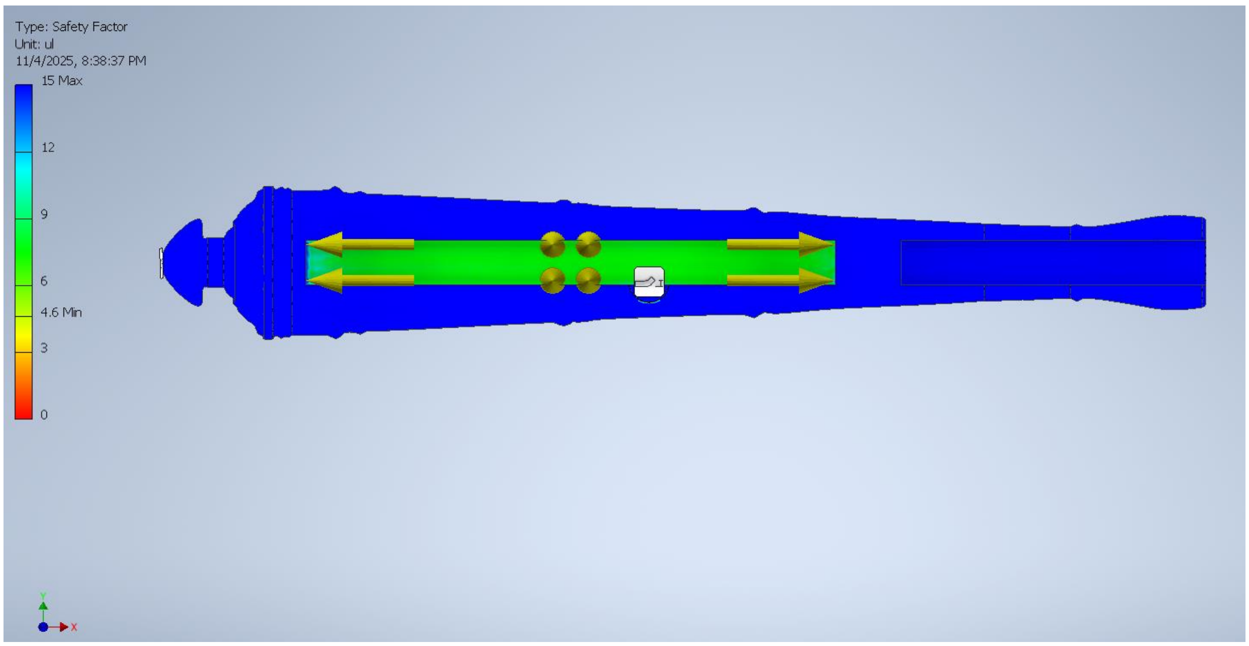

Figure 104: The Factor of Safety graph for UN–01 at 120 cm; actual displacement shown. (Created by James Fowler in Autodesk Inventor.)

Interestingly, the largest displacement happens on the dorsal surface of the bore interior, which mirrors what is found in the archaeological record, displayed in Figure 105. The FoS graph indicates that as the ball travels past the 120 cm (47.24 in) mark, the area behind the ball is subjected to lower FoS values. As the projectile passes the 180 cm (70.87 in) mark, the physical cannon failed. The simulation of this point is depicted in Figure 106. The FoS and Von Mises stress values are below critical, with a minimum FoS of 3.94 and a maximum Von Mises stress of 192.3 MPa (27.9 ksi).

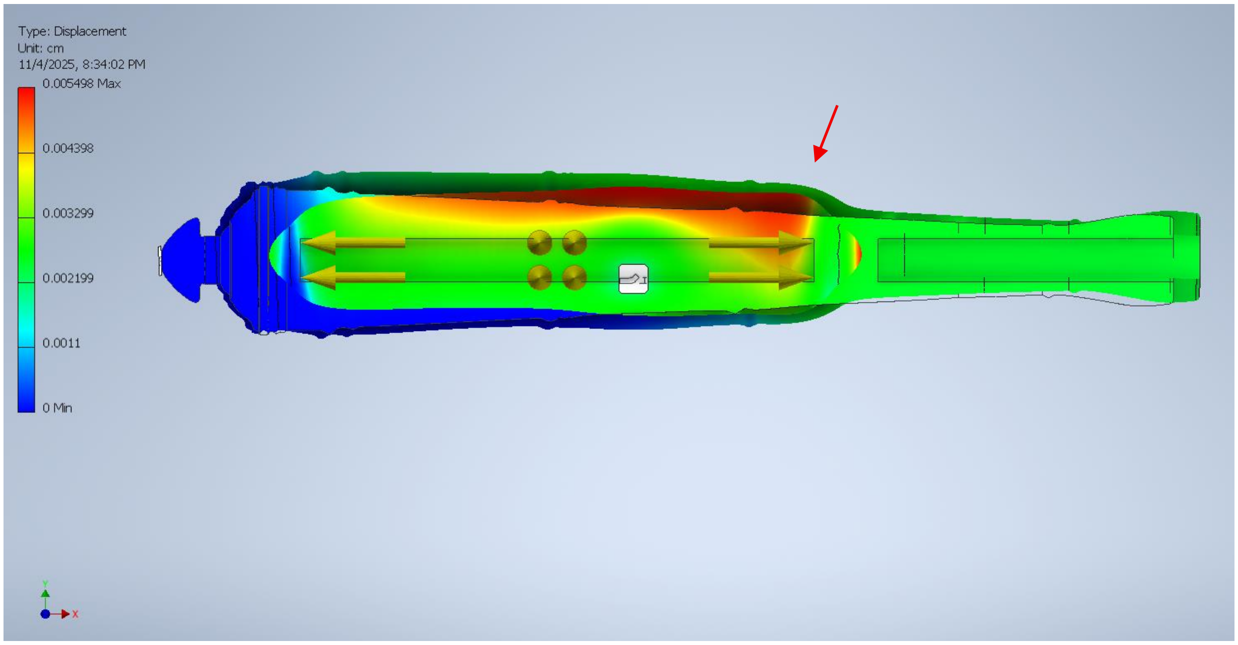

Figure 105: The Displacement graph for UN–01 at 120 cm. Exaggerated displacement shown. Red arrow indicates deformation on the dorsal surface of the interior of the bore. (Created in Autodesk Inventor by James Fowler.)

What is noticeable, however, is the wave of displacement that follows behind the projectile as it leaves the gun (Figure 106). This cyclical loading would slowly build stress fractures in the regions of greatest displacement, which may lead ultimately to failure. From what can be determined by these pressure tests, the cannon was well designed and could sustain repeated loads of this sort. The breech area was subjected to the most stresses, and in places encountered substantial loading. It seems likely that if fatigue occurred, it would be located mostly towards the breech section which saw the highest loading. However, with the inclusion of the spiraling crack, a new picture emerges. When the cannon failed historically, as the projectile moved down the barrel, the barrel deformed upwards, which can be simulated in the present if the projectile is removed and only an interior pressure is exerted on the weapon (Figure 107).

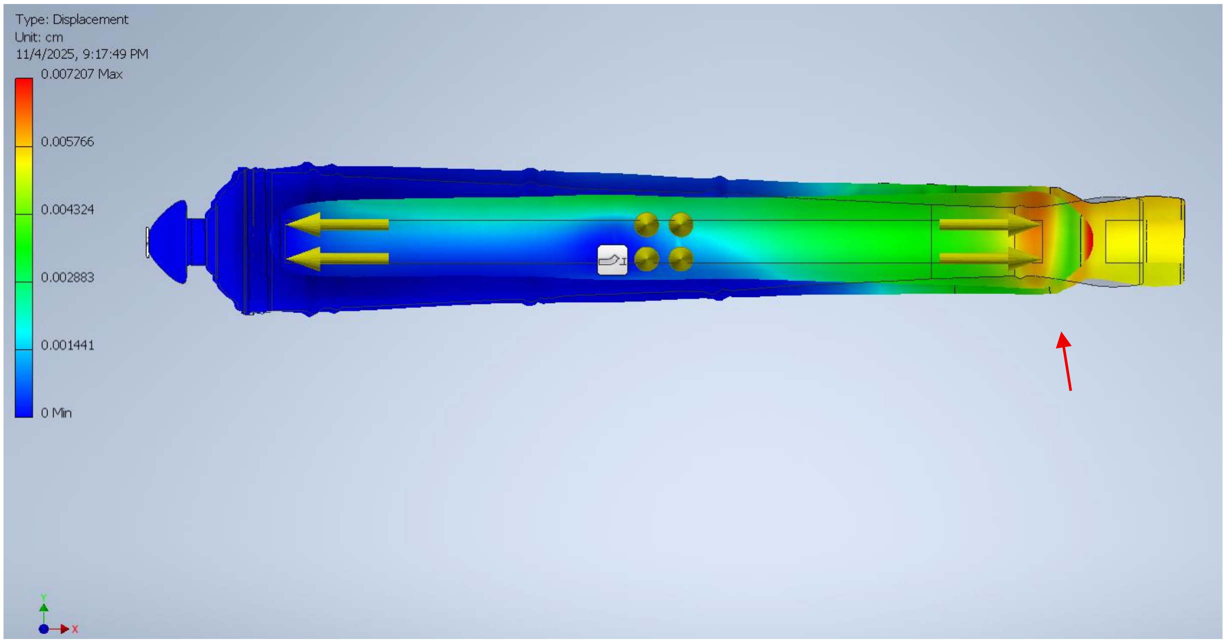

Figure 106: The Displacement graph for UN–01 at 180 cm; exaggerated displacement shown. (Created in Autodesk Inventor by James Fowler.)

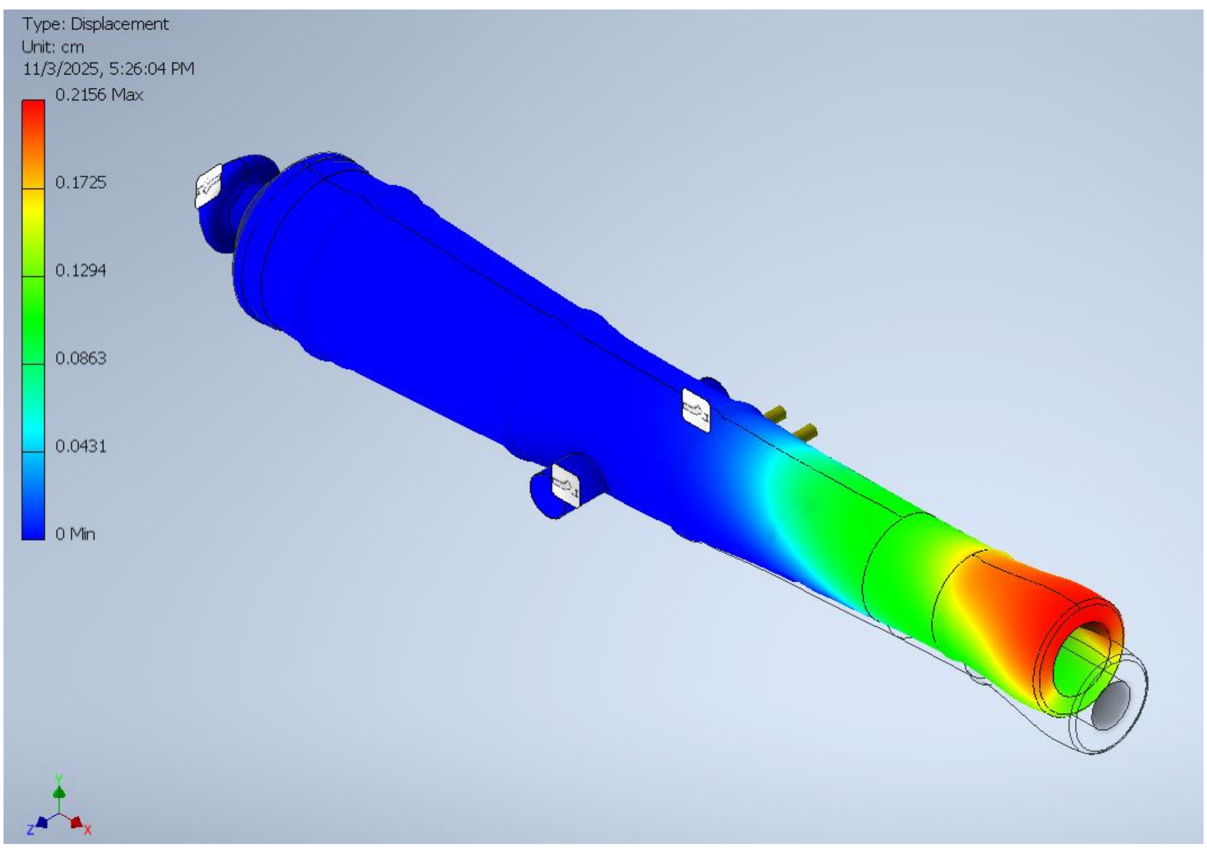

Figure 107: Displacement graph for the UN–01 (created in Autodesk Inventor by James Fowler).

It appears that after the projectile leaves the muzzle, the ventral forward portion of the weapon experiences the greatest displacement. When analyzed in Inventor Nastran FEA software, the lowest FoS was found near the muzzle fracture location. When the divot created by the wire was included in the CAD solid model, and subjected to FEA, the Von Mises stress diagram indicated that an intense stress concentration was present along the length of the spiraling crack. In some key spots, including in exactly the region where the gun failed, the area around the crack displayed stress values 30% higher than the material's yield strength, indicating that each time the cannon was fired, the crack became worse. A close view of this can be seen in Figure 108.

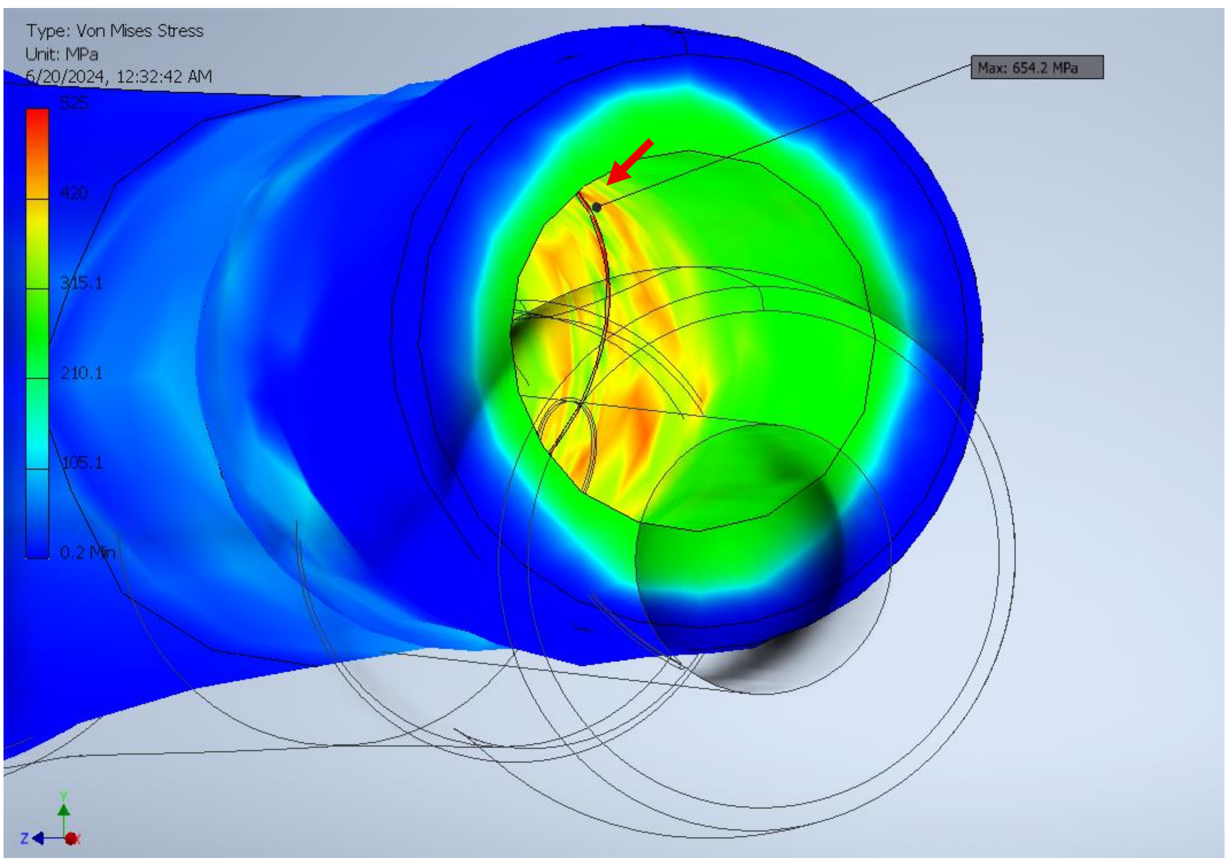

Figure 108: The stress concentration around the spiraling crack in UN–01. Red arrow indicates crack caused by embedded wire. (Created in Autodesk Inventor by James Fowler.)

Further analysis in Inventor Nastran shows a similar pattern in the FoS graph, shown in Figure 109. Although the FoS is still high with a minimum of 3.53, the areas of lowest FoS, and thus most prone to fatigue in this stage of firing, are in the region where the barrel failed.

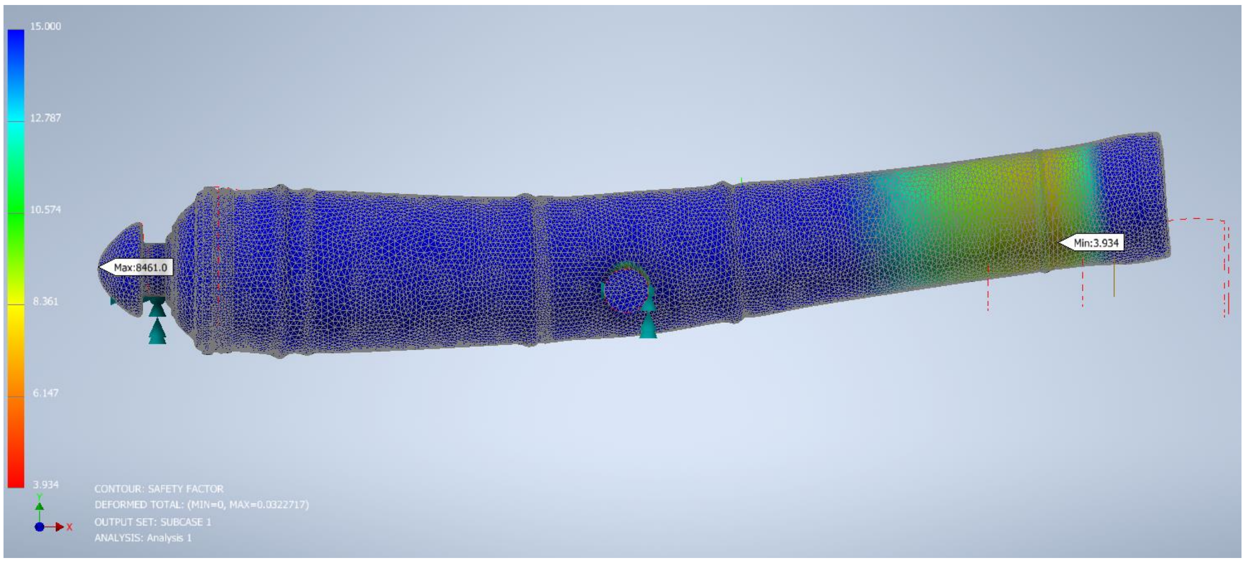

Figure 109: Factor of Safety graph for UN–01 when the projectile is no longer in the barrel. (Created in Autodesk Inventor NASTRAN by James Fowler.)

Muzzle Failure Trends

From an analysis of the FEA simulation results, several notable trends emerge. Clearly the highest stress concentrations in the UN–01 design are primarily in the breech region, near where the peak pressure occurs before the projectile moved down the barrel. However, as the pressure equation dictates, the bore pressure drops off substantially as the projectile moves down the barrel, dropping almost 90% from peak pressure. This is visualized in Figure 101, and means that when the projectile reaches the muzzle, the muzzle is subjected to substantially lower pressure than peak pressure, which rules out the likelihood of an over–pressure failure. All other variables held constant, the shorter the barrel, the more likely for an over–pressure failure. Fatigue failure would likely not cause the muzzle to fail before another region, unless the muzzle was poorly designed or included serious manufacturing defects.

Considering failure of the UN–01 design is less likely caused by fatigue or over–pressure in the muzzle area, this indicates that the UN–01 barrel probably failed due to the manufacturing defect. The embedded wire, possibly combined with poor internal material distribution, likely caused the gun to fail. Additionally, as explained in Chapter Two, the metal in the breech would have solidified last during the casting process, resulting in a tighter grain structure in the breech and a thinner, brittle and more porous composition towards the muzzle, which could result in failure (Greener 1858:277; Guilmartin 2003:307–312).

If we compare UN–01 to other guns which failed in the muzzle, several trends appear. Cannon BR–03 also failed near the muzzle, and the weapon shows signs of pitting and corrosion on the outside of the barrel, and the presence of a large groove that circles the muzzle of the weapon. This may indicate the presence of inclusions or other manufacturing defects within the muzzle of the weapon that resulted in its failure. Cannon BR–05, BR–06 and SW–22 each suffer from similar features, and resulted in similar failures. Cannon BR–04 also failed in the muzzle region, and the weapon also shows signs of severe pitting and corrosion on the outside of the gun, as did BR–05 and BR–06. It is uncertain whether this is due to transformation processes or material defects. Additionally, this weapon fractured in a similar pattern to UN–01, in that the top forward piece of the muzzle broke off in a diagonal fracture from the aft dorsal surface to the forward ventral surface. Perhaps, as indicated in Figure 107, repeated displacement resulting in fatigue in this region, although not enough to result in failure attributable only to fatigue, weakened that area and made the region more prone to failing due to inclusions, porosity, or manufacturing defects. Cannon BR–07 also shows a similar breakage pattern.

It is worth noting, however, that some weapons fractured in an inverse pattern, with the fracture beginning on the ventral aft side and proceeding up and forward to the dorsal forward side. No explanation for this pattern was determined utilizing FEA and causation remains a mystery. Perhaps this is due to vibration fatigue or some combination of resonant frequency during material loading, something that is not covered in this study but provides an avenue for future research. BR–12, BR–06, and SW–07 each display this subcategory of muzzle failure. Alternatively, this pattern of failure could simply result from the random location of manufacturing defects within the muzzles of those individual guns.

To conclude, it appears that muzzle failures are mostly resultant from porosity, muzzle brittleness due to casting technique, manufacturing defects, and propensity for inclusions, but not due to overpressure, as proposed by some historic sources (Greener 1858:277). In the case of UN–01, it seems likely that the gun failed because of the imbedded wire, as first proposed by Jim McKee, but the location of the failure was dependent on the area which experienced the highest displacement. Additionally, the failure due to a casting defect was likely made more probable due to low levels of compounding fatigue. While the design of the gun itself was not overly susceptible to fatigue, any inclusions or spongey regions within the material matrix would have been extremely susceptible to fatigue cracking and may have provided a suitable genesis for expanding fatigue failure.

Type II: Barrel Failure Forward of the Trunnions

Type II failure is similar to a Type I muzzle failure, however, it happens between 30 cm (11.81 in) aft of the muzzle and the region forward of the trunnion. Examples of this kind of failure are observed in BR–01, BR–02, SW–05, and UN–04. Although consideration was given to divesting the Type I category into Type II and Type III failures because they are very similar in origin and result, the decision was made to differentiate them because there are some notable differences in results. Multiple examples were selected for analysis. BR–01 and BR–02 were chosen because they represent drastically different shot weight, being 24– and 65–pounders respectively. Additionally, the latter is a design iteration on the former, representing the culmination of 50 years of technological advancement (McConnell 1988:27–28; Tucker 1989:118; Henry 2004:45).

Barrel Failure Forward of the Trunnions FEA Simulations

The 24–pounder Blomefield (BR-01), was selected for this analysis first. The dimensioned engineering drawing for this cannon is shown in Figure 110, the CAD model in Figure 111, and the pressure graph in Figure 112, while Figure 31 depicts the photogrammetric model.

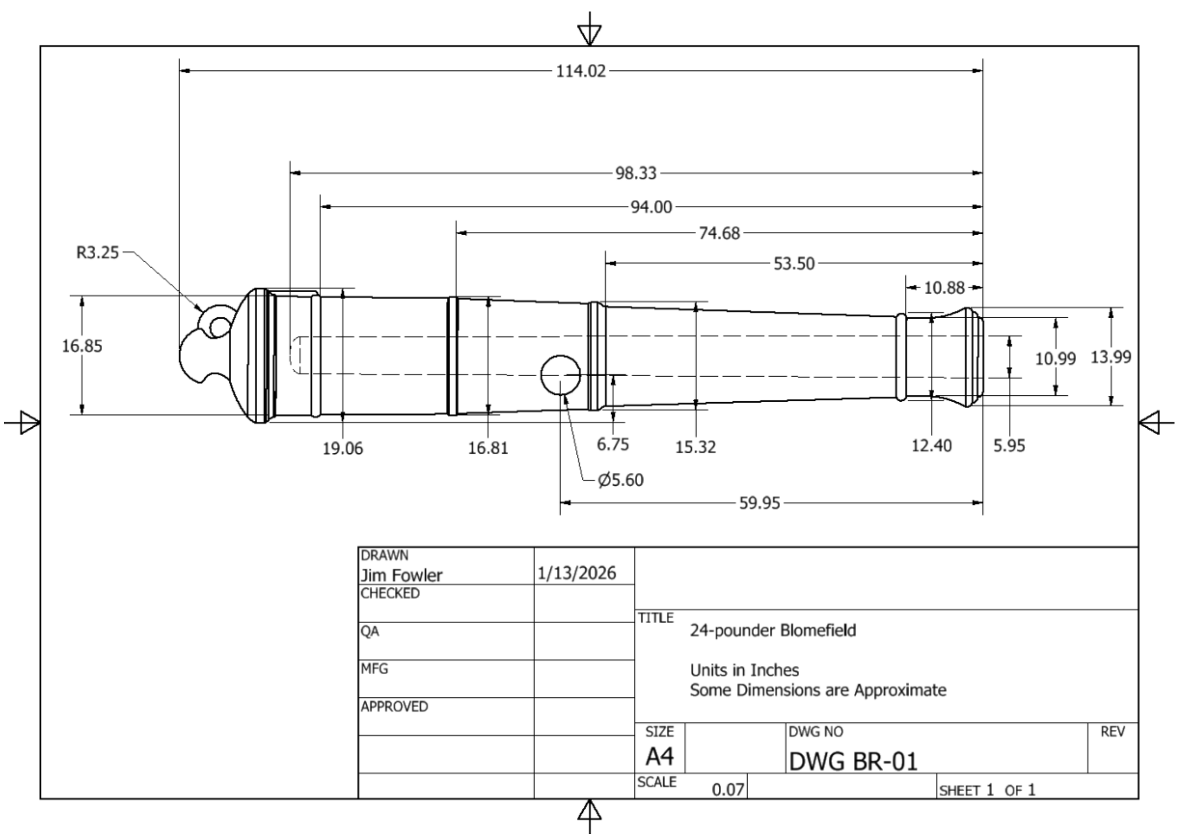

Figure 110: A dimensioned engineering drawing of the BR–01 CAD model. (Created by James Fowler in Autodesk Inventor.)

Figure 111: BR–01 24–pounder Blomefield CAD model. (Created in Autodesk Inventor by James Fowler.)

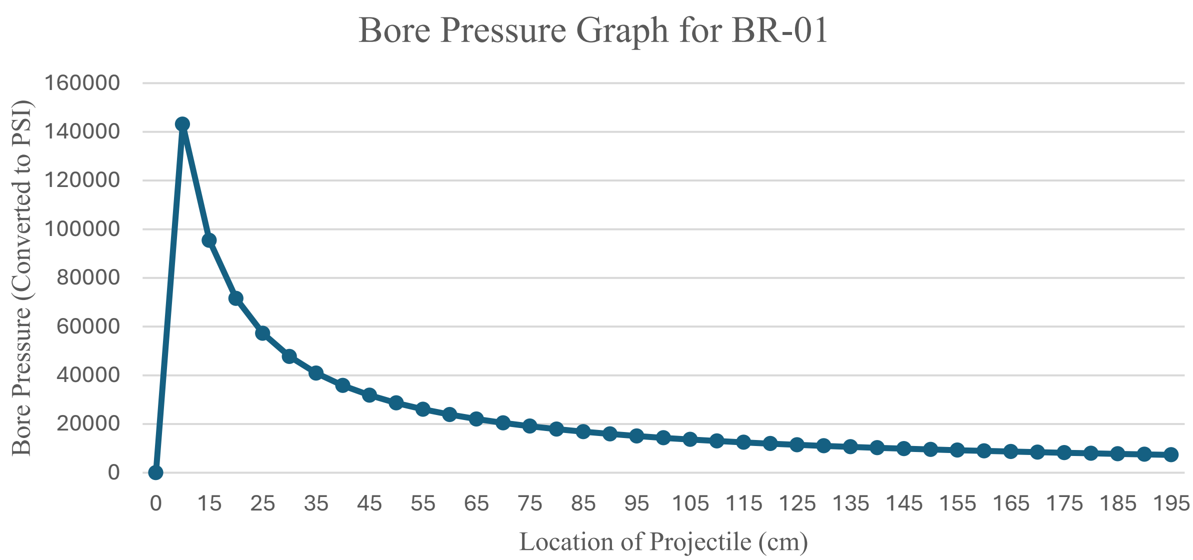

Figure 112: Bore Pressure Graph for BR–01. (Created in Microsoft Excel by James Fowler.)

The 65–pounder Millar–pattern shell gun (BR-02), was the second cannon chosen for analysis. The dimensioned engineering drawing for this cannon is shown in Figure 113, the CAD model is depicted in Figure 114, and photogrammetric model in Figure 33. BR–01 failed approximately 1 meter forward of the trunnions in a diagonal pattern across the weapon, while BR–02 failed directly in front of the trunnions, perpendicular to the axis of the bore. To model the firing of BR–01, the peak bore pressure was calculated to be 143,130.8 psi (986.8 MPa) at 20 cm (7.87 in) distance from the breech face, and the peak bore pressure of BR–02 was calculated to be 170,108.5 psi (1172.8) at 10 cm (3.94 in) distance. The pressure graph for this weapon can be seen in Figure 115.

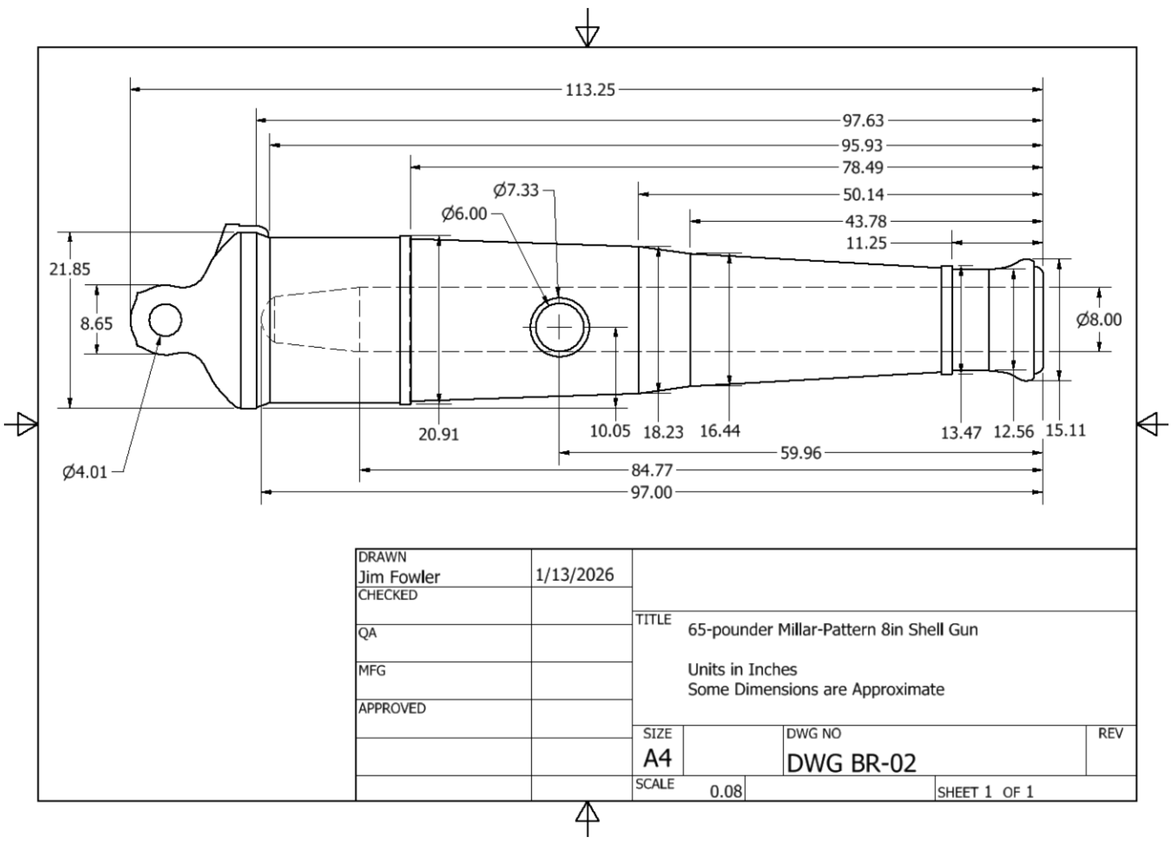

Figure 113: A dimensioned engineering drawing of the BR–02 CAD model. (Created by James Fowler in Autodesk Inventor.)

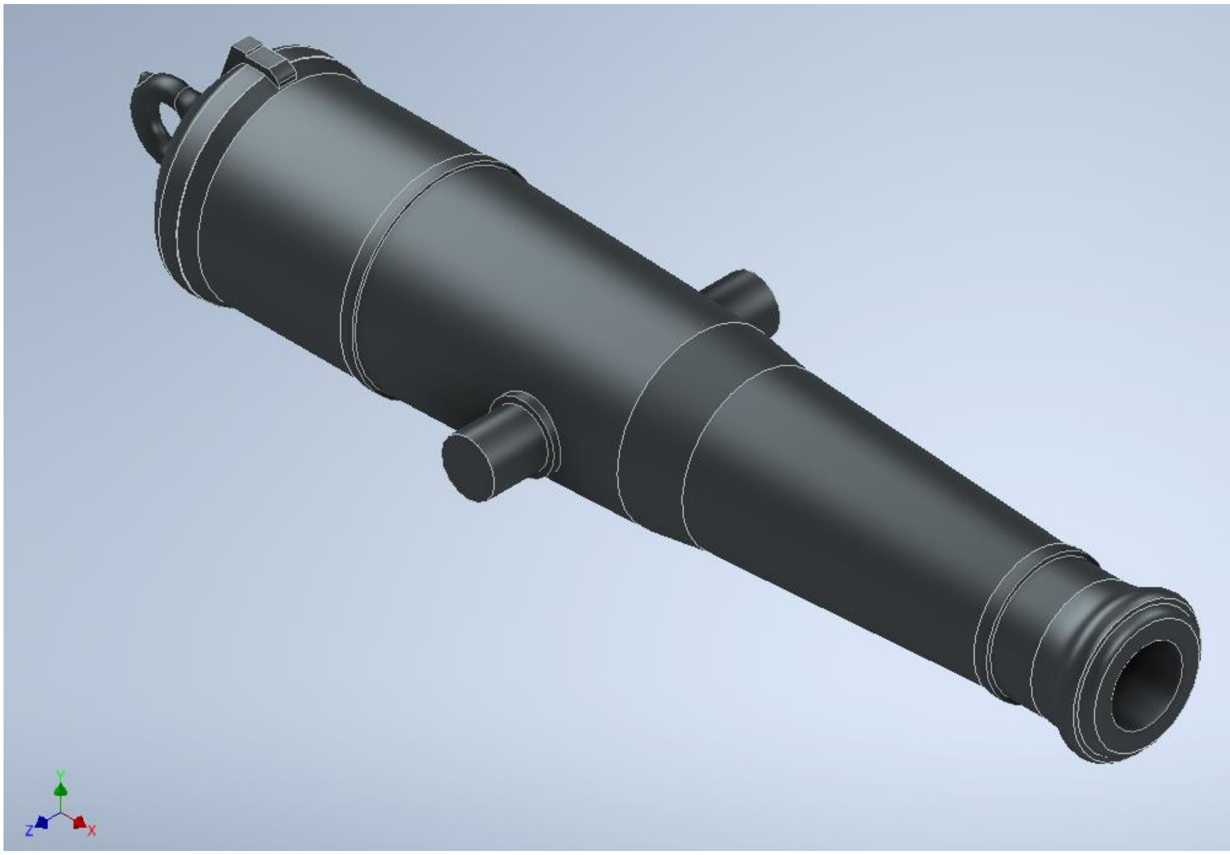

Figure 114: BR–02 65–pounder Millar pattern shell gun CAD model. (Created in Autodesk Inventor by James Fowler.)

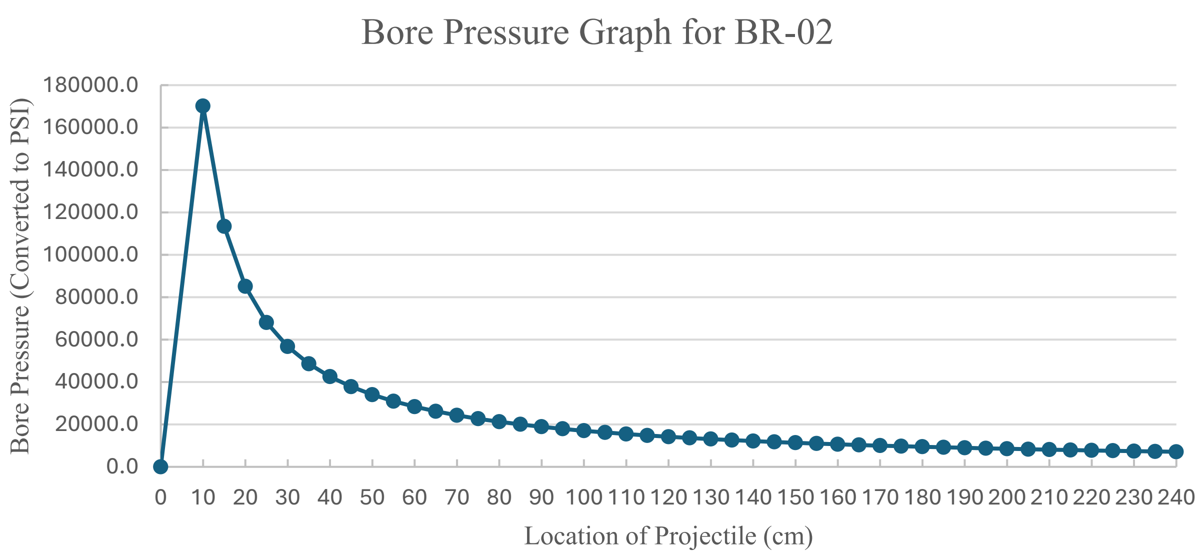

Figure 115: Bore Pressure Graph for BR–02. (Created in Microsoft Excel by James Fowler.)

Example: BR–01

The BR–01 design shows a similar pattern when compared to UN–01. The Von Mises Stress within interior of the bore during peak pressure is 266 ksi (1834.01 MPa), which is substantially more than the material's yield strength (Figure 116). Additionally, the FoS within the bore is very low, even lower than UN–01, at 0.41 (Figure 117). This indicates that like UN–01, the bore is exposed to substantial deformation and stress during firing, enough to exceed the yield strength of the material on the inner surface but not on the outer surface.

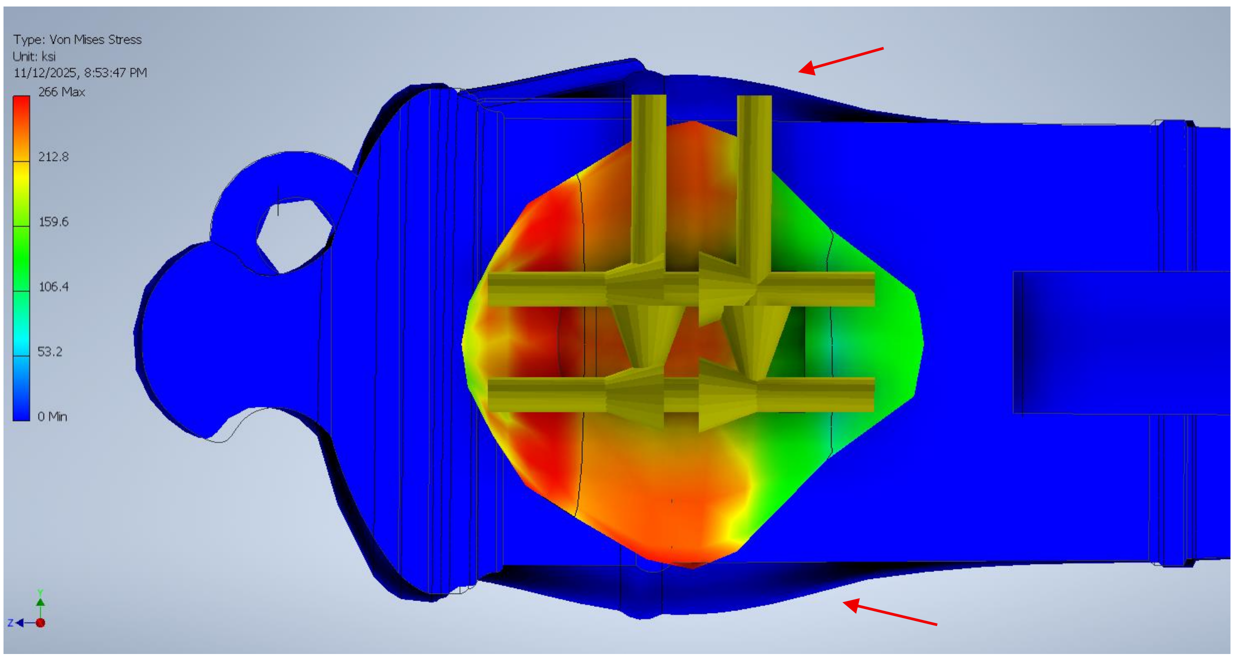

Figure 116: The Von Mises Stress graph for BR–01 at the 10 cm interval. Red arrows indicate exaggerated displacement. (Created in Autodesk Inventor by James Fowler.)

When the projectile is moved forward to the 120 cm (47.24 in) mark, close to where the weapon failed, the pressure is calculated to have dropped significantly to 11,927.6 psi (82.2 MPa). However, in this location where it might be expected to find a design flaw forward of the third reinforcement ring, no substantial design flaw is found. The displacement is low, at around 0.003 inches (0.007 cm). This is displayed in Figure 118. Additionally, a nominal FoS was measured in this region as well with a minimum at around 2.62, as seen in Figure 119, with sustainable levels of Von Mises Stress. This indicates that even with a full load of gunpowder, this region is not susceptible to overpressure failure.

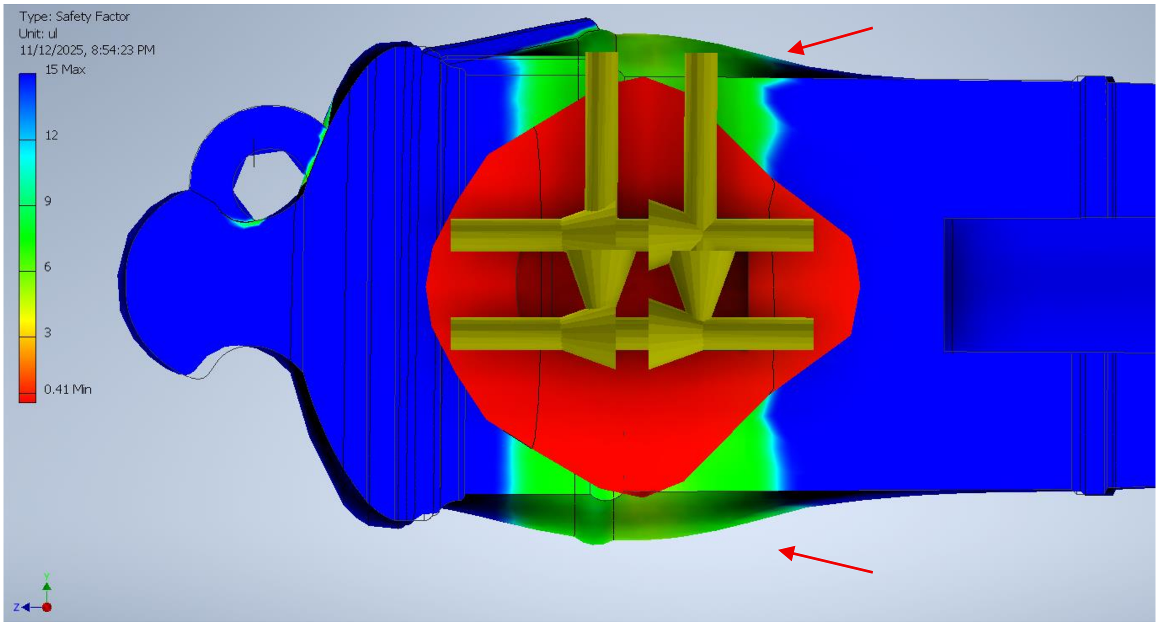

Figure 117: The Factor of Safety graph for BR–01 at the 10 cm interval. Red arrows indicate exaggerated displacement. (Created in Autodesk Inventor by James Fowler.)

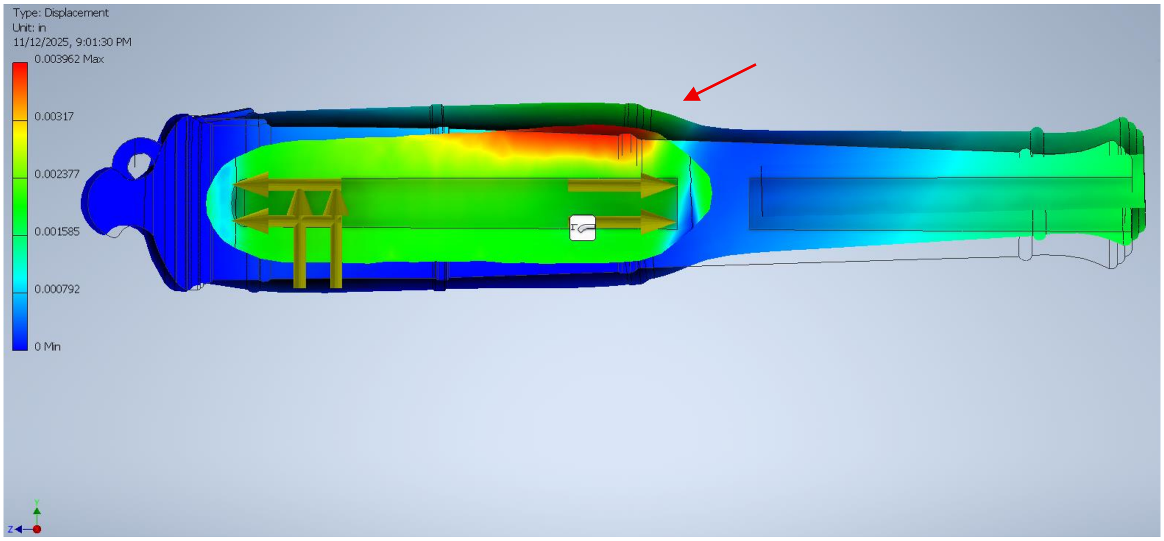

Figure 118: The Displacement graph for BR–01 at the 120 cm interval. Red arrow indicates dorsal deformation region. Exaggerated displacement shown. (Created in Autodesk Inventor by James Fowler.)

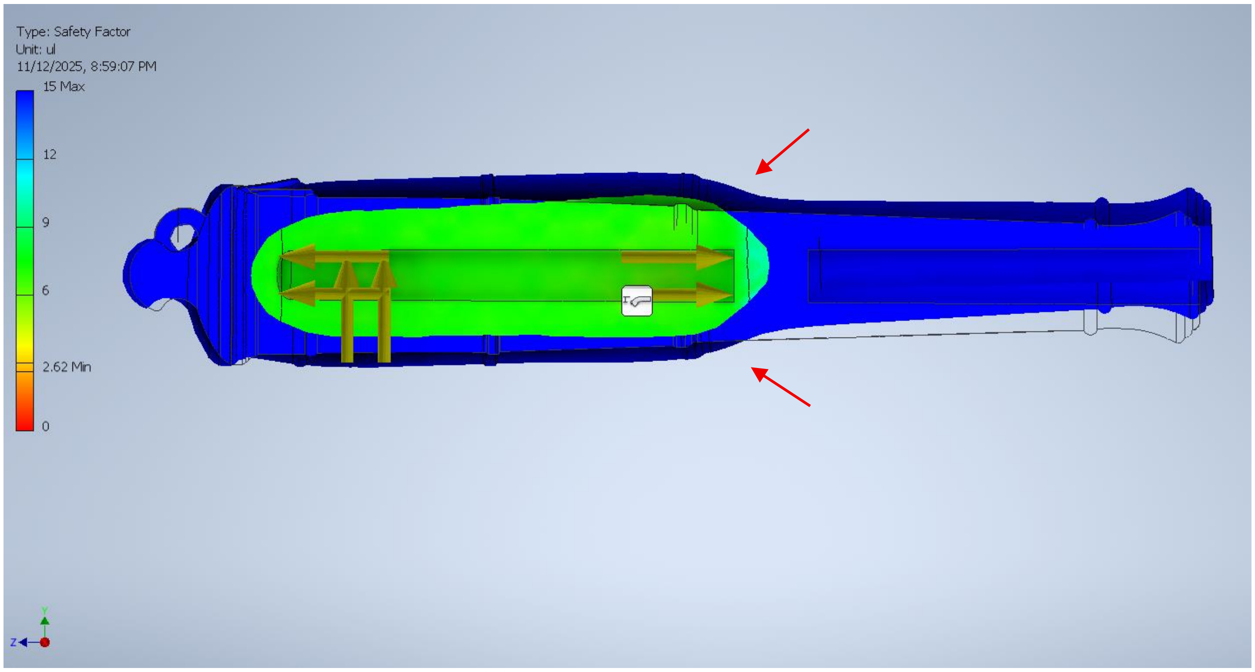

Figure 119: The Factor of Safety graph for BR–01 at the 120 cm interval. Red arrows indicate exaggerated displacement. (Created in Autodesk Inventor by James Fowler.)

To double check the results, a double load of gunpowder was tested and the pressure at the 120 cm (47.24 in) mark was tested at 20,000 psi (137.9 MPs). This load of gunpowder would have likely caused the weapon to burst at the breech, however assuming it survived for the projectile to reach the 120 cm (47.24 in) mark, it was found that the pressure at this point was still low enough not to cause a pressure–related burst in this region. The wall thickness is simply too thick. A minimum FoS of 1.57 was recorded, as displayed in Figure 120. This indicates that the cannon was well designed in this region, but this does not rule out the likelihood of a manufacturing defect or fatigue failure point.

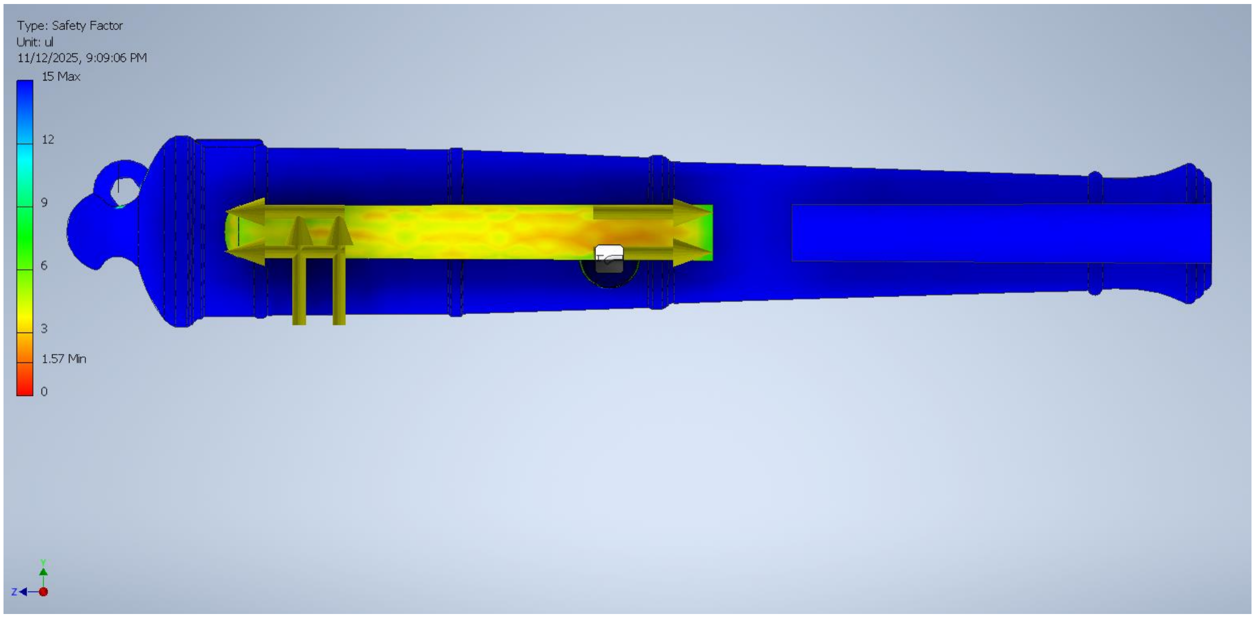

Figure 120: The Factor of Safety graph for BR–01 at the 120 cm interval, given a double charge of gunpowder. Exaggerated displacement shown. (Created in Autodesk Inventor by James Fowler.)

Example: BR–02

The BR–02 design, when tested using FEA at the 10 cm (3.94 in) mark, is deformed by a 305.7 ksi (2107.7 MPa) force, substantially more than the material's yield and tensile strength. (Figure 121). Additionally, the displacement in the region hovers around 0.02 in (0.5 mm), which is substantial, given the nominal ranges described in Chapter Four. The FoS is also very low, at 0.36 in the immediate blast region. However, like many of the examples in this chapter, deformation on the outside of the gun is nominal, and forces dissipate as they propagate towards the outside face of the material. As such, fatigue failure would result after substantial usage, although this reaction is common in other guns.

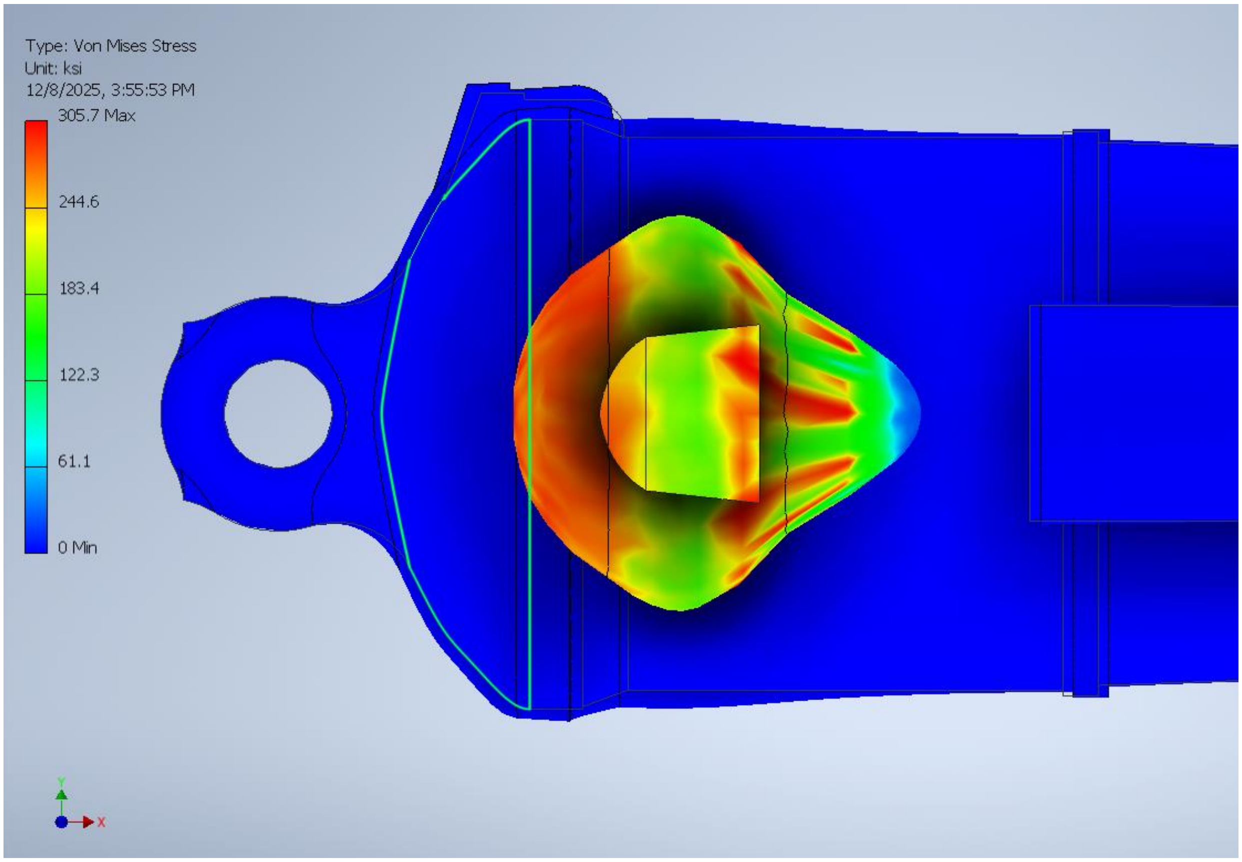

Figure 121: The Von Mises Stress graph for BR–02 at the 10 cm interval. Exaggerated displacement shown. Force vectors removed for clarity. (Created in Autodesk Inventor by James Fowler.)

When the projectile is moved further down the barrel to the 100 cm (39.37 in) region, where the physical cannon failed, the pressure drops substantially to 17,010.8 psi (117.3 MPa), as expected. Notably, however, at this point the FoS rises above the nominal 1.0 into the optimal value region, and the entire model displays a blue color to describe a high FoS value (see Figure 122). The Von Mises Stress graph also corroborates this conclusion, showing a peak stress of 39.3 ksi (271 MPa). This value is roughly equivalent, or less than, the material's yield strength, indicating that the cannon would likely not undergo stress to the point of permanent deformation.

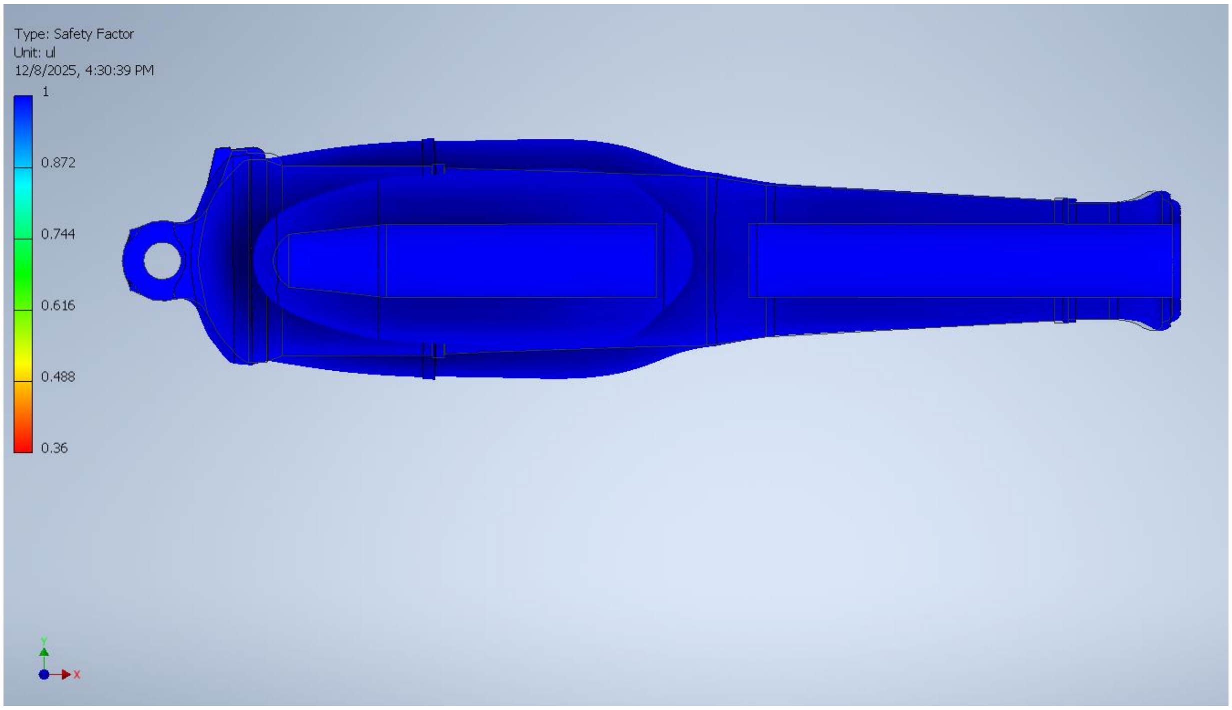

Figure 122: The FoS graph for BR–02 at the 100 cm interval. Exaggerated displacement shown. Force vectors removed for clarity. (Created in Autodesk Inventor by James Fowler.)

In short, although BR–02 experiences large interior stress forces which surpass other cannons in this study, BR–02 performs relatively similarly to other cannons in the initial blast. However, the large failure zone forward of the trunnions is not represented at all in the FEA simulations. The historical and archaeological evidence of this gun must also be compared to the engineering models. BR–02 is located on Malta in Valletta, a city which utilized retired cannons as bollards throughout the port area. Several are still extant, and several locations show signs of bollard removal. The failure region on BR–02 is not consistent with the FEA simulations, which indicate a very slim chance of catastrophic failure in that region. Thus, as observed in Chapter Four, it is more likely that BR–02 was indeed cut by an acetylene torch, in an effort to remove it as a bollard, instead of failing due to an explosion.

Barrel Failure Forward of the Trunnion Trends

Despite efforts to cause both weapons to fail, no cause of failure was determined by the FEA in the failure region of either BR–01 and BR–02. BR–02 showed no sign of failing in the region directly forward of the trunnions, and likely the archaeological evidence shows purposeful cutting of that region instead of bursting failure. Site formation processes may have imitated a failure event, but in reality, the gun was cut or damaged after it entered the archaeological record. Perhaps other guns, such as SW–05, are also results of purposeful, induced failure in the region and not directly due to a catastrophic bursting event. Notably, this is a good example of the complicated cultural/noncultural transformation scenarios encountered by both Alexander D. von Gernet and later P. J. Watson which proved hard to explain through site formation processes alone (von Gernet 1982; Watson 1986:450; Trigger 1989:361). However, the historical record indicates that BR–01 represents a burst gun. When BR–01 was subjected to a double load of gunpowder in the simulation, the failure region did not indicate weakness. This implies that BR–01 did not fail due to overpressure at all, nor to cyclical fatigue due to overpressure. Additionally, the weapon did not fail near the muzzle where manufacturing defects were most common. This analysis leaves several unanswered questions, which will be expounded upon here, and a course of action for future research recommended to enable a complete understanding of this failure mode.

Weapons need to be cleaned thoroughly to avoid “honeycombing,” that is, developing a weakness in the iron structure due to prolonged exposure to corrosives, such as gunpowder residue or iron oxides forming due to saltwater exposure (Griffith 1856:56–57). As stated previously in Chapter Five, this weapon is located on the island of Antigua and was supposed to be neglected before it exploded. Perhaps the development of honeycombing claimed this gun due to poor inspection techniques. Honeycombing was usually inspected for and caught early before resulting in a burst gun, because of the very obvious symptoms and a routine maintenance schedule, including swapping out and brushing out the bore before and during gunnery practice. The only way to confirm or deny this theory would be to conduct a closer inspection of the weapon in Antigua, utilizing the bore scope methodology successfully utilized on guns in Finland. Alternatively, this weapon simply failed due to material weakness in the fracture region. Brittleness and material defects are not confined to only the muzzle area, although it is more common to find such defects in the muzzle. It is possible to find material defects in any region of the gun. Perhaps this weapon suffered from an unpredictable material defect.

Additionally, BR–01 could have failed due to fatigue caused by vibration or resonance frequency. FEA simulation software exists to measure resonance frequency; however, the author does not currently possess the experience to utilize those methods with confidence, and thus they were not employed. This is a path for future analysis. Perhaps BR–01 had failed due to a destructive resonance frequency. Furthermore, the effects of mechanical, low–cycle fatigue are hard to quantify using the methods described above. Perhaps a thermal analysis or thermomechanical fatigue analysis of this gun could help uncover more answers. These are all routes forward.

Perhaps the most reasonable explanation is that this weapon suffered from a combination of the above factors. The gun’s utilization in a neglected coastal fortification meant it likely was not inspected often nor used regularly, resulting in corrosion build up and honeycombing. An unpredictable material weakness in a spot hard to inspect may have compounded factors. Although the region does not show high levels of Von Mises stress, this doesn’t mean that fatigue couldn’t creep into any area compromised by honeycombing or corrosion, regardless of the failure propensity. More research will be needed to determine if Type II failure should be included as a subcategory of Type I or III failure, or if it is due to other factors which are not present in Type I failures.

Type III: Barrel Failure Aft of the Trunnions

This failure is like the Type II failure, however, it occurs between the trunnions and the breech end of the barrel. These failures are often characterized by large explosive bursting events, often deadly to the gun crew (Delano 1817:94–95; United States Congress House Committee on Naval Affairs 1844; Greener 1858:84–85; Greener 1910:28; Leiner 2006:99). As depicted by Figure 101, Figure 114, and Figure 115, the pressures are higher in the regions closer to the breech, and thus the failures likely are related to peak pressures. Cannons SW–01, SW–02, SW–05, SW–23, UN–02, and UN–03 all represent suitable examples of a Type III failure. Notably, four of these weapons are Swedish in origin; UN–03 is also likely Swedish, although this in not confirmed. Additionally, these weapons are of many different caliber guns, from a 36–pounder to a 6–pounder. Type III failures are like some Type II failures, and in some cases the line can be blurred, especially when the gun explodes directly at the trunnion area. For example, SW–05 and BR–02 both failed in similar spots on the gun and in similar fashion, with the former occurring just aft of the trunnions in a clean perpendicular break and the later just forward of the trunnions in a clean perpendicular break.

Barrel Failure Forward of the Trunnions FEA Simulations

For analysis of this failure mode, two weapons were chosen due to similar breakage patterns but with relatively different calibers. SW–01 is a Swedish 36–pounder and represents the largest gun which failed in this manner, and SW–23 is a Swedish 6–pounder that represents the smallest gun which failed in this manner. These guns are depicted earlier in Figure 54 and Figure 86. The dimensioned engineering drawing for SW–01 is shown in Figure 123, and the CAD model for SW–01 can be seen in Figure 124. The pressure graph for SW–01 can be seen in Figure 125.

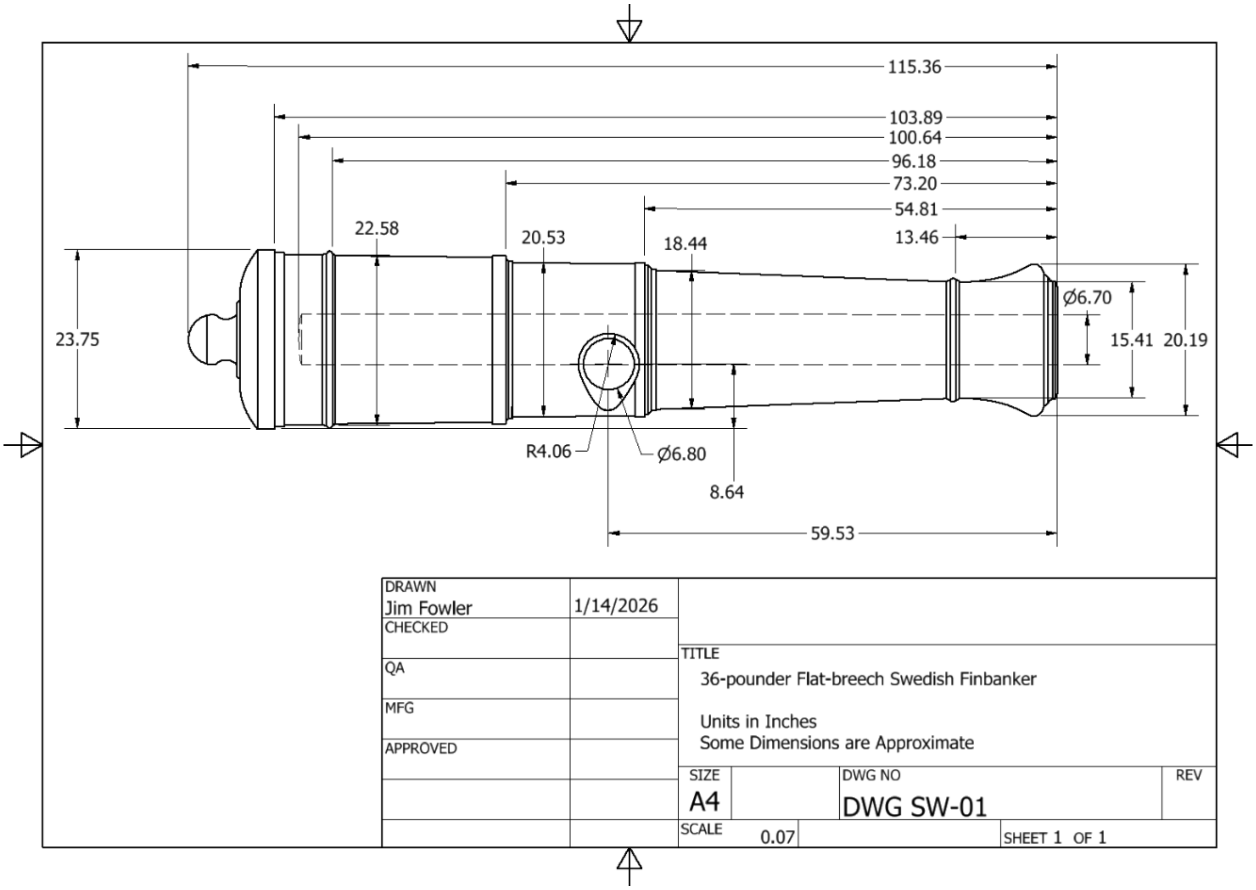

Figure 123: A dimensioned engineering drawing of the SW–01 CAD model. (Created by James Fowler in Autodesk Inventor.)

The CAD model of SW–01 was created utilizing rough dimensions pulled from the MAS photogrammetric models (Maritime Archaeological Society of Finland 2025a, 2025b). Due to the extent of concretion, and the lack of extant plans for a 36–pounder “Flat Breech” Finbanker, consultation of Rudy Roth’s drawings of French 36–pounder flat breeched weapons of the same year for the Royal Arsenal in Woolworth were utilized to confirm proportions (Royal Armouries 2025).

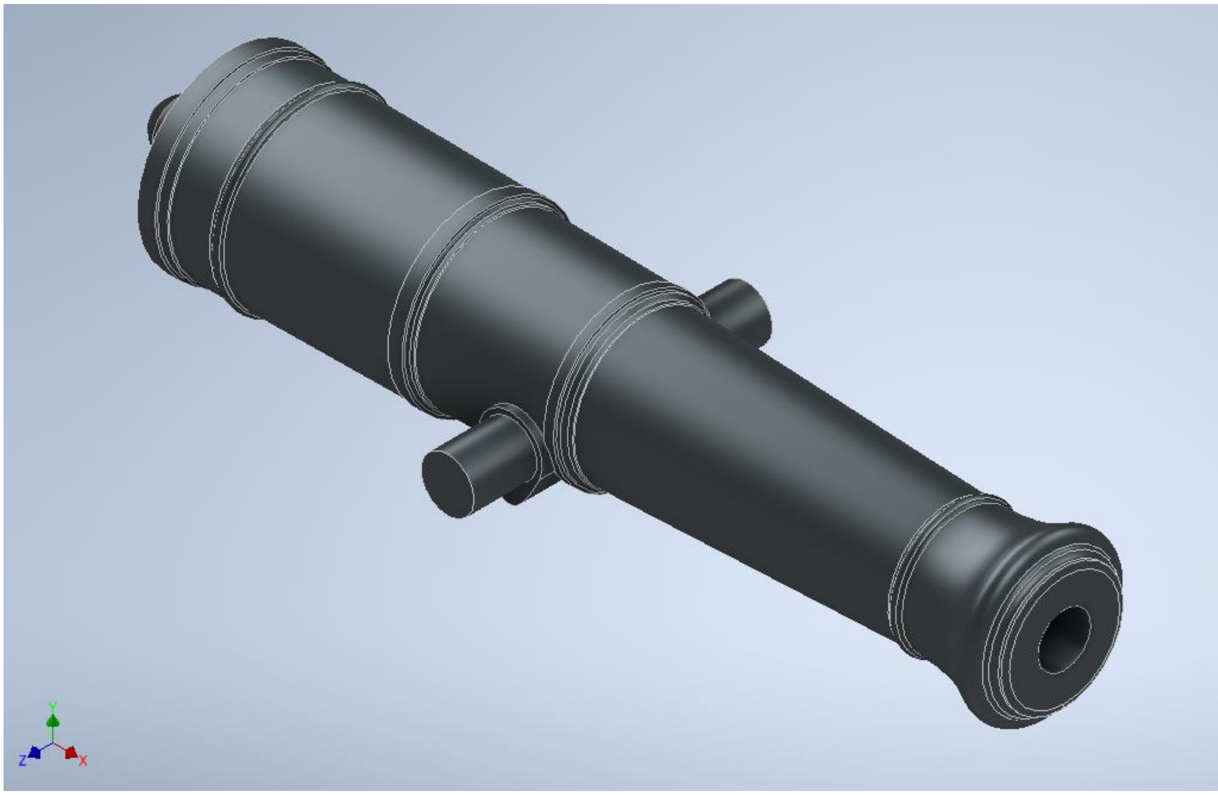

Figure 124: SW–01 36–pounder Finbanker CAD model. (Created in Autodesk Inventor by James Fowler.)

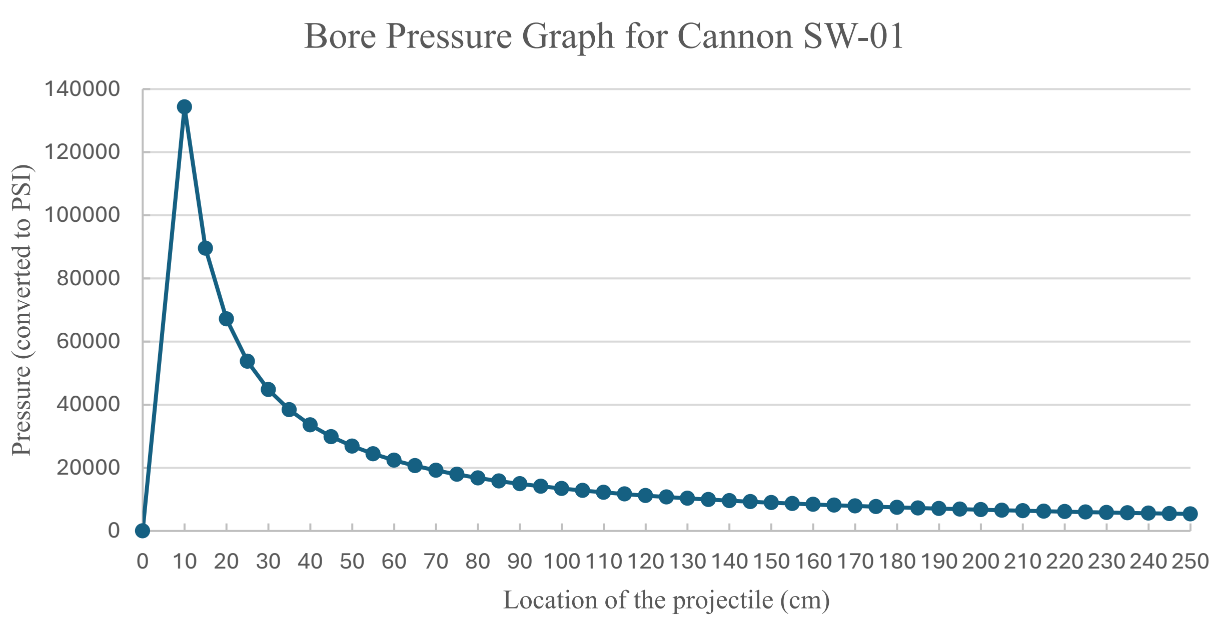

Figure 125: Bore Pressure Graph for SW–01. (Created in Microsoft Excel by James Fowler.)

The CAD model for SW–23 was constructed by utilizing the scaled drawing of SW–23 created by Gordon Cawood of the LCMM, referred to in LCMM literature as artifact 99–01. The final piece of the gun was found only very recently and no official literature published on it as of yet, thus an archaeological drawing of a 6–pounder "Dutch Breech" variety Finbanker was utilized to estimate the location and dimensions of the second reinforcement band. This was selected from Rudi Roth's drawings of Finbankers for the Royal Arsenal in Woolworth (Royal Armouries 2025). The dimensioned engineering drawing for SW–23 is shown in Figure 126, and the CAD model for SW–23 can be viewed in Figure 127. The pressure graph for SW–23, which follows the expected pressure curve generated in Chapter Four, can be seen in Figure 128.

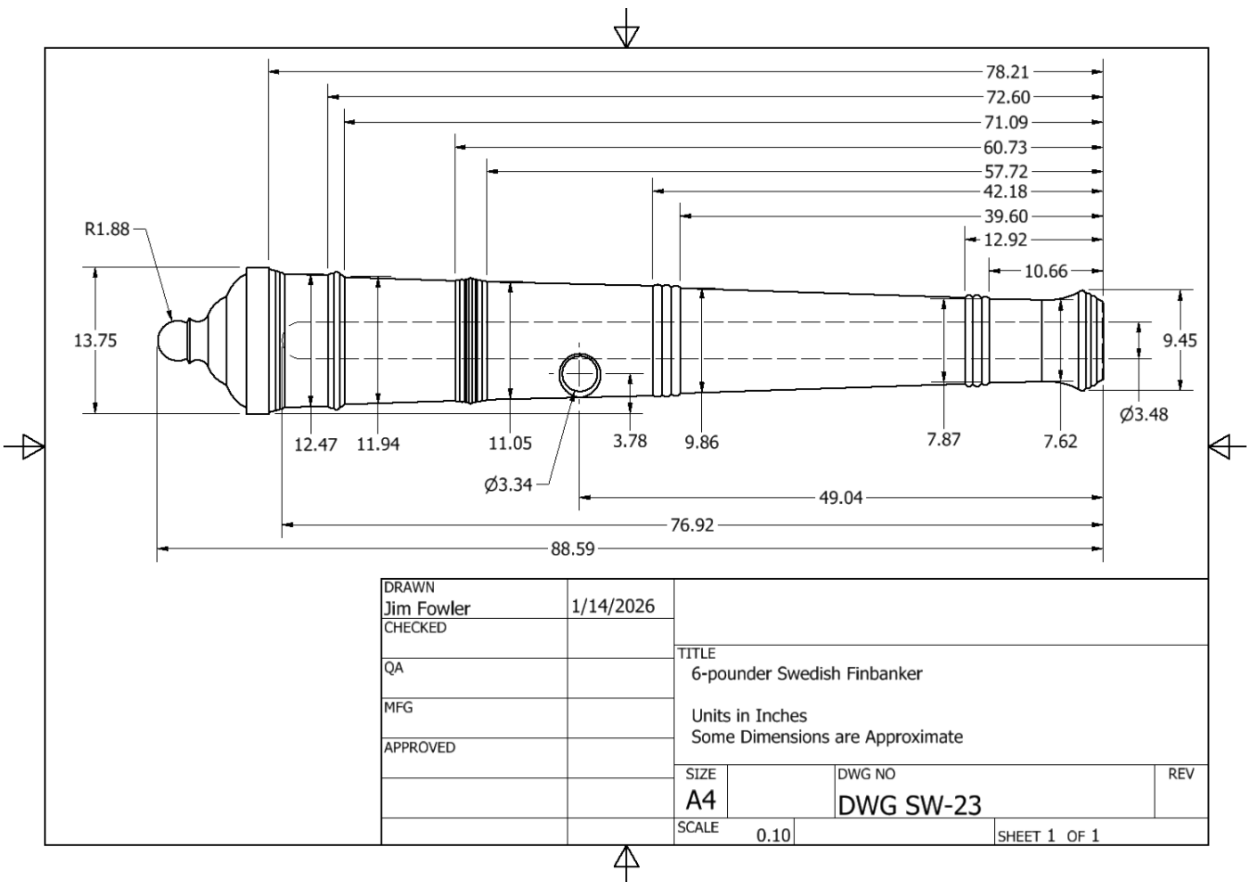

Figure 126: A dimensioned engineering drawing of the SW–23 CAD model. (Created by James Fowler in Autodesk Inventor.)

Figure 127: SW–23 6–pounder Finbanker CAD model. (Created in Autodesk Inventor by James Fowler.)

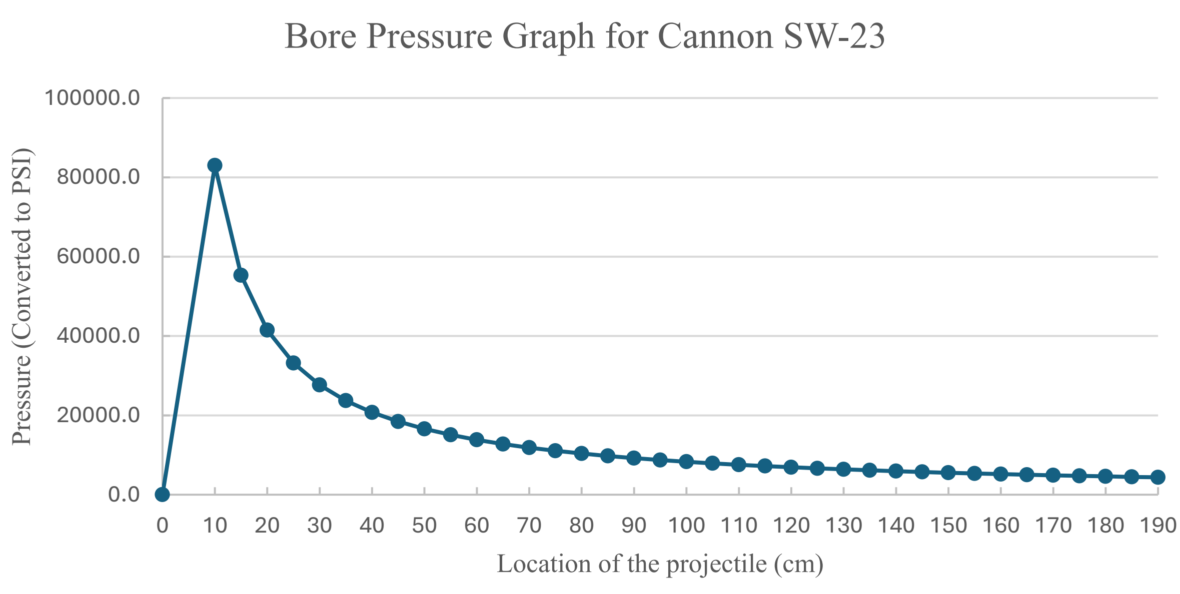

Figure 128: Bore Pressure Graph for SW–23. (Created in Microsoft Excel by James Fowler.)

Both SW–01 and SW–23 were subjected to simulations. To model the firing of these guns, the peak bore pressure was calculated to be 134,310.6 psi (926.0 MPa) at 10 cm (3.84 in) distance from the breech face for SW–01 and 82,982.6 psi (572.1 MPa) at 10 cm (3.84 in) distance from the breech face for SW–23, as depicted in Figure 128.

Example: SW–01

SW–01 was tested first, and the results of these tests are discussed below. As depicted in Figure 129, at the initial location of the projectile, the average Von Mises Stress was around 234.6 ksi (1617.5 MPa), with peak stress at 391.1 ksi (2696.5 MPa). As stated previously, such stresses are significantly above the material's yield strength.

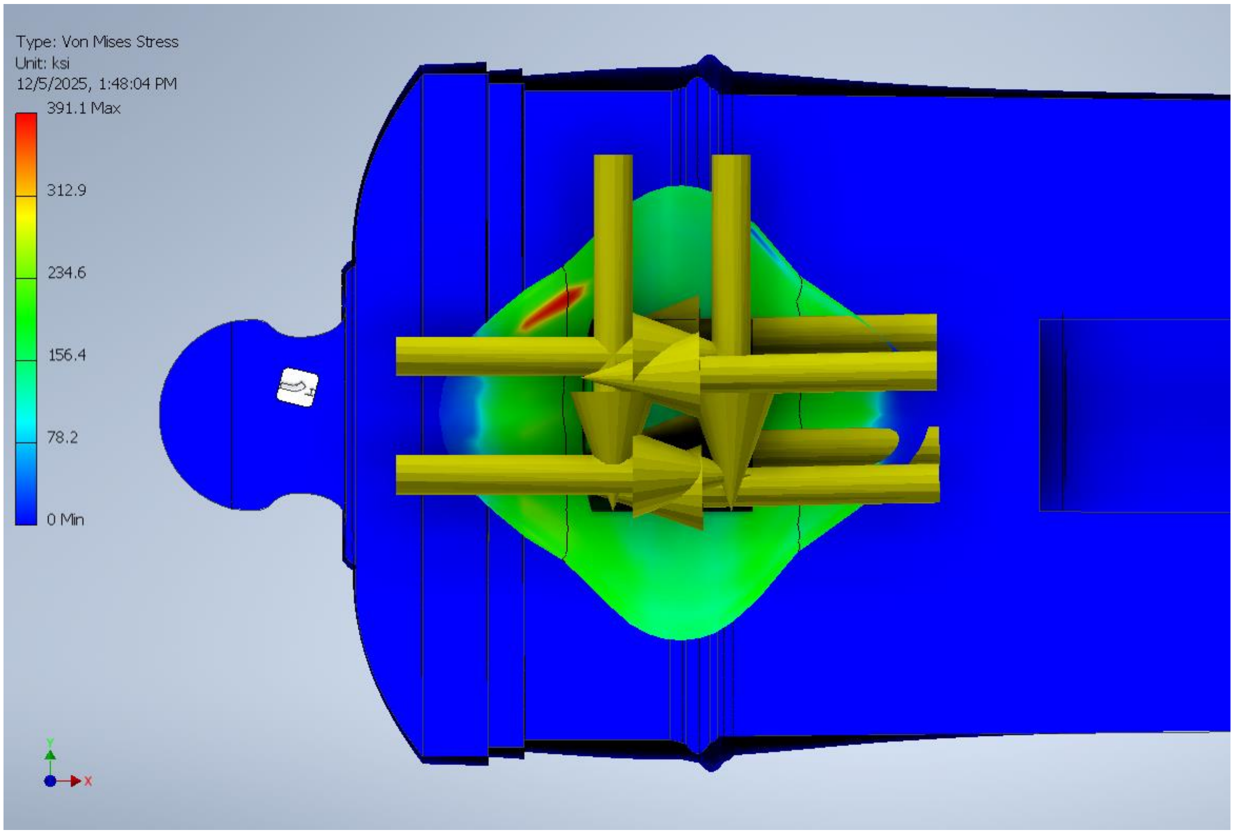

Figure 129: The Von Mises Stress graph for SW–01 at the 10 cm interval. Exaggerated displacement shown. Yellow arrows indicate force vectors. (Created in Autodesk Inventor by James Fowler.)

Unlike some of the previous examples, however, the image in Figure 129 is misleading. As stated in Chapter Four in the Value Parameters for FEA Analysis subsection, the color gradients for all the FEA simulations do not indicate likelihood of failure but are instead evenly distributed between highest and lowest values. Hence, even the dark blue regions in Figure 129 are substantially above the yield strength of cast iron, which has a yield strength of around 39.885 ksi (275 MPa) and an UTS of around 72.519 ksi (500 MPa). Perhaps more telling is the FoS graph, depicted in Figure 130. The minimum FoS is staggeringly low at 0.28, which indicates all red areas would fail imminently.

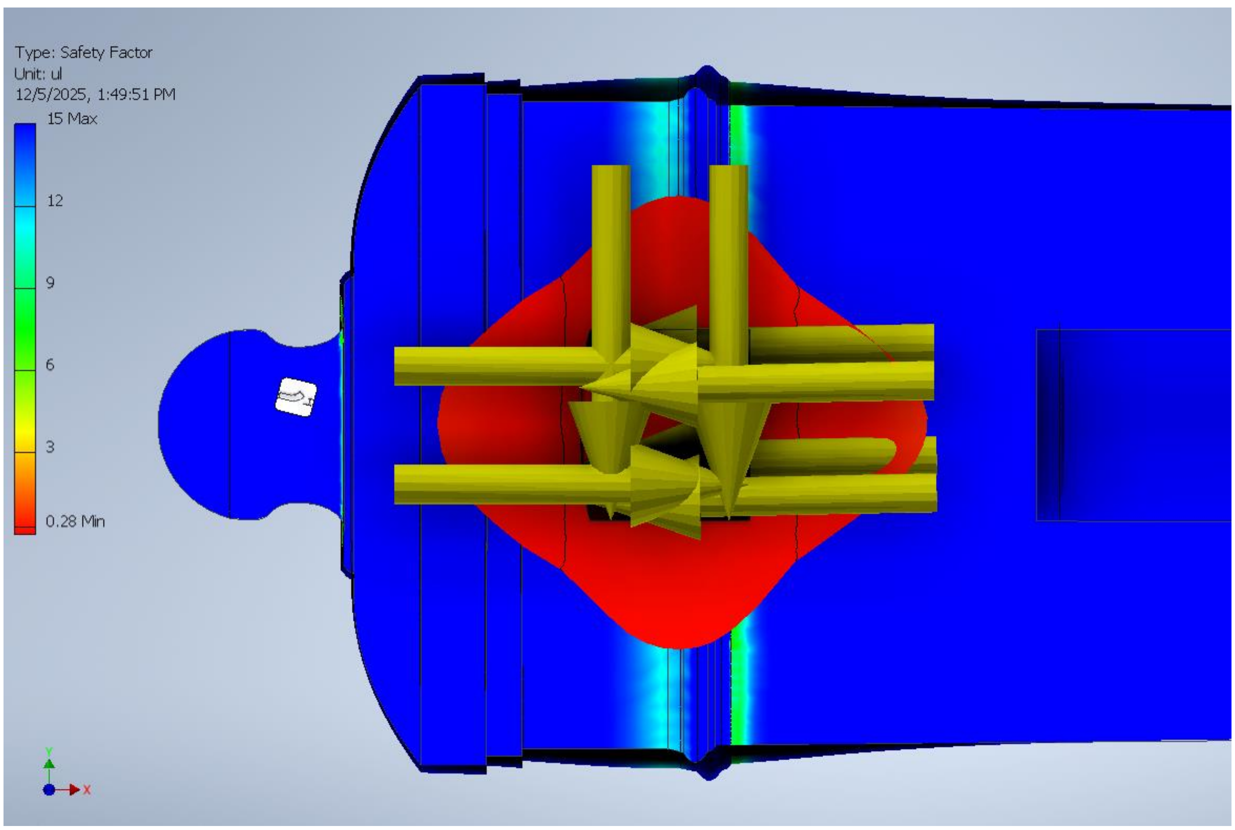

Figure 130: The Factor of Safety graph for SW–01 at the 10 cm interval. Exaggerated displacement shown. (Created in Autodesk Inventor by James Fowler.)

As depicted in Figure 131, however, when the projectile reached the area in which the cannon failed, around 70 cm (27.56 in) down the barrel, the Von Mises Stress dropped off substantially, and the area showed less likelihood of failure, however the stress was still above the material's yield strength. In this instance, it is interesting to compare the FEA simulations to the archaeological and historical record. The gun modeled, SW–01, was located on the wreck of *Kronprince Gustaf Adolf,* and found in situ, broken in half aft of the trunnions. The ship sank in the summer of 1788 during the first few months of the Russo–Swedish War of 1788 (Anderson 1910:246). The twenty-six 36–pounders present on the vessel were utilized only during a wartime outfit, as records indicate that in peacetime the Swedish Navy replaced the 36–pounders with lighter and cheaper 24–pounders (Tredrea and Sozaev 2010:470).

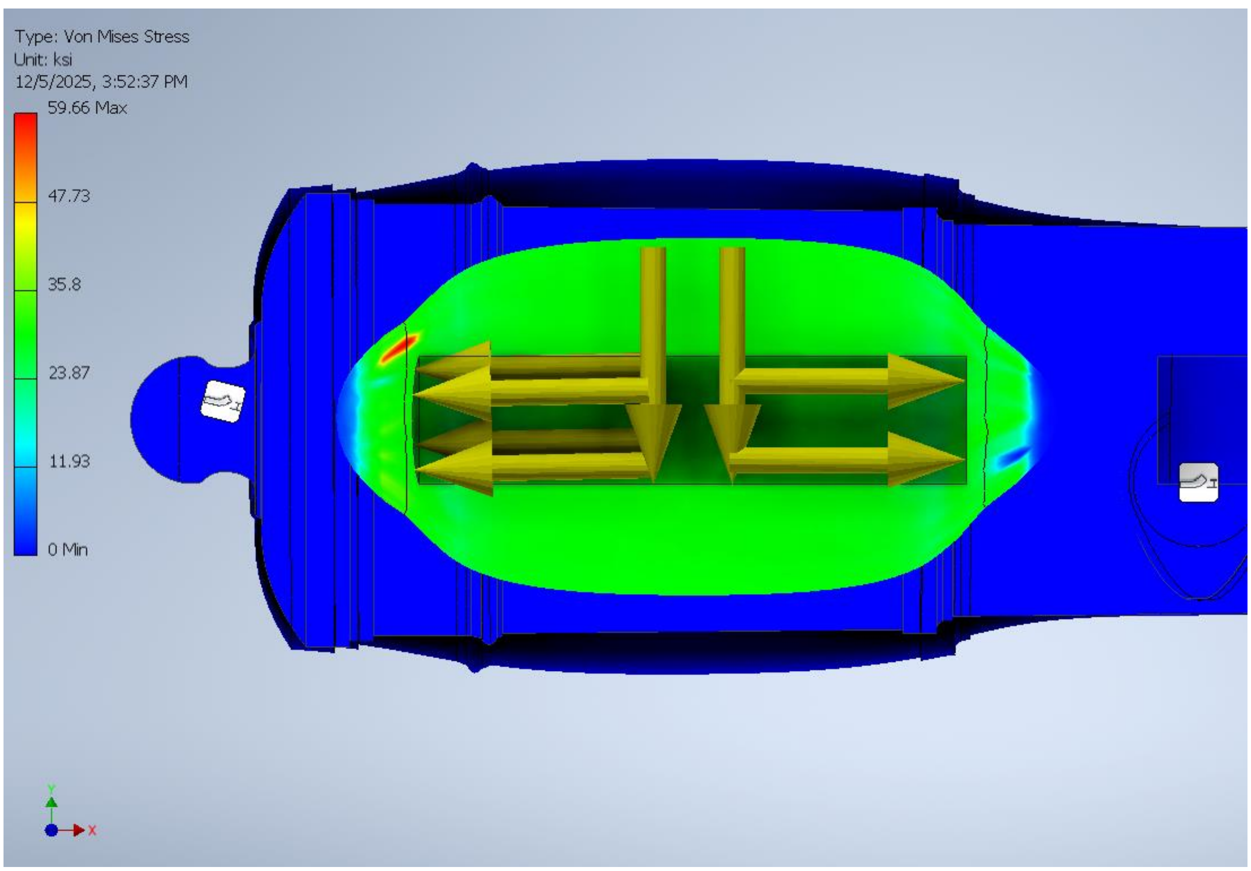

Figure 131: The Von Mises Stress graph for SW–01 at the 70 cm interval. Exaggerated displacement shown. (Created in Autodesk Inventor by James Fowler.)

If indeed this appraisal is accurate and considering that the ship sank in the first few months of the conflict, it is unlikely that these weapons saw much usage at all and likely sat in ordinary (mothballed or in a reserve fleet context) for many years before being quickly fielded with the Swedish fleet. This indicates that corrosion and honeycombing could have been present within the bore to weaken the interior structure of these guns, unless they were routinely inspected and cleaned. Lack of maintenance might have resulted in failure in the area close to the point of max pressure. Additionally, if the weapons were not fielded during peacetime training, it is unlikely that the gun crews of *Kronprince Gustaf Adolf* had substantial experience calculating the correct powder loads to utilize when firing the larger guns, and mistakes due to poor training may have been more prevalent. If the pressure was doubled due to a double load of black powder, the area is subjected to even more pressure, indicating an even higher likelihood of failure.

Also, as can be seen in Figure 124, a large reinforcement band exists exactly at the 70 cm (27.56 in) mark, and the sharp angles in this area would have provided substantial stress concentrations. The presence of fatigue around each of the reinforcement bands is likely, which may relate to failure location. Furthermore, perhaps poor iron was utilized here as well, so inclusions or sponginess could have resulted in weak spots in this area. Until a more uniform survey of very large caliber guns can be conducted, and more case studies examined, it remains difficult to determine if the gun's size played a role in its failure.

Example: SW–23

The results of the SW–01 simulation are useful to compare to the results of the SW–23 simulations depicted in Figure 132. At the initial location of the projectile at 10 cm distance from the inner breech face, the maximum Von Mises Stress was around 143 ksi, (979 MPa). As stated previously, such stress is significantly above the material's yield strength.

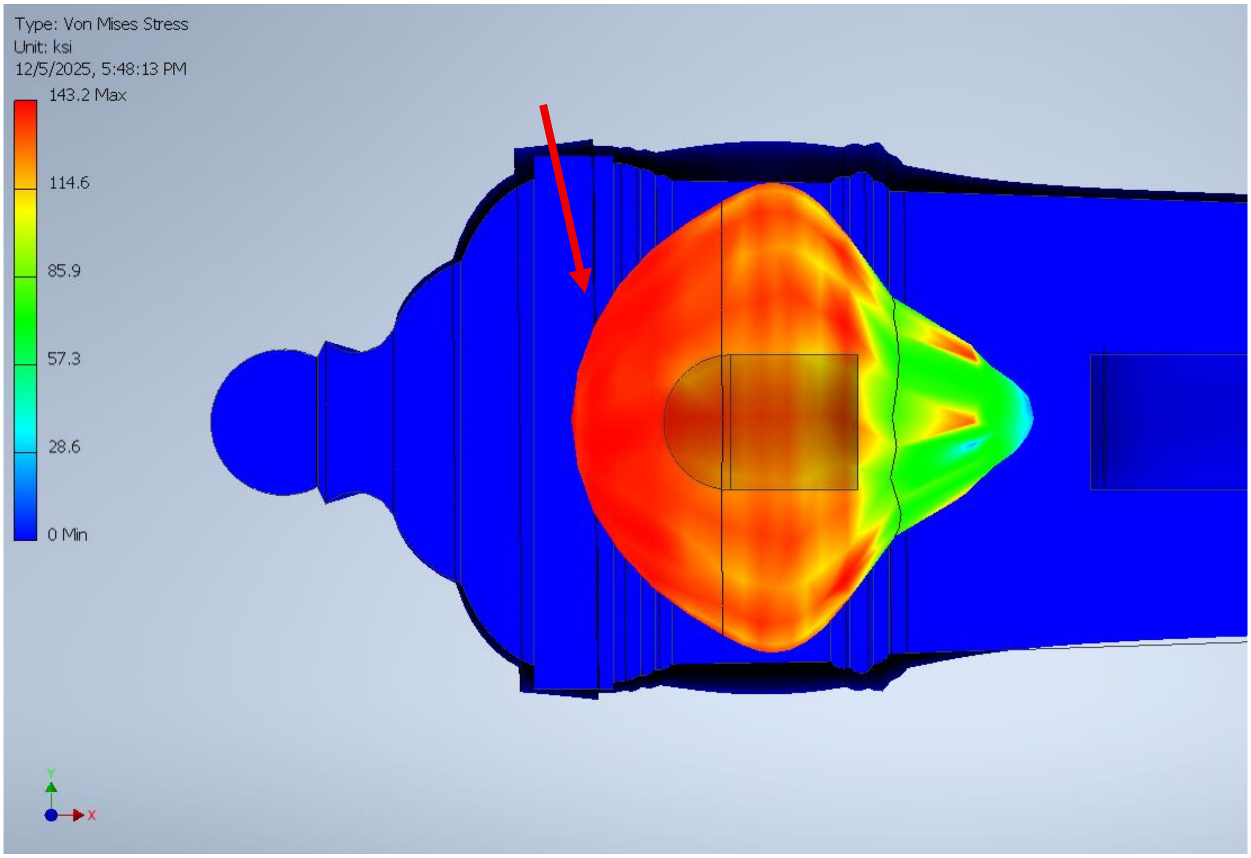

Figure 132: The Von Mises Stress graph for SW–23 at the 10 cm interval. Exaggerated displacement shown. Force vectors removed for visual clarity. Red arrow indicates mushroom–shaped deformation area. (Created in Autodesk Inventor by James Fowler.)

Noticeably, the concave profile of the breech face in this example directs the deformation in the perpendicular direction, with substantial yielding in the back face of the gun. This pronounced mushroom shape of the deformation area is unique to this simulation, caused by the convex interior breech face profile. The FoS graph indicates that a minimum of 0.77 FoS was recorded; since this is below 1.0, it indicates the presence of failure. Curiously, this FoS signature is significantly higher than other examples of failure, such as SW–01. The displacement graph, depicted in Figure 133, further indicates that a ring of high displacement is found in the region perpendicular to the axis of the bore, indicating that it might experience a higher concentration of force. The displacement is relatively low, at around 0.01 inches (0.2 mm).

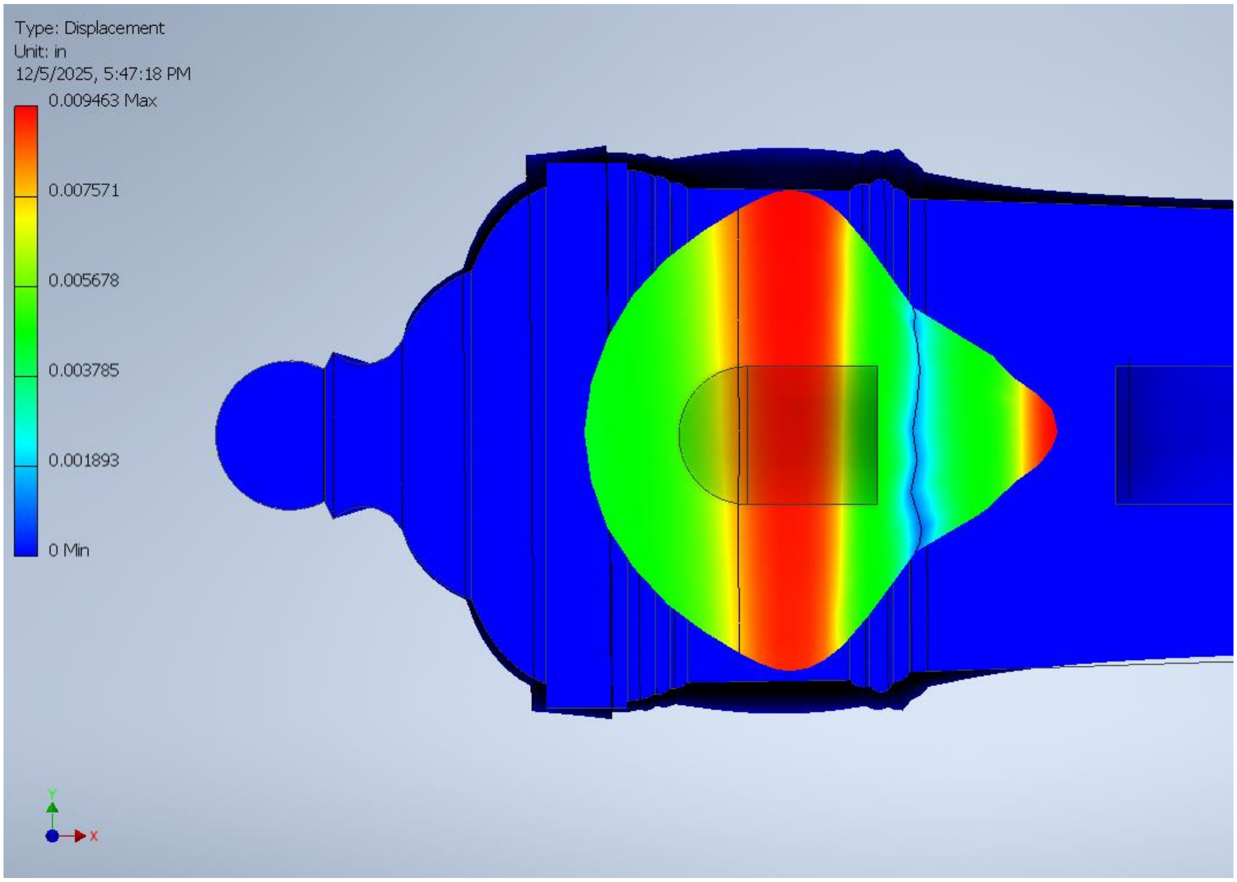

Figure 133: The Displacement graph for SW–23 at the 10 cm interval. Exaggerated displacement shown. Force vectors removed for visual clarity. (Created in Autodesk Inventor by James Fowler.)

When the projectile reaches the area in which the cannon failed, around 30 cm (11.81 in) down the barrel, the simulation indicates that the Von Mises Stress has dropped to 53.8 ksi (370.9 MPa) (Figure 134). Stress at 53.8 ksi (370.9 MPa) is still much higher than the material's yield strength and approaching the tensile strength, but this stress is concentrated on the interior bore, not the exterior. This weapon is another example of failure from the inside out. However, the most interesting graph generated by the simulation is the Displacement graph, (Figure 135).

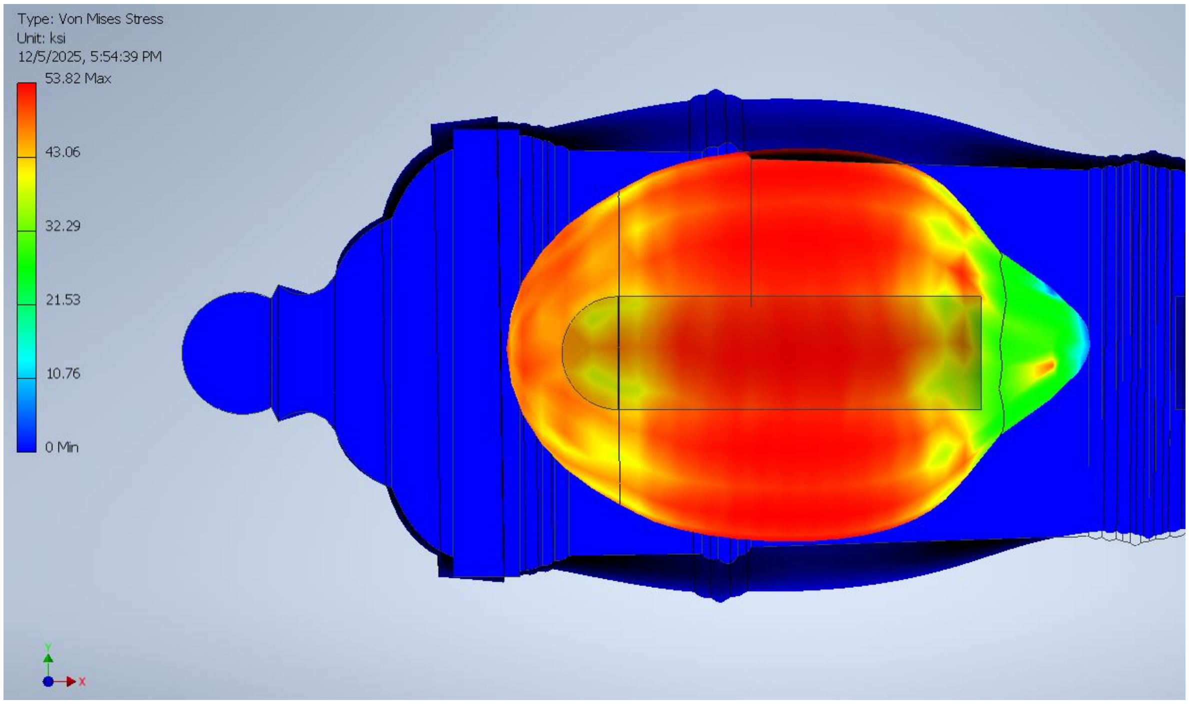

Figure 134: The Von Mises Stress graph for SW–23 at the 30 cm interval. Exaggerated displacement shown. Force vectors removed for visual clarity. (Created in Autodesk Inventor by James Fowler.)

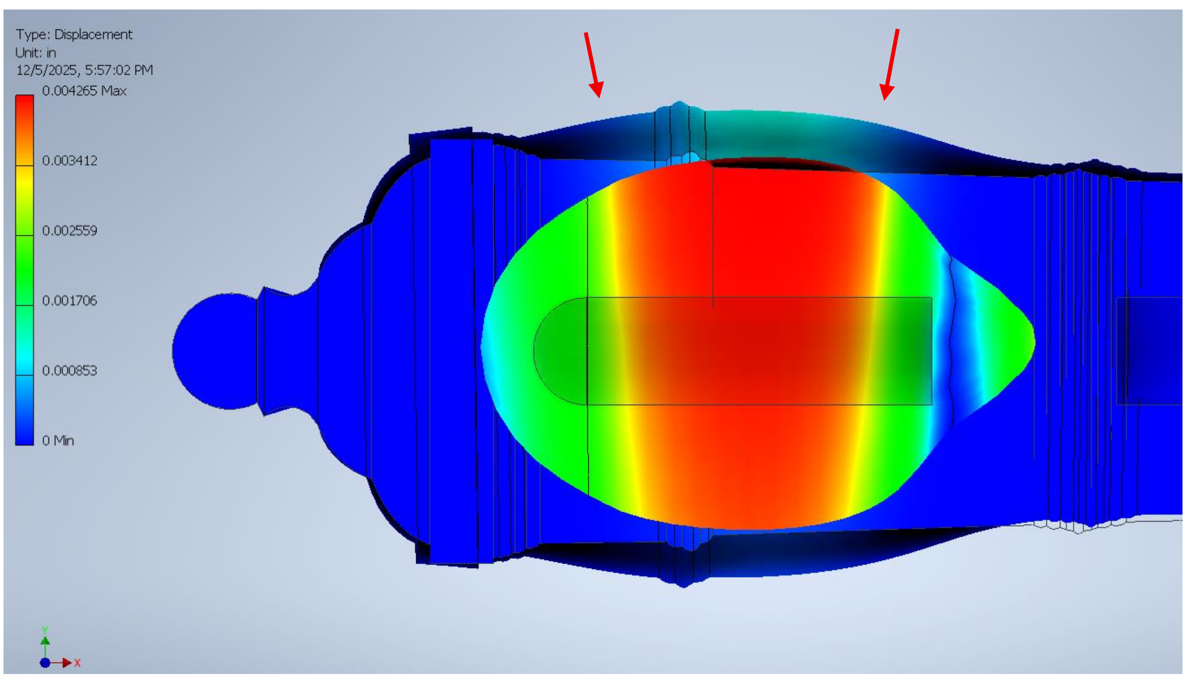

Figure 135: The Displacement graph for SW–23 at the 30 cm interval. Red arrows indicate tapered displacement profile. Exaggerated displacement shown. Force vectors removed for visual clarity. (Created in Autodesk Inventor by James Fowler.)

The slight taper in the displacement indicates that the top of the gun was subjected to more displacement than the bottom of the gun and thus it is likely subjected to more fatigue stress over the course of the weapon's service life.

The results of this simulation are again useful to compare to the historical and archaeological information concerning this weapon. This particular gun was recovered by the LCMM and represents one which exploded in action during the American Revolution (Cohn et al. 2003:86–92). The gun burst near the breech, shattering the barrel into countless pieces but left the muzzle of the weapon intact, and the breech area split but otherwise intact. The thick and full breech area of the weapon, often referred to as the "Dutch breech" Finbanker design, seems to have concentrated the forces in the perpendicular direction resulting in higher deformation in that region than in other weapons analyzed in this study (Mendel 1965:184; Parham et al. 2013:408–409). The Dutch breech design benefits from a larger concentration of solid iron in the area between the inner breech face and the cascabel, and this added mass may have the additional benefit of being significantly harder to deform than the barrel walls.

The concave inner breech face seems to have mitigated failure in the breech face itself, but in doing so redirected forces outward, and thus might have increased the likelihood of failure, although more testing is required to support this claim. Furthermore, the tapered displacement profile also mirrors the archaeological evidence. As displayed in Chapter Five, the cannon exploded upward, and the ventral portion of the barrel is intact further towards the failure region than the dorsal portion. This characteristic is well represented in the simulation evidence as well, with most of the displacement focused on the dorsal region.

Barrel Failure Aft of the Trunnion Trends

The presence of low FOS readings in both SW–01 and SW–23, despite both weapons being of significantly differing caliber dimensions, indicates that weapons that fail near the breech are more likely to do so before high–cycle fatigue could result in fatigue cracking. Thus, weapons that fail near the breech and aft of the trunnions are more likely a result of overpressure due to gunpowder mishandling or some other overpressure scenario. This isn't to say that fatigue wasn't an issue, but these regions are more prone to overpressure failure than the muzzle regions, or other areas where the pressures involved are much lower. If a gun was to be overloaded with powder, it would fail in the breech region before it got the chance to fail anywhere else. No impact of site formation processes were apparent in Type III failures.

Failures in this region might be attributed to poor training, stress of combat, or underutilization of the weapons. Honeycombing and interior bore degradation can represent a compounding factor, and the history of both weapons suggests both had seen extended periods of time with little or no maintenance. Cannon SW–01 might have been relegated to ordinary for many years before being utilized in the Russo–Swedish War, while SW–23 was likely an older weapon pressed into service by the US Army during the American Revolution. Both weapons were also of Swedish manufacture. Further research might determine where one or both of the weapons were cast which could indicate if material defects might have played a role in failure. Archaeological research on SW–01, conducted in conjunction with Finnish Maritime Archaeological Society and the Finnish Heritage Agency, uncovered identifiable marks which might be trackable to foundries in Sweden, where more manufacturing information could be obtained. A report on this information is currently being compiled.

Type IV: Extremity Failure

Cannons BR–08, BR–09, SW–03, SW–04, SW–06, SW–08, SW–09, SW–10, SW–11, SW–12, SW–13, SW–14, SW–15, SW–16, SW–17, SW–18, SW–19, and SW–20 all represent suitable examples of a Type IV failure. Of these weapons, many represent Swedish Finbankers, and thus a Finbanker variety was chosen for modeling. All the cannons documented in Finland are 12– or 18–pounders, which although numerous in the archaeological record, no verifiable engineering drawings or scaled plans were found of these weights within the correct date range and manufacturer. However, scaled drawings of the next smallest variety commonly found – 8–pounder– were readily obtained (Royal Armouries 2025). The dimensioned engineering CAD drawing based on Rudi Roth's illustration of an iron 8–pounder Finbanker in the Royal Arsenal in Woolwich can be seen in Figure 136. A CAD model was constructed in Autodesk Inventor, as depicted in Figure 137.

Extremity Failure FEA Simulations

The cause of extremity failures is difficult to assess due to the multitude of ways a cannon could get damaged in this region. Two possibilities seem most likely: first, the trunnion could fail from repeated recoil of the gun. This seems unlikely due to the low force acting upon the trunnion in the x–axis relative to the force exerted on the interior of the bore. Although it is likely *some* guns failed this way, it is unlikely that the extreme number of extremity failures observed in the archaeological record correlate to this: there are simply too many failed cascabels and trunnions. The second possible cause seems much more likely: the extremities get broken off by force applied perpendicular to centerline of the trunnion or cascabel at the far end of the extremities, resulting in a bending moment and shear force that overcomes the material's ultimate tensile strength. This could happen either intentionally or unintentionally: intentionally to render the gun unusable and unintentionally by dropping the weapon or similar uncontrolled movement of the weapon which resulted in a force to the extremity. Such methods for removing the trunnion of a gun to render them unserviceable recommend either impacting the trunnion with a large sledgehammer or blasting the trunnion off with a point–blank carronade shot (Griffith 1856:57). To facilitate this test, simulations of loads in various directions were applied to the trunnions and cascabel to determine if the weight of the cannon could shear off an extremity, or if a lesser force would suffice.

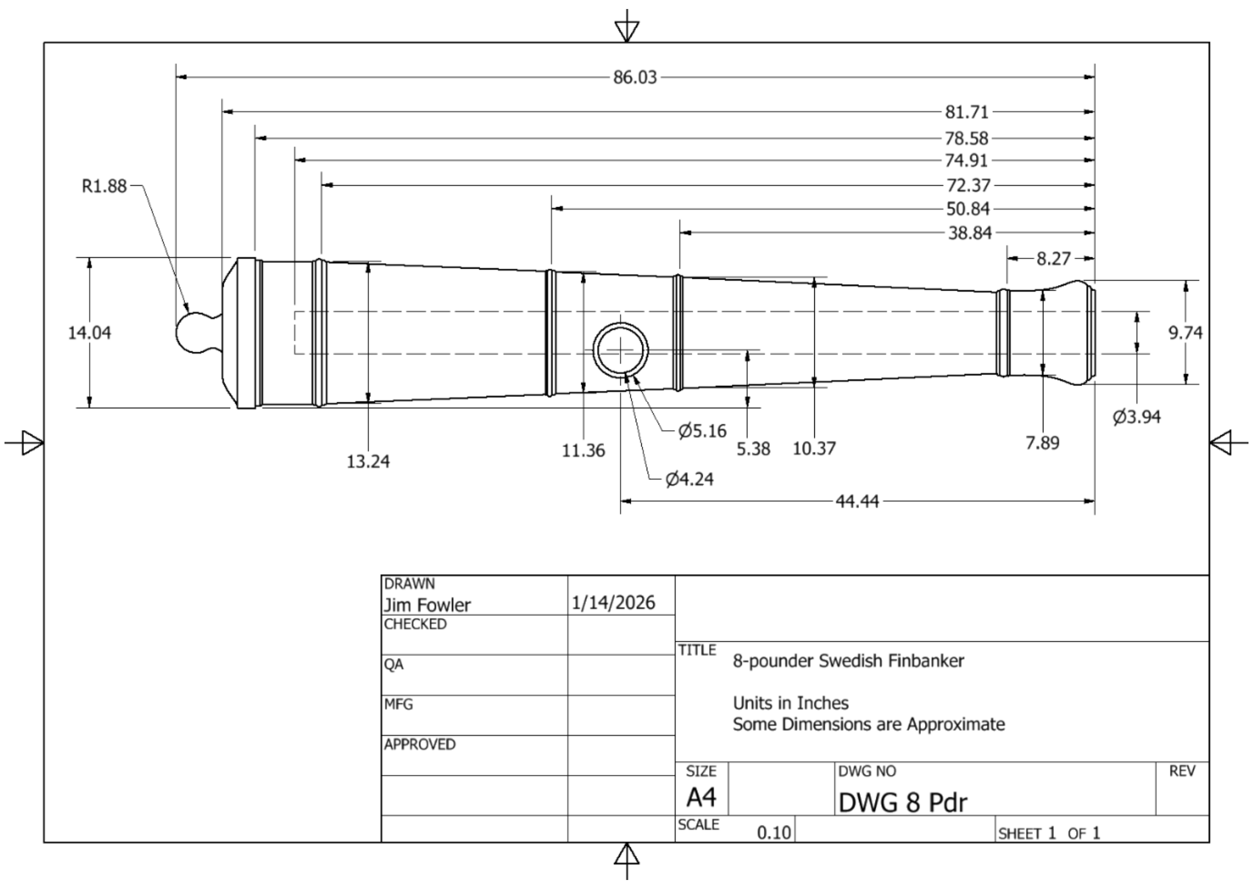

Figure 136: A dimensioned engineering drawing of the 8–pounder Finbanker CAD model. (Created by James Fowler in Autodesk Inventor.)

Figure 137: The 8–pounder Finbanker CAD model, (Created in Autodesk Inventor by James Fowler.)

Example: Cascabel Failure

As depicted in Figure 138, when a force equal to the weight of the cannon (1730 lbs–force or 7695.423 N) was applied to the cascabel along the y–axis, the cascabel was easily able to withstand it. Additionally, the force of a large 20-pound sledgehammer with an acceleration equal to 17 times the force of gravity (a high estimate), resulting in a force of 304 lbs–force (1352.259 N), the cascabel showed negligible sign of damage. On both, a FoS of 15.0 or more was measured. A similar result was found when the same force with similar constraints was imparted on a trunnion.

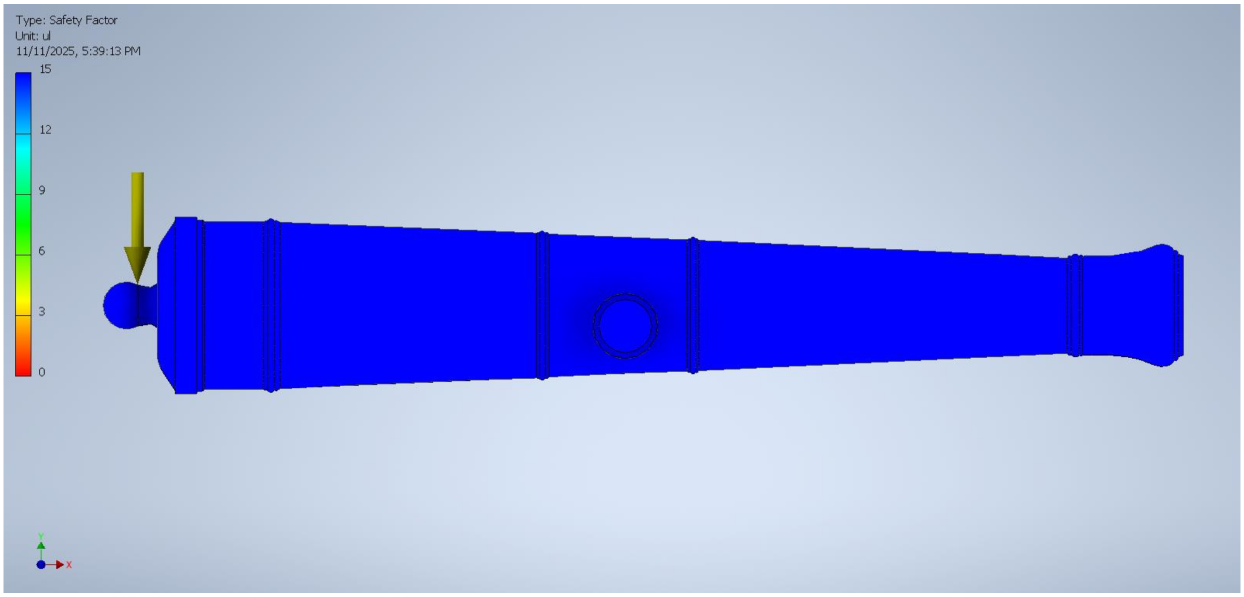

Figure 138: 8–pounder Finbanker model Factor of Safety graph. Yellow force arrow represents the force applied along the y–axis. (Created in Autodesk Inventor by James Fowler.)

When a virtual drop test was conducted on the cannon, however, different results were apparent. The impact work of the weight of the cannon was calculated when dropped from 2 meters, and a much larger force was determined considering the acceleration due to gravity over that distance and the large mass of the cannon. A stopping distance of 0.003 m (0.12 in) was utilized, to simulate a hard stone surface, and 0.03 m (1.18 in), to simulate landing on a hard wooden surface, like the deck of a ship. In the first instance, such a fall resulted in 1,134,170.6 lbf (5,049 kN) imparted to the cascabel, and in the second instance resulted in substantially less at 113,517.1 lbf (504.8 kN). However, both resulted in complete cascabel failure. In the first instance, the cascabel was displaced over 0.44 in (1.1 cm), resulting in total failure. This can be seen in Figure 139. The FoS also indicated instant failure, at 0.07, way lower than the required 1.00 (seen in Figure 140).

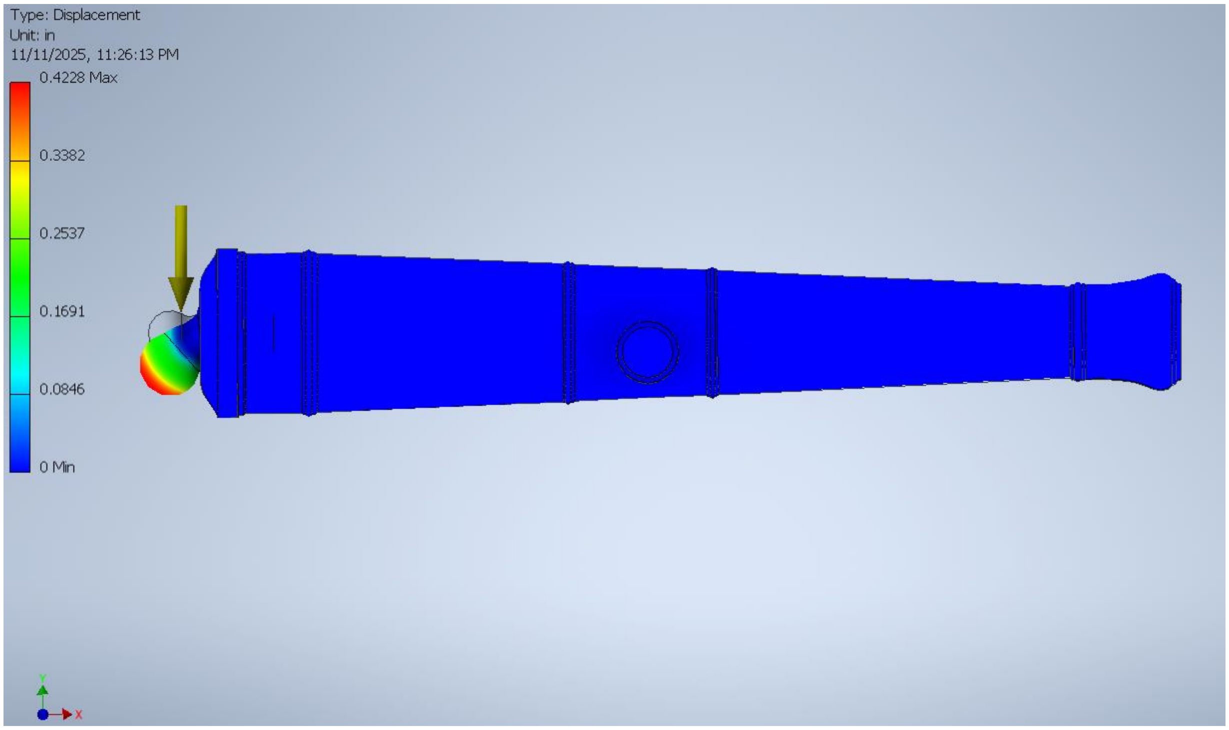

Figure 139: 8–pounder Finbanker model Displacement graph if dropped on the cascabel on a stone surface, displacement exaggerated. (Created in Autodesk Inventor by James Fowler.)

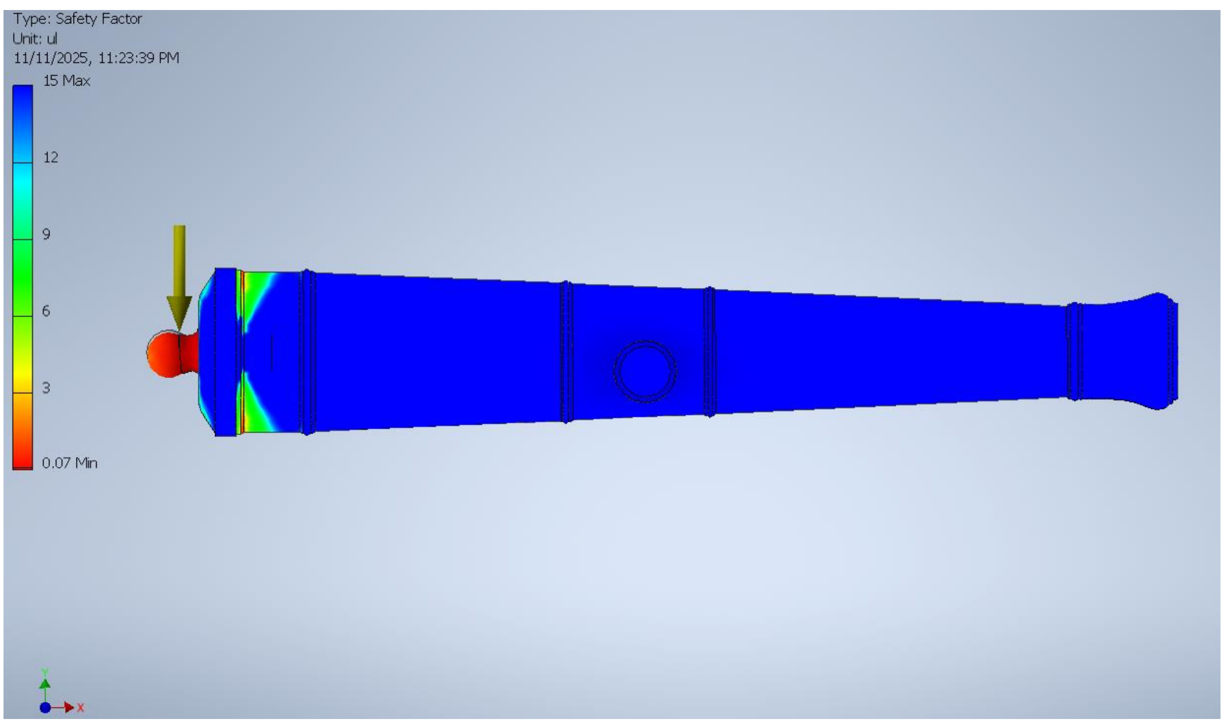

Figure 140: 8–pounder Finbanker model Factor of Safety graph if dropped on the cascabel on a stone surface. (Created in Autodesk Inventor by James Fowler.)

In the second instance –dropped on wood– the cascabel still failed, however the FoS was substantially higher, at 0.71 (seen in Figure 141). This indicates that cascabel failure was less likely if a cannon became dismounted on a wooden surface, such as a ship or dock, when compared to on a harder stone surface, such a stone fortification or cobble wharf. It is more likely that cascabels failed while the cannon was being handled on shore, and substantially less likely if onboard a ship. Perhaps not coincidently, all the cannons with failed cascabels were found on land. So far very few cascabel failures have been found in an underwater context, and none of the cannon in this study exhibit this issue.

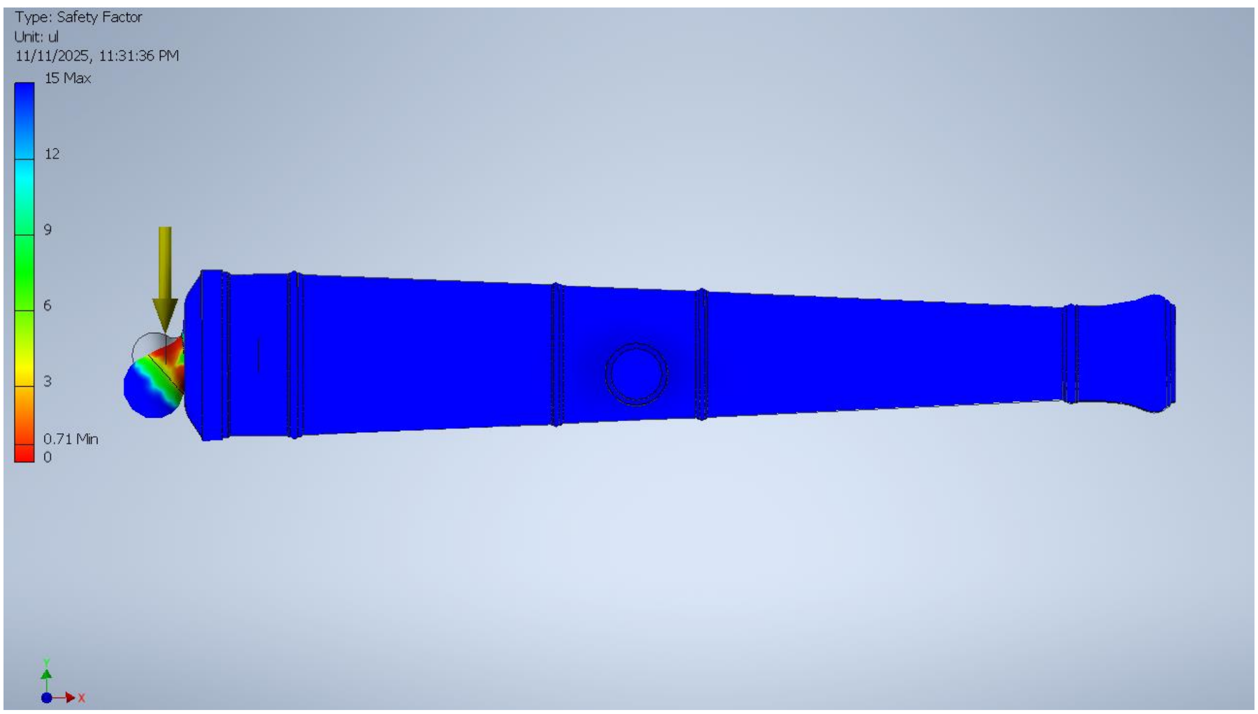

Figure 141: 8–pounder Finbanker model Factor of Safety graph if dropped on the cascabel on a wood surface, displacement exaggerated. (Created in Autodesk Inventor by James Fowler.)

Example: Trunnion Failure

Similarly, simulations for drop tests for both stone and wood surface were conducted on the trunnions of the 8–pounder Finbanker. As expected, the trunnions performed much the same way as the cascabels. A minimum FoS of 0.21 was determined if dropped on a stone surface, and a displacement of 0.128 in. (0.325 cm) was recorded. This would entail an immediate trunnion failure, resulting in the shearing of the trunnion from the body of the cannon. This can be viewed in Figure 142.

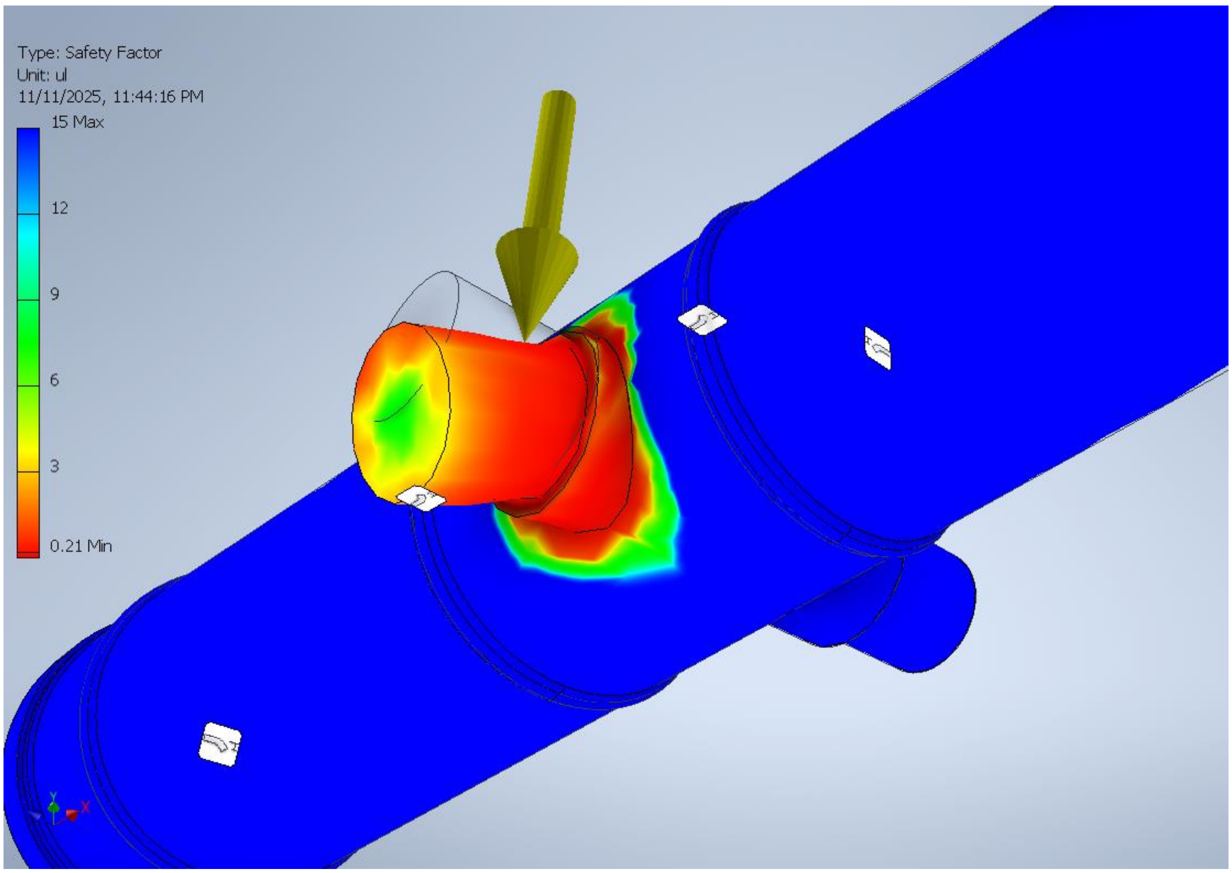

Figure 142: 8–pounder Finbanker model Factor of Safety graph if dropped on the trunnion on a stone surface, displacement exaggerated. (Created in Autodesk Inventor by James Fowler.)

When instead the cannon was dropped on its trunnion on a hard wooden surface, the results did not indicate that the trunnion would fail. As depicted in Figure 143, the FoS remained above 1.0, with a minimum observed at 2.13. The Von Mises Stress graph for the wood surface is displayed in Figure 144. Additionally, the Von Mises Stress remains acceptable at 41.9 ksi (288.9 MPa). Thus, under these conditions, a trunnion is more than capable of surviving such trauma.

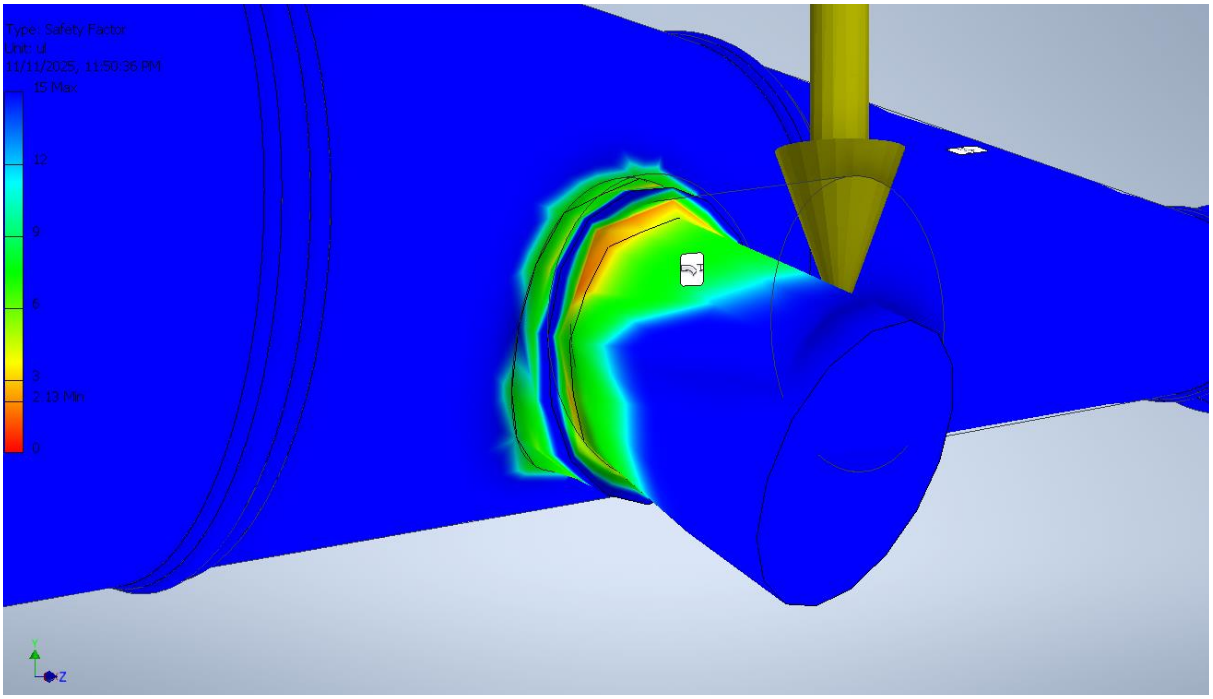

Figure 143: 8–pounder Finbanker model Factor of Safety graph if dropped on the trunnion on a wood surface, displacement exaggerated. (Created in Autodesk Inventor by James Fowler.)

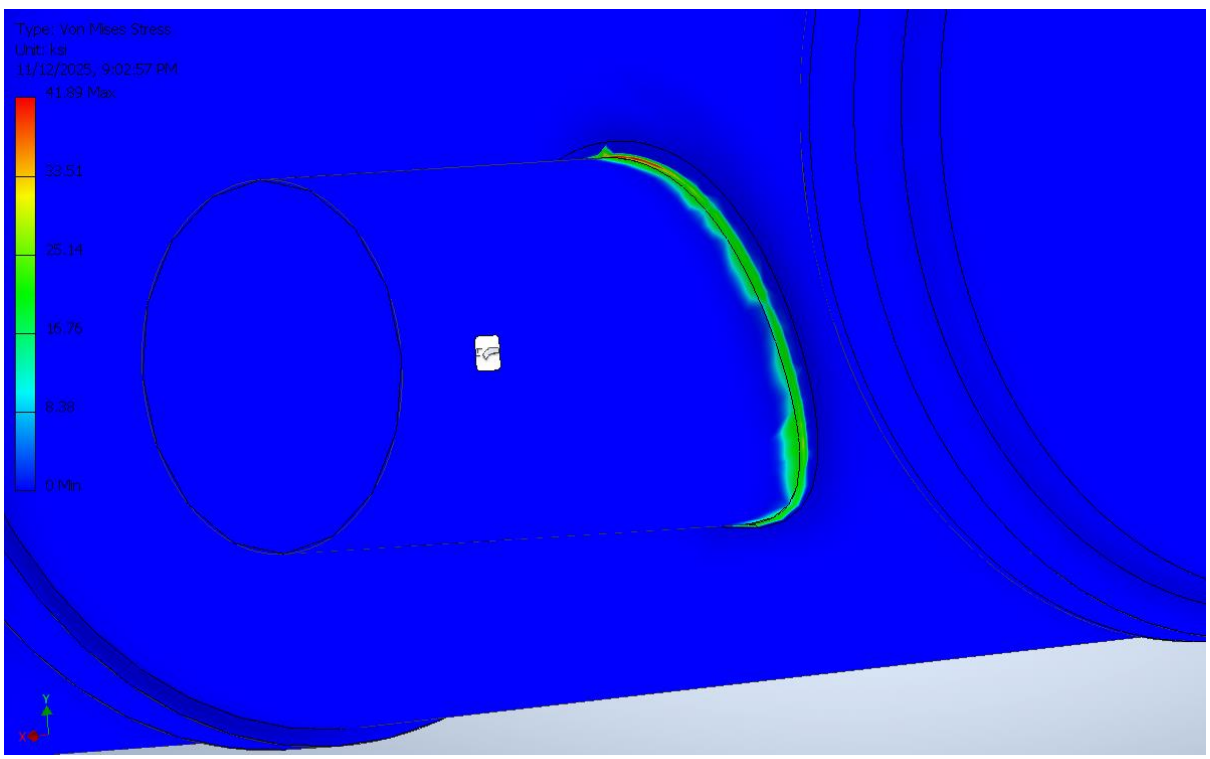

Figure 144: 8–pounder Finbanker model Von Mises Stress graph if dropped on the trunnion on a wood surface, realistic displacement. (Created in Autodesk Inventor by James Fowler.)

Therefore, it is unlikely that trunnions were broken off during service onboard warships, unless perhaps one cannon landed on or struck another cannon. Instead, it is much more likely that they failed while being dropped ashore.

Extremity Failure Trends

From these simulations, it can be ascertained that most failed extremities resulted from mishandling while on shore, likely on hard stone surfaces. The hardest surfaces on a ship are the wooden decks, and even if dropped from a height of 2 meters, under such circumstances the simulations indicate that the cannons trunnions would not fail. The cascabel, narrower at the neck, could fail on either wood or stone surfaces, however it was more likely to fail on stone. From this research, it was determined unlikely that a hammer blow could cause an otherwise–undamaged trunnion or cascabel to fail. This indicates that to disable a cannon, spiking the gun or otherwise rendering it unserviceable would be more effective than trying to cause the cascabel or trunnions to fail with a hammer. Additionally, guns may fail at the extremities due to a wrecking event. As a ship begins to sink and it loses stability, guns higher on the vessel may become dislodged and collide violently with guns located lower on the vessel. This may result in fractured extremities. Guns found in the underwater archaeological context need to be considered for damage which may have occurred during the site formation process. More research is needed to verify these preliminary results, however trends observed in the archaeological record and through in simulations point towards mishandling as the primary cause of a Type IV extremity failure.

It must also be noted that the historical sources, as discussed in Chapter One, indicate that significant testing was done on guns elevated to high angles and fired (Greener 1858:88–89; Holley 1865:56, 121, 582). These guns often failed at the trunnions, shearing them off entirely.

Perhaps guns found in the archaeological record with missing trunnions are the results of high angle firing. No specific testing of high angle firing was conducted in FEA, and the FEA results indicate that even when the trunnions are restrained completely and the gun is fired, little force is exerted on the trunnions. It is also important to note that angling naval guns to high elevations was more difficult onboard warships due to design of the standard naval gun carriages and the typical layout of gundecks. However, if naval gun trunnion failures are due to high angle firing, this indicates that the historical reports of trunnion failure are likely not due to a design issue but instead to a material quality or manufacturing defect issue which resulted in fatigue failure in those regions. More research will be needed to confirm these findings.

Failure Types Not Addressed

This study is focused on explaining failure types encountered in both the archaeological and the historical record, however some failure modes are alluded to but no physical examples have ever been located. These failure modes had too little data associated with them to conduct a rigorous analysis and thus were excluded from the study. An example of such are the failures recorded by the Royal Navy of large sea–borne mortars employed at the Battle of Sveaborg at Suomenlinna during the Crimean War. Sources claim these large–caliber mortars split down the middle when used continuously, effectively cutting the mortar into two halves. Some crude drawings of these exist, however no precise measurements were taken, and little data exists to allow for a faithful replication, despite being mentioned in multiple sources as a constant failure mode during the mid–19th century (Greener 1858:89, Holley 1865:582). Additionally, since no archaeological example of failed mortars has been found to exist, no physical evidence can be analyzed to interpret causation. Thus, such failures and others similar were excluded from this classification. Future research may lend more data to allow further analysis of such incidents.

Additionally, a fifth profile, here referred to as Type V: Material Loss Failure, was also excluded from this study due to lack of substantial material evidence. A Type V failure describes any time a large chunk of the gun detaches itself from the gun, but no bursting or explosive failure occurs. This failure has been observed in only a few archaeological examples and has proven difficult to fully quantify. Examples of this kind of failure are seen in cannons BR–04, BR–07, SW–21, and UN–05. Whether these missing chunks fractured and fell out, are due to corrosion cavities, or result from interior voids in the casting are not known. Such a failure might occur when a gun is struck by an object with substantial mass, velocity, or both, as the damage resembles in some ways bullet pockmarks on concrete or iron surfaces. Perhaps such damage comes from a cannonball strike or ball shot impacting the gun, however this theory has not been tested or analyzed. More likely, it is due to fatigue failure which causes the gun to split in a region that by happenstance does not intersect with the barrel and thus does not cause a pressure burst. More research is needed to understand this failure mode.

Conclusion

The four primary types of failure categories result in four different failure modes. Generally, muzzle failures are caused by vastly different reasons than barrel failures aft of the trunnions. Barrel failures forward of the trunnions represent an anomaly, with these instances resulting from failure modes consistent with muzzle failures and other times with barrel failures aft of the trunnions, and in some limited cases, these guns instead display signs of purposeful destruction. The fourth category, extremity failures, were found to be often caused by drops or falls, but additionally could be resultant of other different non–uniform force concentrations.

The first type simulated was Type I: muzzle failures. FEA testing indicates that muzzle failures are most likely due to muzzle brittleness related to casting techniques, manufacturing defects, and propensity for inclusions. Bursting muzzles do not appear to be caused by overpressure, which represented an initial theory for their proclivity in the archaeological record. This implies that guns bursting at the muzzle are not indicative of poor crew training or other human factors which might induce an overpressure failure. Instead, burst guns indicate poor manufacturing or quality standards, weapons pushed beyond their service life, or poor material sourcing. For instance, UN–01 appears to have failed due to an imbedded wire, which represents a quality defect which should have been identified during the proofing process, and the gun should not have been released but instead culled and scrapped. Additionally, displacement of the barrel seems to also play a role in muzzle failures, with cyclical deformation, or whiplashing, resulting in fatigue failures. Further analysis may uncover relationships between resonance frequency and muzzle failure, thus providing a future avenue for research.

The second failure type analyzed was Type II: barrel failure forward of the trunnions. Barrel failures forward of the trunnions represent an anomalous failure category. This region has been determined by FEA simulations to be the least prone to catastrophic failures of any type. It appears that some failures may be categorized in a similar manner to muzzle failures, and others may be more congruent with Type III barrel failures aft of the trunnions due to overpressure. However, it is highly likely that any catastrophic failure which occurs there is the result of fatigue stress and likely occurred late in the weapon's service life. Simulations show that BR–02 represents a strong design which very likely did not fail but instead was purposefully cut in the region. Simulations on BR–01 show few signs of propensity to fail due to overpressure, even with high gunpowder loads. It was determined that this specific weapon likely failed due to a combination of factors, including neglect, corrosion, and material weakness. Additionally, more research is needed to determine if Type II failures should be included as a subcategory of a different type of failure – or, perhaps only two categories of barrel failure are required: failures towards the muzzle and failures towards the breech. Furthermore, efforts must be made to quantify the effects of resonance frequency, thermal fluctuations, and low–cycle thermomechanical fatigue, however at this point no satisfying conclusion can be made concerning guns in this category.

Type III: barrel failure aft of the trunnions was analyzed third. Both SW–01 and SW–23 displayed very low Factor of Safety numbers, and across all cannons tested, the breech area was consistently the region of highest peak pressure. This indicates that failure in this region is likely to be catastrophic and would occur before high–cycle fatigue could result in significant fatigue cracking. Weapons that burst in this region likely failed due to overcoming the material's yield and tensile strength, resulting in instantaneous disintegration. Thus, weapons that fail near the breech and aft of the trunnions may represent overpressure failures due to gunpowder mishandling. Poor training, combat stress, or mishandling of the weapons could cause such a failure. Additionally, honeycombing and interior bore dilapidation could compound degradation due to fatigue. Both weapons tested, SW–01 and SW–23, likely remained out of service for extended periods of time. Notably, both weapons were also of Swedish manufacture. Further research should be focused on determining if material quality impacted the propensity for catastrophic Type III failures.

The fourth category tested was Type IV: extremity failure. The FEA indicates that most failed extremities are the result of cannon mishandling in areas where very hard surfaces are present. If dropped from a height of 2 meters (6.56 ft) on a wooden deck, FEA indicates that the trunnions would not fail, however, on stone, they would fail. The cascabel, narrower at the neck, could fail on either wood or stone surfaces, however it was more likely to fail on stone.

Considering the FEA results, it is unlikely that a hammer blow could cause an otherwise–undamaged trunnion or cascabel to fail. This indicates that spiking or otherwise rendering a gun unserviceable would be more effective than trying to break an extremity with a hammer. More research is needed to verify these preliminary results, however the trends both in the archaeological record, and the trends observed in the simulations, point towards mishandling as the primary cause of a Type IV extremity failure.

Chapter 7: An Overview and Conclusion

Introduction

The goal of this thesis was to expand the understanding of the causes of naval gun failures utilizing archaeological and engineering methodology. As stated previously, cannons are constantly present in the archaeological record, however up until this point little research has been conducted on the failed specimens often found preserved. To understand how thesis questions were answered, a short synopsis of each chapter is included. In Chapter One, the research questions were outlined, and each of those objectives are revisited in detail and a determination made. Additional research is also proposed, and some key outcomes of this research are expounded upon.

Thesis Overview

In Chapter One, the concept of gun failure is introduced, and several research questions poignant to the study are outlined. Additionally, a brief overview of previous research on this topic is included, and the structure of the thesis is outlined. The history of naval guns, including their design, construction, and deployment is detailed in Chapter Two. Gun casting techniques are analyzed and raw material sourcing for cannons is overviewed along with a history of gun proofing and a comprehensive history of gun failures. To understand gun failure from a highly technical perspective, the theoretical foundations upon which such a study rests are introduced. Chapter Three first outlines the archaeological theory required to understand the context of naval gun material culture, then engineering theory was related to intersect with the tenets of archaeological site formation theory. In short, Chapter Three connects the history of gun failure outlined in Chapter Two with modern engineering and archaeology theory. Chapter Four is based around the implementation of the PFD. Chapter Four outlines the methodology requisite in both historical and archaeological data collection, which leads to the reconstruction of internal ballistics calculations, and implementation of CAD modeling and the FEA process. Chapter Five presents an overview of all the cannons recorded by the author, and many that were recorded by other archaeologists but are of use to this study. British cannons, Swedish cannons, and cannons of unknown origin are all included, and each is assigned a unique identifier, and its location, condition, and dimensions are included, if known. Chapter Six applies FEA software to analyze gun failure patterns. In this chapter, guns were categorized into four failure patterns: Type I muzzle failure, Type II barrel failure forward of the trunnions, Type III barrel failure aft of the trunnions, and Type IV extremity failure. Every gun recorded in Chapter Five is categorized into one of these four categories. In this chapter, archetypal guns, sometimes more than one per failure type, are selected for further analysis, and the results of each of these guns are discussed in length.

Addressing the Research Questions

The secondary research questions are addressed first, because when taken together, they culminate to answer the primary research question. Several secondary objectives were outlined in Chapter One. The initial secondary objective consisted of the following question: Can a categorization of naval gun failure modes be generated? Initially, no obvious way of categorizing cannon failure modes was found, but once all the cannons exhibited in Chapter Five were accounted for and cross-compared, several trends emerged. Cannons seem to fail in four distinct places - many guns failed towards the muzzle and others failed at the extremities. These two categories developed quickly into defined groups. Additionally, some guns exploded near the breech, while others failed forward of the trunnions but not at the muzzle. Thus, four categories were created. However, Type II barrel failure forward of the trunnions may still require some further testing to correctly categorize. This failure mode was very difficult for FEA software to replicate, and although several cannons in the archaeological record exhibit this failure mode, FEA indicated that such a failure is highly unlikely. Further testing may reveal that Type II failures should instead be categorized as a form of either Type I or Type III failures. Furthermore, perhaps categorizing failure modes according to location isn't the correct approach at all, but instead letting FEA dictate the cause of failure would be more accurate. For example, according to the interpretation of the FEA results, failures towards the breech tend to be caused by overpressure, while failures towards the muzzle tend to be caused by fatigue or material defects. An alternative approach would be to categorize failures according to these specifications. Both approaches are viable categorization methods, an observation which became clear upon the completion and analysis of the FEA data. Further research is needed to determine which categorization approach is most effective.

The second secondary objective is as follows: what are the non–engineering related factors influencing instances of historic gun failures? These results indicate that much can be learned about human culture of certain navies and militaries by examining exploded guns. For example, guns that show Type I failure at the muzzle might indicate that the gun was poorly or cheaply manufactured or sourced from an inexperienced iron works. Additionally, a gun burst at the muzzle may indicate a new or unproven design. Guns that exhibit Type III failure and burst in the breech area likely did so due to overpressure, which might indicate a poorly trained gun crew, or a gun which has seen little maintenance since well–maintained guns were less likely to burst at the breech. Guns which show Type IV failure at an extremity were likely mishandled or otherwise damaged in transport. These guns may indicate use as ballast, or a mishandled shipment. Guns which failed in the extremity area could also have failed during a sinking event, as a ship loses stability and guns stored higher in the vessel fall and collide violently with guns lower down, resulting in broken extremities. Additionally, fatigue in the extremity area could result in failure at random and inopportune times.

Such information provides data on the quality of maintenance within a military force, or the level of training received by a ship's crew. Furthermore, the existence of a failed cannon could indicate the dynamics of a wrecking event or the preparedness or budget of a navy at the time of the gun's loss. Additionally, failed guns can indicate the quality of iron sources, which may speak to resource extraction and the strength of global supply chains. The research value failed guns is only as good as the context within which they are found, and thus without intact context, a failed gun becomes much less useful. When archaeologists encounter a failed gun in situ, this study indicates that it should be examined in equal (or in some instance perhaps higher) detail relative to any intact gun. The failed gun may hold the key to further contextual clues which would be absent on intact guns which could provide insight into the entire archaeological site.

While many *engineering*–related factors were identified that influence gun failures, such as fatigue, manufacturing defects, or design flaws, more research is needed into individual militaries to determine other *non–engineering* influences. This thesis does point to human factors being a primary causation in gun failures, however it does not attempt to quantify such factors. Indeed, this thesis supports the need for further historical research into the culture of various militaries, training regimes, and postures of readiness.

The third secondary objective aimed to answer the following question: can engineering software successfully replicate a gun failure to corroborate evidence found in archaeological record? This study proved that failure patterns found in the archaeological record can indeed be replicated using engineering software. For example, as outlined in Chapter Six, cannon UN–01 exhibited a Type I muzzle failure, and was notable due to the wire embedded in the interior of the bore which likely caused failure. When analyzed by engineering software, the cannon indicated a strong design with relatively high FoS in the failed region. However, with the inclusion of the embedded wire, the gun failed in the exact spot recorded in the material culture specimen. Almost every gun analyzed by FEA corroborated or lent insight into the archaeological artifact, and this thesis provides a step in further utilization of engineering software in the context of archaeology.

The fourth secondary objective sought an answer to the question: how do archaeological considerations such as transformation processes and site formation influence the identification of failed guns? This objective proved more challenging to answer than others. Some guns have apparent post–deposition c–transform damage, such as the propellor strike marks on UN–01. Additionally, n–transform damage is apparent on almost every gun in the collection, as shown through severe pitting, spalling, or corrosion. But other guns have significantly less distinct damage, or damage which cannot be fully quantified as n–transform or c–transform, or pre–deposition or post–deposition. For example, BR–01 possibly shows signs of acetylene torch damage. It is not apparent if this occurred during its working life as a gun, as a recycled gun utilized as a bollard, or while it existed within an archaeological context. Such damage is very hard to quantify. This raises the question, when exactly does an object enter the archaeological record, especially if that object was never uncovered in situ? BR–01 was utilized first as a naval gun, then likely as a coastal defense gun, then likely as a bollard, then it either spent some time as an archaeological artifact, or perhaps it was removed from its time as a bollard and placed directly into the care of its museum –its lifespan before it was donated to the museum could not be confirmed. At what point did any in-situ damage occur? More research is needed on this aspect.

The fifth secondary objective asked: how many engineering factors can be identified that influence the failure of guns? This question was in part answered. Factors such as material composition, including choice of metal, and material temperature at the point of failure all play a role. Thermal conductivity and specific heat impact the speed at which a cannon overheats. A material’s yield strength, tensile strength, toughness, and bulk modulus of elasticity indicate how much force a gun can experience before failure or permanent deformation. External stimuli such as work hardening impacts the brittleness of a gun and leads to unpredictable failures. Fatigue is perhaps the biggest factor which impacts the likelihood of failure. Fatigue unavoidably takes root over time, propagating from small cracks caused by the overcoming of a material’s ultimate tensile strength, a phenomenon which analysis of the FEA results in Chapter Six indicate is not uncommon. Additional factors such as surface finish also impact the speed at which fatigue cracks propagate. Furthermore, casting techniques and common casting defects can cause serious weak points in iron’s crystalline structure. Microporosity, non–homogeneous metal, inclusions, and material density all play a role in the likelihood of failure. Cannon design also directly impacts propensity for failure. However, although this list is thorough, more engineering factors are likely at play which could not be fully identified and tested. For example, resonance frequency may have played a role in the failures which standard FEA could not account for. Researchers who are more experienced in this aspect of engineering theory are required to fully explore this possibility and others.

The primary objective of this thesis was to answer the following question: can engineering technology be utilized to broaden knowledge of naval gun failures found in the archaeological record while also aiding in the interpretation of historical instances of cannon failures? The engineering software determined that the location of each gun's failure point can be used with some accuracy to estimate cause of failure. Type I: muzzle failures seem to be caused by poor casting techniques or manufacturing defects, broadly speaking. Type II: barrel failure forward of the trunnions are anomalous failures and were determined by interpretation of the FEA simulations to have occurred in areas least likely to fail. Thus, detailed data on each individual weapon must be collected to help further narrow down the cause of failure. Some Type II failures are likely due to overpressure of some kind, others to manufacturing defects, and some to fatigue. The history of the gun is necessary to fully understand these findings. Type III: barrel failure aft of the trunnions is likely caused by overpressure or fatigue failure due to repeated overpressure. Type IV: extremity failures seem most likely due to poor handling, such as dropping weapons during transportation. FEA simulations indicated that it would be very hard to damage a well–designed cannon via human power alone and thus indicate that missing trunnions or cascabels were likely not removed with a sledgehammer or similar tool. Instead, this damage is likely due to dropping the gun on a hard surface such as a stone floor. It seems unlikely that cast iron guns could fail in the trunnions if dropped at sea, as dropping impacts on wood did not provide enough shock to cause iron to fail in the gun tested. However, if the gun was dropped on another gun at sea, for example, guns rolling around in a hold or dropped into a hold, such a failure could occur.

In short, engineering technology can be utilized to further understand gun failures and does lend insight into historical instances of cannon failure. Such methodology is optimal for projects which do not have the funding or time necessary to complete a rigorous regime of experimental archaeological analysis on artifacts. While physical testing will always be more accurate to determine causes of failure, such methodology can be unobtainable, and engineering software offers an approachable and viable alternative.

Future Research

More work is needed to answer questions which were touched upon but not the primary focus of this research. As mentioned before, several engineering characteristics have not fully been studied. The effects of low–cycle thermomechanical fatigue are not quantified in this study. Furthermore, no thermal analysis was conducted to determine whether applying heat to guns causes them to fail in unpredictable ways or locations. Thermal analysis could shed light on the anomalous examples of Type II barrel failure forward of the trunnions. Additionally, the effects of vibration were not considered but pose a route for future analysis. Resonance frequencies can cause otherwise unpredictable failure profiles, and perhaps such an effect is measurable in cannons. Additionally, dedicated fatigue analysis was not attempted because the data for the fatigue curve for low–grade cast iron could not be reliably sourced or estimated. Perhaps a future researcher with more expertise in material science could gain more ground in this region.

Further research could also be conducted on the archaeological front. Almost certainly more archaeological publications exist which detail instances of exploded guns in the archaeological record. While the author combed archaeological publications for such instances, not enough ground was covered. What instances of failed guns exist within grey literature around the world is unknown, but they are doubtless significant. Furthermore, additional fieldwork could be conducted at archaeological sites which are confirmed to include failed guns. These artifacts may lend further insight not only into the history of the archaeological sites themselves, but also the history of failed naval guns in general.

Additionally, more data is required to build a more robust statistical sample. Appendix D includes a list of all known exploded guns, with links to publications concerning them, their failure modes, and their locations. However, this is a relatively small sample size, significantly less than 100 individual specimens. With more datapoints, a more complete picture can be developed pertaining to trends which may exist. Archaeologists should take extra care to mention and record all failed or otherwise broken guns found in the archaeological context and fully document them to make any future work more statistically viable. Finally, an increased visibility on broken guns within the field of archaeology is required. To fully appreciate the importance of broken guns in understanding the archaeological record, more archaeologists need to invest time and resources into prioritizing broken guns found on sites. This would markedly increase the potential knowledge generated on this subject.

Conclusion

In closing, while this study contributes to the study of failed guns, more work should be conducted by the next generation of scholars to fully unlock the potential knowledge that failed guns hold. More methods should be tested, and more objectives completed. This thesis proved that multidisciplinary approaches can be successfully implemented, and that engineering technology can be utilized to great effect when trying to explain phenomenon found within the archaeological record. Hopefully, the knowledge developed in this work will be utilized outside of simply failed cannons but utilized in a whole variety of archaeological projects in the place of conventional experimental archaeology. Engineering software offers a less expensive and more repeatable alternative to conventional experimental analysis. It is the hoped that thesis inspires those who wish to utilize this methodology for other, more varied archaeological purposes, and that the importance of failed guns is not lost to those who could answer their own research questions by examining failed guns.

References

Agisoft Metashape

2026 Agisoft Metashape User Manual, Professional Edition, Version 2.3. Agisoft LLC <https://www.agisoft.com/pdf/metashape-pro_2_3_en.pdf>. Accessed 28 January 2026.

American Society for Mechanical Engineers

2025 Codes and Standards. AMSE Setting the Standard <https://www.asme.org/codes-standards/find-codes-standards>. Accessed 10 December 2025.

Anderson, R. C.

1910 *Naval Wars in the Baltic during the Sailing–Ship Epoch, 1522–1850.* C. Gilbert–Wood, London, UK.

Andrade, Tonio

2016 *The Gunpowder Age: China, Military Innovation, and the Rise of the West in World History*. Princeton University Press, Princeton, NJ.

Armstrong, Benjamin F. (editor)

2023 *21st Century Mahan: Sound Military Conclusions for the Modern Era*. Naval Institute Press, Annapolis, MD.

Arnold, John H.

2000 *History: A Very Short Introduction*. Oxford University Press, New York, NY.

Auer, Jens

2004 Fregatten Mynden: a 17th-century Danish Frigate Found in Northern Germany. *International Journal of Nautical Archaeology* 2(33):264–280.

Autodesk

2014 Equivalent or Von Mises Stress. Autodesk Inventor 2014 <https://help.autodesk.com/view/INVNTOR/2014/ENU/?guid=GUID-C787792D-BBB1-41A7-BBD7-CBCABCBE7C01>. Accessed 29 January 2026.

2026 Finite element analysis software for accurate engineering simulation. Autodesk Inventor <https://www.autodesk.com/solutions/simulation/finite-element-analysis>. Accessed 29 January 2026.

Axelsson, Yngve.

2021 The history of Swedish iron and steel industry. Jernkontoret <https://www.jernkontoret.se/en/the-steel-industry/the-history-of-swedish-steel-industry/>. Accessed 1 November 2024.

BU Archaeology

2025 SCW0025: 12lb Finbanker Cannon. BU Maritime Archaeology <https://www.bumaritime.org/projects/scw/finds/0026/>. Accessed 9 October 2025.

Batchvarov, Kroum Nickolaev

2002 The Framing of Seventeenth-Century Men-of-War in England and Other Northern European Countries. Master's thesis, Department of Anthropology, Texas A&M University, College Station.

Bindler, Richard, Jon Karlsson, Johan Rydberg, Björn Karlsson, Lena Berg Nilsson, Harald Biester, and Ulf Segerström

2017 Copper-ore mining in Sweden since the pre-Roman Iron Age: lake-sediment evidence of human activities at the Garpenberg ore field since 375 BCE. *Journal of Archaeological Science: Reports* 12(1):99–108.

Benton, J. G.

1862 *A Course of Instruction in Ordnance and Gunnery; Compiled for the Use of the Cadets of the United States Military Academy, 2nd edition.* D. Van Nostrand, New York, NY.

Binford, Lewis. R.

1962 Archaeology as Anthropology. *American Antiquity* 28(2):217–225.

Boëthius, B.

1958 Swedish iron and steel, 1600–1955. *Scandinavian Economic History Review* 6(2):144–175.

Bowens, Amanda (editor)

2009 *Underwater Archaeology: The NAS Guide to Principles and Practice, 2nd edition*. John Wiley & Sons, Chichester, UK.

Brown, David K.

1997 *Warrior to Dreadnought: Warship development 1860–1905.* Chatham, London, UK.

Brown, Ruth

1988 The Woolwich proof registers 1780– 1781, *International Journal of Nautical Archaeology* 17(1):105-111.

1989 Identifying 18th–century trunnion marks on British iron guns: a discussion, *International Journal of Nautical Archaeology* 4(18):321–329.

1990 Guns carried on East Indiamen, 1600–1800, *International Journal of Nautical Archaeology* 19(1):17-22.

2007 Report on Cannon 3 from the Queen Ann's Revenge. Queen Annes Revenge Project: Natural and Cultural Resources. Manuscripts, Queen Annes Revenge Lab, Greenville, NC. <chrome-extension://efaidnbmnnnibpcajpcglclefindmkaj/https://www.qaronline.org/report-cannon-3-queen-annes-revenge/open#:~:text=1.,in%20the%20Baltic%20in%201719.>. Accessed 9 October 2025.

Budynas, Richard G., and J. Keith Nisbett

2015 *Shigley's Mechanical Engineering Design, 10th edition*. McGraw Hill Education, New York, NY.

Carpenter, Austin C.

1993 *Cannon: The Conservation, Reconstruction, and Presentation of Historic Artillery.* Halsgrove Press, Somerset, UK.

Ciarlo, Nicolas, Josefa Marti Solano, Manual Bethencourt, and Elisa Fernandez Tudela

2023 New remarks on the mid-17th-century gunfounding in Northern Europe: archaeometric analysis of scrap bronze ordnance recovered from a Dutch merchant vessel lost off Cadiz, Spain. *Archaeological and Anthropological Sciences* 15(136):1-28.

Cipolla, Carlos M.

1967 *Guns, Sails and Empires: Technological Innovation and the Early Phases of European Expansion 1400–1700.* Minerva Press, New York, NY.

Cohn, Arthur B., Adam I. Kane, Christopher R. Sabick, and Edwin R. Scollon

2003 *Valcour Bay Research Project: 1999-2002 results from the archaeological investigation of a Revolutionary War battlefield in Lake Champlain, Clinton County, New York.* Reports, Lake Champlain Maritime Museum, Vergennes, VT.

Collins, A. R.

2025 Smooth Bore Cannon Ballistics, Miscellany: Miscellaneous technical articles by Dr. A. R. Collins, Arc.id.au. <https://2015fallhw.github.io/arcidau/CannonBallistics.html#:~:text=Atmospheric%20pressure%20is%2014.7%C3%97,of%201600%20is%20more%20appropriate.>. Accessed 3 November 2025.

Conahan, Frank C.

1990 *Battleships, issues arising from the explosion aboard the USS Iowa.* ASIN B00010DRDG. The Office of the Distributor, Government Accountability Office, Washington, DC.

Cooper, Iver P.

2024 *Arming the Warship: Naval Weapons Technology and Gunnery from the Spanish Armada to the Cold War.* McFarland and Co., Jefferson, NC.

Cook, Gregory D., Rachel Horlings, and Andrew Pietruszka

2016 Maritime Archaeology and the Early Atlantic Trade: research at Elmina, Ghana, *International Journal of Nautical Archaeology* 45(2):370-387.

Cooke, A. P.

1875 *A Textbook of Naval Ordnance and Gunnery: Prepared for the Use of the Cadet Midshipmen at the United States Naval Academy*. John Wiley & Sons, New York, NY.

Corbett, Julian S.

1911 *Some Principles of Maritime Strategy.* Longmans, Green, and Co., London, UK.

Dawson, Anthony L., Paul L. Dawson, and Stephen Summerfield

2007 *Napoleonic Artillery*. Crowood Press, Marlborough, UK.

Delano, Amasa

1817 *A Narrative of Voyages and Travels, in the Northern and Southern Hemisphere: Comprising Three Voyages Round the World; Together with a Voyage of Survey and Discovery, in the Pacific Ocean and Oriental Islands.* E. G. House, Boston, MA.

Delgado, James P. and James A. Goold

2022 Background to the 'Black Swan' Case: The Identification as Nuestra Señora de las Mercedes, *International Journal of Nautical Archaeology* 50(2):352-360.

DeLuca, D. P.

2025 Understanding Fatigue. United Technologies Pratt & Whitney, American Society of Mechanical Engineers <https://files.asme.org/igti/knowledge/articles/13048.pdf>. Accessed 1 April 2025.

Ducoing, Cristián and Fredrik Olsson-Spjut

2021 The energy transition in the Swedish iron and steel sector, 1800 – 1939, *Journal of Energy History/Revue d'Histoire de l'Énergie* 1(4):1–12.

ECU Maritime Studies

2022 British Blomefield Cannon (24-pound), Sketchfab <https://sketchfab.com/3d-models/british-blomefield-cannon-24-pound-7dc41a08164d4e0a9717c7a7a1b465c9>. Accessed 9 October 2025.

Edvinsson, Rodney

2012 The international political economy of early modern copper mercantilism: Rent seeking and copper money in Sweden 1624–1776. *Explorations in Economic History* 49(3):303-315.

Eriksson, N. and J. Rönnby

2017 *Mars* (1564): the initial archaeological investigations of a great 16th-century Swedish warship. *International Journal of Nautical Archaeology* 46(1): 92-107.

Fowler, James R.

2025 Exploded Guns, Warships and the Baltic, *Stem to Stern* 42:10.

Fowler, James R. and Markku Luoto

2026 *Report on Analysis of Failed Cannons on the Kronprins Gustav Adolf Wreck Site, MV/00971/2025*. Reports, Finnish Heritage Agency, Helsinki, Finland.

Fox, Kara D.

2015 Matters of Steel: Illustrating and Assessing the Deterioration of the World War II Merchant Freighter *Caribsea*. Master's thesis. East Carolina University, Greenville, NC.

Franklin, Benjamin.

1777 The American Commissioners: Contract with Rey de Morande, 31 October 1777. National Archives <https://founders.archives.gov/documents/Franklin/01-25-02-0082>. 9 October 2025.

Guilmartin, John Francis

1982 The cannon of the Batavia and the Sacramento: early modern cannon founding reconsidered, *International Journal of Nautical Archaeology* 11(2):133-144.

1999 The Development of Artillery, Encyclopedia Britannica <https://www.britannica.com/technology/military-technology/The-development-of-artillery>. Accessed 23 April 2024.

2003 *Gunpowder and Galleys: Changing Technology and Mediterranean Warfare at Sea in the 16th Century.* Naval Institute Press, Annapolis, MD.

Green, Jeremy

2004 *Maritime Archaeology: A Technical Handbook, 2nd edition.* Elsevier Academic Press, San Diego, CA.

Greener, William W.

1858 *Gunnery in 1858: Being a Treatise on Rifles, Cannon, and Sporting Arms, Explaining the Principles of the Science of Gunnery, and Describing the Newest Improvements in Fire–Arms*. Smith, Elder and Company, Cornwall, UK.

1910 *The Gun and Its Development*. Cassell and Company, London, UK.

Griffith, F. A.

1856 *The Artillerist's Manual, and British Soldier's Compendium, 7th edition*. Authority, London, UK.

Groover, Mikell P.

2012 *Introduction to Manufacturing Processes.* John Wiley & Sons, Hoboken, NJ.

Hammond, Carolyn

1996 *Caesar The Gallic Wars: A New Translation by Carolyn Hammond.* Oxford University Press, New York, NY.

Harris, Lynn and Nathan Richards

2018 Preliminary Investigations of Two Shipwreck Sites in Cahuita National Park, Costa Rica. *International Journal of Nautical Archaeology* 47(2):405-418.

He, Li, Fan Fei, Wenbo Wang, and Xuan Song

2019 Layerless Additive Manufacturing of Metal Alloy Lattices Using Immiscible-Interface Assisted Direct Metal Drawing. *Procedia Manufacturing* 34(1):647-654. <10.1016/j.promfg.2019.06.106.> Accessed 1 April 2025.

Henry, Chris.

2004 *Napoleonic Naval Armaments 1792–1815*, Osprey Publishing, Oxford, UK.

Herry, Nolwenn

2004 Blackwell Publishing Ltd Report on Finds from the Saint-Quay-Portrieux Wreck, France, *International Journal of Nautical Archaeology* 33(1):96–105.

Hobson, John M.

2004 *The Eastern Origins of Western Civilisation.* Cambridge University Press, Cambridge, UK.

Hocker, Frederick M., Ed., Cheryl A. Ward.

2004 *The Philosophy of Shipbuilding: Conceptual Approaches to the Study of Wooden Ships.* Texas A&M University Press, College Station.

Hodson, Harry

2003. "The Royal Arsenal at Woolwich - the Master Founders." *Steel Times International*, 6(1): 76.

Holley, Alexander L.

1865 *A Treatise on Ordnance and Armor: Embracing Descriptions, Discussions, and Professional Opinions Concerning the Material, Fabrication, Requirements, Capabilities, and Endurance of European and American Guns for Naval, Sea–Coast, and Iron–Clad Warfare, and their Rifling, Projectiles, and Breech–Loading.* D. Van Nostrand, New York, NY.

Ingalls, James M.

1912 *Interior Ballistics, 3rd edition*. John Wiley & Sons, New York, NY.

Keith, Matthew E. (editor)

2016 *Site Formation Processes of Submerged Shipwrecks*. University Press of Florida, Gainesville.

Koivikko, Minna, Tuomas Aakala, Sami Brchisky, David Cleasby, Kari Hyttinen, Jesse J. Jokinen, Xavier Le Rudulier, and Liisa Näsänen

2026 An Archaeological Study of an Underwater Cannon Site in the Sea Fortress Suomenlinna, the Baltic Sea. *Material culture in the Swedish Navy, c. 1450-1850, 1st edition.* Simon Ekström, Niklas Eriksson, Anna Maria Forssberg, and Leos Müller, editor, Amsterdam University Press, Amsterdam, Netherlands.

Krulikowski, Alex

2013 *Fundamentals of Geometric Dimensioning and Tolerancing.* Effective Training, Livonia, MI.

Lambert, Andrew

2018 *Seapower States: Maritime Culture, Continental Empires, and the Conflict that Made the Modern World.* Yale University Press, New Haven, CT.

Lambert, D. M.

2016 Evaluation of the effect of surface finish on high–cycle fatigue of SLM–IN718. NASA-MSFC Marshall Space Flight Center. In *JANNAF Propulsion meeting*, JANNAF Propulsion meeting, Newport News, VA.

Lavery, Brian (editor)

1992 *The Line of Battle: The Sailing Warship 1650–1840.* Conway Maritime Press, London, UK.

Law, John

1984 On the Methods of Long-Distance Control: Vessels, Navigation and the Portuguese Route to India. *The Sociological Review* 32(5):234–263.

Leiner, Fredrick C.

2006 *The End of Barbary Terror: America's 1815 War Against the Pirates of North Africa*. Oxford University Press, New York, NY.

Lesley, John

1830 *The History of Scotland, From the Death of King James I in the Year M.CCC.XXXVI, to the Year M.D.LXI.* Edinburgh, UK.

Mahan, Alfred Thayer

1890 *The Influence of Sea Power Upon History.* Little, Budynas and Company, Boston, MA.

Mallet, Robert

1856 *On the Physical Conditions Involved in The Construction of Artillery: With An investigation of the relative and absolute values of the materials principally employed, and of some hitherto unexplained causes of the destruction of cannon in service.* Longman, Brown, Green, Longmans, and Roberts, London, UK.

Manucy, Albert

1949 *Artillery Through The Ages: A Short Illustrated History of Cannon, Emphasizing Types Used in America.* National Park Service, Washington, DC.

Maritime Archaeological Society of Finland

2023 G-A Texturoitu, Sketchfab <https://sketchfab.com/3d-models/g-a-texturoitu-6e819bced6fd428f89e15cb269767af6>. Accessed 10 October 2025.

2025a Fowler cannon before [textured] <https://sketchfab.com/3d-models/fowler-cannon-before-textured-649a5f83e1704ff3b7bbb0b8e1907974?>. Accessed 4 December 2025.

2025b Fowler cannon after [textured] <https://sketchfab.com/3d-models/fowler-cannon-after-textured-f9271d5f1e0540e799ecd165b108920c?>. Accessed 4 December 2025.

Martin, Colin J. M.

1972 El Gran Grifon: An Armada Wreck on Fair Isle. *The International Journal of Nautical Archaeology and Underwater Exploration* 1(1):59–71.

2005 The Adelaar: a Dutch East-Indiaman Wrecked in 1728 off Barra, Outer Hebrides, Scotland. *International Journal of Nautical Archaeology* 34(2):179-210.

2020 On War on Board: archaeological and historical perspectives on Early Modern warfare. *International Journal of Nautical Archaeology* 49(2):427-429.

Martin, Lillian Ray

2001 *The Art and Archaeology of Venetian Ships and Boats*. Texas A&M University Press, College Station.

McBride, P.

1976 The *Dartmouth*, a British frigate wrecked off Mull, 1690. *International Journal of Nautical Archaeology* 5(3):189-200.

McConnell, David

1988 *British Smooth-Bore Artillery: A Technological Study to Support Identification, Acquisition, Restoration, Reproduction, and Interpretation of Artillery at National Historic Parks in Canada.* Minister of Supply and Services, National Historic Parks and Sites, Environment Canada-Parks, Ottawa, Canada.

McGrath, Tim

2014 *Give Me a Fast Ship: The Continental Navy and America's Revolution at Sea.* Penguin Random House, New York, NY.

Meide, Chuck

2002 *The Development and Design of Bronze Ordnance, Sixteenth through Nineteenth Centuries.* College of William and Mary, Williamsburg, VA.

Mendel, Peterson

1965 *History under the Sea: A Handbook for underwater exploration.* Smithsonian Institution Press, Washington, DC.

Miles, A. H.

1926 The Princeton Explosion. *Proceedings*, 52(11):2225–2246. < https://www.usni.org/magazines/proceedings/1926/november/princeton-explosion>. Accessed 11 December 2025.

Moran, Michael J., Howard N. Shapiro, Daisie D. Boettner, Margaret B. Bailey

2018 *Fundamentals of Engineering Thermodynamics, 9th edition*. John Wiley & Sons, Hoboken, NJ.

Morrev, P.G., K.I. Kapyrin, L. Kurdyumova, I. Yu Kulikov, N.V. Tatatchenkov, and V.A. Gordon

2019 On construction of SPD stress–strain curve for bronze Cu85–Pb5–Sn5–Zn5. *Materials Science and Engineering: A* 765(1):137889.

Muckelroy, Keith

1978 *Maritime Archaeology.* Cambridge University Press, New York, NY.

Mueller, Hans-Friedrich

2012 *Caesar: Selections from his Commentarii De Bello Gallico.* Bolchazy-Carducci, Mundelein, IL.

Nagesha, A., Kannan, P. Parameswaran, R. Sandhya, K. Bhanu Sankara Rao, and Vakil Singh

2010 A comparative study of isothermal and thermomechanical fatigue on type 316L(N) austenitic stainless steel. *Materials Science and Engineering: A* 527(21–22):5969–5975.

Naval History and Heritage Command

2025 Bonhomme Richard. *Naval History and Heritage Command*. <https://www.history.navy.mil/browse-by-topic/ships/ships-of-sail/bonhomme-richard.html>. Accessed 11 December 2025.

Niderost, Eric

2021 Bloody Revenge at Sluys. *Military Heritage* 23(4):64–74.

O'Brien, Caleb J.

2022 *Norman* and *Grecian*: A Comparative Archaeological Site Formation Analysis of Two Steel–Hulled Great Lakes Bulk Carriers in Lake Huron. Master's thesis, East Carolina University, Greenville, NC.

Oldham, N., Plamer, M., Tyson, J.

1993 The Erme Estuary, Devon, historic wreck site, 1991–3. *International Journal of Nautical Archaeology* 22(4):323–330.

Overmeer, A. B. M.

2012 A Swedish man-of-war in Dutch waters: An archaeological field evaluation of the wreck of the *Sophia Albertina*. *Archaeological Heritage Management Reports 20,* pp. 1–93. Cultural Heritage Agency of the Netherlands, Amersfoort, Netherlands.

Oxford English Dictionary

2026 Gun. *Oxford English Dictionary*. <https://www.oed.com/dictionary/gun_n?tab=meaning_and_use#2344809>. Accessed 18 March 2026.

Padfield, Peter

1974 *Guns at Sea.* St. Martin's Press, New York, NY.

Paulaharju, Jyri, Ove Enqvist, and Keijo Koskinen

2025 The Guns of Suomenlinna, Suomenlinna Museum, Suomenlinna, Finland.

Pawelski, Matthew

2023 From USS *Stars and Stripes* to *Metropolis* (1861-present): Modeling the Life, Loss, and Archaeological Site Formation of a Currituck Beach Shipwreck (Corolla, North Carolina). Master's thesis, East Carolina University, Greenville, NC.

Pearson, L. M.

1966 The "Princeton" and the "Peacemaker": A Study in Nineteenth-Century Naval Research and Development Procedures. *Technology and Culture* 7(2):163-183.

Pedersen, M. M.

2024 *Introduction to Metal Fatigue*. Aarhus University, Aarhus, Denmark.

Phipps, Raymond C.

2024 "Eighty-Nine Years Before the Mast": An Analysis of Human Innovation and Maritime Technological Change in *Bear* (1874-1963). Master's thesis, East Carolina University. Greenville, NC.

2023 "Nelson's Dockyard, English Harbour, Antigua and barbuda. *Stem to Stern* 40:9–12.

Pomey, Patrice; Kahanov, Yaacov; Rieth, Eric.

2012 Transition from Shell to Skeleton in Ancient Mediterranean Ship–Construction: analysis, problems, and future research, *The International Journal of Nautical Archaeology* 41(2):235–314.

Prentiss, A. M.

1923a The Specific Heat and Thermal Diffusivities of Certain Explosives: Part I. *Army Ordnance* 4(20):117–122.

1923b The Specific Heat and Thermal Diffusivities of Certain Explosives: Part II. *Army Ordnance* 4(21):184–188.

PyroGuide

2025 Gunpowder Grades. PyroGuide <https://pyrodata.com/PyroGuide/index.php%5Etitle=Gunpowder_Grades.htm#:~:text=From%20PyroGuide&text=Black%20powder%20that%20passed%20through,are%20used%20for%20different%20purposes.&text=On%20nomenclature:%20The%20number%20of,be%20found%20in%20consumer%20articles.>. Accessed 4 November 2025.

Rees, Mike G.

2012 1813–14 Voyage of the H.M.S. Racoon. Academia, <https://www.academia.edu/33186707/1813_14_Voyage_of_H_M_S_Racoon>. Accessed 11 December 2025.

Renfrew, Colin, and Paul Bahn
2012 *Archaeology Theories, Methods, and Practice, 6th edition.* Thames and Hudson, London, UK.

Robertson, Frederick Leslie
1921 *The Evolution of Naval Armament.* Constable and Company, London, UK.

Robins, Benjamin
1805 *New Principles of Gunnery: Containing the Determination of The Force of Gunpowder, and An Investigation of the Difference in The Resisiting Power of the Air to Swift and Slow Motions. With Several Other Tracts on the Improvement of Practical Gunnery.* F. Wingrave, London, UK.

Roio, Maili (editor)
2022 *The Invisible Heritage Beneath the Waves: Exploring the Underwater Landscape in the Baltic Sea and Along the Coast of Norway.* AS Printon, Tallinn, Estonia.

Roth, Rudi
1989 A proposed standard in the reporting of historic artillery. *International Journal of Nautical Archaeology* 18(3):191–202.

Roquefeuil, Camille de
1823 *A Voyage Round the World Between the Years 1816–1819, in the Ship Le Bordelais.* Richard Phillips and Co., London, UK.

Royal Armouries
2025 Royal Armouries Archives. Royal Armouries Museum <https://royalarmouries.org/collection/archive/archive-390426>. Accessed 9 October 2025.

Sasser, Kirk N., and Jason T. Ford
2020 *Test Report: Black Powder Equivalency*. Safety Management Services, West Jordan, UT. <chrome-extension://efaidnbmnnnibpcajpcglclefindmkaj/https://www.phmsa.dot.gov/sites/phmsa.d

ot.gov/files/2020-10/Black%20powder%20equivalency.pdf>. Accessed 4 November 2025

San Francisco Call

1895 Johnson's Death Blow. *San Francisco Call*, 26 April, 77(137):1. San Francisco, CA. < https://cdnc.ucr.edu/?a=d&d=SFC18950426.2.12>. Accessed 18 March 2025.

Sarrau, M. E.

1883 *Theoretical Researches on the Effects of Gunpowder and Other Explosives.* Gunnery Department, Washington, DC.

Sasse, Ronald A.

1985 *Technical Report Brl-tr-2630: A Comprehensive Review of Black Powder.* US Army Ballistic Research Laboratory, Aberdeen Proving Ground, MD.

Schiffer, Michael B. and James Skibo

1987 Theory and Experiment in the Study of Technological Change. *Current Anthropology* 28:595-622.

Schiffer, Michael B.

1983 Towards the Identification of Formation Processes. *American Antiquity* 48(4):675–706.

1987 *Formation Processes of the Archaeological Record*. University of New Mexico Press, Albuquerque.

1995 *Behavioral Archaeology: First Principles*. University of Utah Press, Salt Lake City.

2002 *Behavioral Archaeology (Foundations of Archaeology).* Percheron Press/Eliot Werner Publications, Clinton, NY.

2010 *Behavioral Archaeology: Principles and Practices*. Routledge, New York, NY.

Seemann, Ute A.

1992 The Amsterdam Battery: A Late 18th Century Dutch Military Installation in Table Bay *South African Field Archaeology* 1:72–79.

Shipwreck Preservation Society of Newfoundland and Labrador

2020 Bauline cannon no. 1, Sketchfab <https://sketchfab.com/3d-models/bauline-cannon-no-1-b2609b189a534996a6ea3216b3b90181>. Accessed 10 October 2025.

Smith, Tim

2017 Early Cannon made in England. *Steel Times International* 41(4):56.

Steffy, J. Richard

1994 *Wooden Ship Building and the Interpretation of Shipwrecks.* Texas A&M University Press, College Station.

Sumida, John, and David Rosenburg

1995 Machines, Men, Manufacturing, Management and Money: The Study of Navies as Complex Organizations and the Transformation of Twentieth Century Naval History. In *Doing Naval History: Essays Toward Improvement*, John Hattendorf, editor, pp. 25-40. Naval War College Press, Newport, RI.

Suresh, Subra.

1998 *Fatigue of Materials, 2nd edition*. Cambridge University Press, New York, NY.

Taylor, John M.

1984 The Old Navy: The *Princeton* Disaster. *Proceedings* 110(9):148–149.

Tredrea, John and Eduard Sozaev.

2010 *Russian Warships in the Age of Sail, 1696–1860: Design, Construction, Careers and Fates*. Seaforth, Barnsley, UK.

Trigger, Bruce G.

1989 *A History of Archaeological Thought.* Cambridge University Press, Cambridge, UK.

Tucker, Spencer

1989 *Arming the Fleet: U.S. Navy Ordnance in the Muzzle-Loading Era.* Naval Institute Press, Annapolis, MD.

The Engineering Toolbox

2003 Specific Heat of Common Materials–Engineering Reference. The Engineering Toolbox <https://www.engineeringtoolbox.com/specific-heat-capacity-d_391.html>. Accessed 1 April 2025.

2005 Metals, Metallic Elements and Alloys - Thermal Conductivities. The Engineering Toolbox <https://www.engineeringtoolbox.com/thermal-conductivity-metals-d_858.html>. Accessed 23 April 2024.

2008a Metals - Strength vs. Temperature. The Engineering Toolbox <https://www.engineeringtoolbox.com/metal-temperature-strength-d_1353.html>. Accessed 23 April 2024.

2008b Metals and Alloys - Bulk Modulus Elasticity. The Engineering Toolbox <https://www.engineeringtoolbox.com/bulk-modulus-metals-d_1351.html>. Accessed 23 April 2024.

United States Congress House Committee on Naval Affairs

1844 Accident on Steam–ship “Princeton”, Report of the Committee on Naval Affairs. Report No. 479, 28th Congress, 1st Session. Blair & Rives, Washington, DC.

Unity Manufacture

2023 *How To Improve Sand Casting Surface Finish.* Unity Manufacture, 19 April. <https://unitymanufacture.com/how-to-improve-sand-casting-surface-finish/>. Accessed 11 April 2024.

Universal Engineering Services

2021 *Elastic analysis of pressure vessels.* Universal Engineering Services, 1 June. <https://www.universalengineeringconsultants.com/post/elastic-analysis-of-pressure-vessels-design-of-pressure-vessel>. Accessed 11 April 2024.

U.S. Department of Energy

1993 *DOE Fundamentals Handbook: Material Science* DOE-HDBK-1017/1-93, U.S. Department of Energy, Washington, DC. <https://engineeringlibrary.org/reference/properties-of-metals-doe-handbook>. Accessed 23 April 2024.

Verbruggen, Jan

2013 'Screws', or tricks of the trade: secret repairs of solid cast cannon. *Smoothbore Ordnance Journal* 6(22):91–100.

Von Gernet, Alexander D.

1982 Analysis of Intrasite Artifact Spatial Distributions: The Draper Site Smoking Pipes. Master's thesis, McGill University. Montreal, QC.

Watson, P. J.

1986 Archaeological Interpretation. In *American Archaeology Past and Future: A Celebration of the Society for American Archaeology 1935–1985,* D. J. Meltzer, D. D. Fowler, and J. A. Sabloff, editors, pp. 439–457. Smithsonian Institution Press, Washington, DC.

Weihed, P.

2022 How commodity prices and technical development has influenced exploration strategies: A case study from Sweden. *Mineral Economics* 35(3-4):409-427.

Wessex Archaeology

2017a Mystery Chesil Beach Shipwreck Designated Following Wessex Archaeology Fieldwork, September 14. Wessex Archaeology <https://www.wessexarch.co.uk/news/mystery-chesil-beach-shipwreck-designated-following-wessex-archaeology-fieldwork>. Accessed 10 October 2025.

2017b Chesil Beach Cannon Site, inshore (Dorset), Sketchfab <https://sketchfab.com/3d-models/chesil-beach-cannon-site-inshore-dorset-c19cc1d3b95c4b6f95fe660bdb33747c>. Accessed 10 October 2025.

2015a Cannon 6002, Gun Rock, Outer Farne Islands, Sketchfab <https://sketchfab.com/3d-models/cannon-6002-gun-rock-outer-farne-islands-0ecd7e2a6fac4b2abbd7fcc32d4d997d>. Accessed 10 October 2025.

2015b Cannon 6011, Gun Rock, Outer Farne Islands, Sketchfab <https://sketchfab.com/3d-models/cannon-6011-gun-rock-outer-farne-islands-0fd413401ff84196af1338e1facec155>. Accessed 10 October 2025.

2013 Gun Rocks, Farne Islands, undesignated site assessment, confidential report. Ref:83803.12. Wessex Archaeology, Salisbury, UK.

Wilkes, Bill St. John

1971 *Nautical Archaeology: A Handbook.* David and Charles, Bristol, UK.

Wilson, G. M.

1988 The Commonwealth Gun. *International Journal of Nautical Archaeology* 1(17):87–99.

Appendix A: Cannon recording proformas

CANNON DATA SHEET

Site name: ______________

Date: ______________

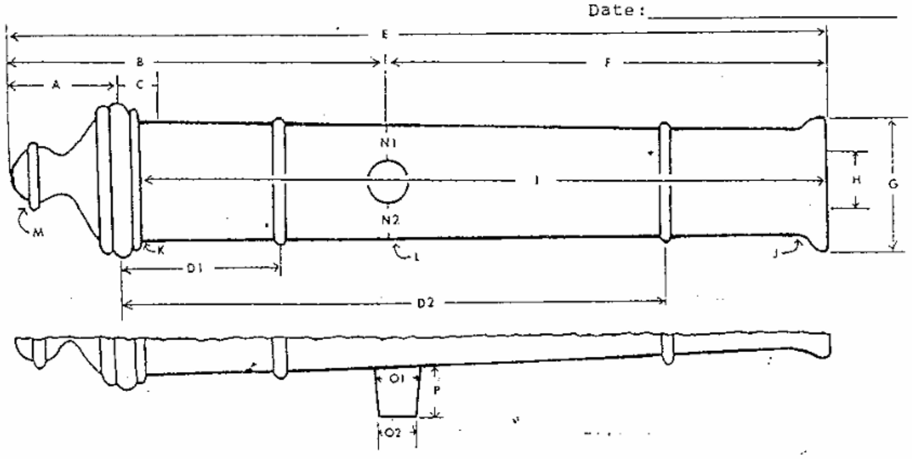

Site location and reference: ______

____

Location of cannon on site: _______

____

Date cannon was located: ____________

Divers: ______________________

____

Recorder: ______________________

METRIC ATTRIBUTES

NOTE: Measurements requiring two readings for left and right sides should be taken viewing the cannon on the touchhole side (dorsal) from the cascabel down the tube.

A. Cascabel to breech reinforce ________

B. Cascabel to trunion ________

C. Reinforce to touchhole ________

D. Breech reinforce to each other reinforce band

	Distance	Thickness
1.	________	________
2.	________	________
3.	________	________
4.	________	________
5.	________	________
6.	________	________

write any additional reinforce measurements on back

E. Overall length ________

F. Trunion to muzzle length ________

G. Muzzle diameter ________

H. Bore diameter ________

I. Bore depth ________

J. Diameter [illegible]
muzzle flare ________

K. Diameter in front of breech reinforce ________

L. Diameter of tube at trunions ________

M. Diameter of cascabel ________

N. Vertical position of trunion on tube

1. trunion to dorsal ________
2. trunion to ventral ________

O. Diameter of trunion

1. at tube left________ right________
2. at ends left________ right________

P. Length of trunions left________ right________

Other: ______________________

____

NON-METRIC ATTRIBUTES

answer on reverse side

1. Depth to and description of bottom.
2. Type of sediment(s).
3. Lifting handles: description & necessary accompanying measurements.
4. Any other pertinent attributes: distinguishing marks, insignias, dates, color, condition, type of metal, etc.

UWARS rev. 3/8/78

Appendix B: Dimensioned CAD Drawings

UN–01 Dimensioned CAD Drawings

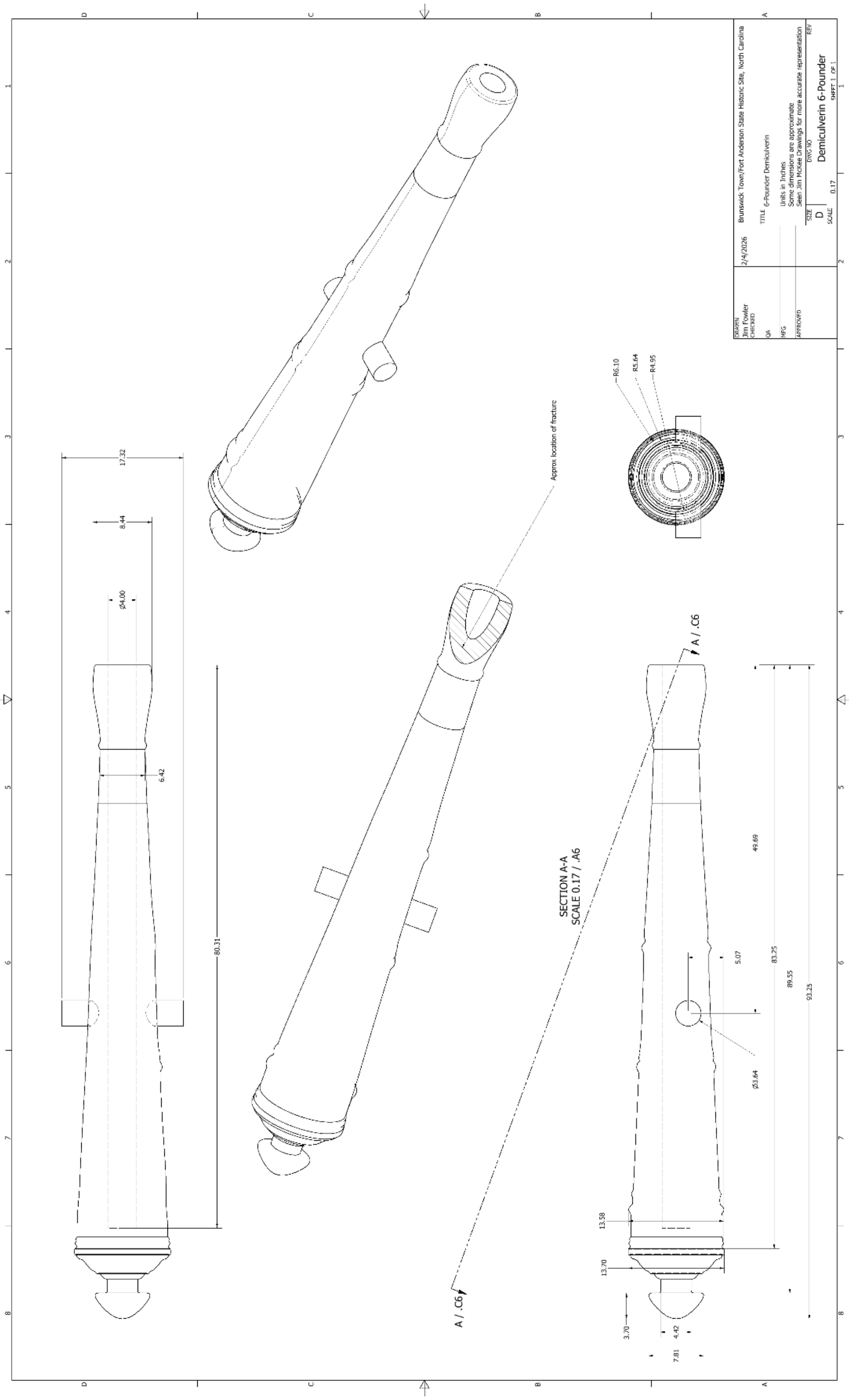

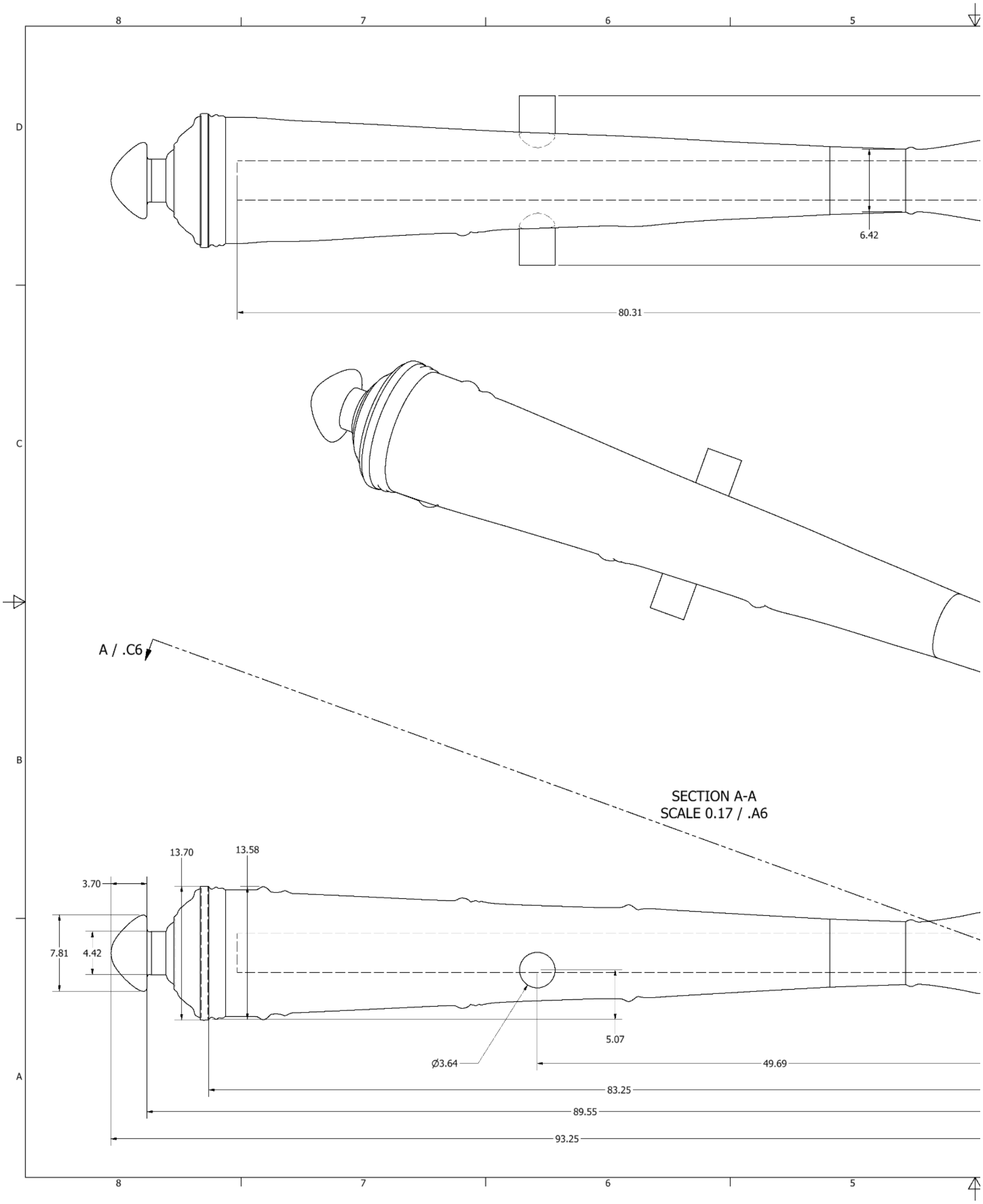
8
7
6
5
D
C
B
A
6.42
80.31
A / .C6
SECTION A-A
SCALE 0.17 / .A6
13.70
13.58
3.70
7.81
4.42
5.07
Ø3.64
49.69
83.25
89.55
93.25

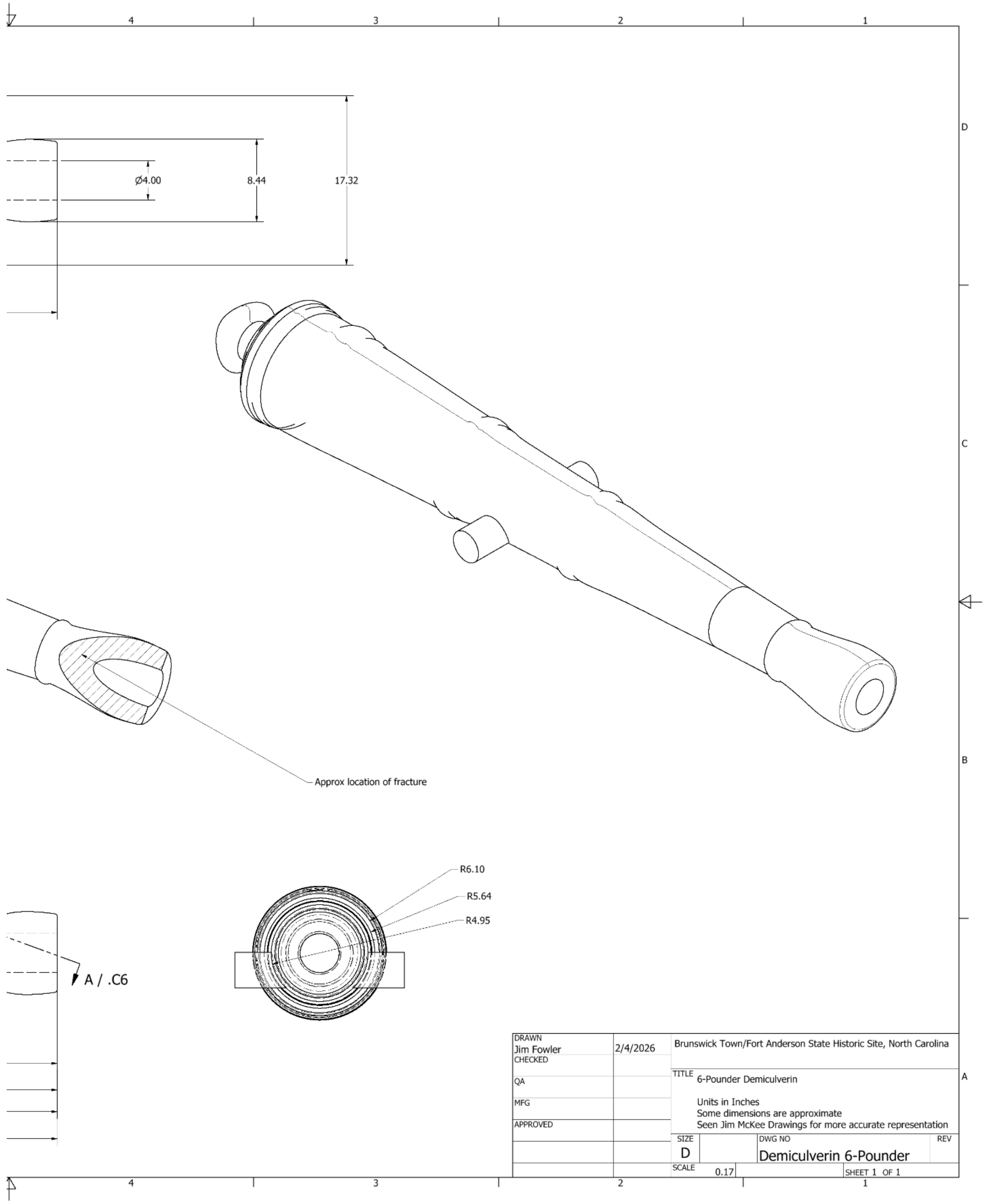

Ø4.00
8.44
17.32
Approx location of fracture
R6.10
R5.64
R4.95
A / .C6
DRAWN
Jim Fowler
2/4/2026
CHECKED
QA
MFG
APPROVED
Brunswick Town/Fort Anderson State Historic Site, North Carolina
TITLE 6-Pounder Demiculverin
Units in Inches
Some dimensions are approximate
Seen Jim McKee Drawings for more accurate representation
SIZE D
DWG NO Demiculverin 6-Pounder
REV
SCALE 0.17
SHEET 1 OF 1

BR–01 Dimensioned CAD Drawings

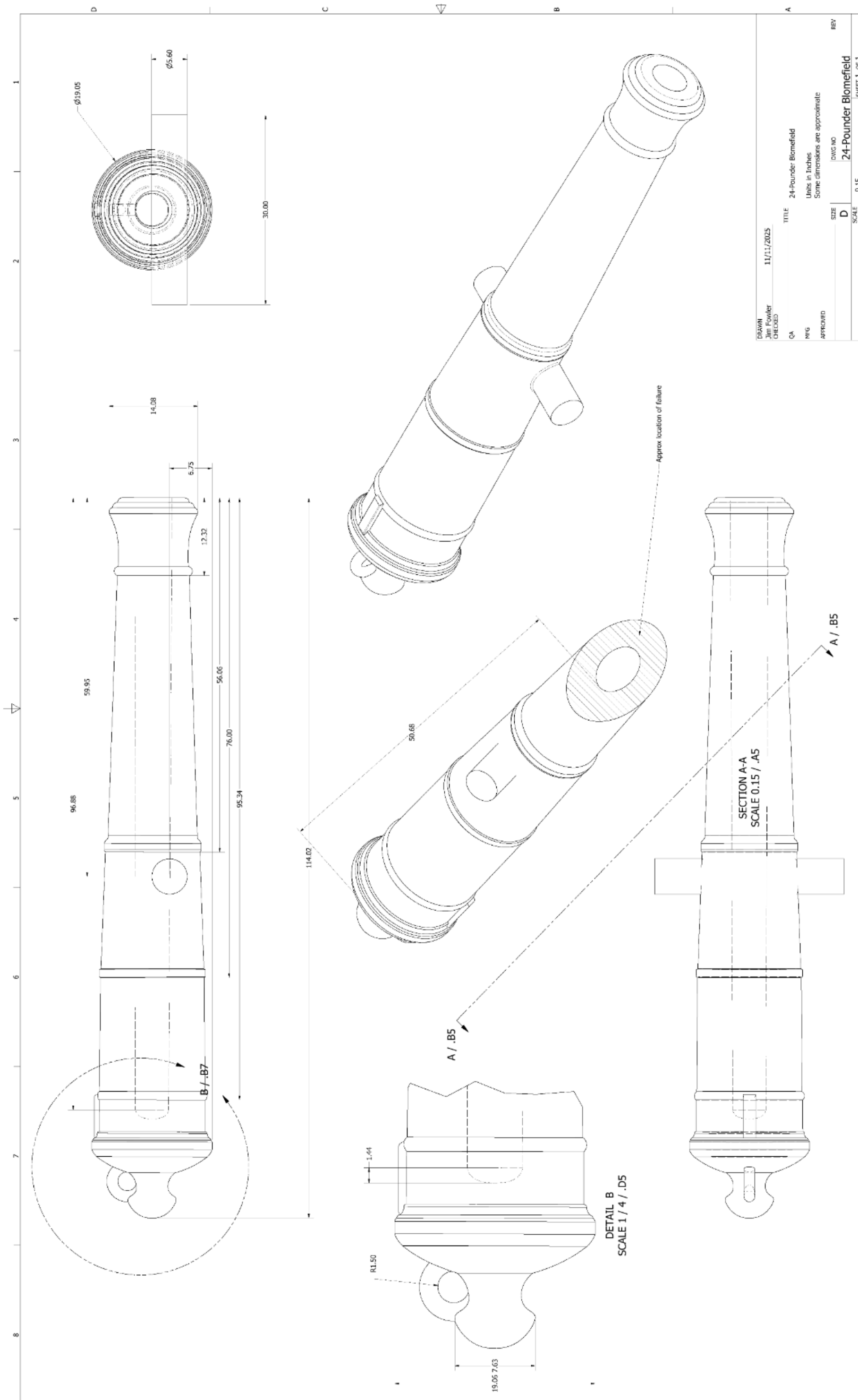

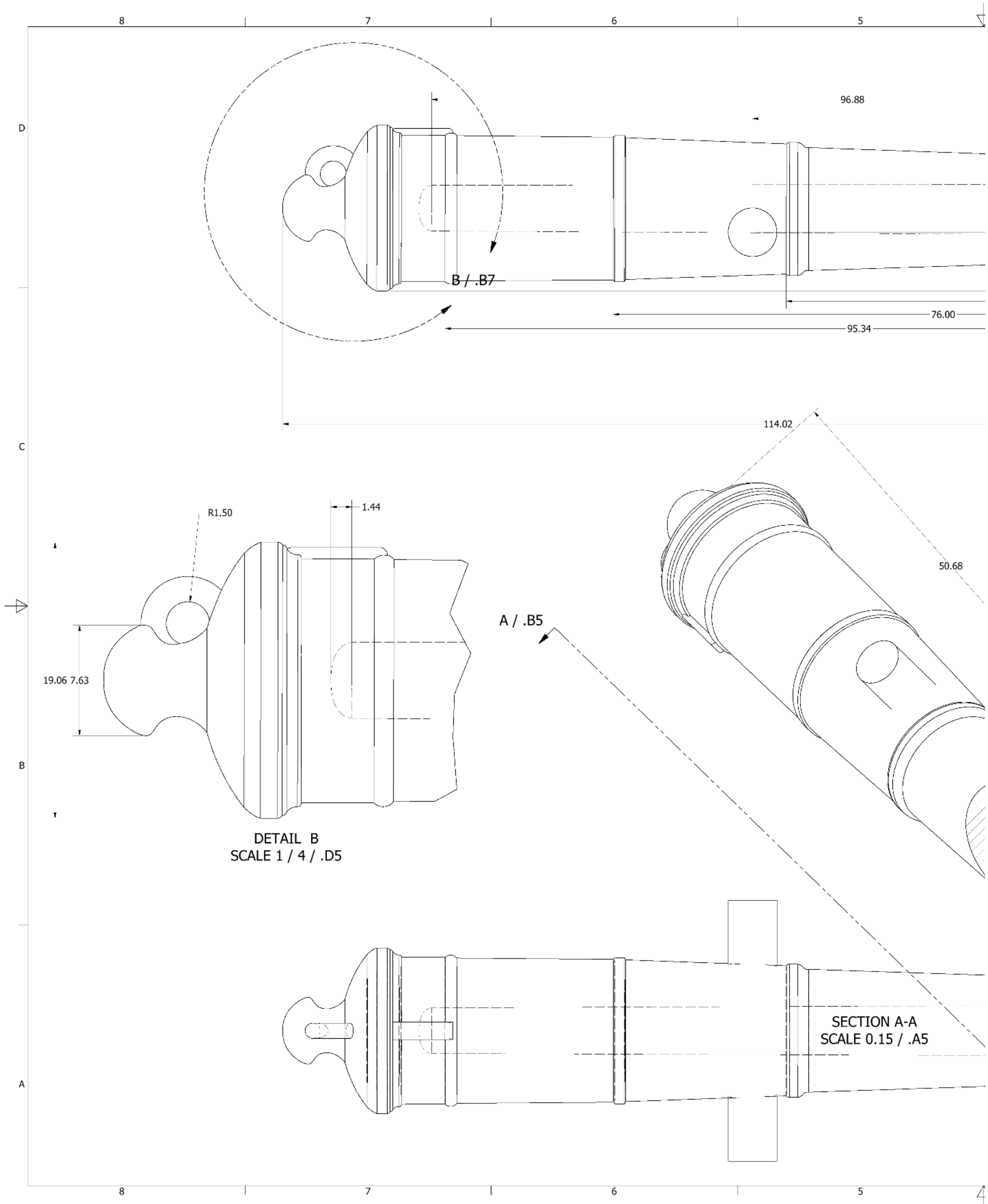
8
7
6
5
D
C
B
A
96.88
B / .B7
76.00
95.34
114.02
50.68
R1.50
1.44
19.06 7.63
A / .B5
DETAIL B
SCALE 1 / 4 / .D5
SECTION A-A
SCALE 0.15 / .A5

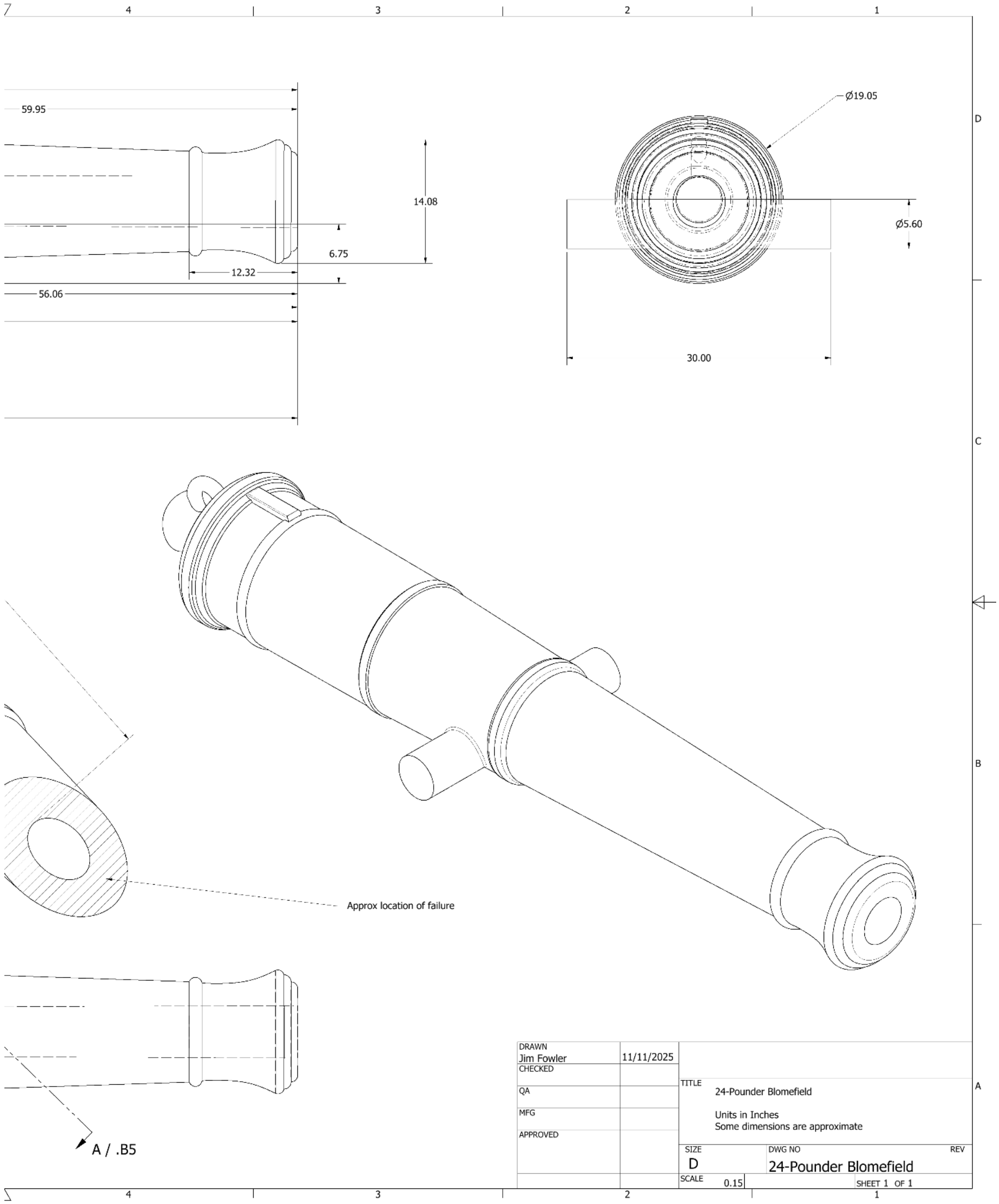

4
3
2
1
D
C
B
A
59.95
14.08
6.75
12.32
56.06
Ø19.05
Ø5.60
30.00
Approx location of failure
A / .B5
DRAWN
Jim Fowler
11/11/2025
CHECKED
QA
MFG
APPROVED
TITLE
24-Pounder Blomefield
Units in Inches
Some dimensions are approximate
SIZE
D
DWG NO
24-Pounder Blomefield
REV
SCALE
0.15
SHEET 1 OF 1

BR–02 Dimensioned CAD Drawings

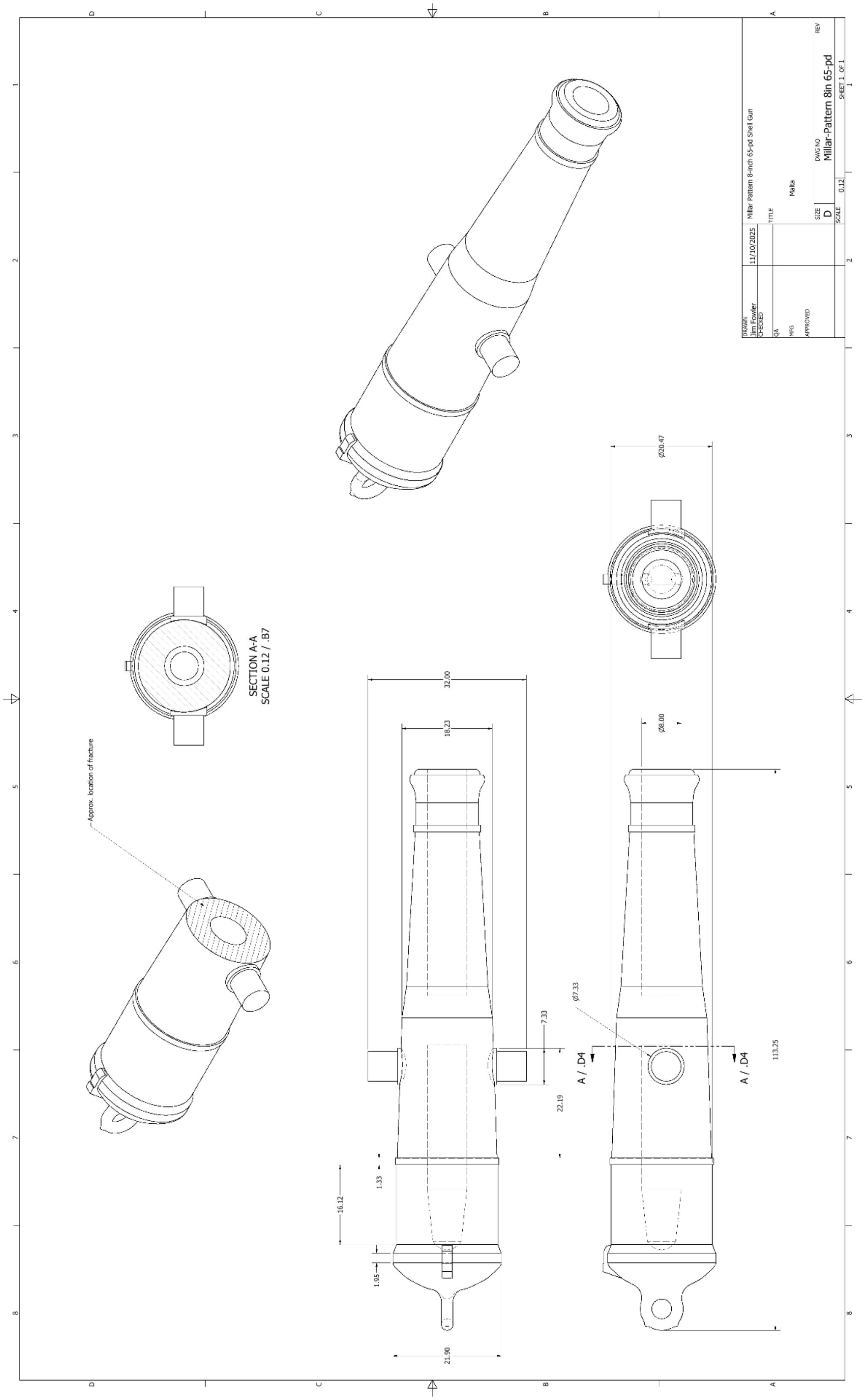

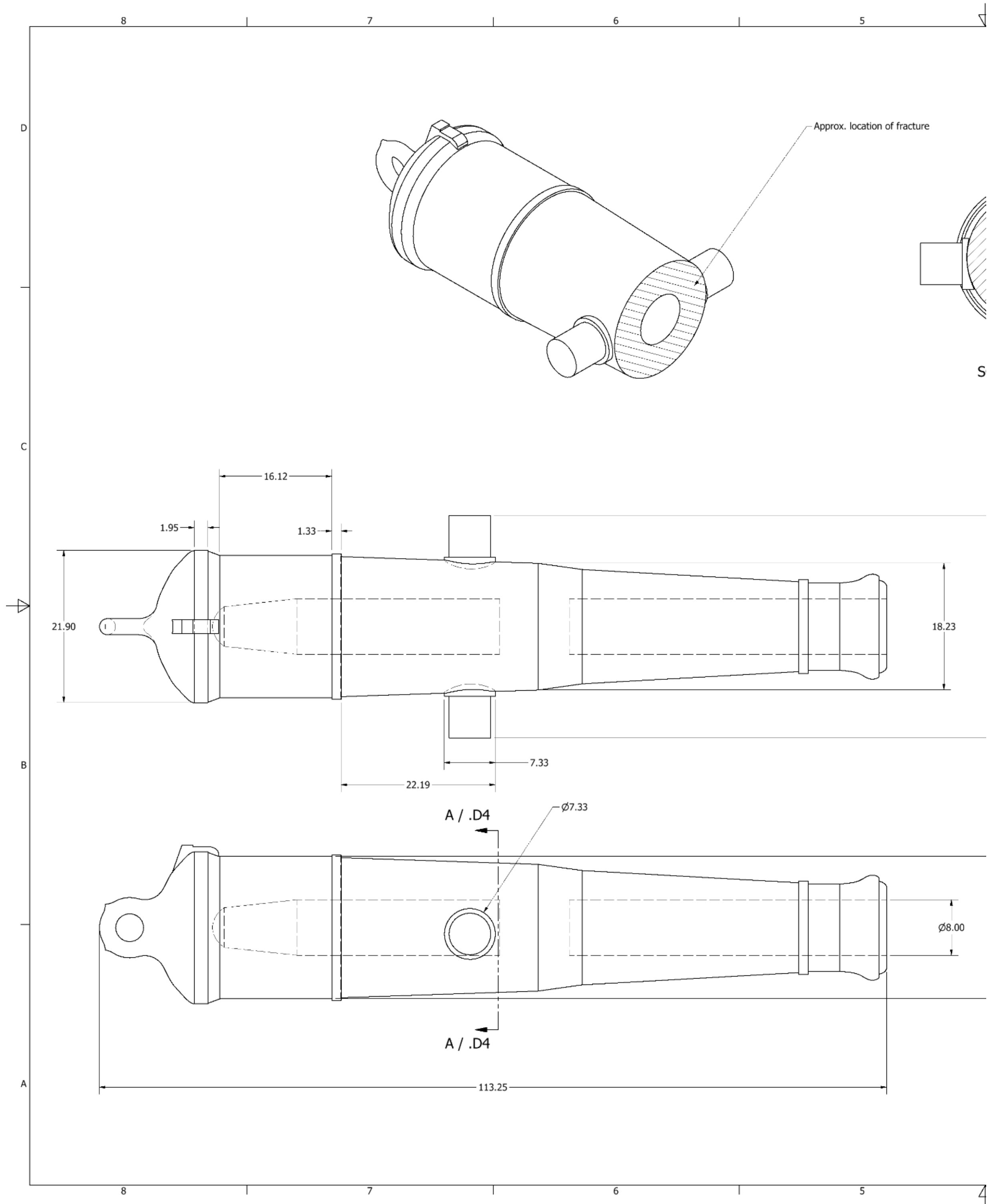
8
7
6
5
D
C
B
A
Approx. location of fracture
16.12
1.95
1.33
21.90
18.23
7.33
22.19
A / .D4
Ø7.33
Ø8.00
A / .D4
113.25

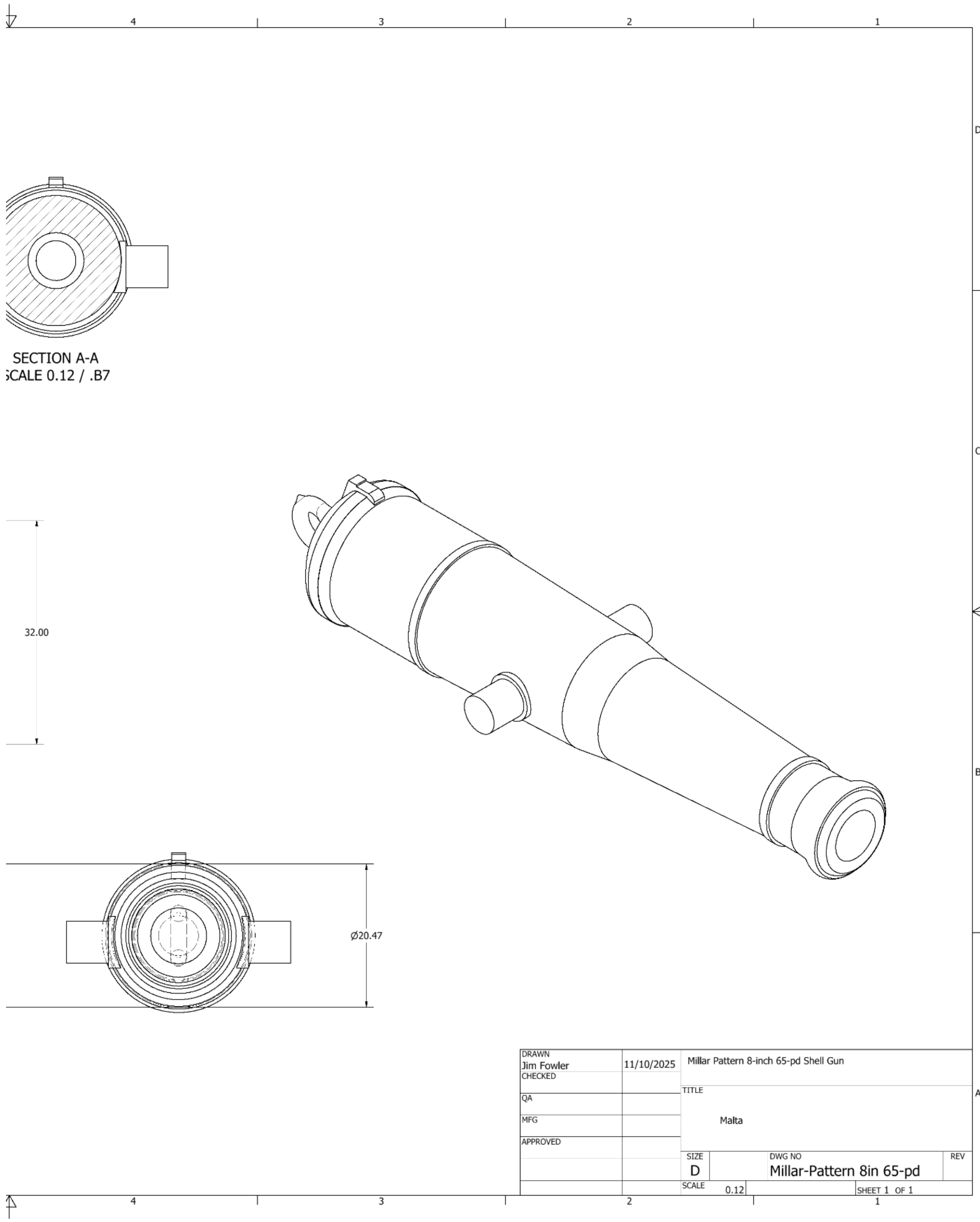
SECTION A-A
32.00
Ø20.47
DRAWN
Jim Fowler
11/10/2025
Millar Pattern 8-inch 65-pd Shell Gun
CHECKED
TITLE
QA
MFG
Malta
APPROVED
SIZE
D
DWG NO
Millar-Pattern 8in 65-pd
REV
SCALE
0.12
SHEET 1 OF 1

SW–01 Dimensioned CAD Drawings

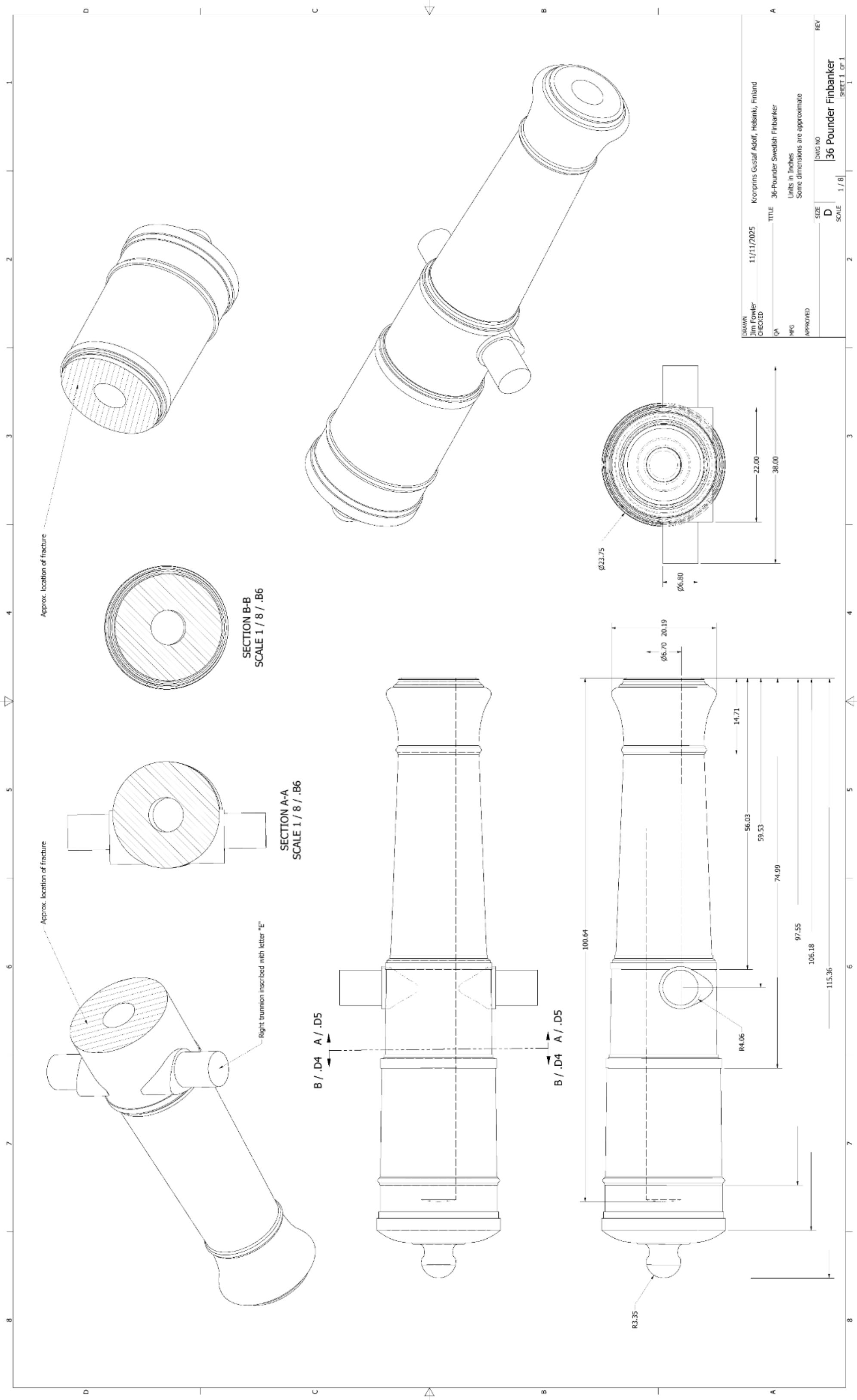

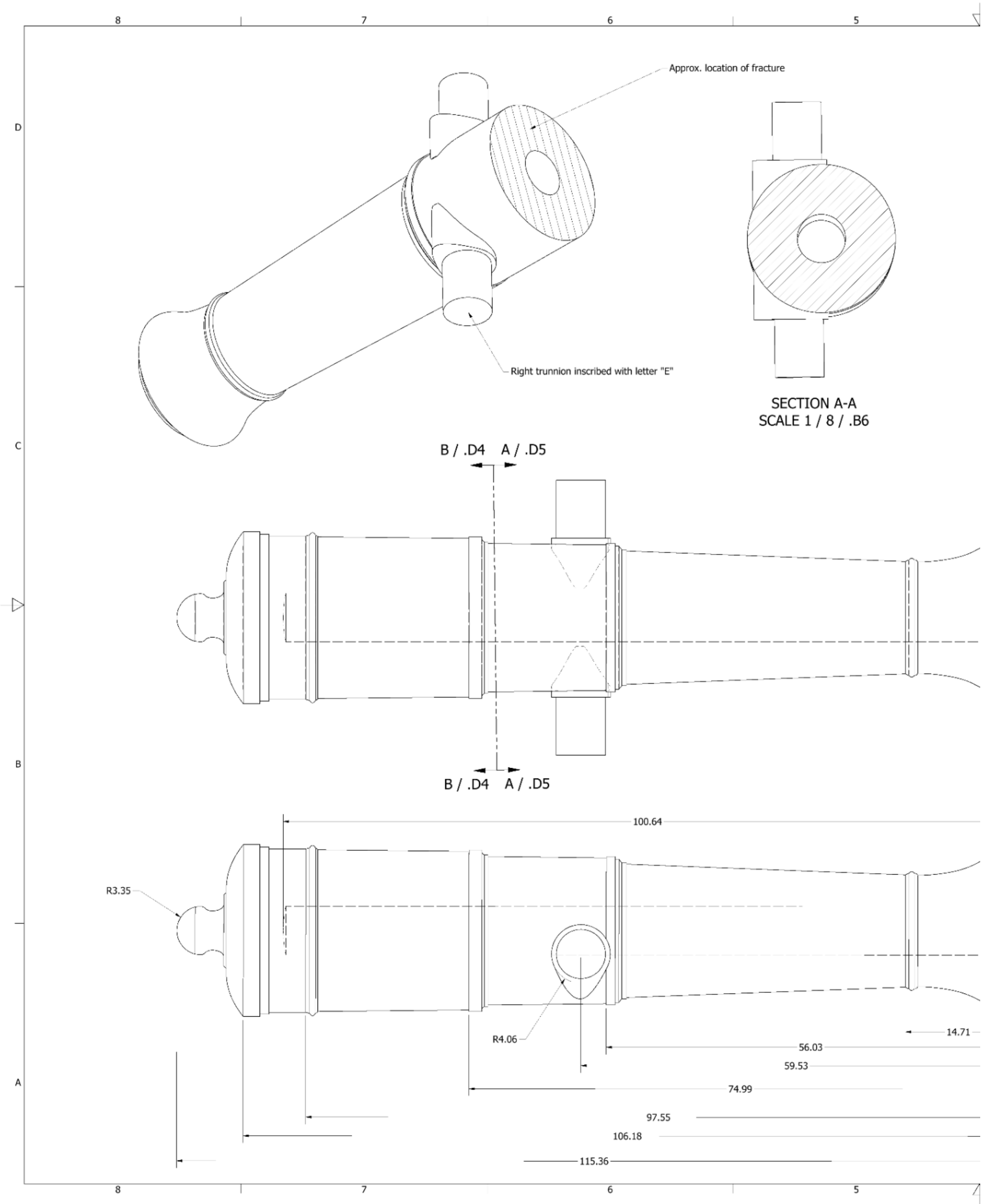
Approx. location of fracture
Right trunnion inscribed with letter "E"
SECTION A-A
SCALE 1 / 8 / .B6
B / .D4
A / .D5
100.64
R3.35
R4.06
14.71
56.03
59.53
74.99
97.55
106.18
115.36

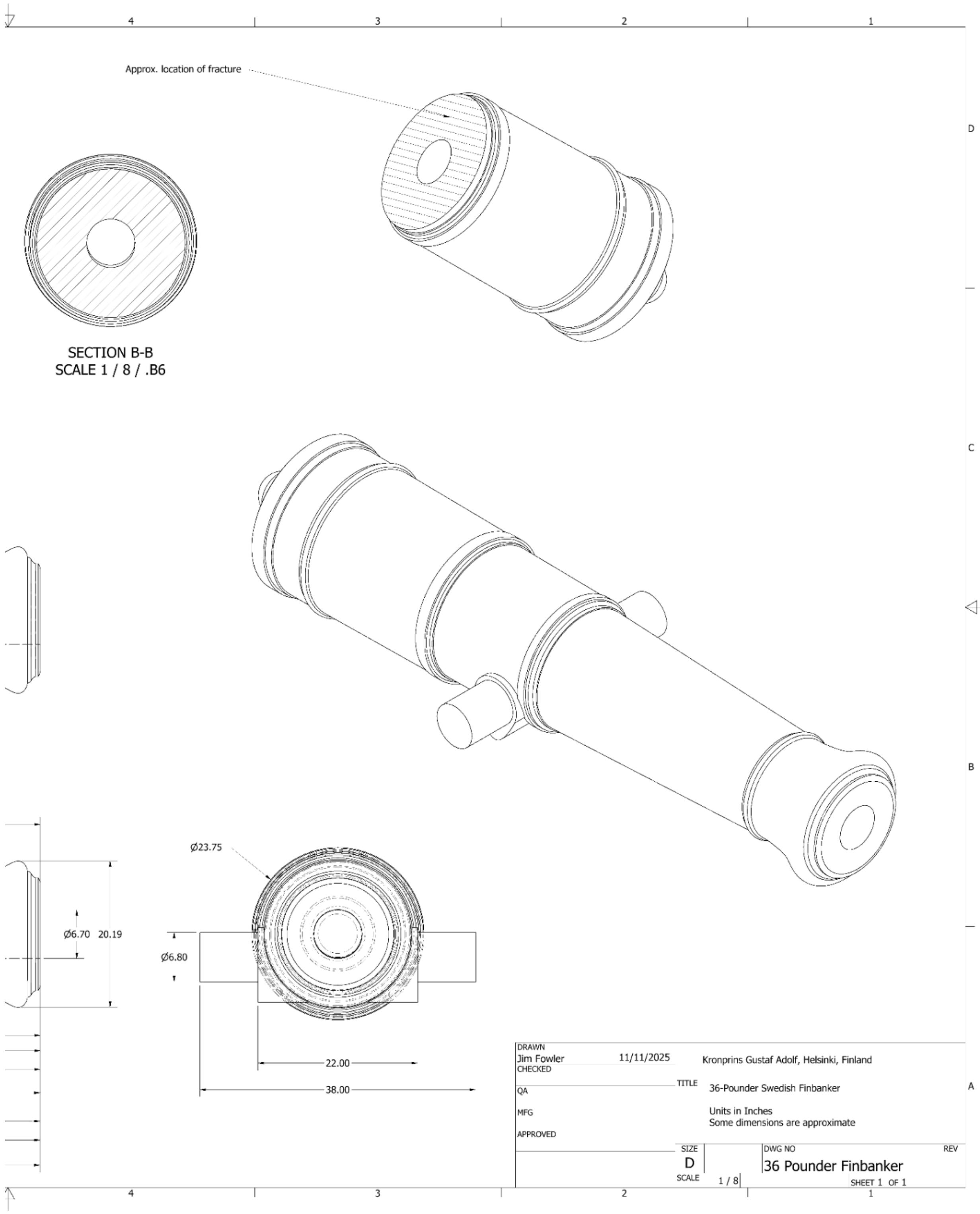

Approx. location of fracture
SECTION B-B
SCALE 1 / 8 / .B6
Ø23.75
Ø6.70
20.19
Ø6.80
22.00
38.00
DRAWN
Jim Fowler
11/11/2025
Kronprins Gustaf Adolf, Helsinki, Finland
CHECKED
TITLE
36-Pounder Swedish Finbanker
QA
MFG
Units in Inches
Some dimensions are approximate
APPROVED
SIZE
D
DWG NO
REV
36 Pounder Finbanker
SCALE
1 / 8
SHEET 1 OF 1

SW–23 Dimensioned CAD Drawings

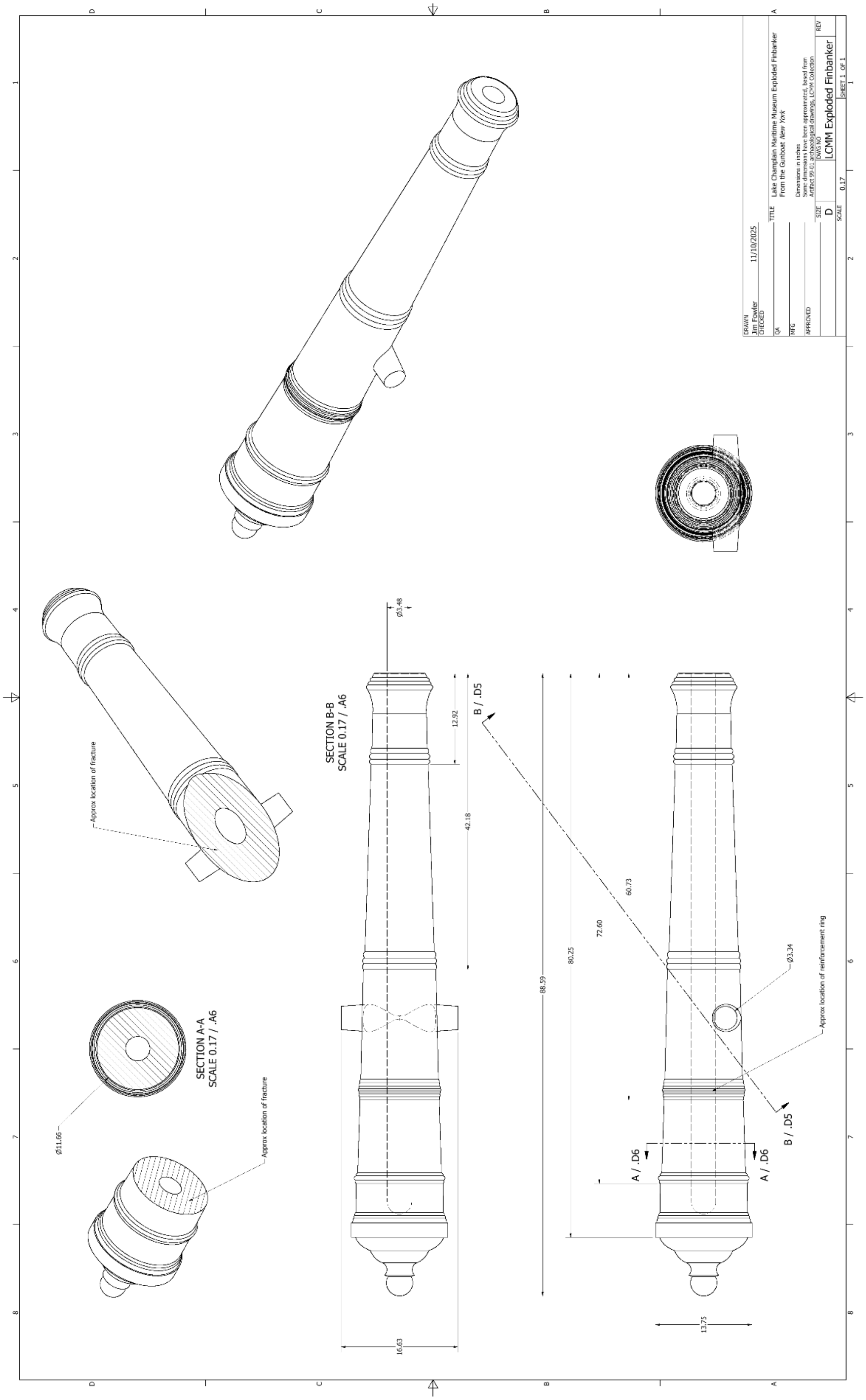

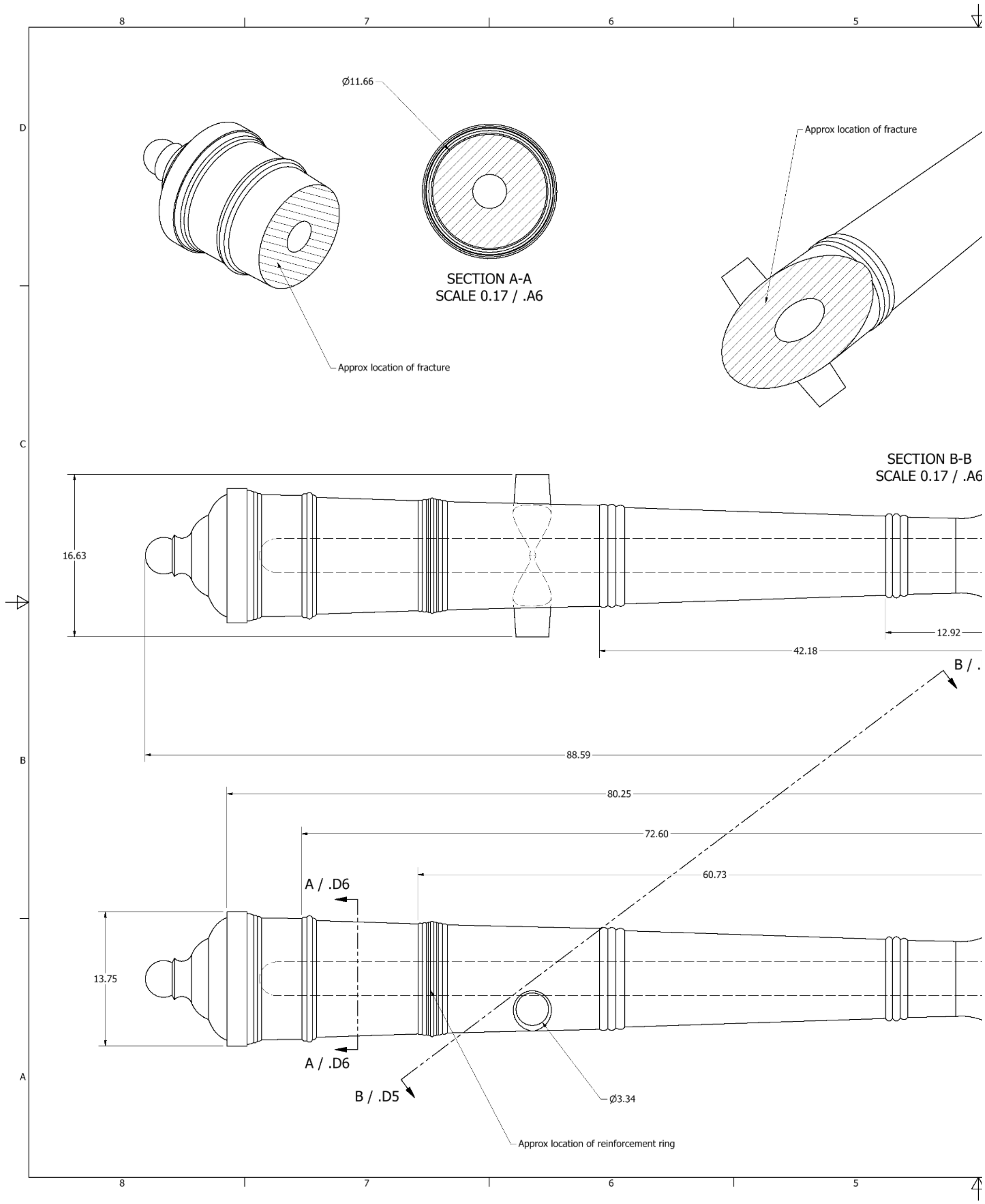
Ø11.66
SECTION A-A
SCALE 0.17 / .A6
Approx location of fracture
Approx location of fracture
SECTION B-B
SCALE 0.17 / .A6
16.63
12.92
42.18
B / .
88.59
80.25
72.60
60.73
A / .D6
13.75
A / .D6
B / .D5
Ø3.34
Approx location of reinforcement ring

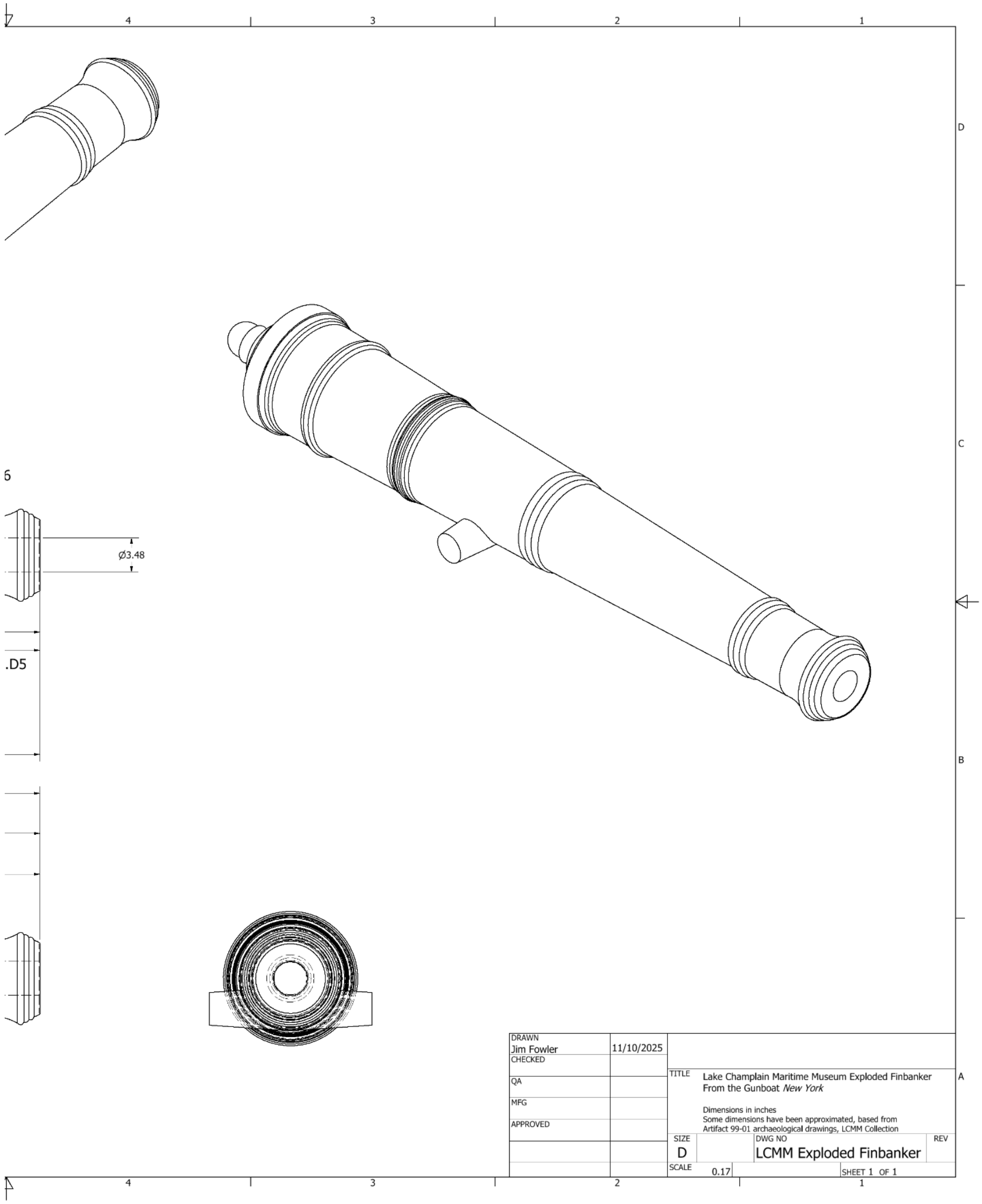
4
3
2
1
D
C
B
A
6
Ø3.48
.D5
DRAWN
Jim Fowler
11/10/2025
CHECKED
QA
MFG
APPROVED
TITLE
Lake Champlain Maritime Museum Exploded Finbanker
From the Gunboat *New York*
Dimensions in inches
Some dimensions have been approximated, based from
Artifact 99-01 archaeological drawings, LCMM Collection
SIZE
D
DWG NO
LCMM Exploded Finbanker
REV
SCALE
0.17
SHEET 1 OF 1

8–Pounder Finbanker Dimensioned CAD Drawings

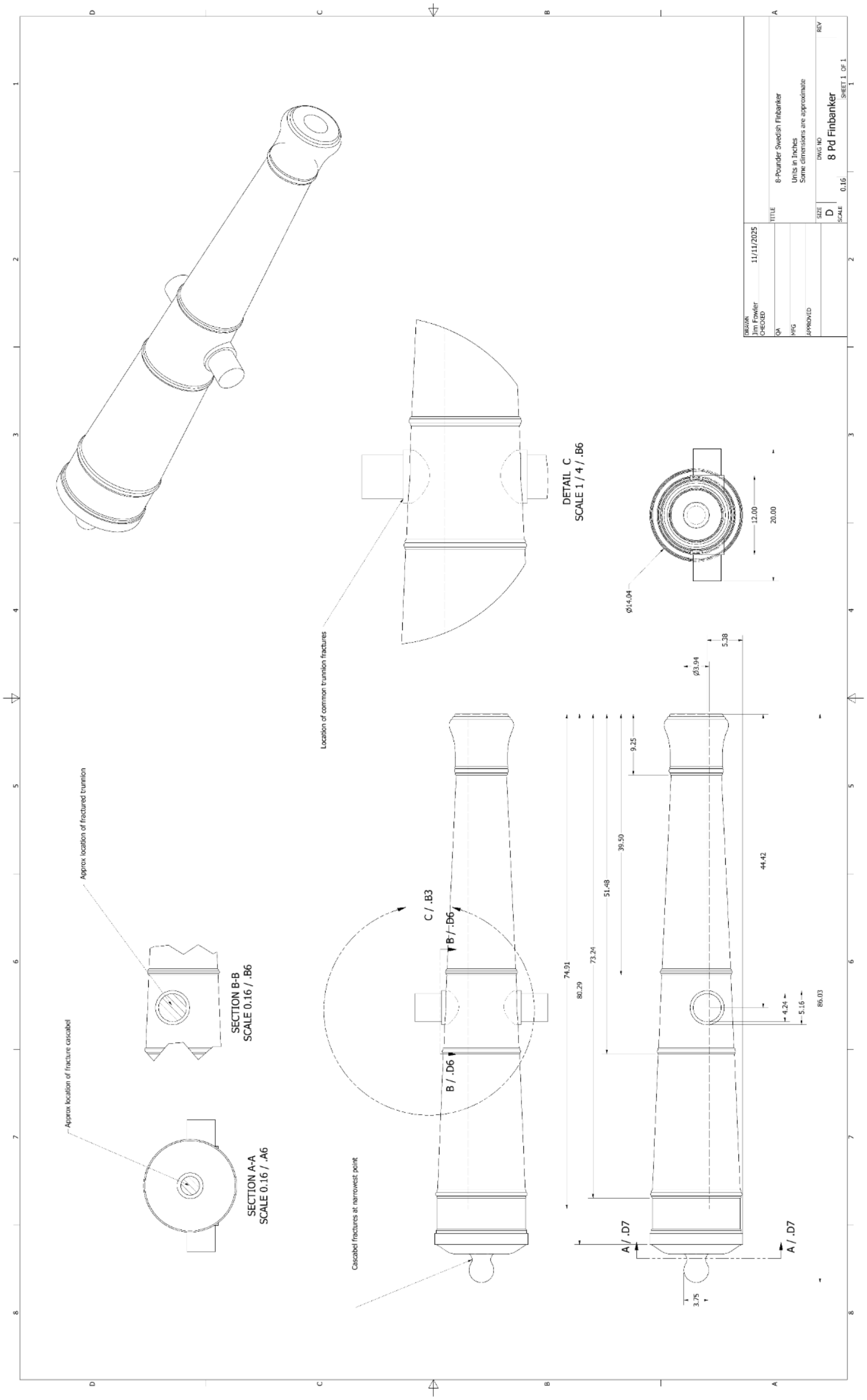

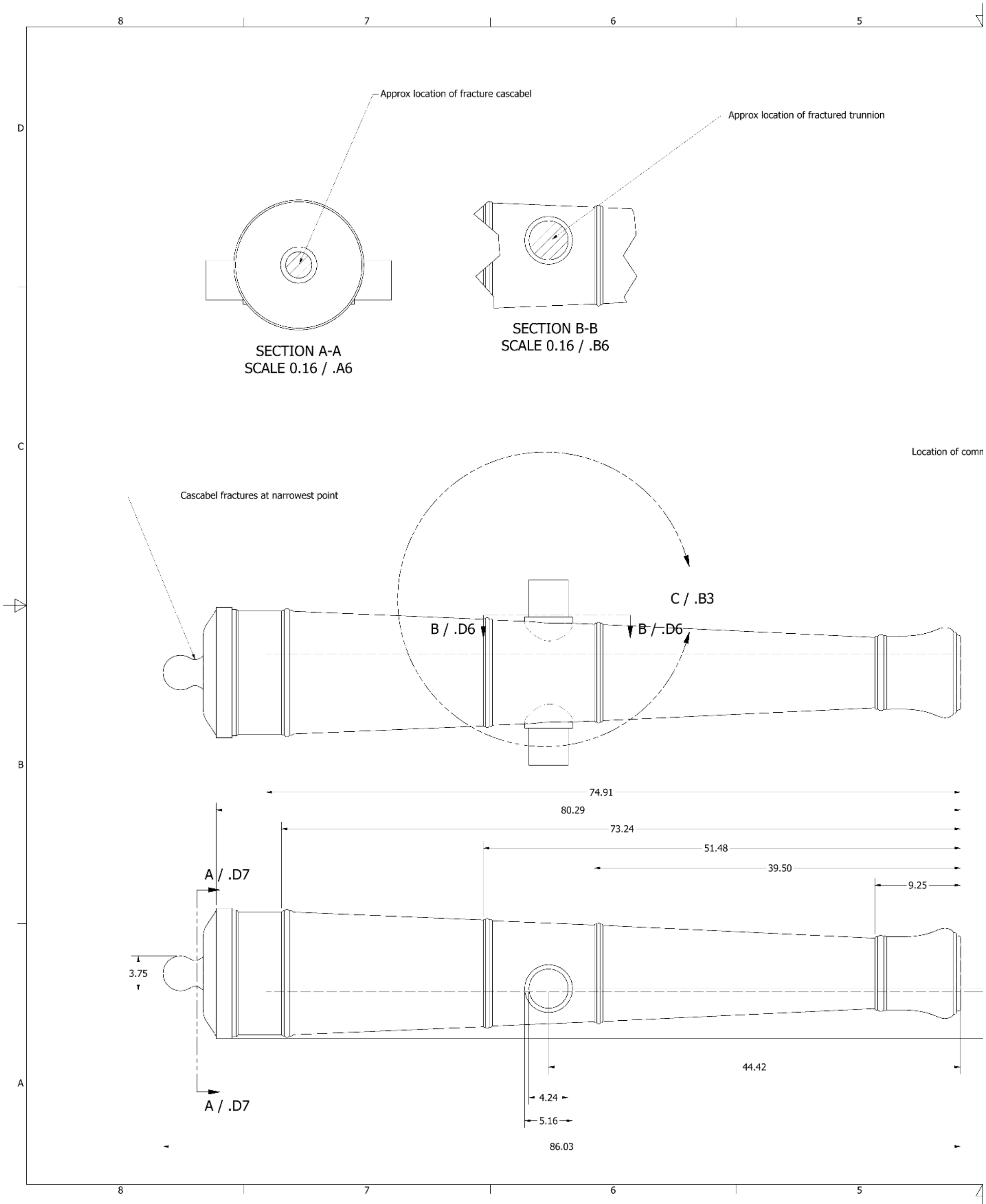
Approx location of fracture cascabel
Approx location of fractured trunnion
SECTION A-A
SCALE 0.16 / .A6
SECTION B-B
SCALE 0.16 / .B6
Location of comn
Cascabel fractures at narrowest point
C / .B3
B / .D6
B / .D6
74.91
80.29
73.24
51.48
39.50
9.25
A / .D7
3.75
44.42
A / .D7
4.24
5.16
86.03

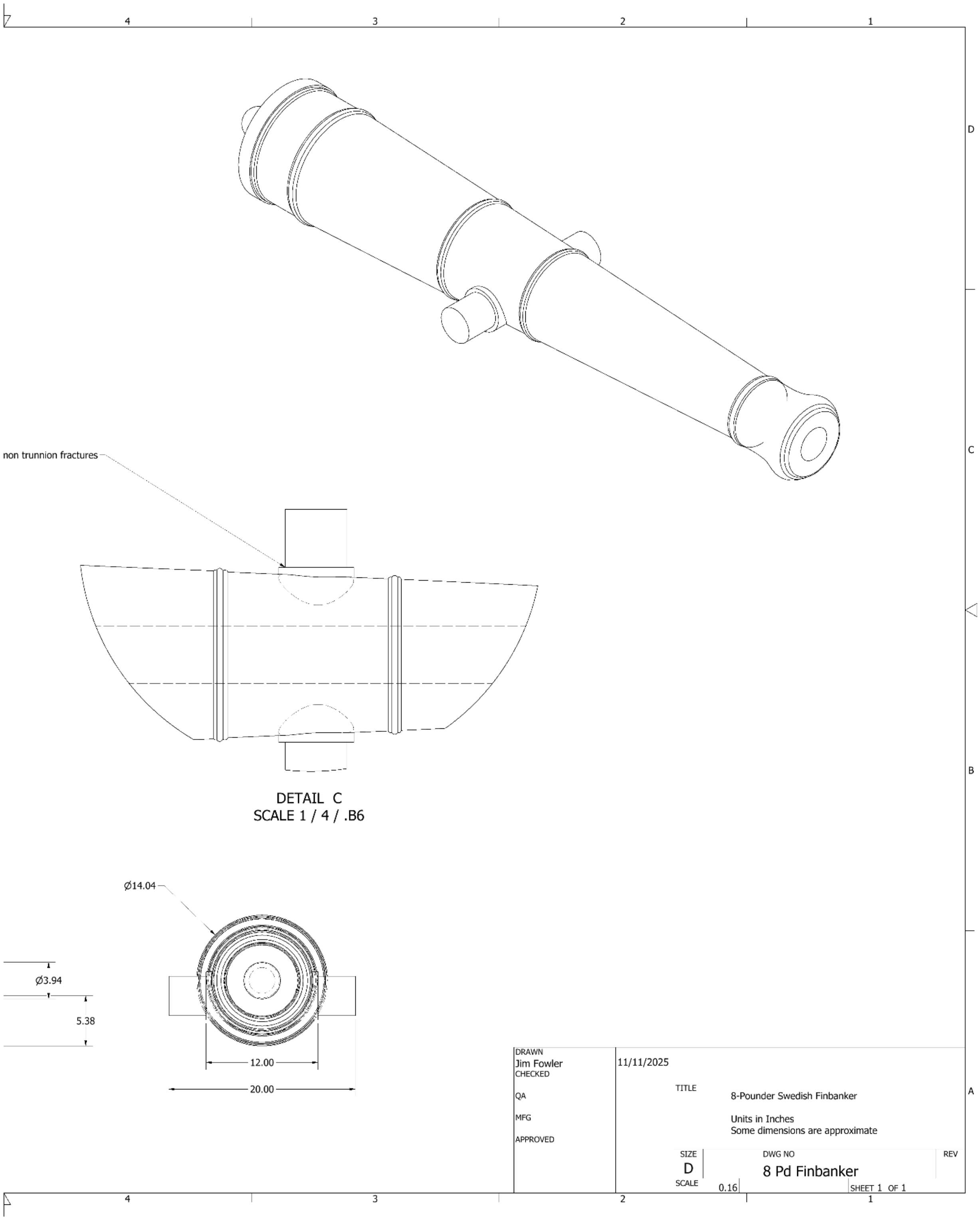
non trunnion fractures
DETAIL C
SCALE 1 / 4 / .B6
Ø14.04
Ø3.94
5.38
12.00
20.00
DRAWN
Jim Fowler
CHECKED
QA
MFG
APPROVED
11/11/2025
TITLE
8-Pounder Swedish Finbanker
Units in Inches
Some dimensions are approximate
SIZE
D
SCALE
0.16
DWG NO
8 Pd Finbanker
REV
SHEET 1 OF 1

Appendix C: Cannon pressure calculations worksheets

Compiled here are the excel worksheets used to calculate interior bore pressure for each analyzed cannon for projectiles at various distances from the breech wall in increments of 10 cm.

UN–01 Pressure Calculations Worksheet

D8 =((H8)*(J8)*(I8)*(G8-1)/(F8))*0.000145038

	A	B	C	D	E	F	G	H	I	J	K
5			Mean:	12100.156							
6		Radius		Pressure	Length of spac	V (m^3)	y	f	q	Mp (Vo*p)	
7		5.8		0	0						
8		5.8		100100.043	10	0.001056801	1.2	0.43	3000000	2.827	
9		5.8		66733.3623	15	0.001585201	1.2	0.43	3000000	2.827	
10		5.8		50050.0217	20	0.002113601	1.2	0.43	3000000	2.827	
11		5.8		40040.0174	25	0.002642002	1.2	0.43	3000000	2.827	
12		5.8		33366.6811	30	0.003170402	1.2	0.43	3000000	2.827	
13		5.8		28600.0124	35	0.003698802	1.2	0.43	3000000	2.827	
14		5.8		25025.0108	40	0.004227202	1.2	0.43	3000000	2.827	
15		5.8		22244.4541	45	0.004755603	1.2	0.43	3000000	2.827	
16		5.8		20020.0087	50	0.005284003	1.2	0.43	3000000	2.827	
17		5.8		18200.0079	55	0.005812403	1.2	0.43	3000000	2.827	
18		5.8		16683.3406	60	0.006340804	1.2	0.43	3000000	2.827	
19		5.8		15400.0067	65	0.006869204	1.2	0.43	3000000	2.827	
20		5.8		14300.0062	70	0.007397604	1.2	0.43	3000000	2.827	
21		5.8		13346.6725	75	0.007926005	1.2	0.43	3000000	2.827	
22		5.8		12512.5054	80	0.008454405	1.2	0.43	3000000	2.827	
23		5.8		11776.4757	85	0.008982805	1.2	0.43	3000000	2.827	
24		5.8		11122.227	90	0.009511205	1.2	0.43	3000000	2.827	
25		5.8		10536.8467	95	0.010039606	1.2	0.43	3000000	2.827	
26		5.8		10010.0043	100	0.010568006	1.2	0.43	3000000	2.827	
27		5.8		9533.33747	105	0.011096406	1.2	0.43	3000000	2.827	
28		5.8		9100.00394	110	0.011624807	1.2	0.43	3000000	2.827	
29		5.8		8704.3516	115	0.012153207	1.2	0.43	3000000	2.827	
30		5.8		8341.67028	120	0.012681607	1.2	0.43	3000000	2.827	
31		5.8		8008.00347	125	0.013210008	1.2	0.43	3000000	2.827	
32		5.8		7700.00334	130	0.013738408	1.2	0.43	3000000	2.827	
33		5.8		7414.81803	135	0.014266808	1.2	0.43	3000000	2.827	
34		5.8		7150.0031	140	0.014795208	1.2	0.43	3000000	2.827	
35		5.8		6903.45127	145	0.015323609	1.2	0.43	3000000	2.827	
36		5.8		6673.33623	150	0.015852009	1.2	0.43	3000000	2.827	
37		5.8		6458.06732	155	0.016380409	1.2	0.43	3000000	2.827	
38		5.8		6256.25271	160	0.01690881	1.2	0.43	3000000	2.827	
39		5.8		6066.6693	165	0.01743721	1.2	0.43	3000000	2.827	
40		5.8		5888.23785	170	0.01796561	1.2	0.43	3000000	2.827	
41		5.8		5720.00248	175	0.018494011	1.2	0.43	3000000	2.827	
42		5.8		5561.11352	180	0.019022411	1.2	0.43	3000000	2.827	
43		5.8		5410.81316	185	0.019550811	1.2	0.43	3000000	2.827	
44		5.8		5268.42334	190	0.020079211	1.2	0.43	3000000	2.827	
45		5.8		5133.33556	195	0.020607612	1.2	0.43	3000000	2.827	

BR–01 Pressure Calculations Worksheet

D8 =((H8)*(J8)*(I8)*(G8-1)/(F8))*0.000145038

	A	B	C	D	E	F	G	H	I	J	K
3											
4				15526.53643							
5						Volume behind ball				Starting mass of gunpowder in kg	Vi in cm^3
6		Radius		Pressure	Length of space	V (m^3)	y	f	q	Mp (Vi*p)	4029.150459
7		7.55		0	0						
8		7.55		143130.8	10	0.001790734	1.2	0.43	3000000	6.849555781	
9		7.55		95420.5002	15	0.0026861	1.2	0.43	3000000	6.849555781	
10		7.55		71565.37515	20	0.003581467	1.2	0.43	3000000	6.849555781	
11		7.55		57252.30012	25	0.004476834	1.2	0.43	3000000	6.849555781	
12		7.55		47710.2501	30	0.005372201	1.2	0.43	3000000	6.849555781	
13		7.55		40894.50009	35	0.006267567	1.2	0.43	3000000	6.849555781	
14		7.55		35782.68758	40	0.007162934	1.2	0.43	3000000	6.849555781	
15		7.55		31806.8334	45	0.008058301	1.2	0.43	3000000	6.849555781	
16		7.55		28626.15006	50	0.008953668	1.2	0.43	3000000	6.849555781	
17		7.55		26023.77278	55	0.009849034	1.2	0.43	3000000	6.849555781	
18		7.55		23855.12505	60	0.010744401	1.2	0.43	3000000	6.849555781	
19		7.55		22020.11543	65	0.011639768	1.2	0.43	3000000	6.849555781	
20		7.55		20447.25004	70	0.012535135	1.2	0.43	3000000	6.849555781	
21		7.55		19084.10004	75	0.013430502	1.2	0.43	3000000	6.849555781	
22		7.55		17891.34379	80	0.014325868	1.2	0.43	3000000	6.849555781	
23		7.55		16838.9118	85	0.015221235	1.2	0.43	3000000	6.849555781	
24		7.55		15903.4167	90	0.016116602	1.2	0.43	3000000	6.849555781	
25		7.55		15066.39477	95	0.017011969	1.2	0.43	3000000	6.849555781	
26		7.55		14313.07503	100	0.017907335	1.2	0.43	3000000	6.849555781	
27		7.55		13631.50003	105	0.018802702	1.2	0.43	3000000	6.849555781	
28		7.55		13011.88639	110	0.019698069	1.2	0.43	3000000	6.849555781	
29		7.55		12446.1522	115	0.020593436	1.2	0.43	3000000	6.849555781	
30		7.55		11927.56253	120	0.021488802	1.2	0.43	3000000	6.849555781	
31		7.55		11450.46002	125	0.022384169	1.2	0.43	3000000	6.849555781	
32		7.55		11010.05772	130	0.023279536	1.2	0.43	3000000	6.849555781	
33		7.55		10602.2778	135	0.024174903	1.2	0.43	3000000	6.849555781	
34		7.55		10223.62502	140	0.02507027	1.2	0.43	3000000	6.849555781	
35		7.55		9871.086228	145	0.025965636	1.2	0.43	3000000	6.849555781	
36		7.55		9542.05002	150	0.026861003	1.2	0.43	3000000	6.849555781	
37		7.55		9234.241955	155	0.02775637	1.2	0.43	3000000	6.849555781	
38		7.55		8945.671894	160	0.028651737	1.2	0.43	3000000	6.849555781	
39		7.55		8674.590927	165	0.029547103	1.2	0.43	3000000	6.849555781	
40		7.55		8419.4559	170	0.03044247	1.2	0.43	3000000	6.849555781	
41		7.55		8178.900017	175	0.031337837	1.2	0.43	3000000	6.849555781	
42		7.55		7951.70835	180	0.032233204	1.2	0.43	3000000	6.849555781	
43		7.55		7736.797314	185	0.03312857	1.2	0.43	3000000	6.849555781	
44		7.55		7533.197384	190	0.034023937	1.2	0.43	3000000	6.849555781	
45		7.55		7340.038477	195	0.034919304	1.2	0.43	3000000	6.849555781	
46		7.55		7156.537515	200	0.035814671	1.2	0.43	3000000	6.849555781	
47		7.55		6981.98782	205	0.036710038	1.2	0.43	3000000	6.849555781	
48		7.55		6815.750014	210	0.037605404	1.2	0.43	3000000	6.849555781	
49		7.55		6657.2442	215	0.038500771	1.2	0.43	3000000	6.849555781	
50		7.55		6505.943195	220	0.039396138	1.2	0.43	3000000	6.849555781	
51											

BR–02 Pressure Calculations Worksheet

D8 =(G8-1)*((H8)*(J8)*(I8)/(F8))*0.000145038

	B	C	D	E	F	G	H	I	J	K	M	N
4												
5		mean:	18453.0309		Volume behind ball				Starting mass of gunpowder g, divided by 1000 to ge	Vi in (m^3)		
6	diameter (m)		Pressure in J/kg, multiplied into PSI	Length of space (m)	V (m^3)	y	f	q in Pascals (j/kg)	Mp (Vi*p) or kg	0.00649	Location of the projectile (c	Pressure (converted to PSI)
7	0.2032		0	0							0	0.0
8	0.2032		170,108.52	0.1	0.00324	1.2	0.43	3000000	14.74175		10	170108.5
9	0.2032		113,405.68	0.15	0.00486	1.2	0.43	3000000	14.74175		15	113405.7
10	0.2032		85,054.26	0.2	0.00649	1.2	0.43	3000000	14.74175		20	85054.3
11	0.2032		68,043.41	0.25	0.00811	1.2	0.43	3000000	14.74175		25	68043.4
12	0.2032		56,702.84	0.3	0.00973	1.2	0.43	3000000	14.74175		30	56702.8
13	0.2032		48,602.43	0.35	0.01135	1.2	0.43	3000000	14.74175		35	48602.4
14	0.2032		42,527.13	0.4	0.01297	1.2	0.43	3000000	14.74175		40	42527.1
15	0.2032		37,801.89	0.45	0.01459	1.2	0.43	3000000	14.74175		45	37801.9
16	0.2032		34,021.70	0.5	0.01621	1.2	0.43	3000000	14.74175		50	34021.7
17	0.2032		30,928.82	0.55	0.01784	1.2	0.43	3000000	14.74175		55	30928.8
18	0.2032		28,351.42	0.6	0.01946	1.2	0.43	3000000	14.74175		60	28351.4
19	0.2032		26,170.54	0.65	0.02108	1.2	0.43	3000000	14.74175		65	26170.5
20	0.2032		24,301.22	0.7	0.0227	1.2	0.43	3000000	14.74175		70	24301.2
21	0.2032		22,681.14	0.75	0.02432	1.2	0.43	3000000	14.74175		75	22681.1
22	0.2032		21,263.57	0.8	0.02594	1.2	0.43	3000000	14.74175		80	21263.6
23	0.2032		20,012.77	0.85	0.02756	1.2	0.43	3000000	14.74175		85	20012.8
24	0.2032		18,900.95	0.9	0.02919	1.2	0.43	3000000	14.74175		90	18900.9
25	0.2032		17,906.16	0.95	0.03081	1.2	0.43	3000000	14.74175		95	17906.2
26	0.2032		17,010.85	1	0.03243	1.2	0.43	3000000	14.74175		100	17010.9
27	0.2032		16,200.81	1.05	0.03405	1.2	0.43	3000000	14.74175		105	16200.8
28	0.2032		15,464.41	1.1	0.03567	1.2	0.43	3000000	14.74175		110	15464.4
29	0.2032		14,792.05	1.15	0.03729	1.2	0.43	3000000	14.74175		115	14792.0
30	0.2032		14,175.71	1.2	0.03891	1.2	0.43	3000000	14.74175		120	14175.7
31	0.2032		13,608.68	1.25	0.04054	1.2	0.43	3000000	14.74175		125	13608.7
32	0.2032		13,085.27	1.3	0.04216	1.2	0.43	3000000	14.74175		130	13085.3
33	0.2032		12,600.63	1.35	0.04378	1.2	0.43	3000000	14.74175		135	12600.6
34	0.2032		12,150.61	1.4	0.0454	1.2	0.43	3000000	14.74175		140	12150.6
35	0.2032		11,731.62	1.45	0.04702	1.2	0.43	3000000	14.74175		145	11731.6
36	0.2032		11,340.57	1.5	0.04864	1.2	0.43	3000000	14.74175		150	11340.6
37	0.2032		10,974.74	1.55	0.05026	1.2	0.43	3000000	14.74175		155	10974.7
38	0.2032		10,631.78	1.6	0.05189	1.2	0.43	3000000	14.74175		160	10631.8
39	0.2032		10,309.61	1.65	0.05351	1.2	0.43	3000000	14.74175		165	10309.6
40	0.2032		10,006.38	1.7	0.05513	1.2	0.43	3000000	14.74175		170	10006.4
41	0.2032		9,720.49	1.75	0.05675	1.2	0.43	3000000	14.74175		175	9720.5
42	0.2032		9,450.47	1.8	0.05837	1.2	0.43	3000000	14.74175		180	9450.5
43	0.2032		9,195.06	1.85	0.05999	1.2	0.43	3000000	14.74175		185	9195.1
44	0.2032		8,953.08	1.9	0.06161	1.2	0.43	3000000	14.74175		190	8953.1
45	0.2032		8,723.51	1.95	0.06324	1.2	0.43	3000000	14.74175		195	8723.5
46	0.2032		8,505.43	2	0.06486	1.2	0.43	3000000	14.74175		200	8505.4
47	0.2032		8,297.98	2.05	0.06648	1.2	0.43	3000000	14.74175		205	8298.0
48	0.2032		8,100.41	2.1	0.0681	1.2	0.43	3000000	14.74175		210	8100.4
49	0.2032		7,912.02	2.15	0.06972	1.2	0.43	3000000	14.74175		215	7912.0
50	0.2032		7,732.21	2.2	0.07134	1.2	0.43	3000000	14.74175		220	7732.2
51	0.2032		7,560.38	2.25	0.07296	1.2	0.43	3000000	14.74175		225	7560.4
52	0.2032		7,396.02	2.3	0.07459	1.2	0.43	3000000	14.74175		230	7396.0
53	0.2032		7,238.66	2.35	0.07621	1.2	0.43	3000000	14.74175		235	7238.7
54	0.2032		7,087.86	2.4	0.07783	1.2	0.43	3000000	14.74175		240	7087.9
55												

SW–01 Pressure Calculations Worksheet

D8 =(G8-1)*((H8)*(J8)*(I8)/(F8))*0.000145038

	B	C	D	E	F	G	H	I	J	K	M	N
5		Mean:	14569.74772		Volume behind ball				Starting mass of gunpowder g, divided by 1000 to ge	Vi in (m^3)		
6	Diameter (m)		Pressure in J/kg, multiplied into PSI	Length of space (m)	V (m^3)	y	f	q in Pascals (j/kg)	Mp (Vi*p), or 1/2 ball weight in kg	0.00455	Location of the projectile (cm)	Pressure (converted to PSI)
7	0.17018		0	0							0	0
8	0.17018		134,310.63	0.1	0.00227	1.2	0.43	3000000	8.164		10	134310.6321
9	0.17018		89,540.42	0.15	0.00341	1.2	0.43	3000000	8.164		15	89540.42141
10	0.17018		67,155.32	0.2	0.00455	1.2	0.43	3000000	8.164		20	67155.31606
11	0.17018		53,724.25	0.25	0.00569	1.2	0.43	3000000	8.164		25	53724.25285
12	0.17018		44,770.21	0.3	0.00682	1.2	0.43	3000000	8.164		30	44770.21071
13	0.17018		38,374.47	0.35	0.00796	1.2	0.43	3000000	8.164		35	38374.46632
14	0.17018		33,577.66	0.4	0.0091	1.2	0.43	3000000	8.164		40	33577.65803
15	0.17018		29,846.81	0.45	0.01024	1.2	0.43	3000000	8.164		45	29846.80714
16	0.17018		26,862.13	0.5	0.01137	1.2	0.43	3000000	8.164		50	26862.12642
17	0.17018		24,420.11	0.55	0.01251	1.2	0.43	3000000	8.164		55	24420.11493
18	0.17018		22,385.11	0.6	0.01365	1.2	0.43	3000000	8.164		60	22385.10535
19	0.17018		20,663.17	0.65	0.01478	1.2	0.43	3000000	8.164		65	20663.17417
20	0.17018		19,187.23	0.7	0.01592	1.2	0.43	3000000	8.164		70	19187.23316
21	0.17018		17,908.08	0.75	0.01706	1.2	0.43	3000000	8.164		75	17908.08428
22	0.17018		16,788.83	0.8	0.0182	1.2	0.43	3000000	8.164		80	16788.82901
23	0.17018		15,801.25	0.85	0.01933	1.2	0.43	3000000	8.164		85	15801.25084
24	0.17018		14,923.40	0.9	0.02047	1.2	0.43	3000000	8.164		90	14923.40357
25	0.17018		14,137.96	0.95	0.02161	1.2	0.43	3000000	8.164		95	14137.96128
26	0.17018		13,431.06	1	0.02275	1.2	0.43	3000000	8.164		100	13431.06321
27	0.17018		12,791.49	1.05	0.02388	1.2	0.43	3000000	8.164		105	12791.48877
28	0.17018		12,210.06	1.1	0.02502	1.2	0.43	3000000	8.164		110	12210.05747
29	0.17018		11,679.19	1.15	0.02616	1.2	0.43	3000000	8.164		115	11679.1854
30	0.17018		11,192.55	1.2	0.02729	1.2	0.43	3000000	8.164		120	11192.55268
31	0.17018		10,744.85	1.25	0.02843	1.2	0.43	3000000	8.164		125	10744.85057
32	0.17018		10,331.59	1.3	0.02957	1.2	0.43	3000000	8.164		130	10331.58709
33	0.17018		9,948.94	1.35	0.03071	1.2	0.43	3000000	8.164		135	9948.935713
34	0.17018		9,593.62	1.4	0.03184	1.2	0.43	3000000	8.164		140	9593.61658
35	0.17018		9,262.80	1.45	0.03298	1.2	0.43	3000000	8.164		145	9262.802215
36	0.17018		8,954.04	1.5	0.03412	1.2	0.43	3000000	8.164		150	8954.042141
37	0.17018		8,665.20	1.55	0.03526	1.2	0.43	3000000	8.164		155	8665.202072
38	0.17018		8,394.41	1.6	0.03639	1.2	0.43	3000000	8.164		160	8394.414507
39	0.17018		8,140.04	1.65	0.03753	1.2	0.43	3000000	8.164		165	8140.03831
40	0.17018		7,900.63	1.7	0.03867	1.2	0.43	3000000	8.164		170	7900.625419
41	0.17018		7,674.89	1.75	0.0398	1.2	0.43	3000000	8.164		175	7674.893264
42	0.17018		7,461.70	1.8	0.04094	1.2	0.43	3000000	8.164		180	7461.701784
43	0.17018		7,260.03	1.85	0.04208	1.2	0.43	3000000	8.164		185	7260.034169
44	0.17018		7,068.98	1.9	0.04322	1.2	0.43	3000000	8.164		190	7068.980638
45	0.17018		6,887.72	1.95	0.04435	1.2	0.43	3000000	8.164		195	6887.724724
46	0.17018		6,715.53	2	0.04549	1.2	0.43	3000000	8.164		200	6715.531606
47	0.17018		6,551.74	2.05	0.04663	1.2	0.43	3000000	8.164		205	6551.738152
48	0.17018		6,395.74	2.1	0.04777	1.2	0.43	3000000	8.164		210	6395.744387
49	0.17018		6,247.01	2.15	0.0489	1.2	0.43	3000000	8.164		215	6247.006145
50	0.17018		6,105.03	2.2	0.05004	1.2	0.43	3000000	8.164		220	6105.028733
51	0.17018		5,969.36	2.25	0.05118	1.2	0.43	3000000	8.164		225	5969.361428
52	0.17018		5,839.59	2.3	0.05231	1.2	0.43	3000000	8.164		230	5839.592701
53	0.17018		5,715.35	2.35	0.05345	1.2	0.43	3000000	8.164		235	5715.346048
54	0.17018		5,596.28	2.4	0.05459	1.2	0.43	3000000	8.164		240	5596.276338
55	0.17018		5,482.07	2.45	0.05573	1.2	0.43	3000000	8.164		245	5482.066617
56	0.17018		5,372.43	2.5	0.05686	1.2	0.43	3000000	8.164		250	5372.425285

SW–23 Pressure Calculations Worksheet

D8 =(G8-1)*((H8)*(J8)*(I8)/(F8))*0.000145038

	A	B	C	D	E	F	G	H	I	J	K	L	M	N	O
4				10266.16849											
5						Volume behind ball				Starting mass of gunpowder g, divided by 1000 to g	Vi in (m^3)				
6		diameter (m)		Pressure in J/kg, multiplied into	Length of space (m	V (m^3)	y	f	q in Pascals (j/k	Mp (Vi*p) or kg	0.001227		Location of the projectile (c	Pressure (converted to PSI)	
7		0.088367		0	0								0	0.0	
8		0.088367		82,982.60	0.1	0.000613	1.2	0.43	3000000	1.36			10	82982.6	
9		0.088367		55,321.74	0.15	0.00092	1.2	0.43	3000000	1.36			15	55321.7	
10		0.088367		41,491.30	0.2	0.001227	1.2	0.43	3000000	1.36			20	41491.3	
11		0.088367		33,193.04	0.25	0.001533	1.2	0.43	3000000	1.36			25	33193.0	
12		0.088367		27,660.87	0.3	0.00184	1.2	0.43	3000000	1.36			30	27660.9	
13		0.088367		23,709.32	0.35	0.002146	1.2	0.43	3000000	1.36			35	23709.3	
14		0.088367		20,745.65	0.4	0.002453	1.2	0.43	3000000	1.36			40	20745.7	
15		0.088367		18,440.58	0.45	0.00276	1.2	0.43	3000000	1.36			45	18440.6	
16		0.088367		16,596.52	0.5	0.003066	1.2	0.43	3000000	1.36			50	16596.5	
17		0.088367		15,087.75	0.55	0.003373	1.2	0.43	3000000	1.36			55	15087.7	
18		0.088367		13,830.43	0.6	0.00368	1.2	0.43	3000000	1.36			60	13830.4	
19		0.088367		12,766.55	0.65	0.003986	1.2	0.43	3000000	1.36			65	12766.6	
20		0.088367		11,854.66	0.7	0.004293	1.2	0.43	3000000	1.36			70	11854.7	
21		0.088367		11,064.35	0.75	0.0046	1.2	0.43	3000000	1.36			75	11064.3	
22		0.088367		10,372.83	0.8	0.004906	1.2	0.43	3000000	1.36			80	10372.8	
23		0.088367		9,762.66	0.85	0.005213	1.2	0.43	3000000	1.36			85	9762.7	
24		0.088367		9,220.29	0.9	0.005519	1.2	0.43	3000000	1.36			90	9220.3	
25		0.088367		8,735.01	0.95	0.005826	1.2	0.43	3000000	1.36			95	8735.0	
26		0.088367		8,298.26	1	0.006133	1.2	0.43	3000000	1.36			100	8298.3	
27		0.088367		7,903.11	1.05	0.006439	1.2	0.43	3000000	1.36			105	7903.1	
28		0.088367		7,543.87	1.1	0.006746	1.2	0.43	3000000	1.36			110	7543.9	
29		0.088367		7,215.88	1.15	0.007053	1.2	0.43	3000000	1.36			115	7215.9	
30		0.088367		6,915.22	1.2	0.007359	1.2	0.43	3000000	1.36			120	6915.2	
31		0.088367		6,638.61	1.25	0.007666	1.2	0.43	3000000	1.36			125	6638.6	
32		0.088367		6,383.28	1.3	0.007973	1.2	0.43	3000000	1.36			130	6383.3	
33		0.088367		6,146.86	1.35	0.008279	1.2	0.43	3000000	1.36			135	6146.9	
34		0.088367		5,927.33	1.4	0.008586	1.2	0.43	3000000	1.36			140	5927.3	
35		0.088367		5,722.94	1.45	0.008892	1.2	0.43	3000000	1.36			145	5722.9	
36		0.088367		5,532.17	1.5	0.009199	1.2	0.43	3000000	1.36			150	5532.2	
37		0.088367		5,353.72	1.55	0.009506	1.2	0.43	3000000	1.36			155	5353.7	
38		0.088367		5,186.41	1.6	0.009812	1.2	0.43	3000000	1.36			160	5186.4	
39		0.088367		5,029.25	1.65	0.010119	1.2	0.43	3000000	1.36			165	5029.2	
40		0.088367		4,881.33	1.7	0.010426	1.2	0.43	3000000	1.36			170	4881.3	
41		0.088367		4,741.86	1.75	0.010732	1.2	0.43	3000000	1.36			175	4741.9	
42		0.088367		4,610.14	1.8	0.011039	1.2	0.43	3000000	1.36			180	4610.1	
43		0.088367		4,485.55	1.85	0.011346	1.2	0.43	3000000	1.36			185	4485.5	
44		0.088367		4,367.51	1.9	0.011652	1.2	0.43	3000000	1.36			190	4367.5	

Appendix D: List of Known Failed Cannons

Failed Cannon	Failure Mode	Location	Origin	Shot Weight	Publication
Cannon BR–01	Type II	Nelson's Dockyard, Antiqua	British	24	N/A
Cannon BR–02	Type II	St Elmo's Fortress, Malta	British	65	N/A
Cannon BR–03	Type I	St Elmo's Fortress, Malta	British	6 or 8	N/A
Cannon BR–04	Type I	St Elmo's Fortress, Malta	British	6 or 8	N/A
Cannon BR–05	Type I	St Elmo's Fortress, Malta	British	6 or 8	N/A
Cannon BR–06	Type I	St Elmo's Fortress, Malta	British	6	N/A
Cannon BR–07	Type I	St Elmo's Fortress, Malta	British	6	N/A
Cannon BR–08	Type I	Brunswick Town/Fort Anderson State Historic Site, NC	British	<1	N/A
Cannon BR–09	Type IV	Edenton, NC	British	3	N/A
Cannon BR–10	Type I	Dorset, UK (underwater)	British	32	Wessex Archaeology 2017b
Cannon SW–01	Type III	*Kronprins Gustav Adolf* , Helsinki, Finland (underwater)	Swedish	32	Maritime Archaeological Society of Finland 2023; Fowler 2025:10
Cannon SW–02	Type III	*Kronprins Gustav Adolf* , Helsinki, Finland (underwater)	Swedish	24	Maritime Archaeological Society of Finland 2023; Fowler 2025:10
Cannon SW–03	Type IV	Soumenlinna, Finland	Swedish	12	Paulaharju et al. 2025
Cannon SW–04	Type IV	Soumenlinna, Finland	Swedish	12	Paulaharju et al. 2025
Cannon SW–05	Type III	Soumenlinna, Finland	Swedish	18	Paulaharju et al. 2025

Cannon SW–06	Type IV	Soumenlinna, Finland	Swedish	12	Paulaharju et al. 2025
Cannon SW–07	Type I	St Elmo's Fortress, Malta	Swedish	6 or 8	N/A
Cannon SW–08	Type IV	Soumenlinna, Finland	Swedish	12	Paulaharju et al. 2025
Cannon SW–09	Type IV	Soumenlinna, Finland	Swedish	12	Paulaharju et al. 2025
Cannon SW–10	Type IV	Soumenlinna, Finland	Swedish	12	Paulaharju et al. 2025
Cannon SW–11	Type IV	Soumenlinna, Finland	Swedish	12	Paulaharju et al. 2025
Cannon SW–12	Type IV	Soumenlinna, Finland	Swedish	12	Paulaharju et al. 2025
Cannon SW–13	Type IV	Soumenlinna, Finland	Swedish	12	Paulaharju et al. 2025
Cannon SW–14	Type IV	Soumenlinna, Finland	Swedish	12	Paulaharju et al. 2025
Cannon SW–15	Type IV	Soumenlinna, Finland	Swedish	12	Paulaharju et al. 2025
Cannon SW–16	Type IV	Soumenlinna, Finland	Swedish	12	Paulaharju et al. 2025
Cannon SW–17	Type IV	Soumenlinna, Finland	Swedish	12	Paulaharju et al. 2025
Cannon SW–18	Type IV	Soumenlinna, Finland	Swedish	12	Paulaharju et al. 2025
Cannon SW–19	Type IV	Soumenlinna, Finland	Swedish	12	Paulaharju et al. 2025
Cannon SW–20	Type IV	Edenton, NC	Swedish	18	N/A
Cannon SW–21	Type II	Outer Farne Islands, UK (underwater)	Swedish	6	Wessex Archaeology 2013:10, 22
Cannon SW–22	Type I	Outer Farne Islands, UK (underwater)	Swedish	6	Wessex Archaeology 2013:1-22
Cannon SW–23	Type III	Lake Champlain Maritime Museum	Swedish	6	Cohn et al. 2003:86–92
Cannon UN–01	Type I	Brunswick Town/Fort Anderson State Historic Site, NC	Unknown	6	N/A
Cannon UN–02	Type II	Chavonnes Battery Museum, Capetown, South Africa	Unknown	12	Chavonnes Battery Museum 2025

Cannon UN–03	Type III	Kiek in de Kök Museum & Bastion Tunnels, Tallinn, Estonia	Unknown	18	N/A
Cannon UN–04	Type III	Castillo De San Marcos, St. Augustine, FL	Unknown	16	Meide 2002:11
Cannon UN–05	Type II	Bauline, Newfoundland (underwater)	Unknown	Unknown	Shipwreck Preservation Society of Newfoundland and Labrador 2020
Cannon 6003	Type I/IV	Outer Farne Islands, UK (underwater)	Swedish	Unknown	Wessex Archaeology 2013:1-22
Cannon 6006	Type I	Outer Farne Islands, UK (underwater)	Swedish	Unknown	Wessex Archaeology 2013:10
Cannon 6009	Type I/IV	Outer Farne Islands, UK (underwater)	Swedish	Unknown	Wessex Archaeology 2013:11
Cannon 6018	Type I	Outer Farne Islands, UK (underwater)	Swedish	Unknown	Wessex Archaeology 2013:12
Cannon 6010	Type II/III	Outer Farne Islands, UK (underwater)	Swedish	Unknown	Wessex Archaeology 2013:1-22
Cannon, El Gran Grifon	Unknown	*El Gran Grifon*, UK (underwater)	Spanish	Unknown	Martin 1972: 63; Muckelroy 1978:104
Cannon, Mars	Unknown	*Mars*, (underwater), recovered, current location unknown	Swedish	Unknown	Eriksson and Rönnby 2017:103
Cannon HA/AG0268	Type I	Unknown	British	Unknown	Parham et al. 2013:409
Cannon HA/AG0274	Type IV	Unknown	Swedish	4 or 6	Parham et al. 2013:409
Cannon HA/AG0278	Type IV	Unknown	British	Unknown	Parham et al. 2013:409
Cannon HA/AG0267	Type IV	Unknown	British	Unknown	Parham et al. 2013:409
Cannon HA/AG0009	Type IV	Unknown	Swedish	4	Parham et al. 2013:409

Cannon HA/AG0002	Type IV	Unknown	Unknown	4 or 6	Parham et al. 2013:410
Cannon HA/AG0003	Type IV	Unknown	Unknown	6 or 8	Parham et al. 2013:410
Cannon HA/AG0289	Type IV	Unknown	Unknown	4	Parham et al. 2013:410
Cannon HA/AG0296	Type IV	Unknown	Unknown	Unknown	Parham et al. 2013:410
Cannon HA/AG0265	Type IV	Unknown	Unknown	6	Parham et al. 2013:410
Cannon HA/AG0004	Type IV	Unknown	Unknown	1 or 2	Parham et al. 2013:410
Cannon, Mynden	Type IV	Landesamt für Bodendenkmalpflege, Germany	Swedish	3	Auer 2004:272
Cannon, Mercedes	Type I/II	*Nuestra Señora de las Mercedes*, (underwater)	Spanish	Unknown	Delgado and Goold 2022:357
Cannon	Type I/II	Crane Point Museum and Nature Center, Florida Keys.	Unknown, (Spanish?)	6 or 8	Pers. Comm. Jason Raupp
Cannon #08	Type II/III	Cannon site, Cahuita Point, Costa Rica	Unknown	Unknown	Harris and Richards 2018:441
Cannon #15	Unknown	Cannon site, Cahuita Point, Costa Rica	Unknown	Unknown	Harris and Richards 2018:441
Cannon #09	Unknown	Cannon site, Cahuita Point, Costa Rica	Unknown	Unknown	Harris and Richards 2018:441